THE INFLUENCE OF PARAMETRIC EFFECTS ON THE APPEARANCE OF SMALL COLOUR DIFFERENCES

by

Dong-Ho Kim

Submitted in accordance with the requirements for the degree of
Doctor of Philosophy

The University of Leeds
Department of Colour Chemistry and Dyeing
April 1997

The candidate confirms that the work submitted is his own and that appropriate credit has been given where reference has been made to the work of others.

ABSTRACT

The effects of the two physical parameters, background and gap, on the perception of small colour differences ($\Delta E^* < 5$) were investigated by use of 248 colour-difference pairs around 21 colour centres made from painted samples. Each pair was assessed by an average of 30 times under each viewing condition using a grey-scale method and/or a paired-comparison method. From the visual data, colour-difference ellipsoids (ellipses) or tolerances were determined by use of a logistic or a probit maximum-likelihood analysis model, or by a least-square method.

The perceived tolerance sizes along the three colour-difference directions ΔL^*, ΔC^* and ΔH^* in the CIELAB space were found to be little influenced by a change of lightness of the grey background but significantly influenced (i.e., decrease in tolerance size) by a 0.5° gap between a pair of samples. The gap factor for the lightness component was greater than that for chroma or hue components, both the latter having similar magnitudes. This could be an explanation for the increase of the lightness relative tolerance ℓ (or parametric factor K_L) by a factor of 2 in the three modified CIELAB formulae (CMC, BFD and CIE94) for acceptability judgements, in which textile samples, having an unclear dividing line between them, are mainly used. In addition, the value of the relative tolerance ℓ used is thought to be practically the ratio between the lightness and chroma tolerances.

The experimental uncertainties from non-physical parameters were also quantified. The degrees of precision (i.e., standard error) of colour measurements and observer judgements were found to be good (±4% and ±7%, respectively). The different methods of scaling and data analysis were found to have little impact on the results.

The lightness, chroma and hue tolerances with respect to the standard colour position in the CIELAB space were studied in detail using the various existing datasets and the set from this study. The lightness tolerance showed a clear dependency upon the metric lightness for medium to light colours, but in the case of dark colours there was a discrepancy between the datasets. Both the chroma and hue tolerances showed dependency upon both the chroma and hue-angle and not the single dependency upon the metric chroma, as assumed in the CIE94 formula.

New weighting functions were derived from the above experimental evidence, and finally a new formula, LCD (Leeds Colour Difference) was proposed. The LCD formula is nearly as simple and flexible as CIE94 but smoothes the individual weighting functions compared to CMC and BFD, especially for lightness tolerances for light colours and chromaticity discrimination near the blue region. It was also found that the reliability of the BFD formula is improved when the size of the chroma weighting function is increased by 1.5 times and the form of lightness weighting function is made parallel to those of the other modified CIELAB formulae.

I dedicate this thesis to my mother and late father.

Acknowledgements

The author thanks Dr. J. H. Nobbs for his supervision and advice during this research.

I am also grateful to all observers for willingly conducting visual assessments and the former and present Korean colleagues in the department for their help and assistance.

My special thanks go to Mr. C.Yoon and Mr. K. Suragul for their intensive observing sessions, Dr. K. Sunwoo for helping me adapt to new circumstances and Jeff Pitchford for making of viewing booth frame and background.

Finally, thanks to all members of my family for their continuing love, support and encouragement and to Ms. I. Kim for her friendship and love.

Table of Contents

List of Figures

List of Tables

1. INTRODUCTION

Colour-difference has long been a subject of interest to the colour scientist. The aim of a colour difference formula is to give a close correlation between visually perceived colour difference and that quantified from instrumental measurement. In the surface colour industries, it is typically used for colour tolerance control, fastness testing, shade sorting and quantification of metamerism.

The Standard Observers (colour matching functions) were established by the CIE colorimetry system [1], but the "Standard Colour-Difference Observer" data has never been achieved. It illustrates the complexity and difficulty of the problem and the need to quantify and control the inherent experimental uncertainties, such as parametric effects, in colour-difference evaluation.

In this introductory chapter, the basics of colorimetry (colour specification, appearance, and difference) and the psychophysical methods of colour-difference assessment are reviewed.

1.1 Colour Specification Systems

Two major colour specification systems are in common use. The first one is based on the colour order system (or colour atlas) which uses collections of colour samples arranged in systematic order of hue, lightness and colourfulness. The second method, the CIE system, defines colours in terms of colorimetric responses of the eye.

1.1.1 Colour order system [2,3]

Among many colour order systems, the most widely known system is the Munsell system[4]. It has served as the main standard for many years since it was first introduced. The Natural Colour System (NCS) [5,6], based on Hering's opponent colour theory, is another representative.

The DIN system [7] by Deutsches Institut für Normung and the OSA-UCS system [8] by the Optical Society of America are the other two comparable systems to Munsell and NCS (e.g., lightness scale).

The Pantone collection is an example of a practical system not based on a colour order

system, in the sense that the colour samples are arranged in a logical order, but a mixing system where a calibrated set of printing inks are mixed in sequence.

1.1.1.1 Munsell system

The Munsell system has been an important model for the formulation and solution of many colorimetric problems. For example, the judgements condition used in deriving it (viewing samples against a neutral grey background of luminance factor of 20%) [2] is still valid for the scaling of colour and colour-difference.

The arrangements of samples are depicted in Fig.1-1. As can be seen, it follows three perceptual attributes: lightness (value), hue, and chroma. The value axis is located in the centre of the Munsell colour solid. It constitutes the grey scale with white at the top designated Munsell value 10, black at the bottom zero, and the greys having values from 1 to 9 as they become lighter. Around the value axis is the hue circle. There are five principal hues: red denoted as Munsell hue 5R, yellow 5Y, green 5G, blue 5B, and purple 5P, and also five intermediate hues (5YR, 5GY, 5BG, 5PB, and 5RP). Between each hue is divided by 10 fine steps but finer divisions are also possible using decimals. The Munsell chroma is represented by the distances of the samples from the neutral value axis.

The full Munsell designation consists of hue, value, / (a slash), and chroma: for example, 2.5YR 5/10. At chroma value 5, one value step corresponds to 2 chroma steps and also 3 hue steps. The CIE tristimulus values of the Munsell chips (Munsell Renotation System) were reported in 1943 [10].

1.1.1.2 Natural colour system (NCS)

The NCS was developed in Sweden by Hård and Sivik and adopted in 1982 as Swedish National Standard. The basis of the NCS is that colour cannot be measured objectively, i.e., in terms of spectral composition, but colour is a subjective visual phenomenon. In this system, the colour is described in the terms of six elementary attributes: whiteness(w), blackness(s), redness(r), green-ness(g), yellowness(y), and blueness(b).

The principles of quantification are as follows:

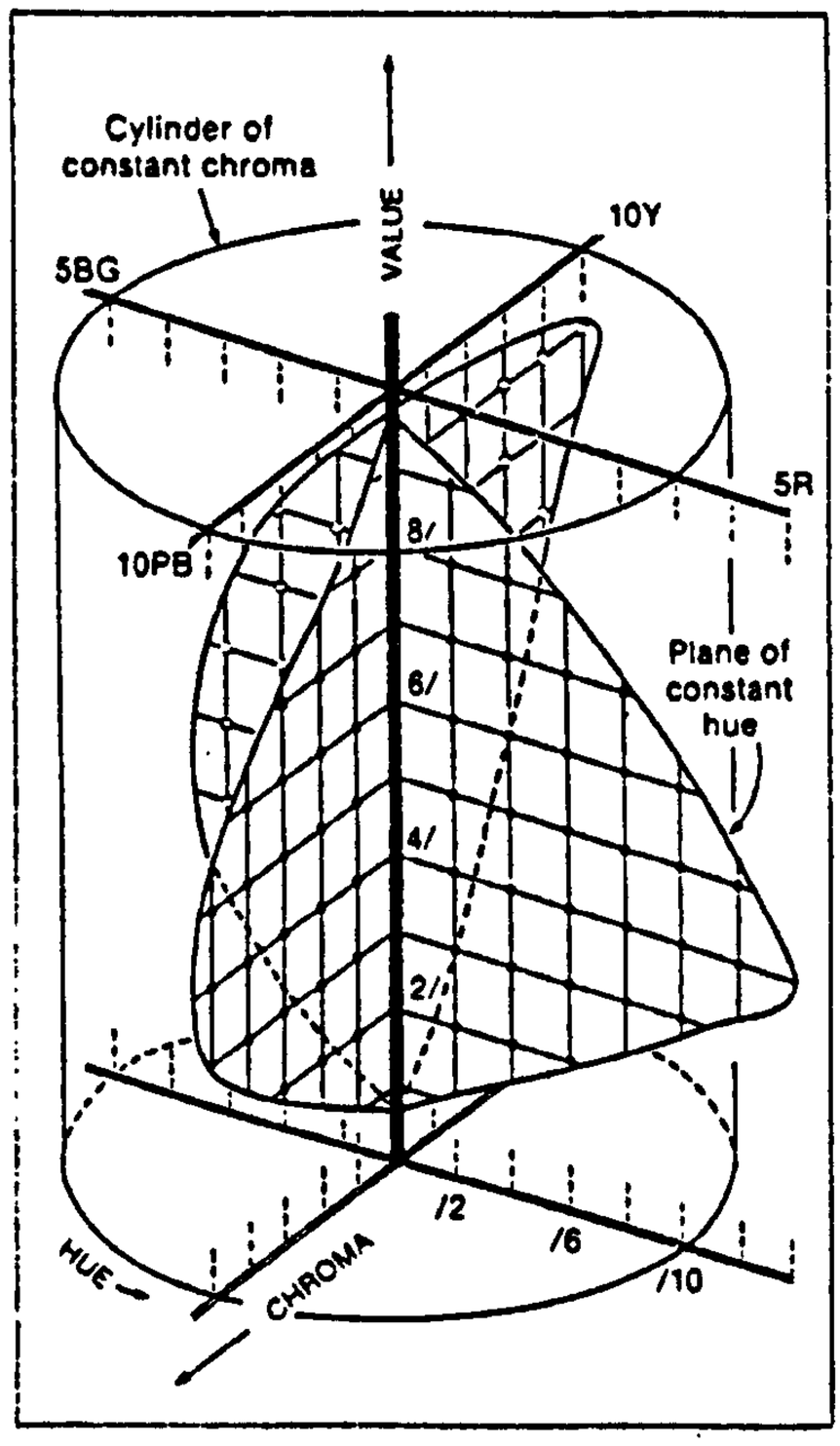

Figure 1-1. Schematic diagram of the Munsell colour solid [9].

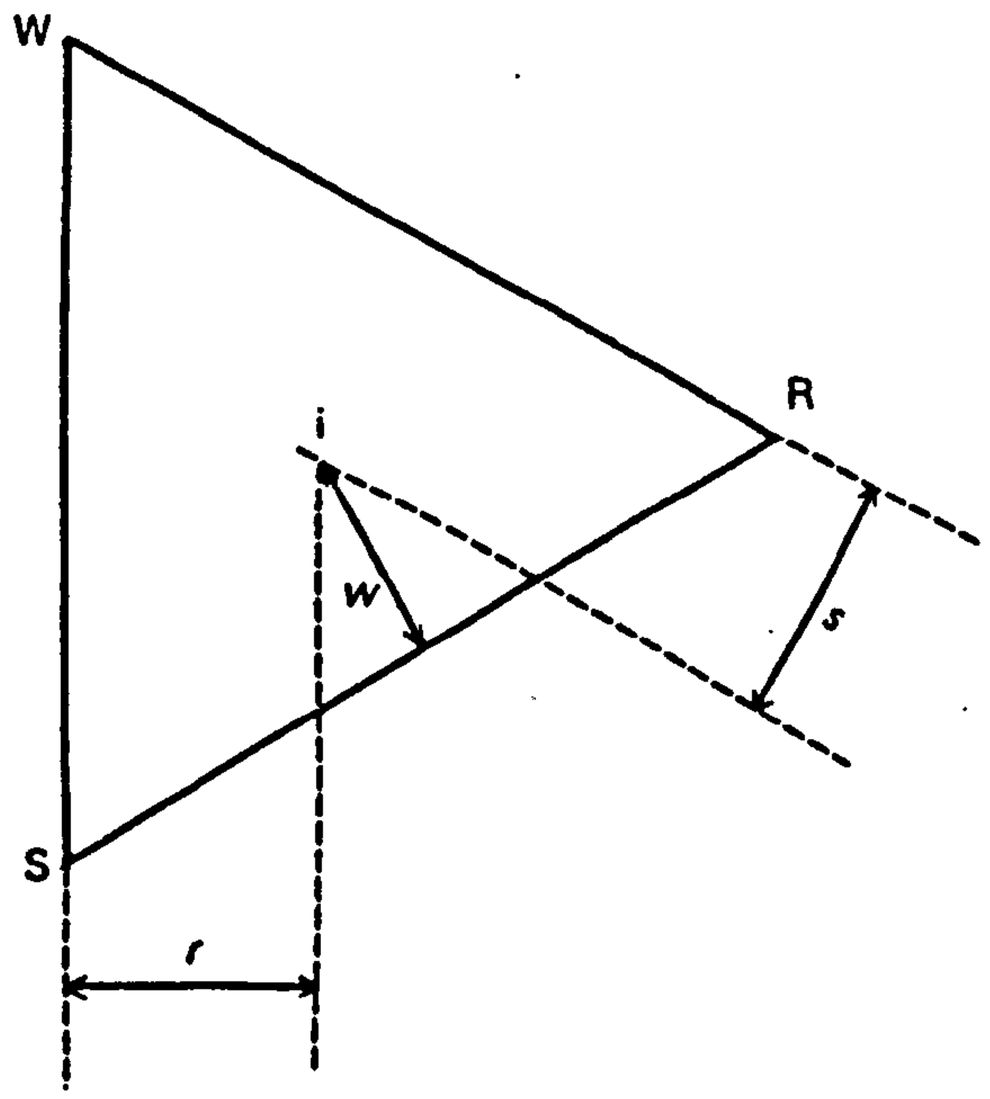

Figure 1-2. Arrangement of colours on a white (W) - black (S) - red (R) plane of the NCS [2].

For every surface colour,

(a) The sum of the elementary attributes always adds up to 100.

(b) The colour can have up to 4 attributes simultaneously.

(c) The colour can also have at the most 2 chromatic elementary attributes and these cannot be an opponent pair.

In architecture, the NCS blackness is said to be more readily perceivable than the Munsell value (lightness). The NCS unique red corresponds to Munsell hue 5R, NCS unique yellow to Munsell 5Y, NCS unique green to Munsell 5G, and NCS unique blue to Munsell 7.5B [2].

Some advantages of using colour order systems include the following: First, they are easy to use and to understand. Second, the spacing and number of samples can be adopted for different purposes. Whereas, there are a number of disadvantages that occur when they are used. First, as there are several colour order systems in use, there is no simple means of transferring results from one system to another. Second, there are large gaps (colour differences) between the samples, and it means that interpolation has to be used to determine the specifications of the samples. Third, the visual comparison between colours and the samples is valid only if it is done using the same illuminant and geometric arrangement as originally adopted in defining the system. Fourth, different observers may make different matches on the same colour (so called "observer metamerism", see section 1.2.4). Fifth, some colours may lie outside the gamut of the samples available in the system.

1.1.2 CIE system [11,12]

The CIE colour specification system was first established in 1931 by the Commission International de l'Eclairage (CIE). It specifies colours in a numerical and objective way, and is used with instrumental measurements. It has been made possible by the development of Standard Observers, Standard Illuminants and Sources, and standard viewing/illumination conditions. It is based on the rules of colour matching by additive colour mixing which were elucidated by Grassman [13].

The Grassman's laws of colour mixing are:

(a) Trichromacy – all colours can be matched by a suitable mixture of three different stimuli. The restriction to the primary stimuli chosen is that no one of them may be matched in colour by any mixture of the other two.

(b) Metamerism – stimuli evoking the same colour appearance produce identical results in additive colour mixing, regardless of their spectral composition.

(c) Additivity – if one component of a colour mixture changes, the colour of a mixture changes correspondingly.

From the contributions of Wright's and Guild's independent work in the 1920's and 30's, the real practical primaries for colour-matching were chosen. They are the monochromatic light of spectral centroids of 700 nm (red), 546.1 nm (green) and 435.8 nm (blue). The amounts of these three primaries are called the tristimulus values: R, G, B. If we match the spectrum colours and the power (Watts) of each spectrum colour is the same, then the relative amounts of three primary lights are called the spectral tristimulus functions: $\bar{r}$, $\bar{g}$, $\bar{b}$ (Fig.1-3). Prior to the CIE 1931 recommendation, the average $\bar{r}$, $\bar{g}$, $\bar{b}$ data obtained from a small number of observers formed the basis of the Standard Observer.

1.1.2.1 CIE tristimulus values

The problem of RGB functions, i.e., real primaries, is that at least one negative term might be produced in the calculation. This reflects the fact that in practice it is not possible to match all the practical primaries with mixtures from three real light sources. It leads to errors, thus the CIE adopted tristimulus specification based on the imaginary primaries that cannot be negative. The tristimulus values for these imaginary primaries are symbolised by X, Y, Z and are called the CIE tristimulus values.

For surface colours, the CIE tristimulus values are obtained by combining the spectral reflectance factor, $R(\lambda)$, covering the visible spectrum, with the relative spectral power distribution of the illuminant, $S(\lambda)$, and with each of the colour matching functions $\bar{x}(\lambda)$, $\bar{y}(\lambda)$, $\bar{z}(\lambda)$.

$$
\begin{aligned}
X &= k \sum R(\lambda)\, S(\lambda)\, \bar{x}(\lambda) \\
Y &= k \sum R(\lambda)\, S(\lambda)\, \bar{y}(\lambda) \qquad (1\text{-}1) \\
Z &= k \sum R(\lambda)\, S(\lambda)\, \bar{z}(\lambda)
\end{aligned}
$$

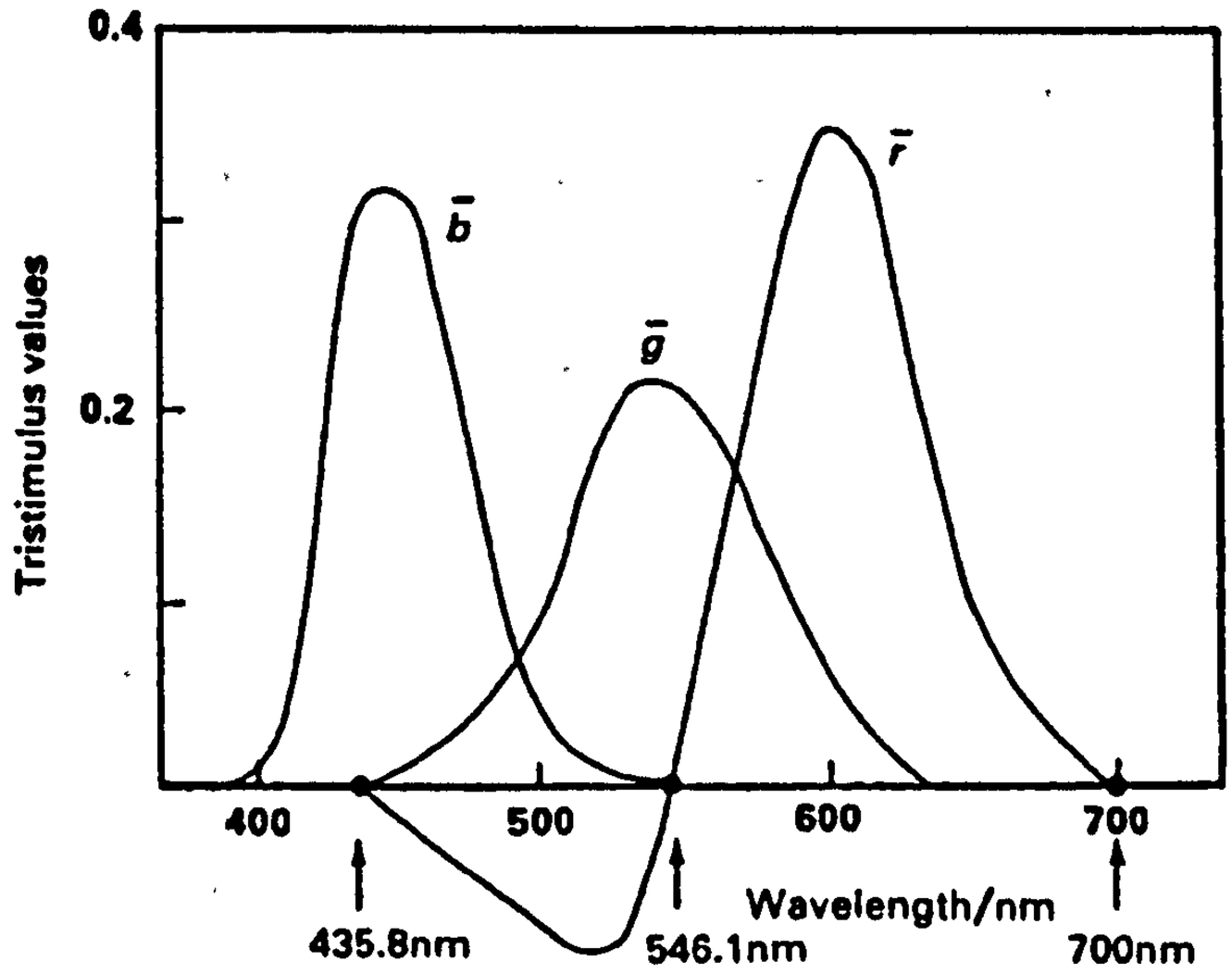

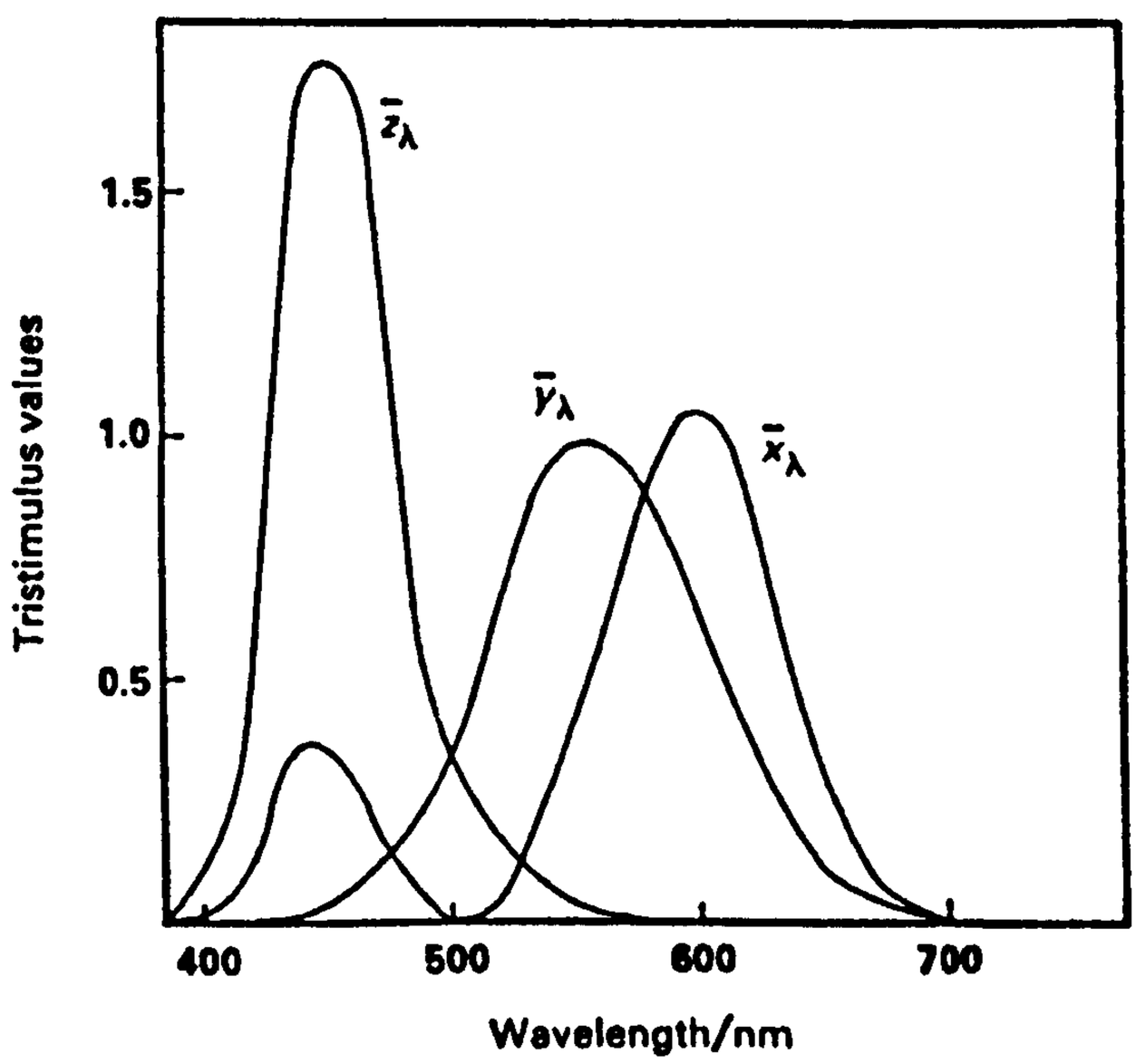

Figure 1-3. CIE spectral tristimulus functions: (a) $\bar{r}$, $\bar{g}$, $\bar{b}$ for colour matching with monochromatic lights of 435.8, 546.1 and 700.0 nm, and (b) $\bar{x}_\lambda$, $\bar{y}_\lambda$, $\bar{z}_\lambda$ for colour matching with imaginary primaries [11].

Where $k = 100 / \sum S(\lambda)\,\bar{y}(\lambda)$, a scaling factor that ensures the Y value of the perfect reflecting diffuser be always equal to 100.

Two different summation methods have been used: the weighted-ordinate method and the selected-ordinate method. The main difference is that in the weighted-ordinate method the summation is done at equally spaced wavelengths but in the selected-ordinate method the wavelength intervals are not equal. (For detailed computational procedures, see MacAdam [14].)

1.1.2.2 CIE Standard Observers (colour matching functions)

The colour matching functions are defined as the relative amounts of tristimulus values needed by the 'Standard Observer' to match a colour of a given wavelength in an equal energy spectrum. The CIE has recommended two Standard Observers for different purposes. The CIE 1931 Standard Colorimetric Observer, also referred to as 2° observer, is originally intended to represent an average observer of normal colour vision when attending a stimulus that subtends 2° diameter in visual subtense. This observer may satisfactorily be used for stimuli whose diameters subtend visual angles up to 4°. The 10° observer, the CIE 1964 Supplementary Standard Observer, is intended to represent an average observer when attending a stimulus that subtends 10° diameter. It is for stimuli with diameters greater than 4°.

In colour-difference assessments, the stimuli generally subtend an angle equal or greater than 4° to the eye, the 10° observer is preferred. However, in colour reproduction application, as most of the elements in the visual field are less than 2°, the 2° observer is preferred.

1.1.2.3 CIE Standard Illuminants and Sources

The CIE has made a distinction between illuminants and sources. An illuminant refers to a specified aim spectral energy distribution, while a source refers to a physical emitter of light such as the sun or a lamp. Thus, an illuminant can readily be specified but may not be realisable. Originally, the CIE recommended only real sources in 1931 but since 1963 illuminants have also been recommended to which no real source exactly corresponds.

In order for colorimetric specifications to be comparable, the particular illuminant used should always be recorded.

The CIE has standardised the following light sources:

(a) Source A - a tungsten filament lamp operating at a colour temperature of 2856°K.

(b) Source B - direct sunlight with a colour temperature of 4874°K.

(c) Source C - average daylight (sunlight + skylight) with a colour temperature of 6774°K.

Because Sources B and C are deficient in ultra-violet content, CIE recommended a series of daylight illuminants based on the studies of spectral power distribution of typical daylight [15]. They represent average daylights having colour temperatures between 4000 and 25000°K. Among them, the Illuminant D65 simulating a colour temperature of 6500°K is now most widely used. Although not being recommended by the CIE, a three-band fluorescent lamp, e.g., TL84, has special high efficiency and gives good reference for comparing metameric properties of surface colours.

1.1.2.4 CIE standard viewing / illumination conditions

The CIE has recommended a set of illumination and viewing conditions for opaque reflecting samples. They are:

(a) 45 / 0 (45° illumination / normal viewing)

(b) 0 / 45 (normal illumination / 45° viewing)

(c) d / 0 (diffuse illumination / normal viewing)

(d) 0 / d (normal illumination / diffuse viewing)

The 45/0 geometry is the original CIE recommendation. The opposite mode (0/45) gives the same result. The d/0 and 0/d geometry were additionally recommended to accommodate the use of spectrophotometers with an integrating sphere. (In 0/45 and 0/d geometries, the axis of the illumination beam need not be exactly normal to the sample surface.) In d/0 or 0/d geometries and for samples of incomplete diffuse reflections, a gloss trap is incorporated in the sphere to reduce the influence of specular reflections. Thus, if a gloss trap is used, specularly reflected light is excluded (SPEX), but if a gloss trap is not used, specularly reflected light is included (SPIN).

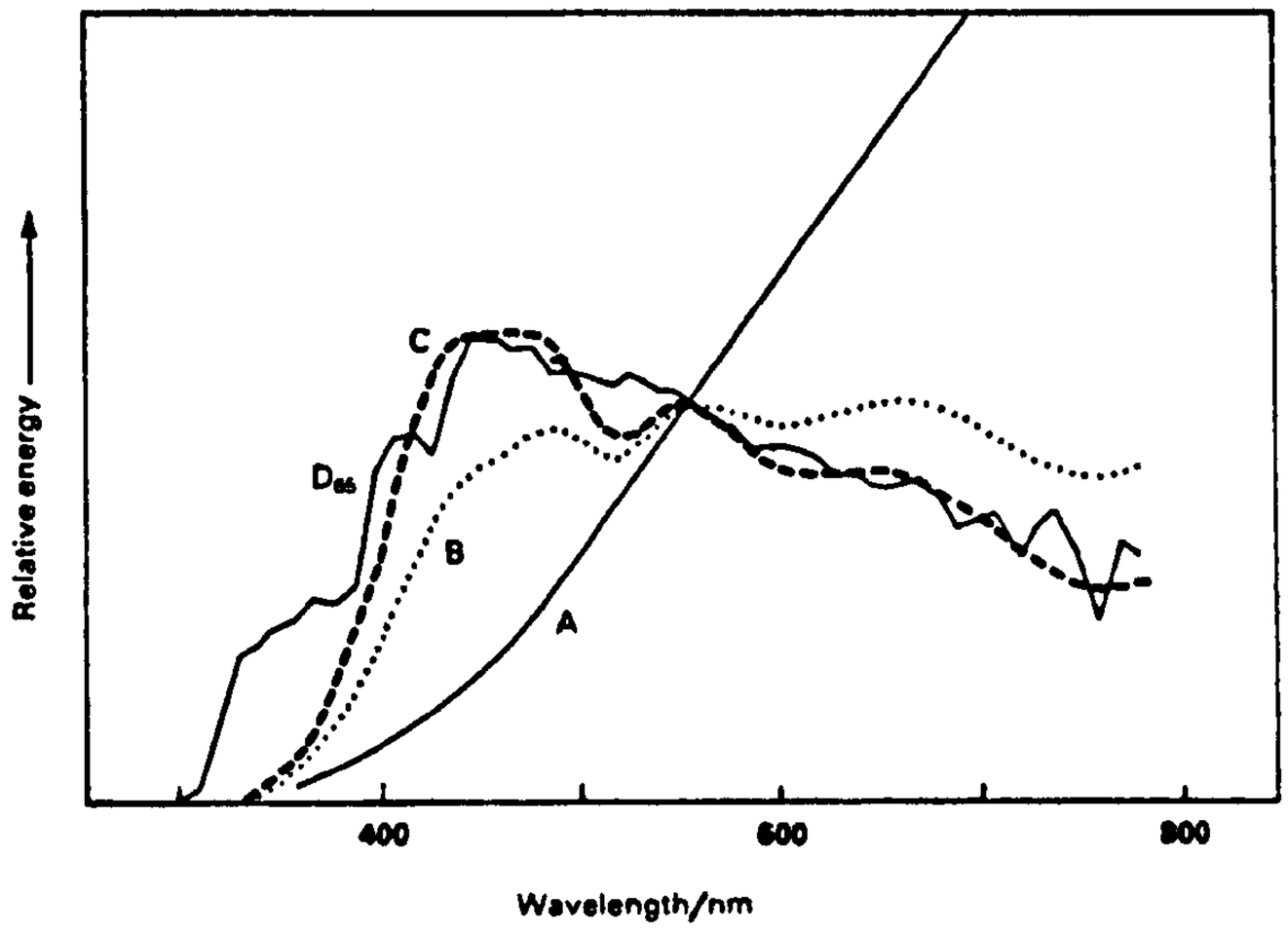

Figure 1-4. Spectral energy distributions of CIE Illuminants A, B, C, D65 [11].

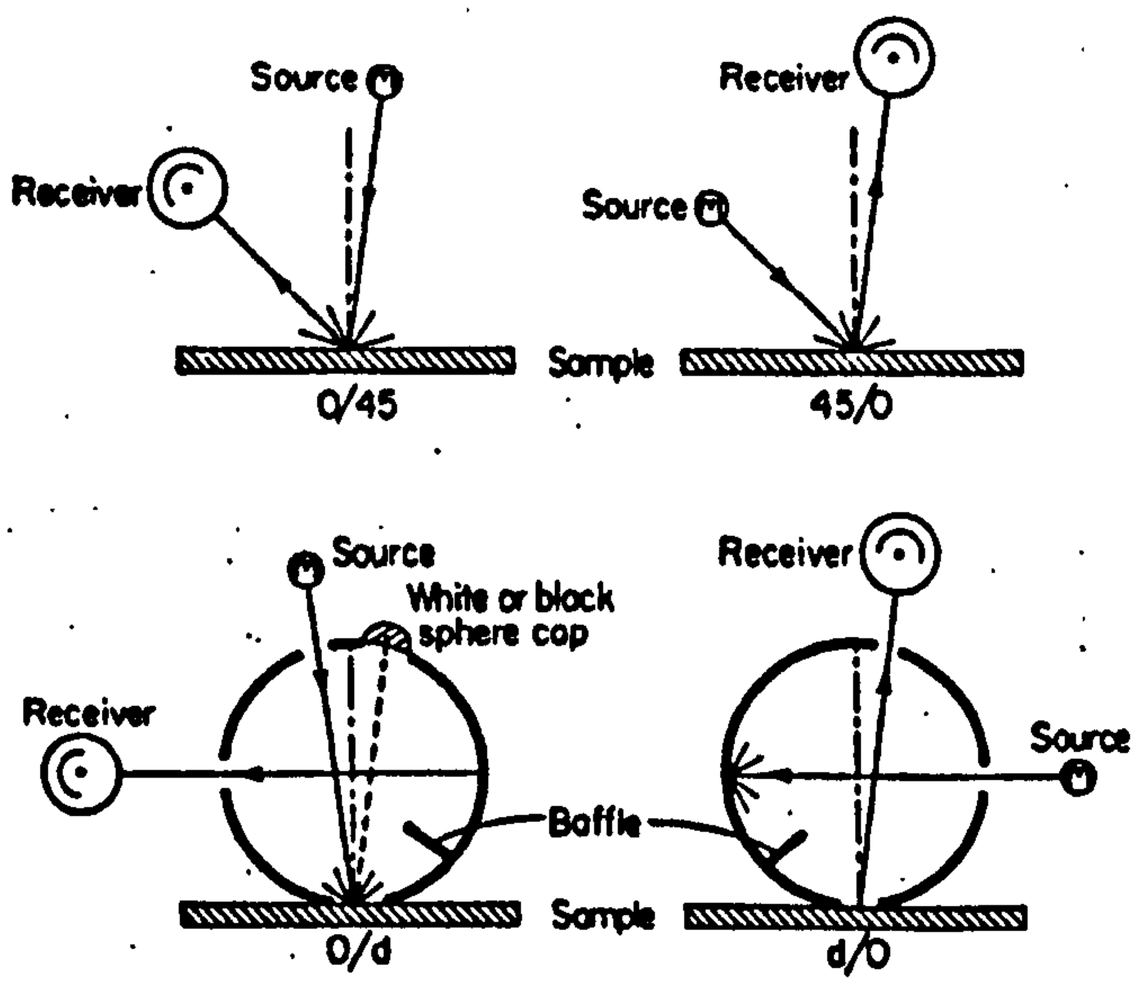

Figure 1-5. CIE recommended illumination and viewing conditions for reflectance measurements [12].

According to McLaren [16], the reflectance is the same if the directions of illumination and viewing are interchanged. Therefore, there are only 3 fundamental illumination / viewing geometries: 0/45, 0/d (SPIN), 0/d (SPEX). As the 0/d (SPIN) geometry approximates well to the reflectance measurements, the SPIN mode is recommended for computer match prediction. However, for the comparison of instrumentally measured colour differences with those from visual assessments, the SPEX mode is preferred [17].

1.1.2.5 CIE chromaticity diagrams

It is not easy to correlate the tristimulus values of an object to the colour appearance. The colour appearance depends not only on the stimulus itself but also on the surround (or background) and the response of the eye. The Y stimulus value is regarded as the lightness attribute of an object, if we consider the colours of the same lightnesses, then we need to deal with only two dimensions at a time. The chromaticity diagram is facilitated if the colour is defined in terms of chromaticity co-ordinates x, y, z and plot y against x (i.e., unit plane of tristimulus space).

$$x = X/(X+Y+Z)$$
$$y = Y/(X+Y+Z) \qquad (1\text{-}2)$$
$$z = Z/(X+Y+Z)$$

and

$$x+y+z = 1 \qquad (1\text{-}3)$$

The line joining the chromaticity co-ordinates of the spectral colours (horse shoe-shaped curve) is known as the spectrum locus. The straight line joining the ends of the spectrum locus is called the purple line (or purple boundary). The area enclosed by the spectrum locus and the purple line represents a maximum chromaticity gamut within which the chromaticities of all real stimuli are found (Fig.1-6).

The dominant wavelength and purity, an alternative set of co-ordinates in the CIE system, correlate more nearly with the visual aspects of hue and chroma. However, still they are not sufficient to be easily interpreted for practical use, and thus there have been attempts to provide a more uniform system, e.g., by linear transformation. These will be reviewed later.

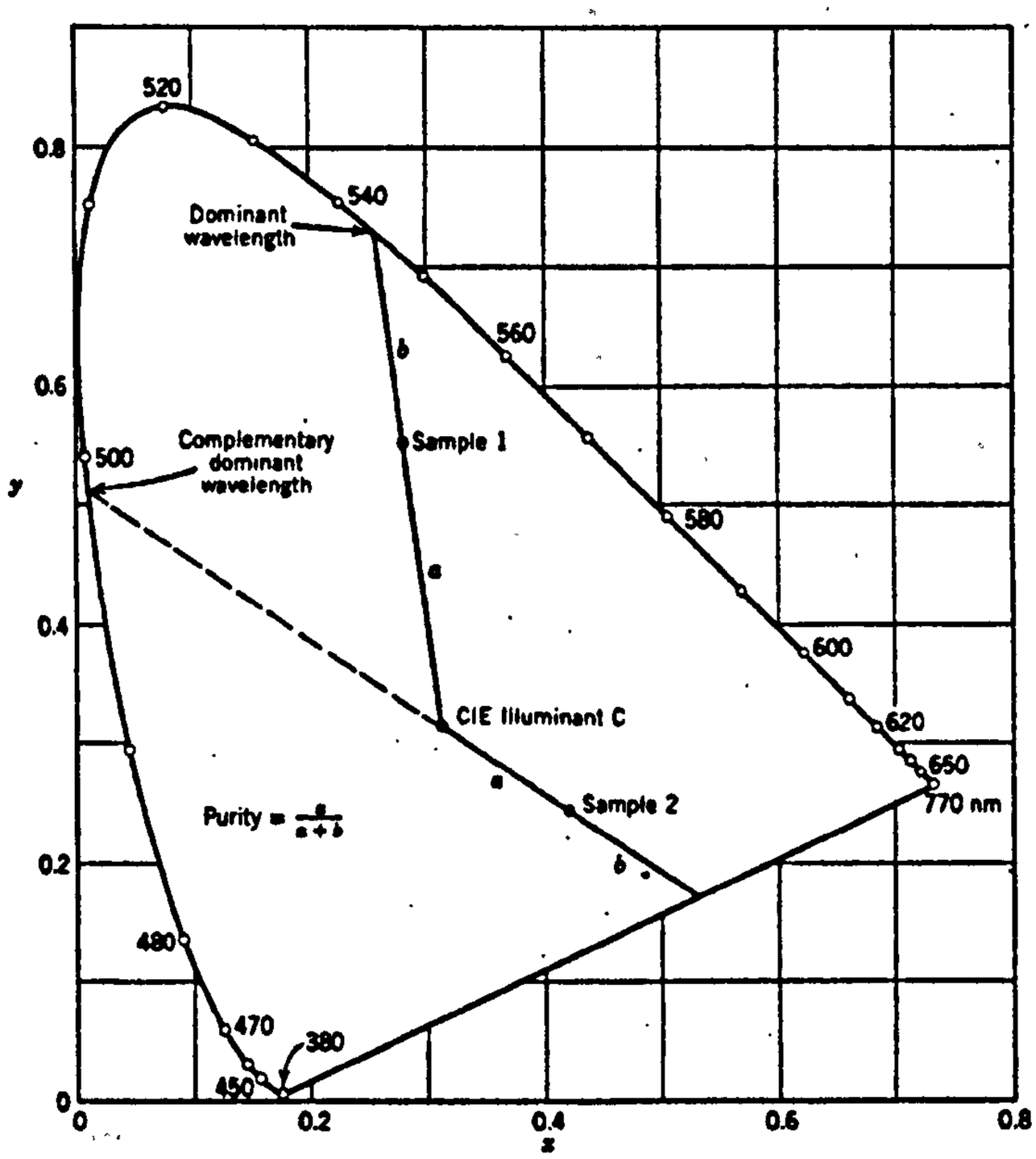

Figure 1-6. CIE 1931 chromaticity diagram [3].

1.2 Colour Appearance Phenomena [11,16,18]

In the previous section, two colour specification systems are reviewed. Both physical and numerical systems provide some basic attributes of colour appearance, but the complex aspects of colour vision phenomena are not satisfactorily explained. At the present time, there does not exist an internationally adopted colour appearance model equivalent in usefulness to the CIE system for specifying colour stimuli. Among the many colour appearance phenomena reported and studied, those thought to be important to this research subject are reviewed here.

1.2.1 Colour constancy

The colour appearance of objects does not change under a considerable range of illuminating conditions. If the illuminant is changed, not only does the observer become accustomed to the new illuminant but also knows well that the object is not changed. So, it is more appropriate to use the terms "object-colour constancy" or "discounting the illuminant".

The observer's adaptation to a new illuminant is usually incomplete, there remains a difference between the colour perceived in one illuminant and that perceived in another illuminant. The resultant colour shift after the observer is adapted to the new illuminant is a combination of colorimetric shift and adaptive colour shift. The colorimetric shift is simply due to the change of the spectral distribution of illuminant and can be calculated by standard colorimetric procedures. The adaptive colour shift is caused by the chromatic adaptation of the visual mechanism. (See Section 1.2.3)

Aspects of object-colour constancy also arise in the effect known as achromatic induction and/or chromatic induction, which seek explanations for such phenomena as lightness contrast, lightness constancy and colour contrast.

1.2.2 Achromatic and chromatic induction

Achromatic or chromatic induction is a visual process that occurs when two or more colour stimuli are viewed side by side, the colour appearance of one particular area is markedly affected by the colour of adjacent area. The change in appearance can be in any combination of the three attributes of colour perception (hue, brightness and colourfulness).

The effect of achromatic and/or chromatic induction is also referred as simultaneous contrast. It is virtually instantaneous process while the chromatic adaptation develops slowly. Simultaneous contrast effects are the visual system's method of enhancing contrast (differences) boundaries, with the retina behaving like a small differential amplifier. That is, these effects are due to lateral inhibition (or interaction) between adjacent wavelength-coded receptive fields within the neural network of the retina. Under the conditions when simultaneous contrast is greatest, the lateral inhibition is maximised. Lateral inhibitions therefore govern the physiological responses generated by the different stimuli in the retina.

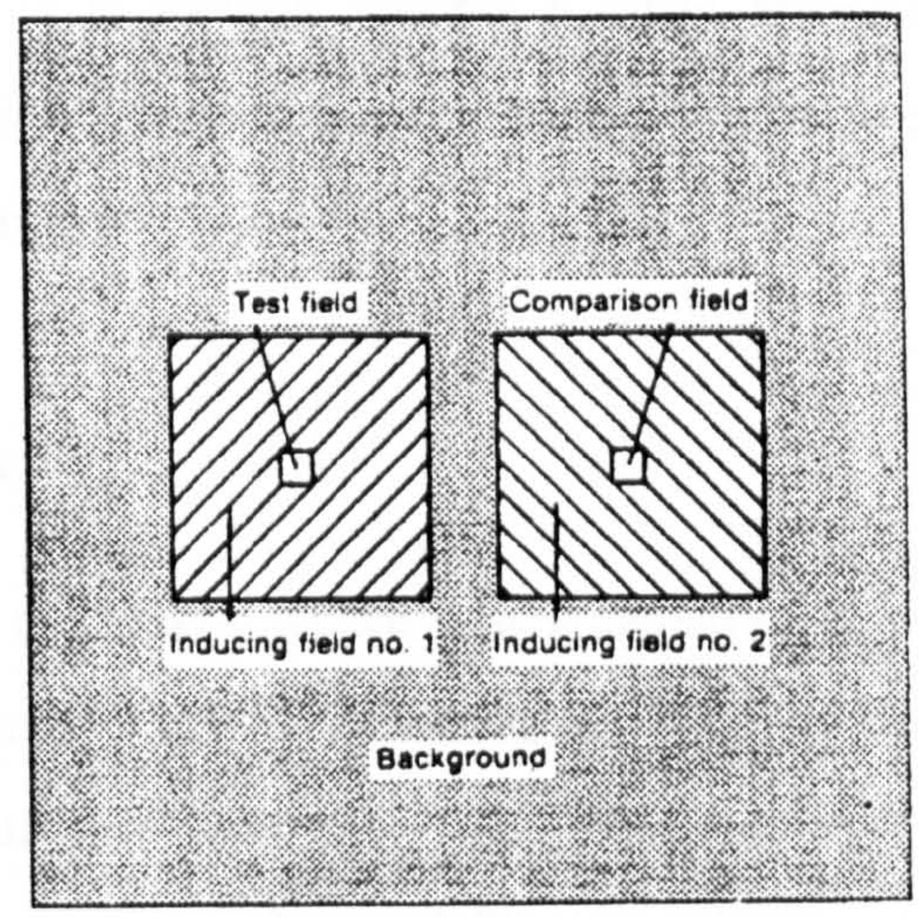

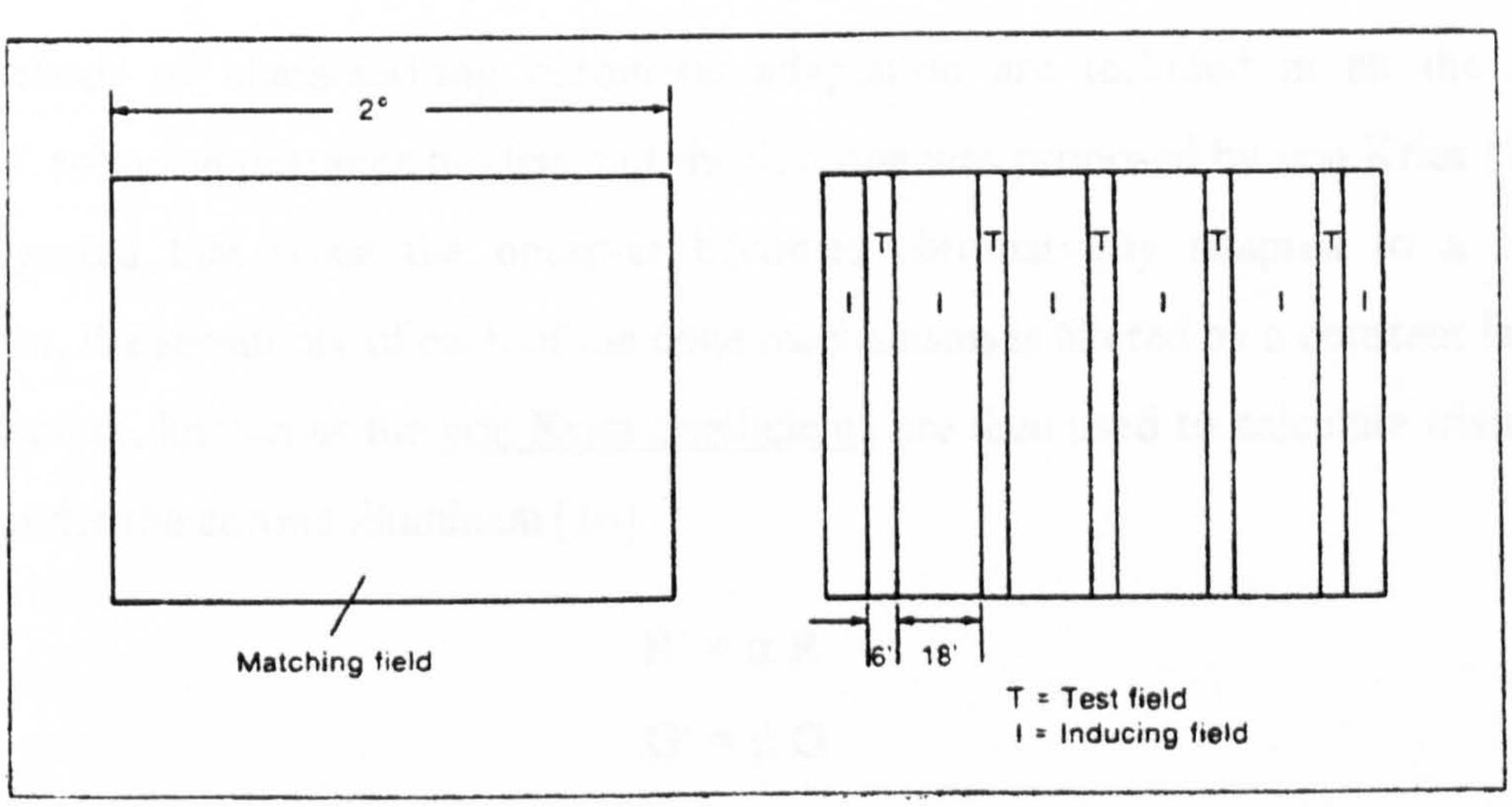

Figure 1-7. Examples of visual field configuration used in (a) achromatic induction, and (b) chromatic induction [18].

Various parameters affect simultaneous contrast (e.g., the stimuli sizes, shapes, separation, etc.), but there is one exception to simultaneous contrast effects. Instead of contrast enhancement the colours of adjacent areas become more alike, which is known as the assimilation or spreading effect. It is prominent when a chromatic object of small visual field (usually < 1°) is viewed against a large area of different chromaticity. Explanations of assimilation effects are made in terms of scattered light within the eye, but are not wholly satisfactory.

1.2.3 Chromatic adaptation

Chromatic adaptation is a process where either sensitivities of the fundamental visual response mechanisms are altered by exposure to light or modification of the visual response is brought about by a chromatic (adapting) stimulus. Many extensive studies have been performed in relation to the modelling of colour appearance, among them the notable ones are that of Hunt [19], Nayatani [20], Fairchild (RLAB) [21], and Luo (LLAB) [22].

Methods of characterising chromatic adaptation are included in all the above workers' colour appearance models, but the first one was proposed by von Kries (1905). He suggested that when the observer becomes chromatically adapted to a second illuminant, the sensitivity of each of the cone mechanisms is altered by a constant factor. These factors, known as the von Kries coefficients are then used to calculate tristimulus values under the second illuminant [16].

$$\begin{aligned} R' &= \alpha R \\ G' &= \beta G \\ B' &= \gamma B \end{aligned} \qquad (1\text{-}4)$$

where R, G, B refer to the original fundamental primaries, and R′, G′, B′ to the altered primaries.

Other chromatic adaptation transforms have the similar principles. That is, it is assumed that a sample represented by a given set of chromaticities under the reference condition would match in colour appearance under a new adaptation condition. This is illustrated in Fig.1-8.

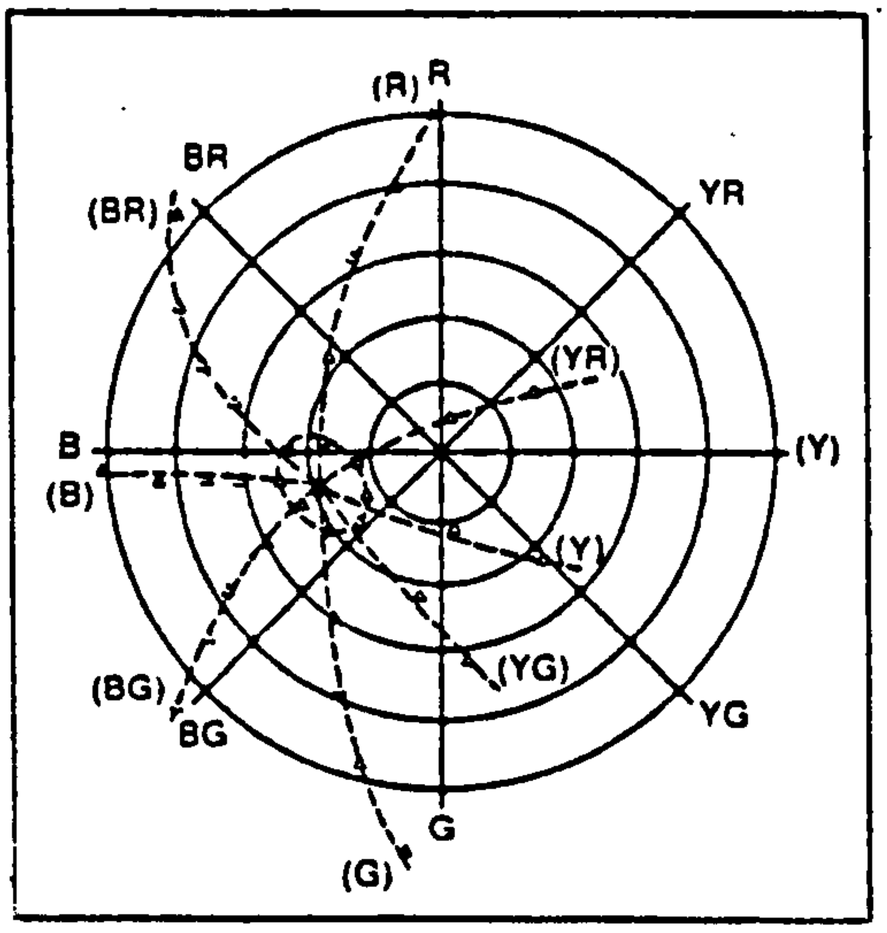

Figure 1-8. Colour appearance diagram for D_{65} adaptation (solid dots) and for A adaptation (open triangles) [23].

1.2.4 Metamerism

For clarity, the distinction between colour constancy, chromatic adaptation, and metamerism is stated again. Firstly, colour constancy is a property of a single sample, while metamerism refers to a pair of sample colours. Secondly, colour constancy refers to the original properties of objects, while chromatic adaptation refers to our eye's compensation for the change of illuminant.

Metamerism is the phenomenon that occurs when two colours match under one set of conditions but fail to match under a second set of conditions. There exist the following types of metamerism [11]:

(a) illuminant metamerism

(b) observer metamerism

(c) geometric metamerism

(d) field-size metamerism

(e) instrument metamerism

Illuminant metamerism occurs when a pair of colours matches under one illuminant but does not match under second illuminant, and is more important than any other types of

metamerism. Also, in the case of illuminant metamerism, there exist three or more cross-over points in the reflectance curves of two test colours (Fig.1-9). Geometric metamerism can occur when the viewing geometry changes. A pair that matches when seen at a distance (small field of view) may no longer match when closer to the eyes (large field) is an example of field-size metamerism. Instrument metamerism occurs in accordance with the instrument used for measurement of the colour parameters.

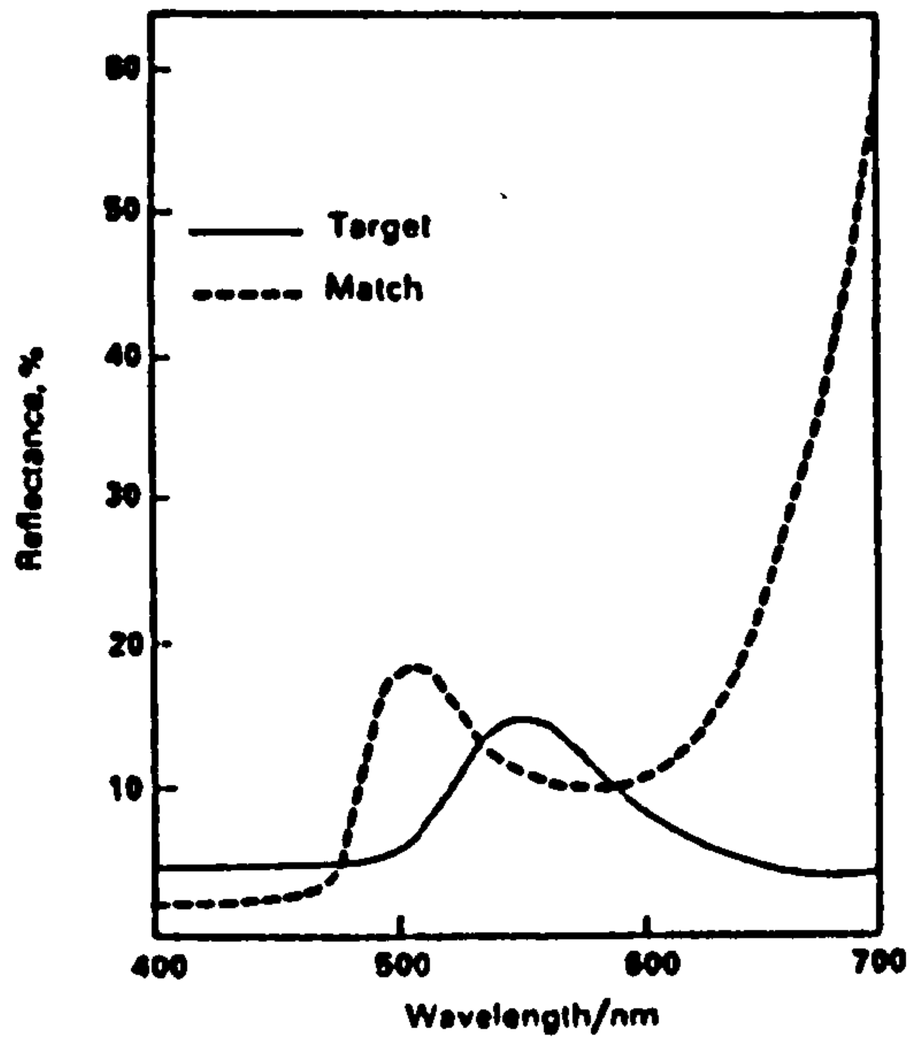

Figure 1-9. Reflectance curves of a target and an attempted match showing metamerism [11].

1.3 Colour-Difference Formulae [3,12,24,25]

Colour-difference formulae have been developed in association with the progress of colour vision theories and uniform colour spaces. Some formulae progress from a purely empirical approach. They can be divided into three groups according to their methodology and history.

(a) Formulae based on the Munsell system

(b) Formulae based on the empirical approach

(c) Formulae based on the theoretical approach

The above classification is, of course, not absolute. Some have aspects of both empirical and theoretical approaches, i.e., composite or hybrid type. The principal trend of recent advanced colour difference formulae is that the colour difference is evaluated by weighted ΔL^*, ΔC^* and ΔH^* values.

1.3.1 Formulae based on the Munsell system

A series of colour difference formulae based on the Munsell colour system have been developed. The first formula is the Nickerson Index of Fading [2] (1936). It is based on the city-block model, in which the distances (differences) in the three directions are simply added. The formula in terms of Munsell units of hue, value and chroma is:

$$\Delta E = \frac{2}{5} C\Delta H + 6\Delta V + 3\Delta C \qquad (1\text{-}5)$$

If C = 5, the coefficients of ΔH, ΔV, and ΔC are 2, 6, and 3, respectively. Their inverses give the relative sizes of these steps, 3H = 1V = 2C.

Balinkin (1941) altered this formula to correspond to Euclidean geometry, in which the distance between two points is the square root of the sum of the squares of each co-ordinate:

$$\Delta E = \left[\left(\frac{2}{5} C\Delta H \right)^2 + (6\Delta V)^2 + \left(\frac{20}{\pi} \Delta C \right)^2 \right]^{1/2} \qquad (1\text{-}6)$$

Since the Nickerson formula, there has been little consideration of the city-block model and colour space is generally assumed to be Euclidean.

Because of the difficulty of calculating Munsell co-ordinates from CIE tristimulus values, these formulae and later modifications are no longer used.

1.3.1.1 CIELAB [26]

The CIE 1976 ($L^*a^*b^*$) colour space is intended to be an approximate uniform colour space representing perceptual colour magnitudes in terms of opponent colour scales. In this colour space, the total colour difference ΔE^*_{ab} between two colours is calculated from

$$\Delta E^*_{ab} = \left[(\Delta L^*)^2 + (\Delta a^*)^2 + (\Delta b^*)^2\right]^{1/2} \tag{1-7}$$

where

$$L^* = 116\left(\frac{Y}{Y_n}\right)^{1/3} - 16 \tag{1-8}$$

$$a^* = 500\left[\left(\frac{X}{X_n}\right)^{1/3} - \left(\frac{Y}{Y_n}\right)^{1/3}\right] \tag{1-9}$$

$$b^* = 200\left[\left(\frac{Y}{Y_n}\right)^{1/3} - \left(\frac{Z}{Z_n}\right)^{1/3}\right] \tag{1-10}$$

for $\frac{Y}{Y_n} > 0.008856$, $\frac{X}{X_n} > 0.008856$, and $\frac{Z}{Z_n} > 0.008856$.

The rectangular colour co-ordinates, L^*, a^*, b^*, are calculated for each colour sample from the X, Y, Z tristimulus values of the sample and the X_n, Y_n, Z_n tristimulus values of a perfect reflecting diffuser with respect to a specified illuminant and observer.(Table1-1)

Procedures for calculating L^*, a^*, b^* when X/X_n or Y/Y_n or Z/Z_n are less than or equal to 0.008856 are also given in CIE recommendations. (Pauli extension [27])

$$L^* = 903.3\left(\frac{Y}{Y_n}\right) \quad \text{for} \quad \frac{Y}{Y_n} \le 0.008856 \tag{1-11}$$

Sève [28] also suggested a set of simplified equations for CIELAB that eliminate the separate equations for low luminance levels. For example,

$$L = 116\left[\frac{Y}{Y_n} + \frac{1}{381(1 + 180\,Y/Y_n)}\right]^{1/3} - 16 \tag{1-12}$$

The perceptual correlates of lightness, chroma, and hue are defined from L^*, a^*, b^*.

CIE1976 lightness Eqs. (1-8) and (1-11)

CIE 1976 a,b chroma
$$C^*_{ab} = \left[(a^*)^2 + (b^*)^2\right]^{1/2} \tag{1-13}$$

CIE 1976 a,b hue-angle
$$h_{ab} = \tan^{-1}\left(\frac{b^*}{a^*}\right) \tag{1-14}$$

The Euclidean distance in ΔL^*, Δa^*, Δb^* rectangular co-ordinates is identical to the Euclidean distance in the rotated rectangular co-ordinates ΔL^*, ΔC^*_{ab}, ΔH^*_{ab}. That is,

$$\Delta E^*_{ab} = \left[(\Delta L^*)^2 + (\Delta C^*_{ab})^2 + (\Delta H^*_{ab})^2\right]^{1/2} \tag{1-15}$$

Hence, CIE 1976 a,b hue-difference is

$$\Delta H^*_{ab} = \left[(\Delta E^*_{ab})^2 - (\Delta L^*)^2 - (\Delta C^*_{ab})^2 \right]^{1/2} \qquad (1\text{-}16)$$

The sign of the hue difference is taken as the same as the sign of the hue-angle difference, Δh_{ab}, between the colour-difference pair. Alternative expressions for ΔH^*_{ab} which make a direct computation of hue difference have been proposed [29-31].

Alternative equation for ΔH^*_{ab} [31]:

$$\Delta H^*_{ab} = \frac{a_1^* b_2^* - a_2^* b_1^*}{\left[0.5 \left(C^*_{ab,1} C^*_{ab,2} + a_1^* a_2^* + b_1^* b_2^* \right) \right]^{1/2}} \qquad (1\text{-}17)$$

The CIELAB space now almost serves as a base colour space, and the conversion of CIELAB co-ordinates to (or from) XYZ tristimulus values is very common. The reverse transform from L^*, a^*, b^* to X, Y, Z (for $Y/Y_n > 0.008856$) [3] is

$$X = X_n \left(\frac{L^* + 16}{116} + \frac{a^*}{500} \right)^3$$

$$Y = Y_n \left(\frac{L^* + 16}{116} \right)^3$$

$$Z = Z_n \left(\frac{L^* + 16}{116} - \frac{b^*}{200} \right)^3 \qquad (1\text{-}18)$$

Table 1-1. Tristimulus values and u', v' co-ordinates of perfect reflecting diffuser [32]. ($Y_n = 100$ in all cases)

Illuminant	Observer	X_n	Z_n	u_n'	v_n'
A	2°	109.850	35.585	0.2560	0.5243
	10°	111.144	35.200	0.2590	0.5242
C	2°	98.074	118.232	0.2009	0.4609
	10°	97.285	116.145	0.2000	0.4626
D_{65}	2°	95.047	108.883	0.1978	0.4683
	10°	94.811	107.304	0.1979	0.4696
TL84 (*)	2°	99.634	63.544	0.2226	0.5027
	10°	102.304	64.368	0.2279	0.5013

(* From Appendices 5 and 6 of Ref.[11])

1.3.2 Formulae based on the empirical approach

The empirical approach relies on the linear transformation of the CIE system. Judd was the first who tried to this method [25]. In 1939, he defined colour difference by using the distance formula in his triangular UCS diagram.

$$\Delta E^2 = \Delta L^2 + \Delta C^2 \qquad (1\text{-}19)$$

where L = lightness and C = chromaticity.

Hunter (1942) suggested the modified version of Judd formula. This formula, the NBS formula, is based on Hunter's rectangular co-ordinate "α-β" chromaticity diagram:

$$\Delta E_{NBS} = G\left\{\left[221\left(\overline{Y}\right)^{1/4}\left(\Delta\alpha^2 + \Delta\beta^2\right)^{1/2}\right]^2 + \left[P\left(\Delta Y^{1/2}\right)\right]^2\right\}^{1/2} \qquad (1\text{-}20)$$

where α and β are calculated from CIE x,y co-ordinates, G is a gloss factor, and P is a proximity factor. As can be seen, NBS is the first formula that includes parametric factors, i.e., gloss and gap.

1.3.2.1 CIELUV

CIELUV is another CIE 1976 recommendation for a new colour space and colour difference formula. In this formula the L^* function was combined with u_n and v_n.

$$\Delta E^*_{uv} = \left[(\Delta L^*)^2 + (\Delta u^*)^2 + (\Delta v^*)^2\right]^{1/2} \qquad (1\text{-}21)$$

where L^* is the same as that of CIELAB.

$$u^* = 13L^*(u' - u_n') \qquad v^* = 13L^*(v' - v_n') \qquad (1\text{-}22)$$

and

$$u' = \frac{4X}{X+15Y+3Z} = \frac{4x}{-2x+12y+3}$$

$$v' = \frac{9Y}{X+15Y+3Z} = \frac{9y}{-2x+12y+3} \qquad (1\text{-}23)$$

The quantities u_n' and v_n' refer to u′ and v′ values for the reference white (Table 1-1).

Also the reverse transform between u',v' and x, y is possible:

$$x = \frac{4.5u'}{3u'-8v'+6} \qquad y = \frac{2v'}{3u'-8v'+6} \qquad (1\text{-}24)$$

As similar to the CIELAB, the components of the CIELUV formula can be divided into the perceptual attributes of lightness, chroma, and hue. In the CIELUV, however, one more term is defined. This is the correlate of psychometric saturation (s_{uv}):

$$s_{uv} = 13\left[(u'-u_n')^2 + (v'-v_n')^2\right]^{1/2} \qquad (1\text{-}25)$$

The advantage of CIELUV to CIELAB is that CIELUV has an associated chromaticity diagram, i.e., linear transform of the CIE x,y diagram. Those who work in the fields such as monitors and video displays prefer to use the CIELUV space and formula.

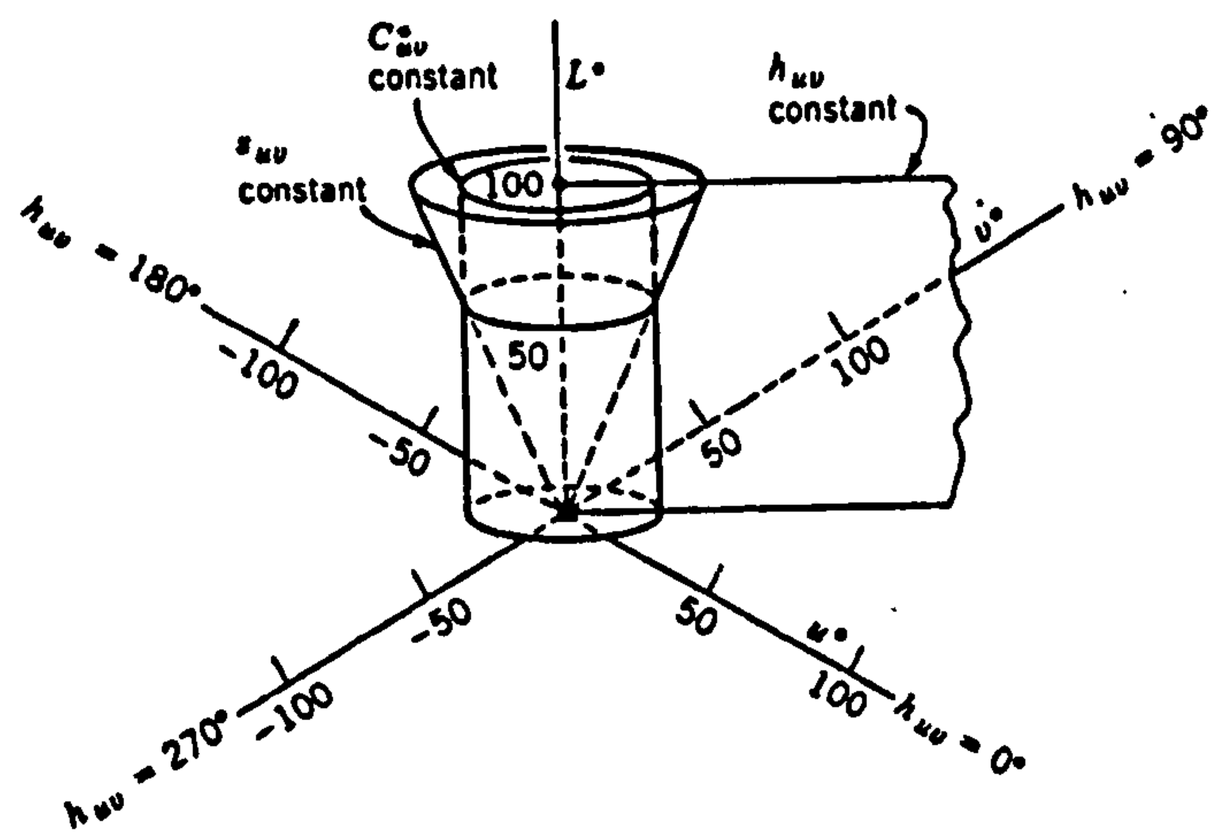

Figure 1-10. CIELUV colour space [1].

1.3.3 Formulae based on the theoretical approach

The line element [33] provides alternative method of colour-difference calculation. It could be used even when the colour space is not Euclidean, that is, all line elements are assumed to have the Riemannian form that defines the colour difference by an ellipsoid equation (quadratic equation). The distance, ΔE, between two points $P_1(x, y, Y)$ and $P_2(x+\Delta x, y+\Delta y, Y+\Delta Y)$ in Riemannian is:

$$\Delta E^2 = g_{11}\Delta x^2 + g_{22}\Delta y^2 + g_{33}\Delta Y^2 + 2g_{12}\Delta x\Delta y + 2g_{13}\Delta x\Delta Y + 2g_{23}\Delta y\Delta Y \qquad (1\text{-}26)$$

The methods of determination of the ellipsoid coefficients are divided into two. One is purely from the colour vision theory, and the other is based on the standard deviation of colour matching which starts from the MacAdam ellipses [34].

MacAdam (1942) published results of experiments that were designed to measure the distance in the x, y diagram for equal threshold colour-difference. Simon and Goodwin (1957) prepared graphic charts for rapid hand computation of colour-difference based on the MacAdam ellipses [35]:

$$\Delta E = \left[\frac{1}{K} (g_{11}\Delta x^2 + 2g_{12}\Delta x\Delta y + g_{22}\Delta y^2 + G\Delta Y^2) \right]^{1/2} \qquad (1\text{-}27)$$

where g_{ik}'s are the constants which depend on x and y, and G and K are the constants which depend on Y.

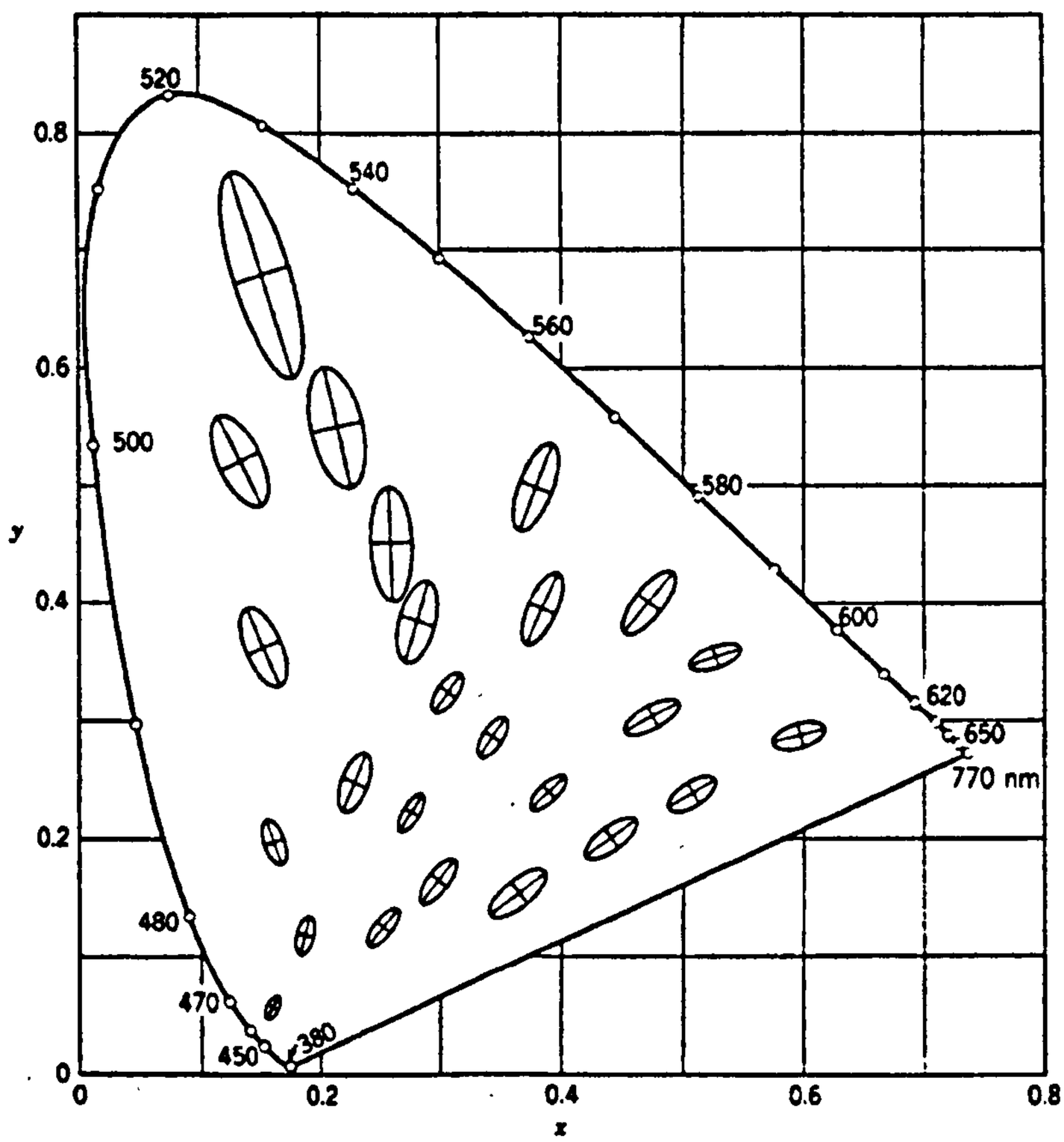

Figure 1-11. MacAdam ellipses plotted on a CIE chromaticity diagram [3].
(The axes of the plotted ellipses are ten times their actual lengths.)

1.3.3.1 FMC [36,37]

FMC colour space and colour-difference formula were developed by collaborated works of Friele, MacAdam and Chickering during the 1960s. FMC space was claimed to be more nearly perceptually uniform than the CIE 1931 space in terms of the MacAdam

1942 ellipses. However, the correlation between calculated difference and perceived difference is not well established and thus, unless confirmed by visual observations, it is not recommended for use. Though it is still included in the American Society for Testing and Materials (ASTM) Standard [38], it is now rarely used.

Other studies related to theoretical approaches were done by Friele [39] (1978) and Seim and Valberg [40] (1986). Friele developed the FCM (Fine Color Metric) formula which is based on the line element concept and is established with various sets of perceptibility and acceptability data of physical samples. Seim and Valberg developed a new theoretical formula of the opponent LAB type.

1.3.4 Advanced colour-difference formulae

Since the CIE recommended two colour-difference models, CIELAB and CIELUV, in 1976, there has been a continuous search for better ones. This led to the development of advanced colour-difference formulae such as CMC [41], BFD [42], and CIE94 [26].

1.3.4.1 CMC, BFD and CIE94

CMC, BFD and CIE94 are all based on the CIELAB space and are similar in most respects. Superior performances of these formulae to CIELAB for small to moderate colour differences originate from the use of different weightings for ΔL^*, ΔC^* and ΔH^* according to the position of the colour in CIELAB space. Thus, the colour spaces associated with these formulae are not Euclidean, and the visual tolerance volume around a standard is defined as an ellipsoid in CIELAB space.

The CMC formula was developed by the Colour Measurement Committee (CMC) of the Society of Dyes and Colourists (SDC) on the basis of McDonald's experiments [43], in which skilled colourists carried out visual pass/fail (acceptability) decisions on polyester thread samples. After more than 10 years of experience, CMC has gained the wide acceptance, especially in textile coloration industries, and is now used extensively. It has been adopted as the British Standard (1988) [44], the American Association of Textile Chemists and Colorists (AATCC) Test Method (1992), and the International Standards Organization (ISO) standard (1995).

(For convenience, the parameters ΔE^*_{ab}, ΔC^*_{ab} and ΔH^*_{ab} will be denoted by ΔE^*, ΔC^* and ΔH^* in the remainder of the thesis.)

CMC(ℓ:c) Formula [41]:

$$\Delta E_{CMC} = \left[\left(\frac{\Delta L^*}{\ell S_L}\right)^2 + \left(\frac{\Delta C^*}{c S_C}\right)^2 + \left(\frac{\Delta H^*}{S_H}\right)^2\right]^{1/2} \qquad (1\text{-}28)$$

where $S_L = \dfrac{0.040975 L^*_{std}}{1 + 0.01765 L^*_{std}}$ unless $L^*_{std} < 16$ when $S_L = 0.511$

$$S_C = \frac{0.0638 C^*_{std}}{1 + 0.0131 C^*_{std}} + 0.638$$

$$S_H = (fT + 1 - f) S_C$$

and

$$f = \left[\frac{(C^*_{std})^4}{(C^*_{std})^4 + 1900}\right]^{1/2}$$

$$T = 0.36 + \left|0.4 \cos(h^\circ_{std} + 35)\right| \quad \text{unless } 164^\circ \le h^\circ_{std} \le 345^\circ \text{ when}$$

$$T = 0.56 + \left|0.2 \cos(h^\circ_{std} + 168)\right|$$

$\ell = c = 1$ for perceptibility of colour differences

$\ell = 2, c = 1$ for pass/fail (acceptability) decisions

Luo and Rigg combined many earlier acceptability and perceptibility data sets and conducted additional experiments using wool serge samples and the grey-scale method[45]. They used these results to derive a new colour-difference equation, the BFD formula. BFD has the following major differences to CMC: (a) the addition of a new term which accounts for the rotation of chromaticity ellipses in the a^*b^* diagram, and (b) the use of a different lightness scale (Fong lightness scale [46], Eq.1-30) and resulting different ΔL^* weighting function.

BFD(ℓ:c) Formula [42]:

$$\Delta E_{BFD} = \left[\left(\frac{\Delta L_{BFD}}{\ell}\right)^2 + \left(\frac{\Delta C^*}{c D_C}\right)^2 + \left(\frac{\Delta H^*}{D_H}\right)^2 + R_T\left(\frac{\Delta C^* \Delta H^*}{D_C D_H}\right)\right]^{1/2} \qquad (1\text{-}29)$$

where $L_{BFD} = 54.6 \log(Y + 1.5) - 9.6$ (1-30)

(For the full specification of BFD, see Appendix 4.)

The CIE94 formula (formerly TC1-29) has recently been recommended by CIE for industrial colour-difference evaluation work. But, as clearly stated in the CIE

report[26], it does not have the status of a CIE standard. The base of CIE94 is the RIT-Dupont data [47] which used paint samples, paired-comparison method and probit analysis to produce visually equivalent tolerances. There has been little work published so far on the comparison of the performance of CIE94 with those of other formulae but in one study [22] it gave the similar performance as CMC or BFD despite its simpler form.

CIE94 Formula [26]:

$$\Delta E^*_{94} = \left[\left(\frac{\Delta L^*}{k_L S_L} \right)^2 + \left(\frac{\Delta C^*}{k_C S_C} \right)^2 + \left(\frac{\Delta H^*}{k_H S_H} \right)^2 \right]^{1/2} \qquad (1\text{-}31)$$

where $S_L = 1$

$S_C = 1 + 0.045\, C^*_{std}$

$S_H = 1 + 0.015\, C^*_{std}$

and $k_L = k_C = k_H = 1$ for most applications

$k_L = 2,\ k_C = k_H = 1$ for the textile industry

1.3.4.2 DCI-95 [48]

Rohner and Rich of Datacolor International have developed a metric, the DCI-95 formula, which is based on logarithms and matches the performance of existing advanced colour-difference models. DCI-95 features:

(a) Logarithmic compression to CIELAB L^* and C^*

(b) Metric hue weighting via C^* as a^*/b^* axes are derived from weighted C^* and h_{ab}

(c) Better uniformity in terms of Munsell hue and chroma spacing at value 5 than any other industrial colour-difference formula evaluated so far

The equations are as follows:

$$L^{**} = G_1 \log_e(1 + P_1 L^*)$$

$$C^{**} = G_2 \log_e(1 + P_2 C^*)$$

$$a^{**} = C^{**} \cos(h_{ab})$$

$$b^{**} = C^{**} \sin(h_{ab})$$

and

$$G_1 = \frac{100}{\log_e(1 + P_1 100)}$$

$$G_2 = \frac{100\left(1 - 0.2\left|\sin(h_{ab})\right|\right)}{\log_e(1 + P_2 100)} \qquad (1\text{-}32)$$

The colour-difference ΔE^{**} is defined as CMC or CIE94 with specific tolerance and parametric factors for lightness, chroma, and hue.

Further work continues to optimise P_1, P_2 and three weighting functions, to improve its uniformity throughout colour space, and especially to explain the behaviour of very dark and very high chroma samples.

1.3.4.3 LLAB [22]

The LLAB model was developed by Luo and co-workers. Unlike other colour-difference models, LLAB provides measures to colour appearance as well as colour difference. It is in effect more close to a colour appearance model. The advantage of LLAB is that it can cope with a wide range of viewing conditions such as change of light source, luminance, and background. However, colour-difference evaluation and colour appearance modelling are substantially different. Small colour differences, larger sample size and a lot of experimental noise are involved in colour-difference work while colour appearance model deals with large colour differences, smaller visual elements and a vast change of viewing conditions. Therefore, the effectiveness of LLAB in conventional industrial colour tolerance work is open to question.

Table 1-2. Summary of colour-difference formulae.

Formula	Comment	References
CIEXYZ	Euclidean colour space	11,12
Nickerson index of fading	The first colour-difference formula (Munsell type & city-block model)	3
Balinkin	Euclidean Munsell type	3
CIELAB	CIE official recommendation	26
NBS	The only formula including gloss and proximity factors	3
CIELUV	CIE official recommendation	2
MacAdam ellipses & Simon-Goodwin	The basis for ellipse formula	34 35
FMC-1, FMC-2	MacAdam based formulae	36,37
FCM	Theoretical approach (line element)	39
SVF	Theoretical LAB type	40
CMC	British Standard & ISO standard AATCC Test Method	41
BFD	Slight improvement on CMC	42
CIE94	Tentative CIE recommendation	26
DCI-95	Logarithm-based formula	48
LLAB	Colour appearance model	22

1.4 Quantifying Visual Colour Difference

1.4.1 General introduction [18,49,50]

There are various scaling methods in visual colour-difference assessments. The terms and definitions are often confused. Here, the types of scales are reviewed first, then the basic concepts and laws of psychophysics and the scaling methods follow. The detailed account of data analysis procedures is given in Chapter 2.

1.4.1.1 Types of scales

The choice of experimental method largely determines the kind of measurement scale. Stevens [49] (1946) has classified scales into four: nominal, ordinal, interval and ratio scales.

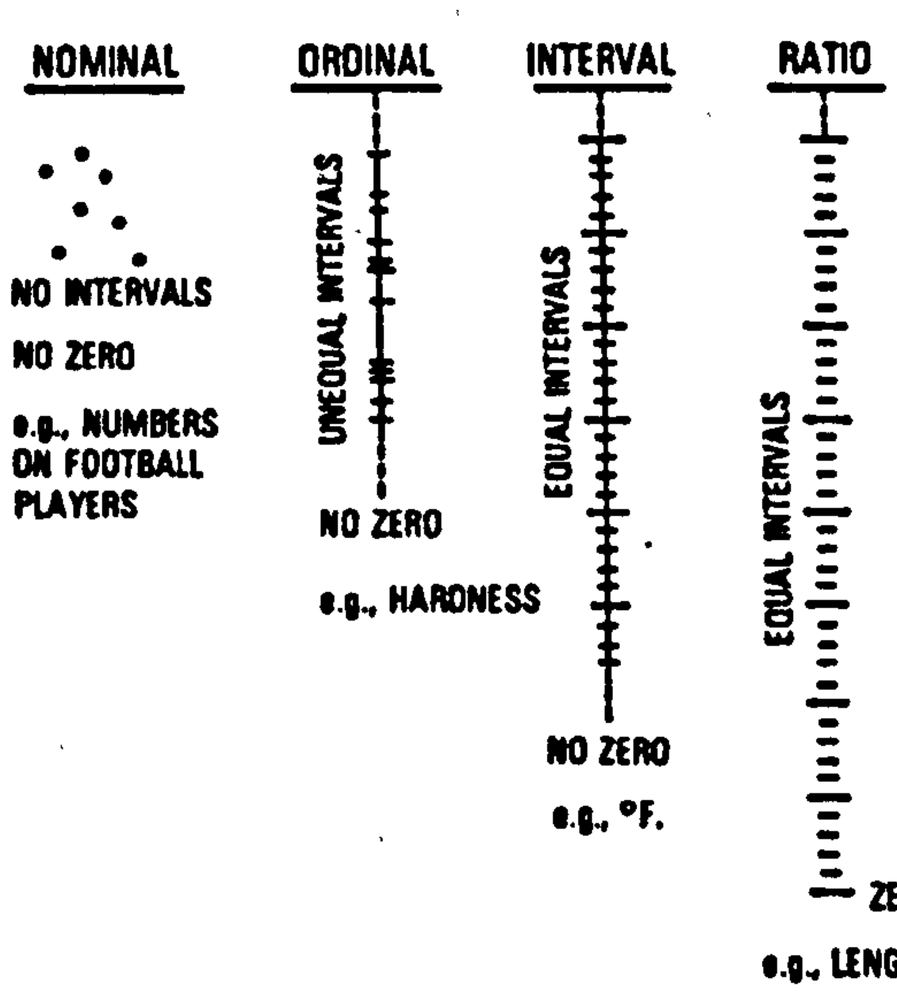

Figure 1-12. Various measurement scales [49].

A nominal scale is the least powerful scale, i.e., it merely uses numbers instead of names to distinguish among members of a group. Many people do not consider it to form a scale.

An ordinal scale consists of an ordered progression of integers but gives no information about the meaning of distances along it.

An interval scale determines order, but it also specifies ratios of differences, so equal distances anywhere along the scale have the same significance.

A ratio scale is an interval scale with a zero point, that is, it additionally defines ratios of magnitudes. Equal ratios as well as equal intervals have the same meaning everywhere along this scale.

1.4.1.2 Psychophysical methods

According to Boynton [49], visual psychophysics concerns the study of lawful stimulus-response relationship and theoretical concepts about explanatory mechanisms. The psychophysical methods are originally defined by Fechner and are divided into three major methods: the method of constant stimuli, the method of limit, and the method of adjustment.

The method of constant stimuli, also called the method of single stimulus, yields results as probability-of-seeing function that constitutes an indirect measure of response magnitude at the bottom end of the sensation scale.

The method of limit is used to get a rough estimate of threshold to determine the range within which to choose the stimuli to use with the constant-stimulus procedure. Here, the threshold is defined as the minimum stimulus or difference in stimuli that can be distinguished as different from standard.

The method of adjustment is similar to the method of limits except that it is the observer, rather than the experimenter, who controls the stimulus. An advantage of this method is that the observer has something more interesting to do than just to say yes or no. It has also been called the method of average error, the method of reproduction, or the method of equivalent stimuli.

1.4.1.3 Weber's law

After he studied the sensitivities of the different senses to stimulus differences, Weber, an anatomist and physiologist, formulated a simple stimulus relation (1834). This, Weber's law, stated that the difference between one stimulus and another that is just noticeably different is a constant fraction of the first. That is,

$$\frac{\Delta x}{x} = k \tag{1-33}$$

where Δx represents the stimulus increment, x is the original stimulus, and k is called the Weber fraction (constant).

Weber's law was adopted by Fechner and he derived another relation known as Fechner's law.

$$s(x) = a + b \log(x + x_0) \tag{1-34}$$

where s(x) is the sensation magnitude, a and b are constants, and x_0 is a threshold. It expresses that sensation increases linearly as a function of logarithm of stimulus intensity. [The Fong lightness scale (Eq.1-30) and the DCI-95 formula (Eq.1-32) follow this form.]

The Weber's law and the Fechner's law play key roles in the basic concepts of psychophysics. Another important concept in psychophysical methods is the Thurstone's law of comparative judgement. The paired-comparison method follows from it. (See Section 1.4.2.2)

1.4.1.4 Representation of data

It is generally assumed that the surface, which represents contours of equal perceived colour-difference from a standard in colour space, is an ellipsoid. In CIExyY space, it is given by Eq.(1-26). In CIELAB space,

$$\Delta E^2 = b_{11}(\Delta a^*)^2 + b_{22}(\Delta b^*)^2 + b_{33}(\Delta L^*)^2 + 2b_{12}\Delta a^*\Delta b^* + 2b_{13}\Delta a^*\Delta L^* + 2b_{23}\Delta b^*\Delta L^* \tag{1-35}$$

The assumption of this representation is justified for two reasons [50]. First, considering the inherent variability of the judgements, it is sufficiently accurate for small colour differences. Second, it is the only expression that can be handled easily by the standard statistical techniques.

The data analysis on colour difference evaluation thus follows as ellipsoid fitting, i.e., deriving g or b coefficients, to optimise the measures of fit between visual difference and calculated difference.

Unlike other data sets, RIT-Dupont data [47] was reported in the form of tolerance vectors in CIELAB space. As the tolerance vectors could not be represented as a single form like an ellipsoid equation, there is no way to compare their data with earlier ones without ellipsoid fitting.

1.4.2 Scaling methods [45,49]

1.4.2.1 Ranking method

The ranking method is easy to use when the number of stimuli is small, but with large number of stimuli it becomes cumbersome. Some [51,52] tried this method in their experiments but it has been rarely used in colour-difference assessments. The observation procedure is normally as follows [51].

> The observer was asked to compare each sample to the standard and sort them according to the magnitude of the perceived colour difference from the standard: Smallest difference first and largest difference last. The ranking was recorded on the sheet.

From the raw data, the following three ranks are calculated: simple ranks, comparative ranks, and normalised ranks. The simple ranks are the very ranks ordered by the observer and used to derive comparative ranks and normalised ranks. The comparative ranks determine the interval scale, i.e., visual scale, and the determination follows the law of comparative judgement. (See Section 1.4.2.2.) The normalised ranks also estimate an interval scale. The term 'normalised' means the normalised ranks are assumed to form a normal distribution with respect to the scaled attribute. (For a detailed procedure of deriving visual scale, see Bartleson [49]).

1.4.2.2 Paired-comparison method

The judgmental mode in a paired-comparison experiment [53] is usually as follows: "whether the colour difference is larger or smaller than a given standard difference". The perceptibility (or discrimination) and the acceptability (or pass/fail) judgements also require similar judgements. "Whether two colours are distinguishable or not" or "whether the difference is perceptible or not" is the judgement in a perceptibility experiment [54]. In an acceptability test [43], samples are judged to be acceptable or not acceptable as matches to a standard. All of these experimental methods can be regarded as the binary judgement method.

The law of comparative judgements plays a key role in the paired-comparison method. It was set down by Thurstone [49] (1927) as an equation relating the difference

between the two stimuli to the probability of one stimulus **i** being judged greater than the other stimulus **j**. For instance, if we do the scaling experiment by the paired-comparison method and postulate this process follows a normal distribution, then the equation for the law of comparative judgements is

$$\Delta E_i - \Delta E_{std} = \left[N^{-1}(P_i)\right]\left[\sigma_i^{\,2} + \sigma_{std}^{\,2} - r_i \sigma_i \sigma_{std}\right]^{1/2} \qquad (1\text{-}36)$$

where ΔE_i and ΔE_{std} represent the colour-difference stimulus of the ith pair and the standard pair, respectively. N^{-1} denotes the inverse of cumulative normal distribution, P_i is the probability that the pair **i** is judged greater than the standard pair, σ_i and σ_{std} represent the standard deviations of ΔE_i and ΔE_{std}, and r_i is their correlation coefficient.

Eq.(1-36) represents the complete law of comparative judgement, but in practice it is assumed that $\sigma_i = \sigma_{std} = \sigma/\sqrt{2}$ = constant and $r = 0$. Thus

$$\Delta E_i - \Delta E_{std} = \sigma\, N^{-1}(P_i) \qquad (1\text{-}37)$$

Above case is stated as Thurstone's Case V.

The transform process of visual data to an interval scale is illustrated in Fig.1-13.

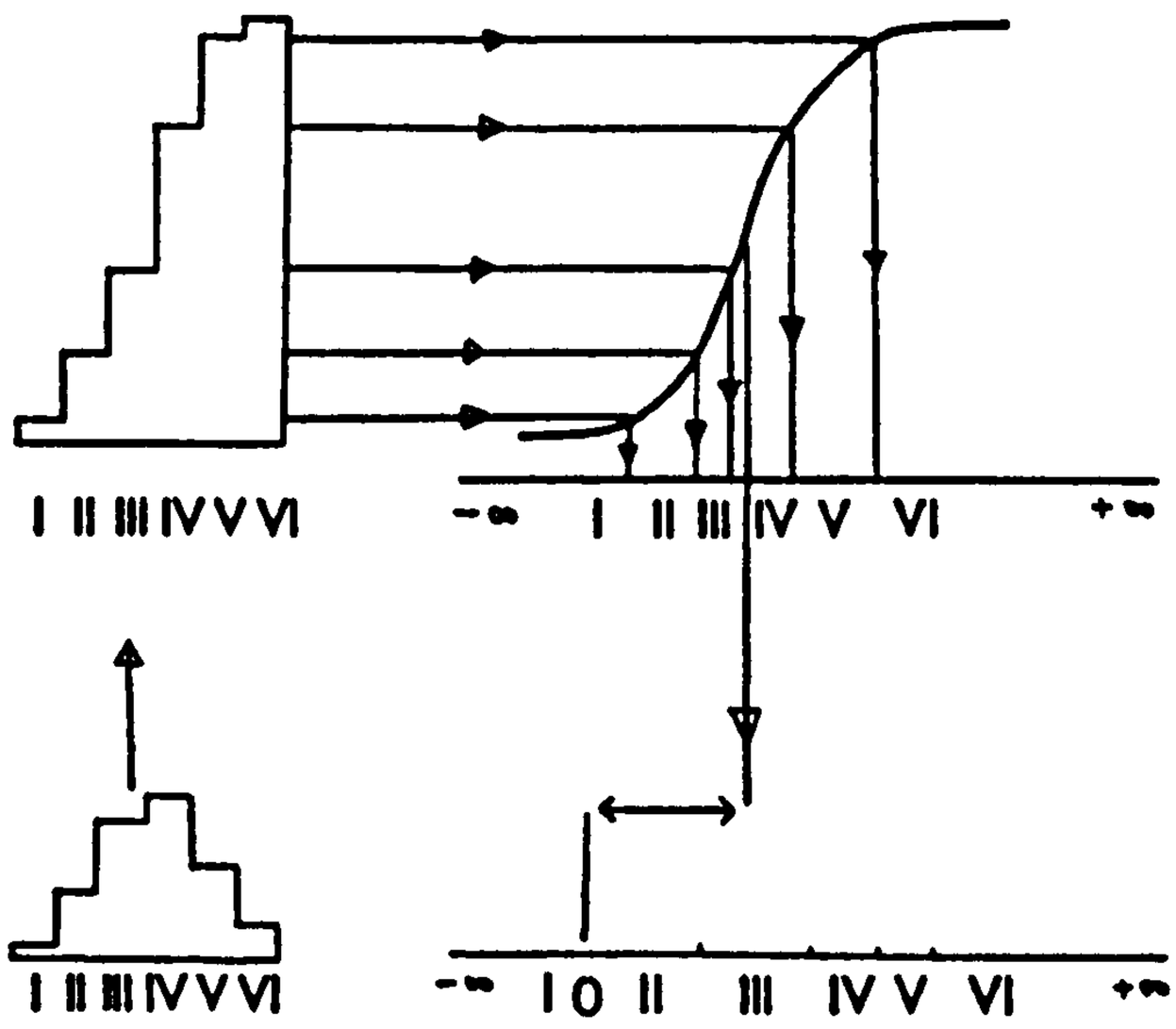

Figure 1-13. Transformation of visual data to an interval scale [55]: (lower left) frequency matrix, (upper left) proportion matrix, (upper right) z matrix, and (lower right) scale value.

First, the raw data is converted into a frequency matrix. Next, it is converted to a proportion matrix (The proportion P is determined as $P = f/N$, where N is the number of observations). Then the values of the proportion matrix are converted to cumulative normal distribution. It is called the z matrix . The scale values can be obtained by taking the sum of each of the columns in the z matrix.

However, in general practice, the scale conversion process is omitted. Instead, the coefficients of Eqs.(1-26) or (1-35) are directly derived by ellipsoid optimisation.

1.4.2.3 Category method

The law of categorical judgements [49] (Torgerson, 1954) is an extension of Thurstone's law of comparative judgements. It is expressed as:

$$\Delta E_j - \Delta E_k = \left[N^{-1}(P_{jk})\right]\left[\sigma_j{}^2 + \sigma_k{}^2 - 2r_{jk}\sigma_j\sigma_k\right]^{1/2} \qquad (1\text{-}38)$$

where ΔE_j = the colour-difference stimulus of the jth pair

ΔE_k = the mean colour-difference stimulus of the kth category

N^{-1} = the inverse of cumulative normal distribution function

P_{jk} = the probability that the pair **j** is placed below category boundary **k**

σ_j and σ_k = the standard deviation of ΔE_j and ΔE_k

r_{jk} = the coefficient of correlation between momentary positions of **j**th pair and boundary **k**.

As can be seen from the expression, it is the same form of Eq.(1-36) and has the same assumption of normal distribution. But the law of categorical judgement relates to the relative positions of a particular colour-difference pair with respect to category boundaries rather than with respect to another pair.

Morley [55] and Robinson [56] have undertaken category scaling experiments. Both studies rated their samples to a six-point category, however Robinson analysed the data by dividing the first three categories as acceptable and the last three as unacceptable. Thus, Robinson's study is, in effect, an acceptability experiment. Morley asked the observer to assess the colour differences in terms of the following categories:

I. No difference

II. Just noticeable difference

III. Noticeable difference

IV. Fairly large difference

V. Large difference

VI. Very large difference

However, they did not attempt to fit an ellipsoid as well.

There are two methods that determine scale values from the raw data: (a) mean-category value method, and (b) categorical-judgement method. In the mean-category value method, the category mean is simply obtained by taking the arithmetic means of each column in the raw data sheet. The categorical judgement method is to derive an interval scale by invoking the law of categorical judgements. The mathematical technique is nearly the same as the paired comparison method.

1.4.2.4 Ratio method

The magnitude estimation is the most frequently used ratio method. In magnitude estimation method, the observer is asked to match a number to the magnitude of the perceptual attribute. In colour difference evaluation, visual assessments are carried out as following [57]:

> The observer was presented with two pairs of samples, one pair always being the standard pair and asked to express the colour difference for the sample pair as a ratio of the difference for the standard pair. Any multiple or fraction was allowed.

After the experimental data were recorded for a sample pair, they were averaged by taking their geometric means.

$$\overline{\Delta V_i^*} = \left(\Pi \Delta V_i^*\right)^{1/n} \tag{1-39}$$

where $\overline{\Delta V^*}$ is the mean of observed ratios (ΔV^*), n represents the number of observation, **i** stands for a particular stimulus, and Π designates cumulative products.

Then, the true visual difference (ΔV) can be related to ΔV^* by

$$\Delta V = \left(\overline{\Delta V^*}\right)^{\alpha} \tag{1-40}$$

where α varies with the particular group of observers. The value of α in Eq.(1-40) can be estimated during the ellipsoid fitting.

1.4.2.5 Grey-scale method

The grey scale method was proposed by Luo [45]. Direct visual scaling is possible for both grey-scale and ratio methods. But the grey scale method is preferred because it enables results obtained at different times to be compared directly, i.e., all results are obtained on a common scale that could be reproduced.

In Luo's experiment, grey scale samples were prepared to have the same size and material as the samples being assessed. The colorimetric specification of grey scale samples followed British Standard BS1006: A02–Grey Scale for Assessing Change in Colour. In the test, these samples served as a kind of standard pair.

After the assessments, the arithmetic mean grey-scale rating (GS) for each pair is calculated. To convert GS into ΔV (visual difference), an equation which relates the grey scale grades and the ΔE^* values of those grades is required. For example,

$$\Delta E^* = C_0 + C_1 e^{-GS/C_2} \tag{1-41}$$

These ΔE^* values are proportional to the differences seen and can thus be taken as ΔV values. Luo used the following equation.

$$\Delta V = -1.078 + 23.56\, e^{-GS/1.709} \tag{1-42}$$

1.5 Thesis Aims

The present state of colour-difference evaluation can be summarised by the following:

(a) CIELAB has served as a base colour space since it was recommended by the CIE in 1976.

(b) CMC is now used extensively in textile coloration industries and to a lesser extent in other industries.

(c) CIE94 is the simplified version of CMC and so far as is known its performance is similar to CMC.

(d) There has been little research work reported on the experimental uncertainties arising from either human or from physical causes such as parametric effects.

The principal aim of this project is to investigate the influence of the parametric effects on the appearance of small colour differences. Sample panels were prepared using paints applied to paper and board, and observer tests were conducted under different parametric viewing conditions. From these, data analysis has been carried out to investigate the following points:

(a) Parametric effects of background and gap, and corresponding correction factors.

(b) Colour measurement error and observer variability.

(c) Comparison between data analysis methods.

(c) Performance testing of major colour-difference formulae.

(d) Modifications of existing formulae and/or development of the new formula.

1.6 References

1. CIE Proc. 8th Session, Cambridge, 1931.

2. R.W.G.Hunt, Measuring Colour, 2nd ed., Ellis Horwood, 1991.

3. F.W.Billmeyer and M.Saltzman, Principles of Color Technology, 2nd ed., Wiley, 1981.

4. A.H.Munsell, Atlas of the Munsell Color system, Wadsworth-Howland, Boston, 1915.

5. A.Hård and L.Sivik, NCS - Natural Color System: A Swedish Standard for Color Notation, Col. Res. Appl., **6**, 129-138 (1981).

6. Swendish National Standard SS 01 91 00, CIE co-ordinates is available as SS 01 91 01, and atlas as SS 01 91 02 (1982).

7. M.Richter and K.Witt, The Story of the DIN Color System, Col. Res. Appl., **11**, 138 (1986).

8. D.L.MacAdam, Uniform Color Scales, J. Opt. Soc. Am, **64**, 1691-1702 (1974).

9. D.B.Judd and G.Wyszecki, Color in Business, Science and Industry, Wiley, New York, 1975.

10. S.M.Newhall, D.Nickerson and D.B.Judd, Final Report of the O.S.A. Subcommittee on the Spacing of the Munsell Colors, J. Opt. Soc. Am., **33**, 385 (1943).

11. R.McDonald (Ed.), Colour Physics for Industry, SDC, Bradford, 1987.

12. F.Grum and C.J.Bartleson (Eds.), Optical Radiation Measurements, Vol.2: Color Measurement, Academic, London, 1980.

13. H.G.Grassman, Poggendorf's Ann., **89**, 69 (1853); Phil. Mag., **4**, 254 (1854).

14. D.L.MacAdam, Color measurement: Theme and Variations, Springer-Verlag, Berlin, 1981.

15. D.B.Judd, D.L.MacAdam and G.Wyszecki, Spectral Distribution of Typical Daylight as a Function of Correlated Color Temperature, J. Opt. Soc. Am., **54**, 1031-1040 (1964).

16. K.McLaren, The Colour Science of Dyes and Pigments, Adam Hilger, Bristol, 1983.

17. D.S.J.Atkin, E.Coates and B.Rigg, Effects of Gloss on Colour-Difference Measurements, JSDC, **97**, 333-334 (1981).

18. G. Wyszecki, Color Appearance, In Handbook of Perception and Human Performance, Vol.1: Sensory Processes and Perception, K.R.Boff, L.Kaufman and J.P.Thomas (Eds.), Wiley, New York, pp.9.1-9.57, 1986.

19. R.W.G.Hunt, An Improved Predictor of Colourfulness in a Model of Colour Vision, Col. Res. Appl., **19**, 23-26 (1994).

20. Y.Nayatani, Revision of Chroma and Hue Scales of a Nonlinear Colour-Appearance Model, Col. Res. Appl., **20**, 143-155 (1995).

21. M.D.Fairchild, Refinement of the RLAB Color Space, Col. Res. Appl., **21**, 338-346 (1996).

22. M.R.Luo, M.C.Lo and W.G.Kuo, The LLAB(ℓ:c) Color Model, Col. Res. Appl., **21**, 412-429 (1996).

23. C.J.Bartleson, Changes in Color Appearance with Variations in Chromatic Adaptation, Col. Res. Appl., **4**, 119-138 (1979).

24. R.McDonald, A Review of the Relationship between Visual and Instrumental Assessment of Colour Difference, J. Oil Col. Chem. Assoc., **65**, 43-53, 93-106 (1982).

25. R.S.Hunter and R.W.Harold, The Measurement of Appearance, 2nd ed., Wiley, 1987.

26. CIE Publ. No.116, Industrial Colour-Difference Evaluation, CIE Central Bureau, Vienna, 1995.

27. H.Pauli, Proposed Extension of the CIE Recommendation on "Uniform Color Spaces, Color Difference Equations, and Metric Color Terms", J. Opt. Soc. Am., **66**, 866-867 (1976).

28. R.Sève, New Cube-Root Equations for Lightness and $L^*a^*b^*$ Colour Space, Proc. 7th Cong. AIC Colour 93, Budapest, Vol. B, C195-C198, 1993.

29. R.Sève, New Formula for the Computation of CIE 1976 Hue Difference, Col. Res. Appl., **16**, 217-218 (1991).

30. M.Stokes and M.H.Brill, Efficient Computation of ΔH^*_{ab}, Col. Res. Appl., **17**, 410-411 (1992).

31. R.Sève, Practical Formula for the Computation of CIE 1976 Hue Difference, Col. Res. Appl., **21**, 314 (1996).

32. ASTM E308, Standard Practice for Computing the Colors of Objects by Using the CIE System, 1995 Annual Book of ASTM Standards, Vol.06.01.

33. G.Wyszecki and W.S.Stiles, Colour Science, 2nd ed., Wiley, New York, 1982.

34. D.L.MacAdam, Visual Sensitivities to Color Differences in Daylight, J. Opt. Soc. Am., **32**, 247-274 (1942).

35. F.T.Simon and W.J.Goodwin, Rapid Graphical Computation of Small Color Differences, Am. Dyest. Rep., **47**, 105-112 (1958).

36. K.D.Chickering, Optimization of the MacAdam-Modified 1965 Friele Color Difference Formula, J. Opt. Soc. Am., **57**, 537-561 (1967).

37. K.D.Chickering, FMC Color-Difference Formulas: Clarification Concerning Usage, J. Opt. Soc. Am., **61**, 118-122 (1971).

38. ASTM D2244, Standard Test Method for Calculation of Color Differences From Instrumentally Measured Color Differences, 1995 Annual Book of ASTM Standards, Vol.06.01.

39. L.F.C.Friele, Fine Color Metric (FCM), Col. Res. Appl., **3**, 53-64 (1978).

40. T.Seim and A.Valberg, Towards a Uniform Color Space: A Better Formula to Describe the Munsell and OSA Color scales, Col. Res. Appl., **11**, 11-24 (1986).

41. F.J.J.Clarke, R.McDonald and B.Rigg, Modification to the JPC79 Colour Difference Formula, JSDC, **103**, 128-132 (1984).

42. M.R.Luo and B.Rigg, BFD(ℓ:c) Colour-Difference Formula, JSDC, **103**, 86-94, 126-132 (1987).

43. R.McDonald, Industrial Pass/Fail Colour Matching, JSDC, **96**, 372-376, 418-433, 486-499 (1980).

44. BS6923: Calculation of Small Colour Differences, BSI, 1988.

45. M.R.Luo and B.Rigg, Chromaticity-Discrimination Ellipses for Surface Colours, Col. Res. Appl., **11**, 25-42 (1986).

46. E.Coates, K.Y.Fong and B.Rigg, Uniform Lightness Scales, JSDC, **97**, 179-183 (1981).

47. R.S.Berns, D.H.Alman, L.Reniff, G.D.Snyder and M.R.Balonon-Rosen, Visual Determination of Suprathreshold Color-Difference Tolerances Using Probit Analysis, Col. Res. Appl., **16**, 297-316 (1991).

48. P.J.Alessi, The 1995 AIC Interim Meeting on Colorimetry: A summary Report, Col. Res. Appl, **21**, 146-160 (1996).

49. C.J.Bartleson and F.Grum (Eds.), Optical Radiation Measurements, Vol.5: Visual Measurements, Academic, London, 1984.

50. A.R.Robertson, CIE Guidelines for Coordinated Research on Colour-Difference Evaluation, Col. Res. Appl., **3**, 149-151 (1978).

51. R.G.Kuehni and R.T.Marcus, An Experiment in Visual Scaling of Small Color Differences, Col. Res. Appl., **4**, 83-91 (1979).

52. E.Coates, S.Day, J.R.Provost and B.Rigg, Measurement and Assessment of Colour Differences for Industrial Use. III - Methods of Scaling Visual Assessments, JSDC, **88**, 186-190 (1972).

53. D.Strocka, A.Brockes and W.Paffhausen, Influence of Experimental Parameters on the Evaluation of Color-Difference Ellipsoids, Col. Res. Appl., **8**, 169-175 (1983).

54. K.Witt and G.Döring, Parametric Variations in a Threshold Color-Difference Ellipsoid for Green Painted Samples, Col. Res. Appl., **8**, 153-163 (1983).

55. D.I.Morley, R.Munn and F.W.Billmeyer, Small and Moderate Colour Differences: II - The Morley Data, JSDC, **91**, 229-242 (1975).

56. F.D.Robinson, Acceptability of Colour Matches, J. Oil Col. Chem. Assoc., **52**, 15-45 (1969).

57. M.Cheung and B.Rigg, Colour-Difference Ellipsoids for Five CIE Colour Centres, Col. Res. Appl., **11**, 185-195 (1986).

2. THEORY

Chapter 2 deals with the theoretical grounds of the research subject in detail. The order of description is as follows.

(a) Data analysis methods: Maximum-likelihood method and least-square method

(b) Ellipsoid visualisation: Principal axes, tilting and transform

(c) Measures of fit: Performance factor and tolerance standard deviation

(d) Colour measurement error: Precision and accuracy, ASTM and DIN methods

(e) Observer assessments: Colour discrimination tests and observer uncertainty

(f) Parametric effects: Physical parameters

2.1 Analysis of Visual Data

Several different data analysis methods have been suggested in the literature. They are generally dependent on the colour-difference scaling methods used, in which the most common types are that of paired-comparison and direct visual scaling. According to these two scaling methods, the data analysis schemes are mainly divided into two: the maximum-likelihood method and the least-square method.

2.1.1 Maximum-likelihood method

The maximum-likelihood method is a regression method that requires a probability distribution assumption, and it is mostly used for the binary judgement type (i.e., paired-comparison) experiments. Conventionally, this method means that the likelihood function, constructed from the binomial combination of the observer response function and the complementary function, is maximised in the calculation of the ellipsoid coefficients. The observer responses are described by the cumulative normal distribution function, Eqs.(1-36) and (1-37), or equivalently by the logistic function.

The probit analysis is another kind of maximum-likelihood method. The distribution of observer responses is also assumed to be a cumulative normal, and the coefficients of a linear regression equation that relates the transformed z-value of the observer response probability to the colour-difference value are estimated by a maximum-likelihood method.

2.1.1.1 Logistic function

The technique using the logistic function was set forth in the CIE guideline by Robertson[1], which is the extension of the Rich's method [2].

As reviewed in Chapter 1, the contours of equally perceived colour-differences from a colour centre are assumed to be ellipsoidal. In CIELAB space, it is given by Eq.(1-35). The task of an observer in the paired-comparison experiment is to judge whether the test colour-difference pair is smaller or larger than that of the standard. (The "smaller than" responses are usually assigned to 0 and the "larger than" responses to 1). The judgements are repeated sufficient times to provide reliable results for the subsequent analysis.

For each pair, the observer response probability P_i that the sample pair **i** is judged to have a difference greater than that of the standard pair is assigned. Then, the relation formed between P_i and ΔE_i is intuitively shown as a sigmoid curve (S-shaped). It can be described by the cumulative normal distribution (Gaussian function):

$$P_i = N(x_i) = \int_{-\infty}^{x_i} \frac{1}{\sigma\sqrt{2\pi}} e^{-\frac{(t-\mu)^2}{2\sigma^2}} dt \quad \text{or} \quad P_i = N(z_i) = \int_{-\infty}^{z_i} \frac{1}{\sqrt{2\pi}} e^{-\frac{w^2}{2}} dw \qquad (2\text{-}1)$$

where x_i is a colour-difference stimulus (i.e., ΔE_i), μ and σ are the mean and the standard deviation on a scale of colour-difference (T), and $z_i = (x_i - \mu)/\sigma$, $w = (t - \mu)/\sigma$, respectively. In practice, instead of using a Gaussian function, the logistic function that is a fairly good approximation to the cumulative normal can be used (Fig.2-1):

$$P_i = \frac{1}{1 + e^{\alpha - \beta \Delta E_i}} \qquad (2\text{-}2)$$

where α and β are parameters to be optimised and ΔE_i is taken from the ellipsoid eq.(1-35). (β could be eliminated by setting $\beta = \alpha/\Delta E_{std}$, where ΔE_{std} is a colour-difference of the standard pair.)

Next, by the binary nature of the paired-comparison method, the probabilities for two answers (larger and smaller) are binomially combined into a likelihood function (L). The logarithm of L (i.e., ln L) is given by

$$\ln L = \sum_{i=1}^{N} [r_i \ln P_i + (n - r_i) \ln(1 - P_i)] \qquad (2\text{-}3)$$

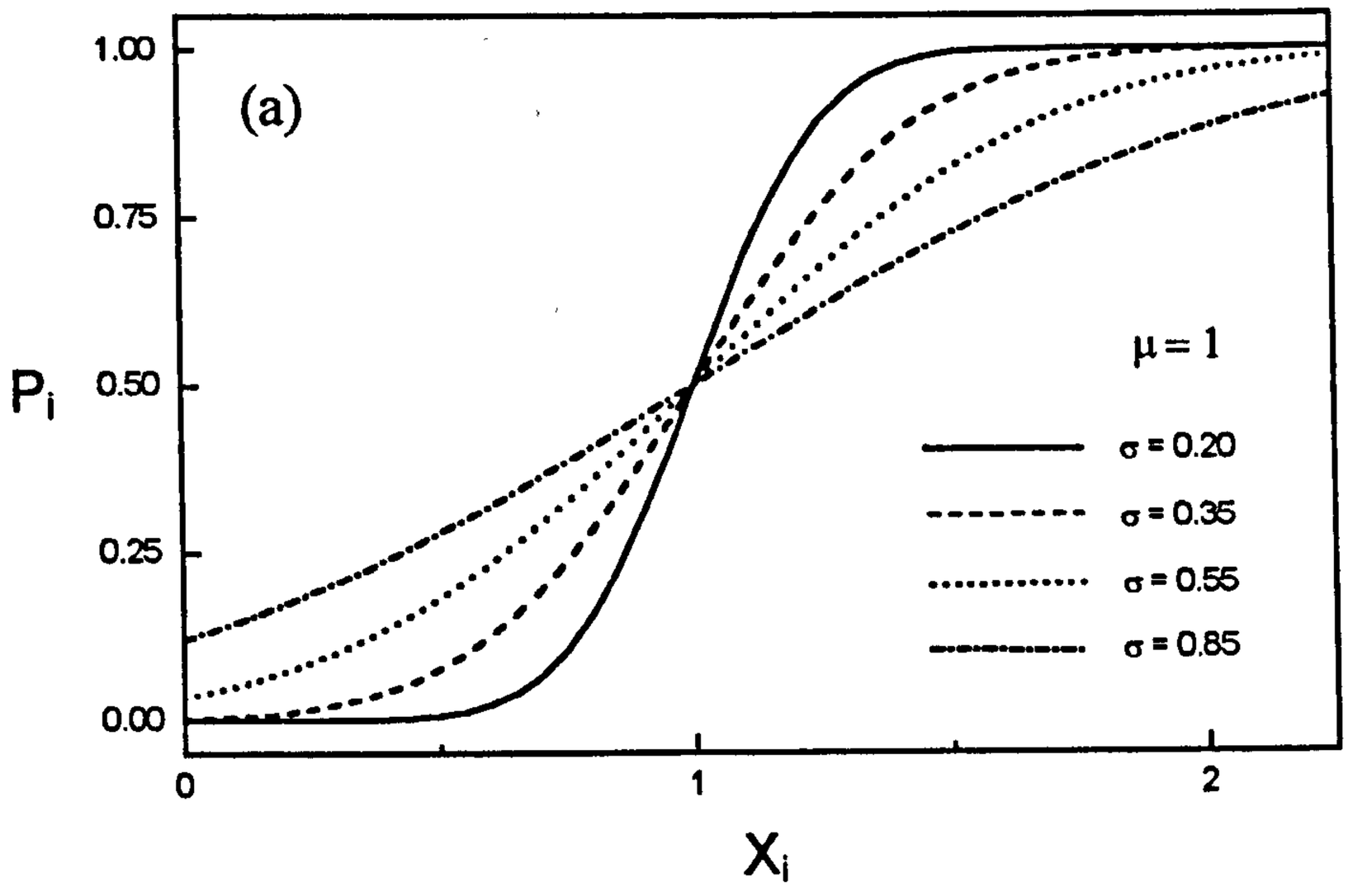

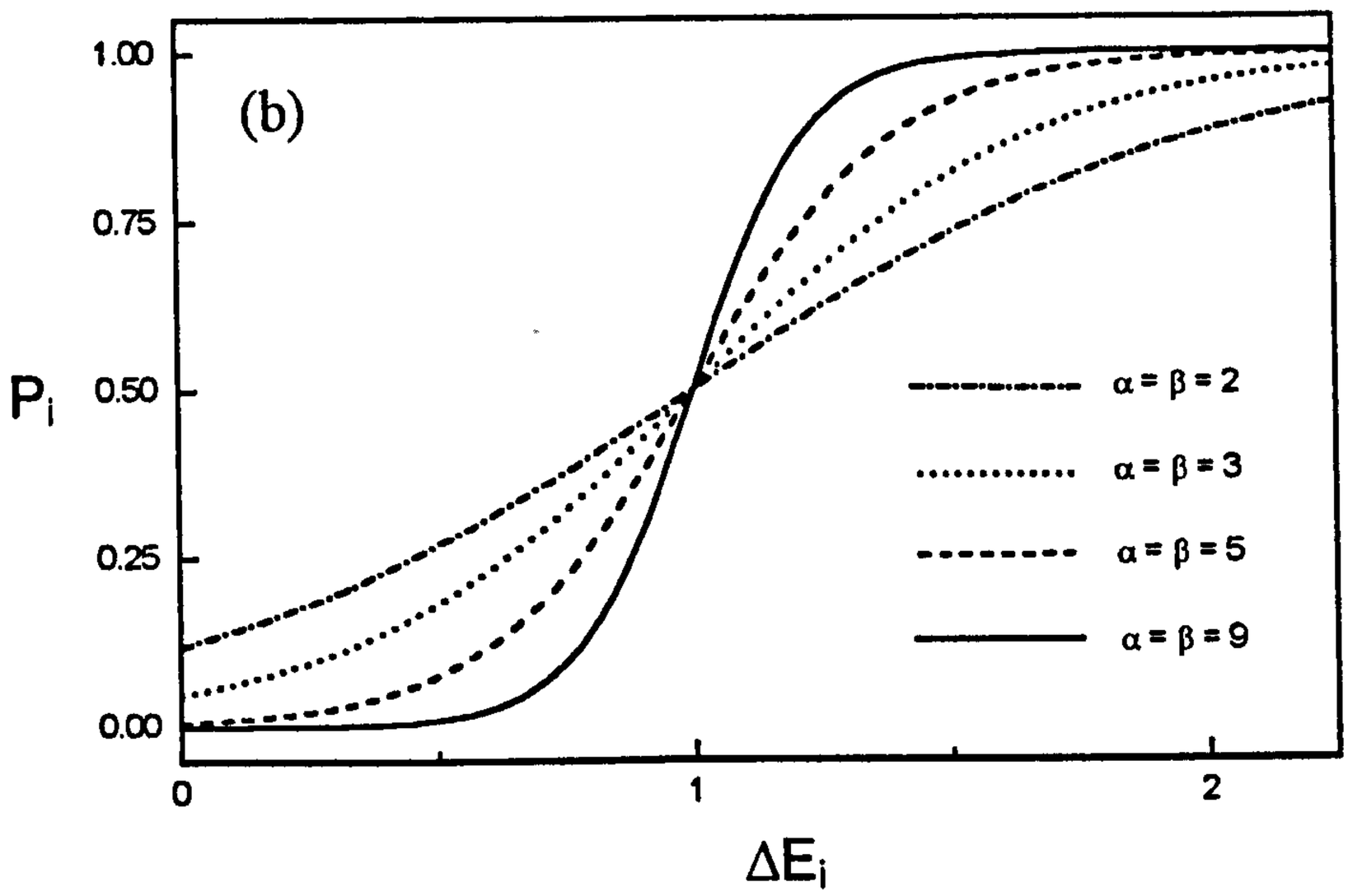

Figure 2-1. Distribution of observer responses: (a) Gaussian function (cumulative normal), and (b) logistic function (with $\beta = 1.7/\sigma$ and $\alpha = \beta\mu$, it shows a good approximation to the cummulative normal).

where N is the number of sample pairs, n is the total number of presentation of each pair, and r_i is the number of "larger than" responses. The ellipsoid coefficients and parameters α,β are estimated by minimising $-\ln L$ (equivalent to maximising L). Since this method is maximising the likelihood function, it is called the maximum-likelihood method. In other words, the coefficients that make observed results most "likely" are selected.

For the function minimisation, three methods were used by earlier workers: Powell's Direction-Set method[2], Downhill Simplex method[3], and Quasi-Newton algorithm[4]. Each method uses quite a different algorithm, but it has been found that all these methods produce virtually identical results. Thus, any function minimisation method can be used as the optimised ellipsoid is insensitive to the method of fitting.

2.1.1.2 Probit analysis

As mentioned above, the basic assumptions of the probit model are identical to the logistic model, namely a normal distribution and maximum-likelihood estimation. However, the probit analysis has limitations. The colour-difference stimuli must vary along only one dimension and the analysis should be performed in each direction individually. (The sampling design and its verification method are reviewed in the next section.)

The processes in the probit analysis are composed of two steps: transform and regression. First, the observer response probability (P_i) is transformed into z-values by the inverse cumulative normal distribution, i.e., from Eq.(2-1)

$$P_i = N(z_i)$$

Thus

$$z(P_i) = N^{-1}(P_i) \tag{2-4}$$

With the transformed z-values at different colour-difference magnitude ΔE_i, the regression coefficients are obtained by a linear maximum-likelihood model [5]:

$$z(\Delta E_i) = c_0 + c_1 \cdot \Delta E_i \tag{2-5}$$

And because

$$z(\Delta E_i) = (\Delta E_i - \mu) / \sigma \tag{2-6}$$

we obtain

$$\mu = -c_0/c_1 \quad \text{and} \quad \sigma = 1/c_1 \tag{2-7}$$

Here μ is the colour-difference visually equivalent to that of the standard pair (denoted as T50, median tolerance) and σ is the population standard deviation. In addition to μ and σ, more statistical parameters are readily available to estimate experimental uncertainties. Along with the T50, asymmetric 95% confidence interval (denoted as UFL and LFL, upper and lower fiducial limits) is also calculated. The size of the confidence interval is known to depend on fit to a cumulative normal distribution (χ^2 test), standard deviation (σ), degrees of freedom (= no. of colour-difference pairs – 2), and number of observers.

2.1.1.3 Sampling

Colour-difference pairs for probit analysis are prepared along regular directions in colour space. Producing these pairs by random sample-pair combination is restricted and consequently many samples are needed. However, it is in addition very difficult to get an even spatial distribution by random sampling. Thus, as far as regular directions in colour space is concerned, the direction sampling method seems to be a good alternative approach. For example, in the CIELAB space, all possible sign combinations of L^*, a^*, and b^* co-ordinates could yield uniformly distributed vector directions.

Table 2-1. Vector directions in CIELAB space. (Assuming symmetry to the origin, two opposite directions are regarded as the same.)

L^*	a^*	b^*	Vector direction	Description
+	0	0	(A)	$-L^*$ ↔ $+L^*$
0	+	0	(B)	$-a^*$ ↔ $+a^*$
0	0	+	(C)	$-b^*$ ↔ $+b^*$
0	+	+	(D)	$-a^*$ $-b^*$ ↔ $+a^*$ $+b^*$
0	+	–	(E)	$-a^*$ $+b^*$ ↔ $+a^*$ $-b^*$
+	+	+	(F)	$-L^*$ $-a^*$ $-b^*$ ↔ $+L^*$ $+a^*$ $+b^*$
+	–	+	(G)	$-L^*$ $+a^*$ $-b^*$ ↔ $+L^*$ $-a^*$ $+b^*$
+	–	–	(H)	$-L^*$ $+a^*$ $+b^*$ ↔ $+L^*$ $-a^*$ $-b^*$
+	+	–	(I)	$-L^*$ $-a^*$ $+b^*$ ↔ $+L^*$ $+a^*$ $-b^*$
+	+	0	(J)	$-L^*$ $-a^*$ ↔ $+L^*$ $+a^*$
+	–	0	(K)	$-L^*$ $+a^*$ ↔ $+L^*$ $-a^*$
+	0	+	(L)	$-L^*$ $-b^*$ ↔ $+L^*$ $+b^*$
+	0	–	(M)	$-L^*$ $+b^*$ ↔ $+L^*$ $-b^*$

For the verification of the sampling scheme in which colour differences are required to vary in single directions in colour space, PCA (principal component analysis) [6] is used. PCA is a statistical technique used for analysing multivariate data, i.e., not to determine the relation between independent and dependent variables but to decide on the inter-relationship between variables. The basic idea of PCA is to describe a new set of orthogonal co-ordinates that order the sample variances. The actual PCA procedures in this case are:

First, the covariance matrix is calculated for the L^*, a^*, b^* co-ordinates of all samples that form the colour-difference pairs in each direction. Then the eigenvectors and eigenvalues of the covariance matrix are calculated. The largest eigenvalue indicates the percent sample position variance, and its associated eigenvector identifies the principal vector direction of colour-difference pairs in CIELAB space.

One advantage of the direction sampling is that the experimenter could correct for uncertain observer judgements. For each vector direction, the graph of each observer's responses vs. metric colour-difference is generally expected to show a step (monotonic) function. However, this is not the case in the real experiments. The filtering algorithm devised by Berns [7] can be applied to the visual results to alleviate this problem. (It is, of course, applied on a vector by vector basis for each observer.)

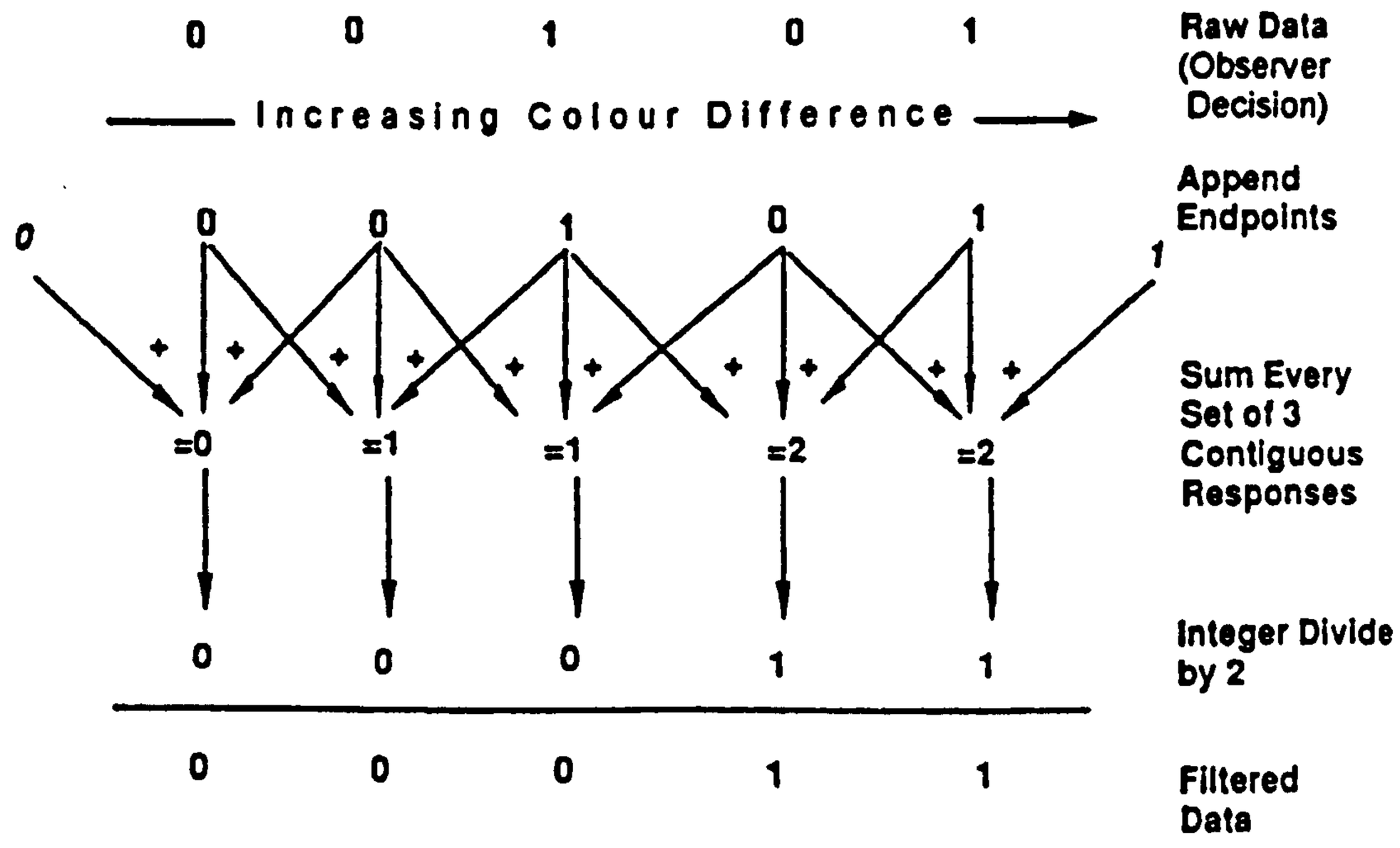

Figure 2-2. Depiction of filtering algorithm applied to nonmonotonic observer responses [7].

2.1.2 Least-square method

Another principal method used in obtaining the tolerance boundary (ellipsoid) is the least-square method. It is also a regression (curve-fitting) method that requires no distribution assumption. When the data are normally distributed, both the maximum-likelihood method and the least-square method yield essentially the same results.

The true visual difference (ΔV) can be obtained directly by the scaling methods such as the grey-scale and the ratio methods. To calculate the b_{ik} values in Eq.(1-35), the sum square difference between the ΔV values and the ΔE values (calculated differences, given by Eq.1-35) are minimised. That is,

$$S^2 = \sum_{i=1}^{N} (\Delta V_i - \Delta E_i)^2 \qquad (2\text{-}8)$$

where S^2 is the sum of squares to be minimised. It was used by Alder [8].

The values of S^2 depend on the number of sample pairs (N), and a more meaningful quantity is the coefficient (**e**) defined as:

$$\mathbf{e} = \sqrt{\frac{S^2}{N}} \qquad (2\text{-}9)$$

That is, **e** expresses the goodness of a fitted ellipsoid.

Other values of S^2 could be considered. For example, Robertson [1]:

$$S_1^2 = \sum_{i=1}^{N} \left(1 - \frac{\Delta V_i}{\Delta E_i}\right)^2 \qquad (2\text{-}10)$$

or Friele [9] used,

$$S_2^2 = \sum_{i=1}^{N} \left(\Delta V_i^2 - \Delta E_i^2\right)^2 / \Delta V_i^2 \qquad (2\text{-}11)$$

This method can be applied to the paired-comparison method as well (i.e., χ^2 minimum). Strocka [10] used the following:

$$S^2 = \sum_{i=1}^{N} \left(P_i - \overline{P_i}\right)^2 \qquad (2\text{-}12)$$

where P_i is the observed probability of positive answers (i.e., "larger than" responses) and $\overline{P_i}$ is the expected probability of positive answers.

2.2 Visualisation of the Ellipsoid

Given the coefficients of the colour-discrimination ellipsoid, it is difficult to know its spatial orientation in colour space. When comparing two ellipsoids, detailed conclusions are arrived at only when the location and the orientation of each ellipsoid are accessible. The positions of its principal axes generally determine the spatial orientation of an ellipsoid. Thus, for the visualisation of an ellipsoid we need to calculate its principal axes.

2.2.1 Calculation of principal axes [11]

The ellipsoid equation (1-35) is conveniently represented by a matrix form. Let us define a symmetric matrix **B** and a column vector **D** as follows:

$$\mathbf{B} = \begin{pmatrix} b_{11} & b_{12} & b_{13} \\ b_{12} & b_{22} & b_{23} \\ b_{13} & b_{23} & b_{33} \end{pmatrix}, \quad \text{and} \quad \mathbf{D} = \begin{pmatrix} \Delta a^* \\ \Delta b^* \\ \Delta L^* \end{pmatrix} \tag{2-13}$$

Then Eq.(1-35) becomes

$$\Delta E^2 = \mathbf{D}^T\mathbf{B}\mathbf{D} = b_{11}(\Delta a^*)^2 + b_{22}(\Delta b^*)^2 + b_{33}(\Delta L^*)^2 + 2b_{12}\Delta a^*\Delta b^* + 2b_{23}\Delta b^*\Delta L^* + 2b_{13}\Delta a^*\Delta L^* \tag{2-14}$$

The following 3 conditions are necessary and sufficient that the coefficients b_{ik} describe an ellipsoid:

(a) b_{11}, b_{22} and $b_{33} > 0$, i.e., $\mathrm{tr}(\mathbf{B}) > 0$

(b) $b_{11}b_{22} - b_{12}^2 > 0$, $b_{22}b_{33} - b_{23}^2 > 0$ and $b_{11}b_{33} - b_{13}^2 > 0$, i.e., $\Sigma B_{ii} > 0$

(c) $|\mathbf{B}| > 0$ (2-15)

where $\mathrm{tr}(\mathbf{B}) = b_{11} + b_{22} + b_{33}$, the trace of matrix **B**

$$|\mathbf{B}| = b_{11}b_{22}b_{33} + 2b_{12}b_{23}b_{13} - b_{11}b_{23}^2 - b_{22}b_{13}^2 - b_{33}b_{12}^2, \text{ the determinant of } \mathbf{B}$$

$$\Sigma B_{ii} = B_{33} + B_{11} + B_{22} = (b_{11}b_{22} - b_{12}^2) + (b_{22}b_{33} - b_{23}^2) + (b_{11}b_{33} - b_{13}^2) \tag{2-16}$$

(B_{ii} is the cofactor of **B**, i.e., a product of $(-1)^{i+i}$ and determinant of 2 × 2 matrix obtained from **B** after deleting i-th row and i-th column.)

To calculate the principal axes of an ellipsoid, we need to first compute the gradient

on the ellipsoid surface $S = \Delta E^2$, i.e., Eq.(2-14); as the gradient has the property that it is parallel to each of the ellipsoid axes and is normal to the ellipsoid surface.

$$\text{grad } S = \left(\frac{\partial S}{\partial(\Delta a^*)}, \frac{\partial S}{\partial(\Delta b^*)}, \frac{\partial S}{\partial(\Delta L^*)} \right) = 2 \begin{pmatrix} b_{11}\Delta a^* + b_{12}\Delta b^* + b_{13}\Delta L^*, \\ b_{12}\Delta a^* + b_{22}\Delta b^* + b_{23}\Delta L^*, \\ b_{13}\Delta a^* + b_{23}\Delta b^* + b_{33}\Delta L^* \end{pmatrix} = 2\,\mathbf{BD} \tag{2-17}$$

And also,

$$\frac{1}{2}\text{grad } S = \mathbf{BD} = \lambda \mathbf{D} = (\lambda \Delta a^*, \lambda \Delta b^*, \lambda \Delta L^*) \tag{2-18}$$

This relation leads to 3 equations for the three unknown co-ordinates, each for one principal axis of the ellipsoid.

For Eq.(2-18) to have the solutions for Δa^*, Δb^* and ΔL^*, the characteristic polynomial of $\mathbf{B}$ (i.e., $|\mathbf{B} - \lambda \mathbf{I}|$) must vanish. It gives the following secular equation of $\mathbf{B}$:

$$|\mathbf{B} - \lambda \mathbf{I}| = \begin{vmatrix} b_{11} - \lambda & b_{12} & b_{13} \\ b_{12} & b_{22} - \lambda & b_{23} \\ b_{13} & b_{23} & b_{33} - \lambda \end{vmatrix} = \lambda^3 - a_2\lambda^2 + a_1\lambda - a_0 = 0 \tag{2-19}$$

where $\mathbf{I}$ = identity matrix, and $a_0 = |\mathbf{B}|$, $a_1 = \Sigma B_{ii}$, $a_2 = \text{tr}(\mathbf{B})$.

In this way, $\mathbf{B}$ becomes a diagonal matrix in which three diagonal elements (nonzero, and all real) are occupied by the roots (eigenvalues) of Eq.(2-19): λ_A, λ_B, and λ_C. Each eigenvalue is associated with each of the ellipsoid axes (eigenvectors) A, B, and C, respectively. That is, Eq.(2-14) is simplified by use of the ellipsoid principal axes A, B, C instead of the original axes Δa^*, Δb^*, ΔL^*:

$$\lambda_A(\Delta a^*)^2 + \lambda_B(\Delta b^*)^2 + \lambda_C(\Delta L^*)^2 = 1 \tag{2-20}$$

and

$$\frac{(\Delta a^*)^2}{A^2} + \frac{(\Delta b^*)^2}{B^2} + \frac{(\Delta L^*)^2}{C^2} = 1 \tag{2-21}$$

Thus, the lengths of the principal axes are

$$A = \frac{1}{\sqrt{\lambda_A}}, \qquad B = \frac{1}{\sqrt{\lambda_B}}, \qquad C = \frac{1}{\sqrt{\lambda_C}} \tag{2-22}$$

The ratios of the direction cosines of the axis $A = (A_{a^*}, A_{b^*}, A_{L^*})$ are given by

$$A_{a^*} : A_{b^*} : A_{L^*} = [b_{23}{}^2 - (b_{22} - \lambda_A)(b_{33} - \lambda_A)] : [b_{12}(b_{33} - \lambda_A) - b_{13}b_{23}] : [b_{13}(b_{22} - \lambda_A) - b_{12}b_{23}]$$

$$= u_A : v_A : 1 \tag{2-23}$$

With the principal axis A and from Eqs.(2-22) and (2-23):

$$A^2 = \frac{1}{\lambda_A} = A_{a^*}^2 + A_{b^*}^2 + A_{L^*}^2 \tag{2-24}$$

And,

$$A_{L^*} = \left[\lambda_A (u_A^2 + v_A^2 + 1)\right]^{-1/2}$$

$$A_{a^*} = u_A A_{L^*}$$

$$A_{b^*} = v_A A_{L^*} \tag{2-25}$$

and similar solutions for B and C.

The axis directions can also be characterised in terms of the polar co-ordinate angles ϕ (longitude) and θ (latitude).

$$\tan\phi_A = \frac{A_{b^*}}{A_{a^*}} = \frac{v_A}{u_A}$$

$$\tan\theta_A = \frac{\sqrt{A_{a^*}^2 + A_{b^*}^2}}{A_{L^*}} = \sqrt{u_A^2 + v_A^2} \tag{2-26}$$

and similarly for ϕ_B, θ_B and ϕ_C, θ_C.

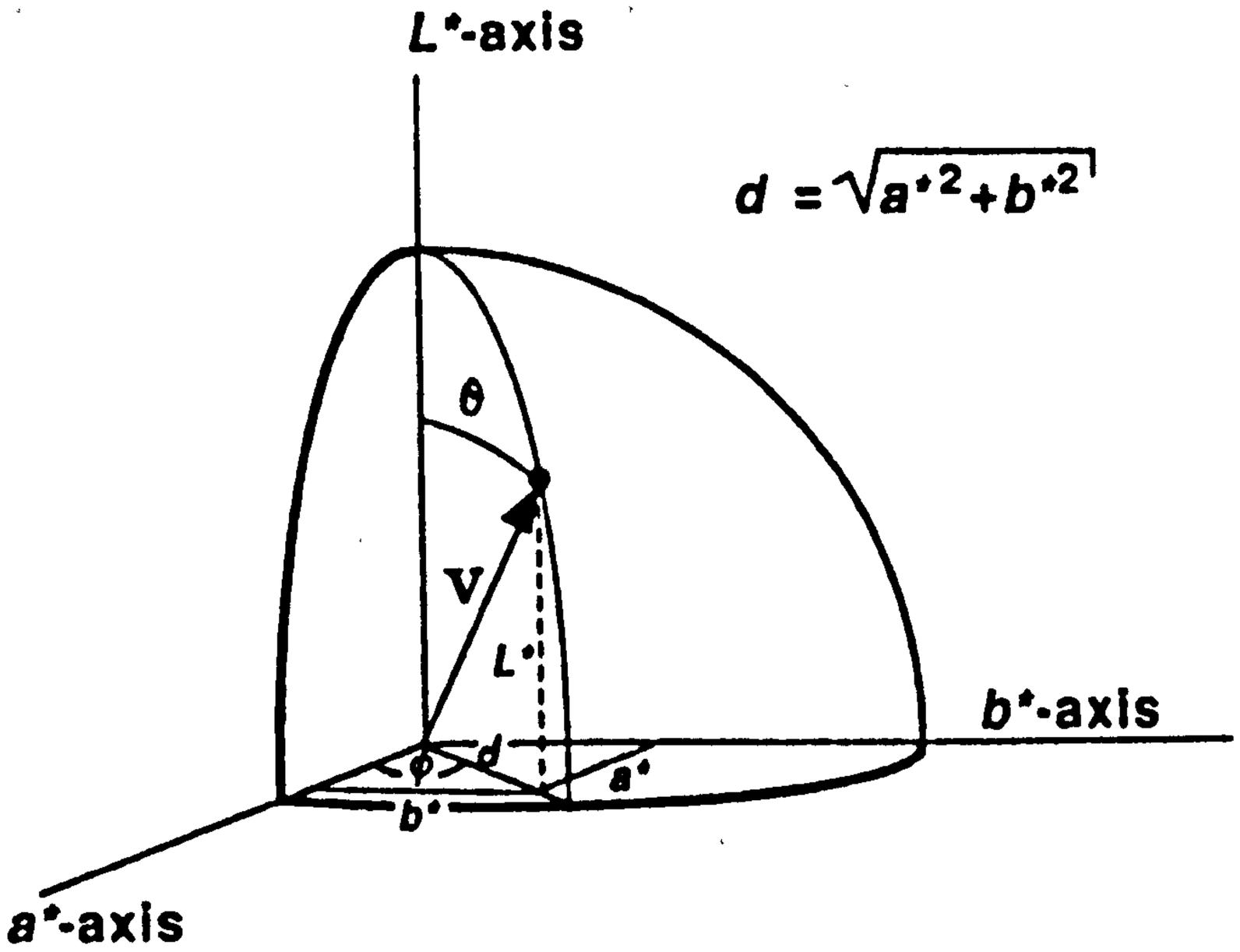

Figure 2-3. Three dimensional polar co-ordinates [11].

2.2.2 Ellipsoid tilting [12]

Though the degree of the ellipsoid tilting could be judged by the angle θ, a more comprehensive information is given by the displacement of the highest point of the ellipsoid projected onto the chromaticity plane. The highest point of ΔL^* for an ellipsoid is (i.e., where grad S has no Δa^* and Δb^* components):

$$\Delta L^*_m = \left[\frac{B_{33}}{|\mathbf{B}|}\right]^{1/2} \tag{2-27}$$

The chromaticity displacements of this points in $\Delta a^* \Delta b^*$ plane are proportional to ΔL^*_m and given by:

$$\Delta a^*_m = \left(\frac{B_{13}}{B_{33}}\right)\Delta L^*_m = \left(\frac{b_{12}b_{23} - b_{22}b_{13}}{b_{11}b_{22} - b_{12}^2}\right)\Delta L^*_m$$

$$\Delta b^*_m = \left(\frac{B_{23}}{B_{33}}\right)\Delta L^*_m = \left(\frac{b_{12}b_{13} - b_{11}b_{23}}{b_{11}b_{22} - b_{12}^2}\right)\Delta L^*_m \tag{2-28}$$

2.2.3 Ellipse parameters

As an ellipse is the simplified case of an ellipsoid involving only 2 dimensions, it is much easier to visualise. It is not difficult to calculate the ellipse parameters (major and minor axes, and orientation angle) by use of the 2nd order secular equation analogous to Eq.(2-19). However, another approach could be considered. That is, the rotation of an ellipse from the original position. (In the following, some notations are the same as those for an ellipsoid, but this does not cause confusion. Also, for brevity, Δa^* and Δb^* are denoted as Δa and Δb, respectively.)

A chromaticity discrimination ellipse is the cross section through the centre of an colour discrimination ellipsoid, i.e., $\Delta L^* = 0$ and

$$(\Delta E)^2 = b_{11}(\Delta a)^2 + 2\,b_{12}(\Delta a)(\Delta b) + b_{22}(\Delta b)^2 = 1 \tag{2-29}$$

Identically,

$$\mathbf{D}^T\mathbf{B}\,\mathbf{D} = \begin{pmatrix}\Delta a & \Delta b\end{pmatrix}\begin{pmatrix}b_{11} & b_{12}\\ b_{12} & b_{22}\end{pmatrix}\begin{pmatrix}\Delta a\\ \Delta b\end{pmatrix} = 1 \tag{2-30}$$

Let the new co-ordinates $\Delta a'$, $\Delta b'$ (parallel to the ellipses axes) differ from the original co-ordinates (Δa, Δb) by a rotation angle θ. Then

$$\mathbf{D}' = \begin{pmatrix} \Delta a' \\ \Delta b' \end{pmatrix} = \begin{pmatrix} \cos\theta & \sin\theta \\ -\sin\theta & \cos\theta \end{pmatrix} \begin{pmatrix} \Delta a \\ \Delta b \end{pmatrix} = \mathbf{R}\,\mathbf{D} \tag{2-31}$$

Conversely,

$$\mathbf{D} = \mathbf{Q}\,\mathbf{D}' \tag{2-32}$$

where $\mathbf{Q} = \mathbf{R}^{-1} = \begin{pmatrix} \cos\theta & -\sin\theta \\ \sin\theta & \cos\theta \end{pmatrix}$, rotation (transform) matrix.

In the case of an ellipsoid, **Q** could be represented by the product of three orthogonal transform matrices having three angles of rotation [13]. That is,

$$\mathbf{Q} = \begin{pmatrix} \cos\theta & -\sin\theta & 0 \\ \sin\theta & \cos\theta & 0 \\ 0 & 0 & 1 \end{pmatrix} \begin{pmatrix} \cos\theta' & 0 & -\sin\theta' \\ 0 & 1 & 0 \\ \sin\theta' & 0 & \cos\theta' \end{pmatrix} \begin{pmatrix} 1 & 0 & 0 \\ 0 & \cos\theta'' & -\sin\theta'' \\ 0 & \sin\theta'' & \cos\theta'' \end{pmatrix} \tag{2-33}$$

Substituting **D** into Eq.(2-30) yields

$$(\mathbf{Q}\,\mathbf{D}')^{T}\,\mathbf{B}\,(\mathbf{Q}\,\mathbf{D}') = (\mathbf{D}')^{T}\,(\mathbf{Q}^{T}\,\mathbf{B}\,\mathbf{Q})\,\mathbf{D}' = 1 \tag{2-34}$$

Equivalently,

$$\begin{pmatrix} \Delta a' & \Delta b' \end{pmatrix} \begin{pmatrix} \lambda_A & 0 \\ 0 & \lambda_B \end{pmatrix} \begin{pmatrix} \Delta a' \\ \Delta b' \end{pmatrix} = 1 \tag{2-35}$$

where $\begin{pmatrix} \lambda_A & 0 \\ 0 & \lambda_B \end{pmatrix} = \mathbf{Q}^{T}\,\mathbf{B}\,\mathbf{Q}$

$$= \begin{pmatrix} b_{11}\cos^2\theta + 2b_{12}\sin\theta\cos\theta + b_{22}\sin^2\theta & b_{12}(\cos^2\theta - \sin^2\theta) - (b_{11} - b_{22})\cos\theta\sin\theta \\ b_{12}(\cos^2\theta - \sin^2\theta) - (b_{11} - b_{22})\cos\theta\sin\theta & b_{11}\sin^2\theta - 2b_{12}\sin\theta\cos\theta + b_{22}\cos^2\theta \end{pmatrix} \tag{2-36}$$

From Eq.(2-36), the angle (θ) of the major axis with the positive Δa axis, and the half lengths of major and minor axes (A and B) are given by:

$$\theta = 0.5\tan^{-1}\left(\frac{2b_{12}}{b_{11} - b_{22}}\right) \tag{2-37}$$

where $\theta < 90°$ when $b_{12} < 0$, and $\theta > 90°$ when $b_{12} > 0$.

$$A = \frac{1}{\sqrt{\lambda_A}} = \frac{1}{\sqrt{b_{22} + b_{12}\cot\theta}}$$
$$B = \frac{1}{\sqrt{\lambda_B}} = \frac{1}{\sqrt{b_{11} - b_{12}\cot\theta}} \tag{2-38}$$

Inversely, the b_{ik} values of an ellipse in terms of θ, A, and B are:

$$b_{11} = \frac{\cos^2\theta}{A^2} + \frac{\sin^2\theta}{B^2}$$

$$b_{12} = \left(\frac{1}{A^2} - \frac{1}{B^2}\right)\sin\theta\cos\theta$$
$$b_{22} = \frac{\sin^2\theta}{A^2} + \frac{\cos^2\theta}{B^2} \qquad (2\text{-}39)$$

2.2.4 Ellipsoid (ellipse) transform

The results of earlier colour-difference evaluation studies were generally given by CIExyY ellipsoids or ellipses. For comparison purposes, new experimental data need to be expressed in CIExyY space. As it is well known, however, the CIELAB system is currently most widely used, and most of the advanced colour-difference formulae such as CMC or CIE94 are all based on it. Thus, it is preferable that the comparison of experimental results is carried out in the CIELAB space.

Melgosa [14] already transformed Luo data [4] (132 x,y chromaticity ellipses) to the CIELAB space. So, as it is thought to be not necessary to give all the details of procedures (see Melgosa [15]), only the general steps are described here.

First, the xyY ellipsoid is cut into several equispaced ellipses along the Y axis. In each ellipse, regularly spaced points along the periphery are computed. All these points are assumed to have unit visual difference (i.e., $\Delta V = 1$) from the centre, and translated to the L^*, a^*, b^* co-ordinates. Then, the coefficients b_{ik} of Eq.(2-14) are estimated by use of the least-square method. (The transformed ellipsoid may have distortions but it is generally accepted that they are too small to merit any special analytical treatment.)

In the CIELAB space, it is often useful to convert the a^*b^* ellipse to that of the $\Delta C^*\Delta H^*$ microspace. In the $\Delta C^*\Delta H^*$ plane, A and B are retained but θ is replaced by $\Delta\theta$ - orientation from the hue angle h° (Fig.2-4). That is,

$$(\Delta E)^2 = s_{11}(\Delta C^*)^2 + 2s_{12}\Delta C^*\Delta H^* + s_{22}(\Delta H^*)^2 \qquad (2\text{-}40)$$

And,

$$\Delta\theta = 0.5\tan^{-1}\left(\frac{2s_{12}}{s_{11} - s_{22}}\right)$$
$$A = \frac{1}{\sqrt{s_{22} + s_{12}\cot\Delta\theta}}$$
$$B = \frac{1}{\sqrt{s_{11} - s_{12}\cot\Delta\theta}} \qquad (2\text{-}41)$$

Also,

$$s_{11} = \frac{\cos^2(\Delta\theta)}{A^2} + \frac{\sin^2(\Delta\theta)}{B^2}$$

$$s_{22} = \frac{\sin^2(\Delta\theta)}{A^2} + \frac{\cos^2(\Delta\theta)}{B^2}$$

$$2s_{12} = \left(\frac{1}{A^2} - \frac{1}{B^2}\right)\sin(2\Delta\theta) \qquad (2\text{-}42)$$

By analogy to Eq.(2-36), the conversion equations from b_{ik} to s_{ik} are given by:

$$s_{11} = b_{11}\cos^2 h^\circ + b_{12}\sin(2h^\circ) + b_{22}\sin^2 h^\circ$$

$$s_{12} = b_{12}\cos(2h^\circ) + 0.5(b_{22} - b_{11})\sin(2h^\circ)$$

$$s_{22} = b_{11}\sin^2 h^\circ - b_{12}\sin(2h^\circ) + b_{22}\cos^2 h^\circ \qquad (2\text{-}43)$$

Or, reversely

$$b_{11} = s_{11}\cos^2 h^\circ - s_{12}\sin(2h^\circ) + s_{22}\sin^2 h^\circ$$

$$b_{12} = s_{12}\cos(2h^\circ) + 0.5(s_{11} - s_{22})\sin(2h^\circ)$$

$$b_{22} = s_{11}\sin^2 h^\circ + s_{12}\sin(2h^\circ) + s_{22}\cos^2 h^\circ \qquad (2\text{-}44)$$

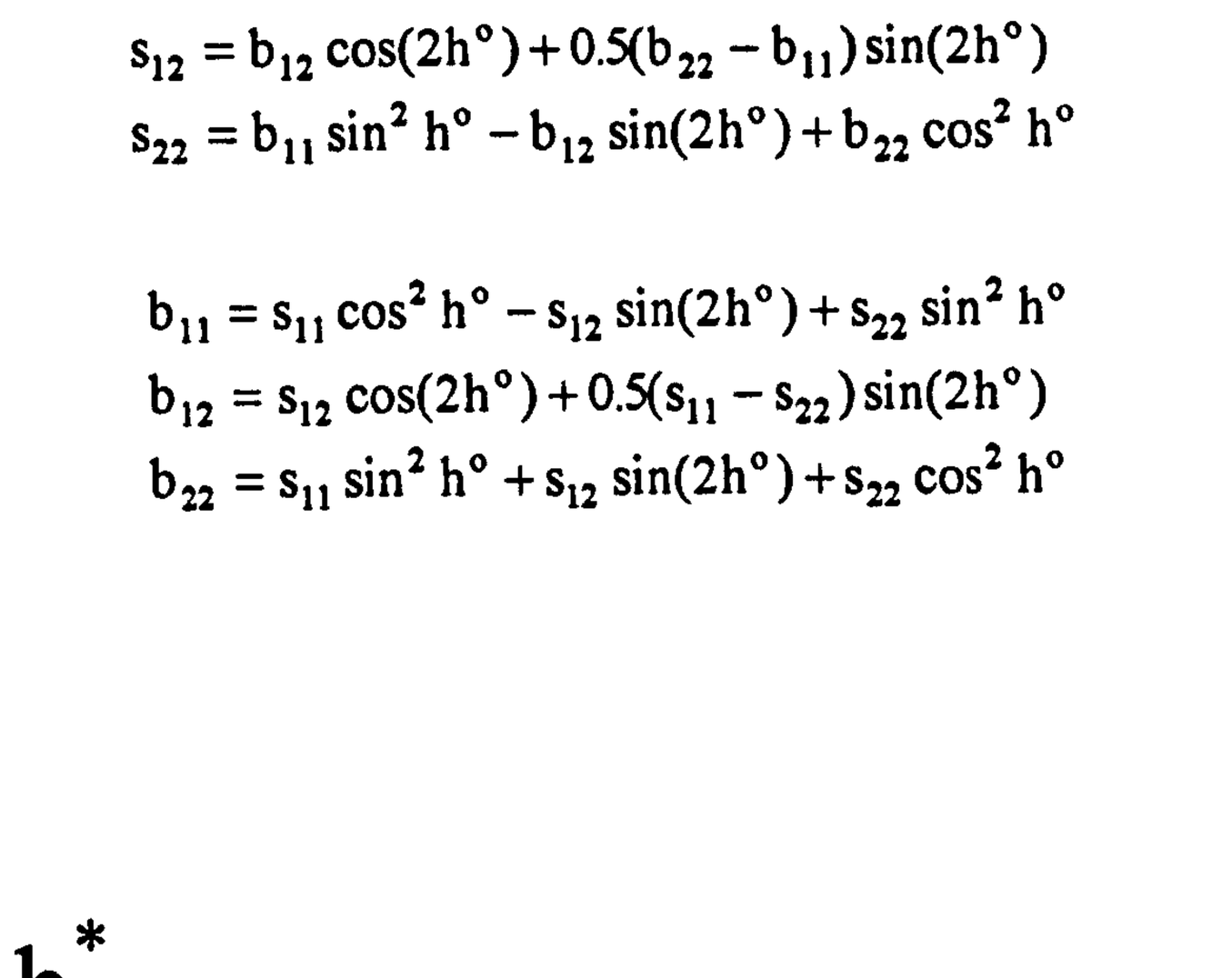

Figure 2-4. Chromaticity-discrimination ellipse in a^*b^* diagram.

2.3 Measures of Fit

Even after the experimental data are visualised as either an ellipsoid or tolerance vectors, it is hard to find which colour-difference formula fits the visual data better. Naturally, for each individual colour centre, the ellipsoid equation for that centre is the ideal formula. But in a normal sense it cannot be regarded as a colour-difference formula. To test the performance of a colour-difference formula, a kind of measure is needed.

Various indicators of goodness of fit of a colour-difference formula were developed. Among them the most informative and all-around is the PF (or PF′) value devised by Luo [16]. This composite indicator combines the correlation coefficient (r), coefficient of variation (CV), γ [8] and V_{AB} [10], and gives the degree of disagreement between ΔV (true visual difference) and ΔE (calculated colour difference):

$$PF(\%) = \left[\left(V_{AB} + \gamma - r\right) \times 100 + CV\right] \tag{2-45}$$

$$PF'(\%) = \left[\left(V_{AB} + \gamma - 1\right) \times 100 + CV\right] \tag{2-46}$$

(As the maxima of PF and PF′ are 400 and 300% respectively, in practice it is better to use the PF/4 and PF′/3.)

V_{AB}, γ, r, and CV are defined by the following equations.

$$V_{AB} = \left(\frac{1}{N}\sum \frac{(\Delta E - F\Delta V)^2}{\Delta E \cdot F \cdot \Delta V}\right)^{1/2} \tag{2-47}$$

where $F = \left(\sum \frac{\Delta E}{\Delta V} \Big/ \sum \frac{\Delta V}{\Delta E}\right)^{1/2}$, a factor for adjusting the ΔV values to the same scale as ΔE, and N is a number of sample pairs.

γ is the antilog of the standard deviation of $\log(\Delta E/\Delta V)$ values, that is,

$$\log(\gamma) = \sqrt{\frac{1}{N}\sum\left[\log\left(\frac{\Delta E}{\Delta V}\right) - \overline{\log\left(\frac{\Delta E}{\Delta V}\right)}\right]^2} \tag{2-48}$$

It is also devised to avoid the unit of ΔV or ΔE affecting the result.

The correlation coefficient is calculated as

$$r = \frac{\sigma_{\Delta E \cdot \Delta V}}{\sigma_{\Delta E}\sigma_{\Delta V}} = \frac{N(\sum \Delta E \cdot \Delta V) - \sum \Delta E \cdot \sum \Delta V}{\sqrt{N\sum \Delta E^2 - (\sum \Delta E)^2}\sqrt{N\sum \Delta V^2 - (\sum \Delta V)^2}} \tag{2-49}$$

where $\sigma_{\Delta E}$ and $\sigma_{\Delta V}$ are the standard deviations of ΔE and ΔV, and $\sigma_{\Delta E \cdot \Delta V}$ is covariance

of ΔE and ΔV.

And
$$CV = \frac{\sqrt{\frac{1}{N}\sum(\Delta E - f\Delta V)^2}}{\overline{\Delta E}} \times 100 \qquad (2\text{-}50)$$

where $f = \frac{\sum \Delta E \cdot \Delta V}{\sum (\Delta V)^2}$, the proportionality constant between ΔV and ΔE.

For perfect agreement, PF, V_{AB}, CV would be 0, and γ, r would be 1.

The PF and other measures above are directly applied to visual results which are given in the form of ΔV values (e.g., that from grey-scale method). If the data is obtained from a paired-comparison method and analysed by the logistic model, the results are expressed as the observer response probability (P_i). In such a case, the original P_i values are converted to ΔV_i values using the following eq.(from Eq.(2-2)):

$$\Delta V_i = \Delta E_{std}\left[1 - \frac{1}{\alpha}\ln\left(\frac{1-P_i}{P_i}\right)\right] \qquad (2\text{-}51)$$

Here ΔV_i cannot be calculated for $P_i = 0$ and $P_i = 1$.

When the data is given in the form of colour-difference (tolerance) vectors, i.e., from a paired-comparison method and analysed by the probit model, another measure TSD (tolerance standard deviation) [17] can be used.

$$TSD = SD / \overline{\Delta E} \qquad (2\text{-}52)$$

Where SD and $\overline{\Delta E}$ are the standard deviation and the mean of the unit visual tolerances calculated by a particular colour-difference formula, respectively.

Similar to the PF value, TSD indicates the percentage disagreement between each formula's prediction and visual results.

In the case when the TSD measure is difficult to apply because the number of tolerance vectors is small (< 10), i.e., the vectors are obtained for only one colour centre, then ΔV_i and so the PF values are computed in a similar way to the logistic model. That is, for each vector direction, ΔV_i corresponding to the rejection probability P_i is calculated as (from Eqs.(2-4) to (2-7)):

$$\Delta V_i = \frac{1}{\mu}\left[\sigma \cdot z(P_i) + \mu\right] = -\frac{z(P_i)}{c_0} + 1 = \frac{\Delta E_i}{\mu} \qquad (2\text{-}53)$$

Again, the ΔV values for $P_i = 0$ and $P_i = 1$ cannot be determined.

2.4 Errors in Colour Measurement

The errors involved in colour measuring instrument can be divided into two types: random and systematic [18]. Random errors result from sample presentation, sensitivity variation and electronic noise. Common sources of systematic errors (or bias) are wavelength, detector linearity, non-standard geometry and polarisation. Random errors affect precision (sometimes referred to as repeatability or reproducibility) while systematic errors affect accuracy. That is, precision means the consistency between repeated test results while accuracy means the absolute agreement with a reference value. Therefore, in instruments for colour-difference measurement, precision is more important than accuracy.

Billmeyer [19] reported the precision of colour and colour-difference measurement. With three commercial spectrophotometers, for a wide range of samples, means of colour-differences from the mean (MCDMs) of a set of measurements (5 times) were less than about 0.1 CIELAB unit. The coefficients of variation (CV) of three repeated colour-difference measurements of the porcelain-enamel tiles and textile samples were between 2.7 – 8.9 (%). It seems that these or slightly lower levels of the precision are typically expected for a modern colour measuring instrument. Billmeyer also found that the distributions of tristimulus values show large deviations from normality. Thus neither the spectral data nor the CIELAB co-ordinates (non-linear cube-root transforms) can be assumed to be normally distributed.

The practice for reducing the error in the mean results of colour (or colour-difference) measurements is provided in the ASTM standard E1345 [20]. The successive steps in this method are:

(1) Determine the standard deviation of instrument s_i, using a stable standard specimen without removing between measurements (≥ 10).

(2) Determine the standard error goal $s_{e,g}$ as the greater of $2\,s_i$ or $0.1\times$(tolerance).
(The tolerance is the total allowable range of the colour or colour-difference scale value considered.)

(3) Determine the standard deviation **s** and the standard error s_e of measurement of the sample.

$$s_e = s / N^{0.5} \qquad (2\text{-}54)$$

Where **N** is the sampling number (≥ 10), which is either the number of multiple measurements or the number of multiple specimens. Note that $N = 1$, $s_e = s$.

(4) Determine the required measurement number N_F to meet the criteria ($s_{e,g} > s_e$ for $N = 1$) for each colour or colour-difference scale. By analogy to Eq.(2-54):

$$N_F = (s_e / s_{e,g})^2 \qquad (2\text{-}55)$$

Select the largest of the rounded values of N_F as the final sampling number.

(5) Determine the final standard error goal.

This method assumes the normal distribution of colour measurement values. But, as was reviewed previously, the distribution of each colour co-ordinate is not well described by the normal distribution. In addition, it should be used when measured values are to be compared to an established tolerance.

The German standard DIN55600 (Part 2) provides a thorough treatment of colour measurement errors [11]. The underlying principles of this method are identical to the techniques used by Brown and MacAdam [12] in their colour matching error studies. That is, the normal distribution of the triplet colour measurement values is represented by an ellipsoid. (The extension of the normal distribution from one to three dimensions) The general procedures, using CIELAB co-ordinates (similarly applied to the colour-difference values), are as follows:

(1) Calculate the arithmetic means of the CIELAB co-ordinates.

(2) Calculate the variances of L^*, a^*, b^* and the covariances between L^*, a^*, b^* to form a covariance matrix $V = v_{ik}$:

$$V = \begin{pmatrix} \mathrm{Var}(a^*) & \mathrm{Cov}(a^*,b^*) & \mathrm{Cov}(a^*,L^*) \\ \mathrm{Cov}(a^*,b^*) & \mathrm{Var}(b^*) & \mathrm{Cov}(b^*,L^*) \\ \mathrm{Cov}(a^*,L^*) & \mathrm{Cov}(b^*,L^*) & \mathrm{Var}(L^*) \end{pmatrix} = \begin{pmatrix} v_{11} & v_{12} & v_{13} \\ v_{12} & v_{22} & v_{23} \\ v_{13} & v_{23} & v_{33} \end{pmatrix} \qquad (2\text{-}56)$$

(3) Invert the matrix **V** to get a matrix **G** ($= g_{ik}$) whose elements are the coefficients of the standard deviation ellipsoid:

$$G = \begin{pmatrix} g_{11} & g_{12} & g_{13} \\ g_{12} & g_{22} & g_{23} \\ g_{13} & g_{23} & g_{33} \end{pmatrix} = V^{-1} \qquad (2\text{-}57)$$

and $$\delta s^2 = g_{11}(\delta a^*)^2 + g_{22}(\delta b^*)^2 + g_{33}(\delta L^*)^2 + 2g_{12}\delta a^*\delta b^* + 2g_{23}\delta b^*\delta L^* + 2g_{13}\delta a^*\delta L^* = 1 \qquad (2\text{-}58)$$

(4) Calculate the errors in the measured CIELAB co-ordinates. Each is equal to the radius of the ellipsoid in the specified direction of corresponding colour co-ordinate.

$$\sigma_{a^*} = \frac{1}{\sqrt{g_{11}}}, \qquad \sigma_{b^*} = \frac{1}{\sqrt{g_{22}}}, \qquad \sigma_{L^*} = \frac{1}{\sqrt{g_{33}}}$$

$$\sigma_{C^*} = \frac{C^*}{\sqrt{g_{11}(a^*)^2 + 2g_{12}a^*b^* + g_{22}(b^*)^2}}$$

$$\sigma_{h^*} = \tan^{-1} \frac{1}{\sqrt{g_{11}(b^*)^2 - 2g_{12}a^*b^* + g_{22}(a^*)^2}} \qquad (2\text{-}59)$$

(5) The ellipsoid obtained in step 3 contains only 20% of all measurement values ($\delta s^2 = 1$, i.e., 20% confidence limit). If the different confidence interval is required, the value of δs^2 should be changed. For instance, the δs^2 values for 70% and 95% confidence limits (i.e., the equivalents of $\pm 1\sigma$ and $\pm 2\sigma$ levels of the one dimensional normal distribution) are 3.665 and 7.81, respectively.

2.5 Observer Assessments

The assessment of observers should be made throughout the visual tests. That is, the tasks of the experimenter before, during and after the visual test are summarised as: selection, control, and evaluation of observers.

For the selection of colour normal observers the colour vision (deficiency) test is generally used, of which the most common type is the confusion charts. The Ishihara Colour Blindness Tests [21] is the well-known test of this kind, and is preliminarily administered to the observers.

The colour discrimination test also can be used either as an adjunct test for the analysis of colour defectives or as an independent test for the discrimination level of colour normal observers. Though they were not applied to the observers, the discrimination tests are reviewed here as they are thought to be directly linked to this research subject.

2.5.1 Colour discrimination tests [22]

2.5.1.1 Farnworth-Munsell 100 Hue Test [23]

The Farnworth-Munsell Test measures the observers' level of discrimination of small colour differences. The chips in this test consist of 85 coloured papers varying in hue at approximately constant value and chroma. The observers are asked to place the test chips in correct order. For the purposes of assessing colour (more precisely, hue) discrimination, the test results are examined for the presence of wide margins in one or more limited regions of the hue circle. (For the colour vision test, the presence of an approximately constant but significant error level in the arrangement of the test chips throughout the hue circle are examined.) This may be interpreted as an inability to discriminate the small colour differences between neighbouring chips. While a weakness of this type might, for example, interfere with an observer's ability to participate in threshold scaling experiments, the observer might still be competent to perform magnitude scaling of large differences among specimens.

2.5.1.2 Triangle Test [24]

The Triangle Test is a part of a series known as the Japanese Color Aptitude Test. The observers are shown, one at a time, a series of 20 sets of three coloured chips each. In each set, two of the chips are identical and the third is slightly different in colour. The observer is asked to identify which one is different, the differences being so small that there is considerable uncertainty in the judgement. A lower than average score in this test indicates that the observer does not differentiate small differences well.

2.5.1.3 HVC (Hue, Value, and Chroma) Color Vision Skill Test [25]

The HVC test is designed to assess the ability of the observer to discriminate between specimens having colour differences in hue, value, and chroma. The test is a general indicator of accuracy in making colour matches. It consists of a set of 36 loose specimens for one-at-a-time comparison with 36 mounted specimens in a prescribed sequence. The specimens are of one of four hues (red, yellow, green, and blue) with nine specimens each in subgroups that vary in hue, value, and chroma around a centre point. The colour differences among the specimens correspond roughly to industrial colour matching tolerances.

2.5.2 Observer uncertainty

It is essential to provide optimum observing conditions for the observers to get reliable results. In this section, the basic considerations required in the design of the typical observer test (excluding physical parameters) are treated: e.g., number of observations, observation time (duration), and inherent uncertainty in psychophysical experiment. The evaluation of the visual results, i.e., error estimate and observer variability, is reviewed in the later part.

A few comments on the number of observations (both the number of observers and the number of repetitions) required for visual test and data analysis can be found in Refs.[10,26]. In a paired-comparison experiment, if a set of about 50 samples is assessed, then 30 observations (15 observers × 2 tests each) are reported to be necessary to get a colour-difference ellipsoid with sufficient accuracy [10]. For single observer analysis (i.e., in-observer variability) in threshold perceptibility experiment, the repetition number of 10 is claimed as a lower limit [26].

The performance of the observers could degrade with increase in length of the observing session. It is known [27] that the visual judgement of colour differences is affected if the state of adaptation of the observer's eye is changed, since the sensitivity of the eye to colour differences decreases for the colours corresponding to the adapting colour. On examination of a colour-difference pair under normal conditions (unless the pair specimens are unusually small) their mean colour is the adapting colour, and prolonged viewing can lead to adaptation to that colour and a decrease in sensitivity to the colour difference. It is therefore usual to view small colour differences in quick glances, as they tend to appear less prominent on prolonged viewing.

The surface colour matching (or threshold perceptibility) experiment may involve the false alarm rate. (Rich [2]) That is, sometimes the observer judges a sample pair having colorimetrically zero difference not to be a match. This could be represented by an additive constant to the Gaussian function, i.e., the probability (P_i) that a sample pair judged as a match is:

$$P_i = (1 - f_a)\exp\left(-\frac{\Delta E_i^2}{2}\right) \tag{2-60}$$

or that for perceptibility judgements is

$$P_i = 1 - (1 - f_a)\exp\left(-\gamma \cdot \Delta E_i^2\right) \qquad (2\text{-}61)$$

where f_a is a false alarm rate, and ΔE_i is calculated from the ellipsoid eq. (Refer to Section 2.1.1.1)

The threshold (i.e., perceptible / not perceptible boundary) probability in Eq.(2-61) should not be $P_i = 0.5$, but a slightly higher value $f_a + (1 - f_a)/2$ [3].

The variability (or error) in observer judgements is estimated in various ways. The precision of the overall visual results is usually computed first. Then, based on this error estimate, the degree of observer variability (either in- or between-) for single observers or for observer groups is estimated.

2.5.2.1 Precision of visual results

The methods and estimates given here are for the two representative data sets - Luo [4] and RIT [7].

Luo [4] reported the standard error of ±8.9% for his data, which was based on grey-scale assessments of textile sample pairs. He used a simplified method assuming a normal distribution of the grey scale (GS) values. The example of calculation is as follows:

For all observer sessions, the overall mean and the standard deviation of GS values for 20 assessments were 3.44 and 0.44, respectively. Thus the standard deviation of the mean GS values is $0.098 = \frac{0.44}{\sqrt{20}}$.

That is, if the whole experiment was repeated many times, for a typical pair 68% of the mean GS values should fall within ±0.098 of the original mean.

For a GS value of 3.44, the 68% limits (1σ level) are 3.34 and 3.54. These limits were converted to ΔV values using the equation that relates GS and ΔV (Eq.1-42), giving 1.89 and 2.26.

The mean for the ΔV values is thus 2.08 with a standard deviation of 0.185.

Finally, the precision is $8.9(\%) = \frac{0.185}{2.08} \times 100$.

Berns[7] reported the standard error of the RIT data is ±5.7%. The RIT data consists

of 156 unit visual tolerances obtained from the paired-comparison experiment and the probit analysis. As reviewed in Section 2.1.1.2, the advantage of probit analysis is that statistical parameters are readily available to estimate experimental uncertainties: e.g., mean (T50), standard deviation (σ), fiducial limits (UFL and LFL), etc.

The fiducial limits are the asymmetric 95% confidence intervals ($\pm 2\sigma$ level), i.e., twice the standard error. Hence, the error of the measured tolerances is computed as:

$$\pm \frac{1}{2}\left[\frac{(\overline{UFL} - \overline{LFL})/2}{\overline{T50}} \times 100\right] \qquad (2\text{-}62)$$

where $\overline{UFL}$, $\overline{LFL}$, $\overline{T50}$ are the averages of the UFL, LFL, T50 values, respectively.

2.5.2.2 Observer variability

From the results of the probit analysis, the measure of observer variability is rather easily estimated. Unless the observers made repeated judgements, the standard deviation could be regarded as between (or inter) observer variability. The coefficient of variation (CV), the standard deviation normalised by the mean tolerance, of the RIT data [7] was about 30%.

The colour-difference sensitivity is naturally quite different from observer to observer. The comparison of colour-difference ellipsoids (or ellipses) for the observers (either individual or groups) could provide the estimate of the observer variability.

In tristimulus space, at a green colour centre, the between-observer variability of threshold (perceptibility) ellipsoids for two extreme observer groups was the order of 1.4 (max./min. size factor) [3].

The standard error estimate is used to simulate the variation of ellipsoids for single observers or for observer groups. The simulation technique is proposed by Alder [28] which is based on the Monte-Carlo method. The idea is to produce the random deviates of mean observer responses (ΔV in this case) and check the newly fitted deviation ellipsoids. These ellipsoids conceptually describe the shells of uncertainty inherent in the data. (This method was also used to test the variability of ellipsoids caused by colour measurement error [4], but the randomisation by assuming the normal distribution of each colour-difference value is inconsistent with the results of the previous colour measurement error studies. (Section 2.4))

For the threshold ellipsoids of the four CIE colour centres (grey, red, yellow and blue), shells of uncertainty in groups of observers were given by variabilities 1.2 to 2.0 (max./min. size factor) [26].

2.6 Physical Parameters

Colour-difference perception is changed by various sources: i.e., by both scaling methods and physical parameters, and as reviewed earlier also by colour measurement error and observer variability. In a broad sense, the changes caused by all these variables are regarded as parametric effects, but use of the term is generally confined to those from physical changes of the viewing environment. Here, the physical parametric effects involved in the colour-difference sensation of pairs of surface colours (i.e., object viewing mode) are reviewed.

A significant parametric factor changes perceptual colour difference in relation to the reference conditions, which represent common levels of the experimental variables. The CIE technical committee 1-28, Parameters Affecting Colour Difference Evaluation, specified the reference conditions as [29]:

Table 2-2. Physical parameters and CIE TC1-28 reference conditions [29].

Physical parameter	TC1-28 reference conditions
Sample size	$\geq 4°$
Sample separation	Direct edge contact
Surface structure (texture)	Homogeneous
Lightness of background	Neutral grey $L^* = 50$
Lightness of sample	–
Other factors	
Illuminant	D65
Illuminance	1000 lx
Viewing mode	Object
Colour-difference magnitude	$\Delta E^* \cong 0 - 5$

An ideal colour-difference formula thus could adjust and correlate closely the shift of colour-difference perception by changes from these reference conditions. Assume that it has 3 major colour-difference components which are the approximations to those along physiologically relevant colour directions: lightness, chroma and hue. Defining the formula in CIELAB space gives us the following, which are similar in structure to CMC or CIE94.

$$\Delta E = \left[\left(\frac{\Delta L^*}{k_L S_L} \right)^2 + \left(\frac{\Delta C^*}{k_C S_C} \right)^2 + \left(\frac{\Delta H^*}{k_H S_H} \right)^2 \right]^{1/2} \tag{2-63}$$

or

$$\Delta E = \left[\left(\frac{\Delta L^*}{k_L S_L} \right)^2 + \frac{\left(\Delta C^* / S_C \right)^2 + \left(\Delta H^* / S_H \right)^2}{k_{CH}^{\ 2}} \right]^{1/2} \tag{2-64}$$

or

$$\Delta E = \frac{1}{k_E} \left[\left(\frac{\Delta L^*}{S_L} \right)^2 + \left(\frac{\Delta C^*}{S_C} \right)^2 + \left(\frac{\Delta H^*}{S_H} \right)^2 \right]^{1/2} \tag{2-65}$$

where k_L, k_C, k_H are the parametric correction factors for lightness, chroma and hue differences, respectively. Also, k_{CH} for chromaticness difference and k_E for total colour difference. (The values of correction factors are set at unity for the reference condition. Numbers larger than 1 indicate the decrease, and those smaller than 1 indicate the increase in perceived tolerance size.)

S_L, S_C, S_H are the weighting functions which (for a fixed experimental set-up) smooth non-uniformities of the scales along different directions of colour-difference.

2.6.1 Gap effect

The gap (sample separation) is a parameter of high industrial interest. Ordinarily, the more the samples in a pair are separated, the greater the colour-difference sensitivity is reduced. As a result, the observer becomes more lenient (or less biased) to colour differences.

Witt [30] has studied the effect of gap systematically. Five sets (CIE colour centres[1]) of colour-difference pairs of painted samples having 10° angular subtense were judged by a perceptibility (threshold) method. A 3 mm dividing line, of near centre lightness and of same background colour, between samples (=0.5°) was introduced.

Factors due to the effect are given for the approximate directions of total, lightness, chroma and hue differences, i.e., ΔE^*, ΔL^*, ΔC^* and ΔH^*.

Table 2-3. Correction factors for the 0.5° gap [30]. (Averages for 4-6 observers)

Colour centre	CIELAB coordinates			Gap/non-gap factor			
	L^*	a^*	b^*	k_E	k_L	k_C	k_H
Grey	62.5	-0.3	1.0	**1.6**	2.0	1.3	1.3
Red	44.7	37.3	23.2	**2.1**	1.7	2.4	2.0
Yellow	86.6	-6.9	47.3	**1.6**	1.4	1.7	1.5
Green	56.3	-31.2	0.2	**1.8**	1.5	2.7	1.4
Blue	35.6	4.6	-30.2	**2.6**	2.9	2.1	2.0

Based on this work, the CIE TC1-28 suggested a tentative correction for the 0.5° or more gap compared to direct contact of samples in a pair as follows:

$k_E = 2.6$ in dark colours ($L^* < 40$)

$k_E = 2.0$ in medium colours ($40 < L^* < 60$)

$k_E = 1.6$ in light colours ($L^* > 60$)

2.6.2 Background effect

The background effect on surface colour-difference judgements was also reported in the same study reviewed above [30]. At three out of 5 CIE colour centres (red, yellow and blue), the effect of the lightness of the grey background was investigated.

Table 2-4. Correction factors for the background lightness [30].

Colour centre	Lightness (L^*)			Background factor			
	Background		Sample	k_E	k_L	k_C	k_H
	Param.	Ref.					
Red	87	41	44.7	**1.1**	1.0	0.9	1.3
Yellow	41	87	86.6	**1.0**	1.0	0.7	1.1
Blue	87	41	35.6	**1.4**	1.8	0.9	1.8

Both the invariability in case of the yellow and the change of the blue were explained as the results of the local adaptation to the lightest element of the visual field.

TC1-28 recommendation of tentative correction for change of background lightness: For the large sample size (10°), the colour discrimination at different lightness of grey background is related to that at similar sample lightness by approximately setting to:

$k_E = 1.4$ in dark colours ($L^* < 36$)

$k_E = 1.0$ in medium to light colours ($L^* > 45$)

2.6.3 Other effects

The effect of the sample size is possibly connected with the background parameter. Increasing the sample size of a colour-difference pair seems to decrease the effect of the background.

The surface structure (texture) of samples, together with the gap, is believed to influence parametric factor values in the textile industry. However, its effect has not been investigated fully with a wide range of structures (homogeneous to very coarse).

The change of illuminant could greatly complicate the colour-difference description. It requires a chromatic adaptation transform, and also addresses the problem of the (illuminant) metamerism. The use of complex colour appearance model may be necessary. (The illuminant parameter was originally not included in the TC1-28 program[29].)

The size of a colour-difference could be another parameter. The tests of the additivity of colour-difference scale values within a small range (±5 threshold units) showed that they were typically linear [31]. But the question remains whether they extend linearly from very small (threshold) to very large differences (found in colour-order systems).

Most of the earlier studies on the parametric effects were conducted by use of the visual colorimeter. Though there is no close correspondence with results from surface colours, they are briefly summarised in Table 2-5.

Table 2-5. Parametric factors from experiments with visual colorimeter [29].

Parameter	Field size	Luminance	Background	k_L	k_{CH}
Sample size	2° to 12°	central field 10-44	white black	1 1	2 1.4
Background	2°	central field 10-44	large to no contrast (grey + chromatic)	1	2.6
Luminance	2°	sample + background 1000 to 100	white	0.7	

2.7 References

1. A.R.Robertson, CIE Guidelines for Coordinated Research on Colour-Difference Evaluation, Col. Res. Appl., **3**, 149-151 (1978).

2. R.M.Rich, F.W.Billmeyer and W.G.Howe, Method for Deriving Color-Difference Perceptibility Ellipses for Surface-Color Samples, J. Opt. Soc. Am., **65**, 956-959, 1389 (1975).

3. K.Witt and G.Döring, Parametric Variations in a Threshold Color-Difference Ellipsoid for Green Painted Samples, Col. Res. Appl., **8**, 153-163 (1983).

4. M.R.Luo and B.Rigg, Chromaticity-Discrimination Ellipses for Surface Colours, Col. Res. Appl., **11**, 25-42 (1986).

5. B.Treutwein, Adaptive Psychophysical Procedures, Vision Res., **35**, 2503-2522 (1995).

6. B.Flury and H.Riedwyl, Multivariate Statistics: A Practical Approach, Chapman & Hall, New York, 1988.

7. R.S.Berns, D.H.Alman, L.Reniff, G.D.Snyder and M.R.Balonon-Rosen, Visual Determination of Suprathreshold Color-Difference Tolerances Using Probit Analysis, Col. Res. Appl., **16**, 297-316 (1991).

8. C.Alder, K.P.Chaing, T.F.Chong, E.Coates, A.A.Khalili and B.Rigg, Uniform Chromaticity Scales - New Experimental Data, JSDC, **98**, 14-20 (1982).

9. L.F.C.Friele, Fine Color Metric (FCM), Col. Res. Appl., **3**, 53-64 (1978).

10. D.Strocka, A.Brockes and W.Paffhausen, Influence of Experimental Parameters on the Evaluation of Color-Difference Ellipsoids, Col. Res. Appl., **8**, 169-175 (1983).

11. H.G.Völz, Industrial Color Testing: Fundamentals and Techniques, VCH, Weinheim, Germany, and New York, 1995.

12. W.R.J.Brown and D.L.MacAdam, Visual Sensitivities to Combined Chromaticity and Luminance Differences, J. Opt. Soc. Am, **39**, 808-834 (1949).

13. T.Indow and M.L.Morrison, Construction of Discrimination Ellipsoids for Surface Colors by the Method of Constant Stimuli, Col. Res. Appl., **16**, 42-56 (1991).

14. M.Melgosa, E.Hita, J.Romero and L.Jimènez del Barco, Color-Discrimination Thresholds Translated from the CIE (x,y,Y) Space to the CIE 1976 (L^*,a^*,b^*), Col. Res. Appl., **19**, 10-18 (1994).

15. M.Melgosa, E.Hita, J.Romero and L.Jimènez del Barco, Some Classical Color Differences Calculated with New Formulas, J. Opt. Soc. Am. A, **9**, 1247-1254 (1992).

16. M.R.Luo and B.Rigg, BFD(ℓ:c) Colour-Difference Formula: Part 1–Development of the formula, JSDC, **103**, 86-94 (1987).

17. D.H.Alman, R.S.Berns, G.D.Snyder and W.A.Larsen, Performance Testing of Color-Difference Metrics Using a Color Tolerance Dataset, Col. Res. Appl., **14**, 139-151 (1989).

18. R.W.G.Hunt, Measuring Colour, 2nd ed., Ellis Horwood, 1991.

19. F.W.Billmeyer and P.J.Alessi, Assessment of Color-Measuring Instruments, Col. Res. Appl., **6**, 195-202 (1981).

20. ASTM E1345, Standard Practice for Reducing the Effect of Variability of Color Measurement by Use of Multiple Measurements, 1995 Annual Book of ASTM Standards, Vol.06.01.

21. S.Ishihara, Tests for Colour-Blindness, 2nd ed., Kanehara Shuppan, Tokyo, 1959.

22. ASTM E1499, Standard Guide to the Selection, Evaluation, and Training of Observers, 1995 Annual Book of ASTM Standards, Vol.06.01.

23. D.Farnworth, The Farnworth-Munsell 100 Hue and Dichotomous Tests for Color Vision, J. Opt. Soc. Am., **33**, 568-578 (1943).

24. Japanese Color Aptitude Test, Japan Color Research Institute, 3-1-19 Nishiazabu, Minato-ku, Tokyo 106, Japan, 1994.

25. HVC Color Vision Skill Test, Graham and Associates, Inc., 1207 Colonial Ave., Greensboro, NC 27408.

26. K.Witt, Three-Dimensional Threshold of Color-Difference Perceptibility in Painted Samples: Variability of Observers in Four CIE Color Regions, Col. Res. Appl., **12**, 128-134 (1987).

27. R.M.Evans, An Introduction to Color, Wiley, New York, NY, 1948.

28. C.Alder, A Monte Carlo Method for the Validation of Discrimination Ellipse Data, JSDC, **97**, 514-517 (1981).

29. CIE Publ. No.101, Parametric Effects in Colour-Difference Evaluation, CIE Central Bureau, Vienna, 1993.

30. K.Witt, Parametric Effects on Surface Color-Difference Evaluation at Threshold, Col. Res. Appl., **15**, 189-199 (1990).

31. K.Witt, Linearity and Additivity of Small Color Differences, Col. Res. Appl., **20**, 36-43 (1995).

3. EXPERIMENTAL

This chapter describes the details of the materials, apparatus and methods used in the experiments reported in Chapters 4 and 5.

3.1 General

The main experiments (observer tests) were divided in 3 parts and carried out over 2 years. 248 colour-difference pairs around 21 colour centres were judged by 12-15 colour normal observers under one reference (grey background) and 3 parametric viewing conditions (black and white backgrounds, and gap). Two methods, paired-comparison and grey-scale, were used in colour-difference scaling.

3.2 Sampling

Colour-difference pairs, standard pairs (for the paired-comparison method), and grey scale (for the grey-scale method) were sampled as described in the following schemes. Full colorimetric specifications of all samples are given in Appendix 1.

3.2.1 Part one - data analysis methodology

The major concern of Part 1 was the data analysis methodology, particularly the comparison between logistic and probit models. In CIELAB space, 45 colour-difference pairs near the CIE Red colour centre [1] were sampled by direction basis, i.e., five pairs along each of 9 uniformly spaced vector directions. These directions were chosen as following:

Among the vector directions listed in Table 2-1, four directions were selected in each of a^*b^*, a^*L^*, and b^*L^* planes: two parallel to the co-ordinates axes and two diagonal directions. These correspond to nine vector directions A to E and J to M. (Fig.3-1) It is not easy to certify univariate sampling adequacy of sample pairs varying all three component colour differences simultaneously. But it is much easier, as in this study, to vary only one or two dimensions. This approach is also good for visualising the tolerance vectors or discrimination ellipses in each plane.

Along each direction, paired combinations of samples yielded colour-differences ranged from about 0.5 to 3.5 CIELAB units.

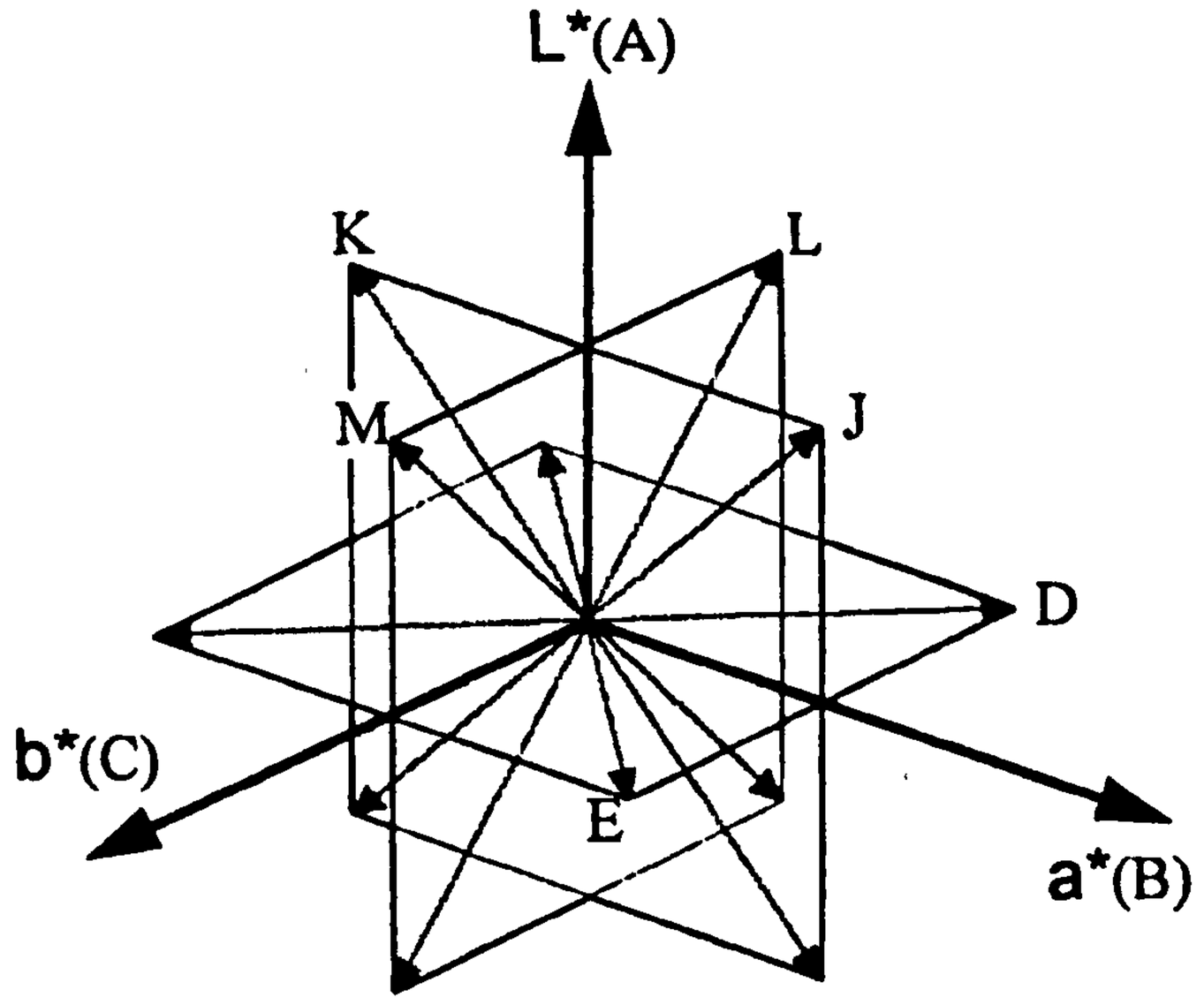

Figure 3-1. Vector directions A, B and C which sample along L^*, a^* and b^* axes, and D, E, J, K, L and M which sample diagonal directions in a^*b^*, a^*L^* and b^*L^* planes.

3.2.2 Part two - study of lightness tolerances

The main aim of Part 2 was to study the lightness tolerances. Four CIE colours, and 7 neutral grey colours from dark to light ($L^* \cong 30 - 90$) with $10L^*$ intervals were selected. For each colour, 5 pairs having virtually only lightness differences ($\Delta L^* \cong 0.5 - 3.0$) were sampled.

Table 3-1. Colour centres selected for checking lightness tolerances (Part 2).

Colour Centre	L^*	a^*	b^*	C^*	h°
L90	**89**	0	0	-	-
Yellow	**86**	-7	46	46	98
L80	**79**	0	0	-	-
L70	**67**	0	0	-	-
L60 (Grey)	**61**	0	0	-	-
Green	**56**	-32	0	32	180
L50	**51**	0	0	-	-
Red	**45**	40	22	46	29
L40	**41**	0	0	-	-
Blue	**38**	-6	-27	27	257
L30	**29**	0	0	-	-

Two CIE colour centres (Blue and Grey) were also selected for other independent investigation. Around the Blue centre, 3 or 4 colour-difference pairs along each of 7 vector directions in a^*b^* plane (total 26 pairs) were sampled. Near the Grey centre, 24 colour-difference pairs that cover the centre in completely random manner were sampled.

3.2.3 Part three - study of hue angle dependence

In Part 3, special attention was paid to the variation of chromaticity discrimination (more precisely ΔH^*) with hue-angle. One neutral grey ($L^* \cong 50$) centre, and 14 colour centres along the hue-circle with 20 - 30 h° intervals were selected (Table 3-2 and Fig.3-2). In the a^*b^* plane, 5 colour-difference pairs around each colour centre were sampled referring to unit chromaticity ellipses of CMC, BFD and CIE94 formulae. (Fig.3-3)

The lightness tolerances of 11 colours studied in Part 2 were re-checked sampling 2 colour-difference pairs in each centre (3 pairs for yellow centre).

Table 3-2. Colour centres sampled for testing the hue-angle dependence (Part 3).

Colour Centre			Co-ordinates		
No	Name	(Abbr.)	L^*	C^*	h°
1	Neutral Grey	(N)	49	-	-
2	Purplish Red	(PR)	54	41	**10**
3	Red	(R)	44	43	**30**
4	Yellowish Red	(YR)	60	40	**48**
5	Reddish Yellow	(RY)	80	31	**75**
6	Yellow	(Y)	87	47	**98**
7	Greenish Yellow	(GY)	66	30	**123**
8	Yellowish Green	(YG)	61	34	**153**
9	Green	(G)	55	32	**179**
10	Bluish Green	(BG)	53	18	**210**
11	Greenish Blue	(GB)	61	32	**237**
12	Blue	(B)	36	28	**260**
13	Violet	(V)	47	32	**290**
14	Purple	(P)	46	18	**323**
15	Reddish Purple	(RP)	53	18	**354**

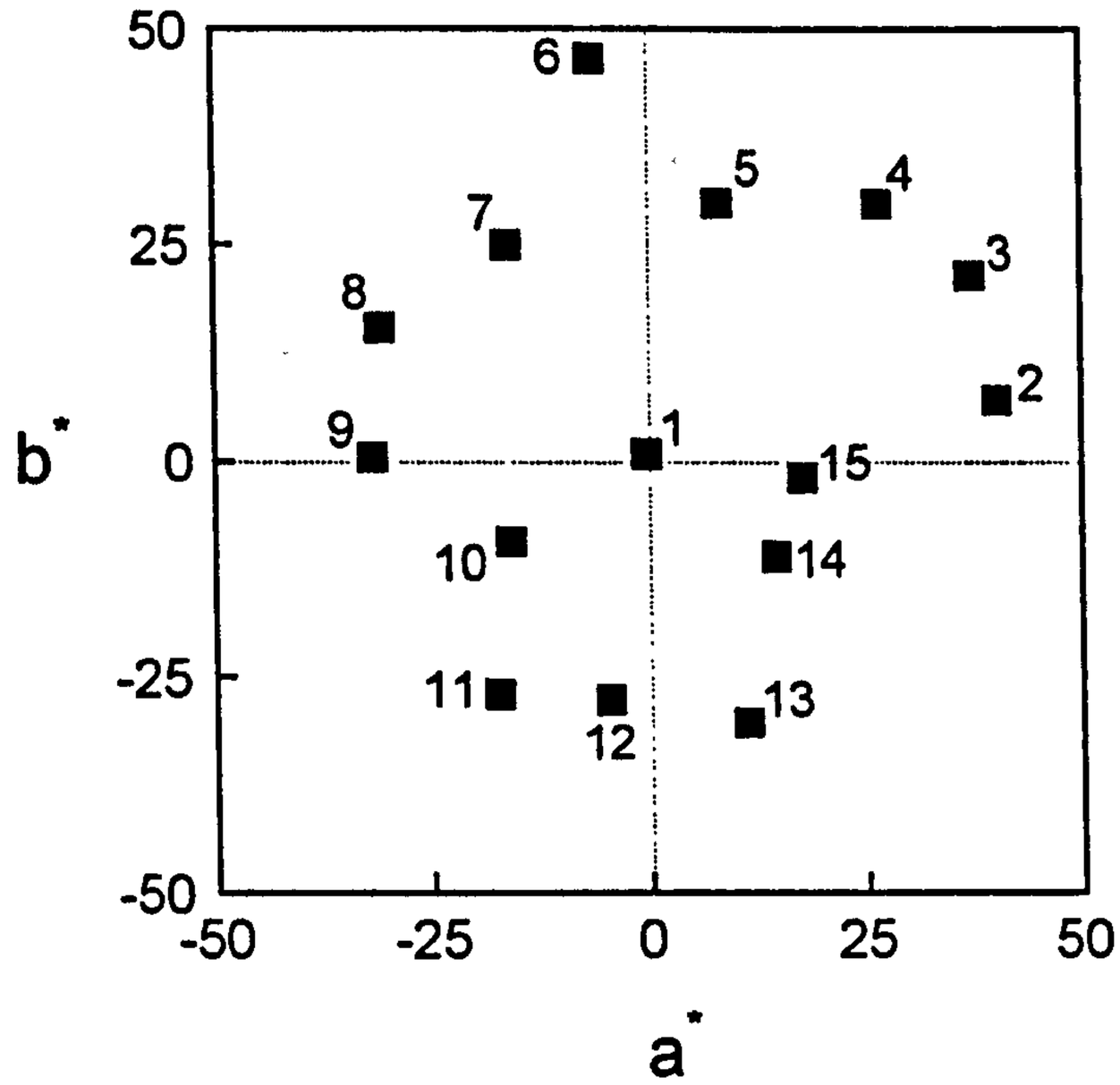

Figure 3-2. Positions of 15 colour centres in a^*b^* diagram.

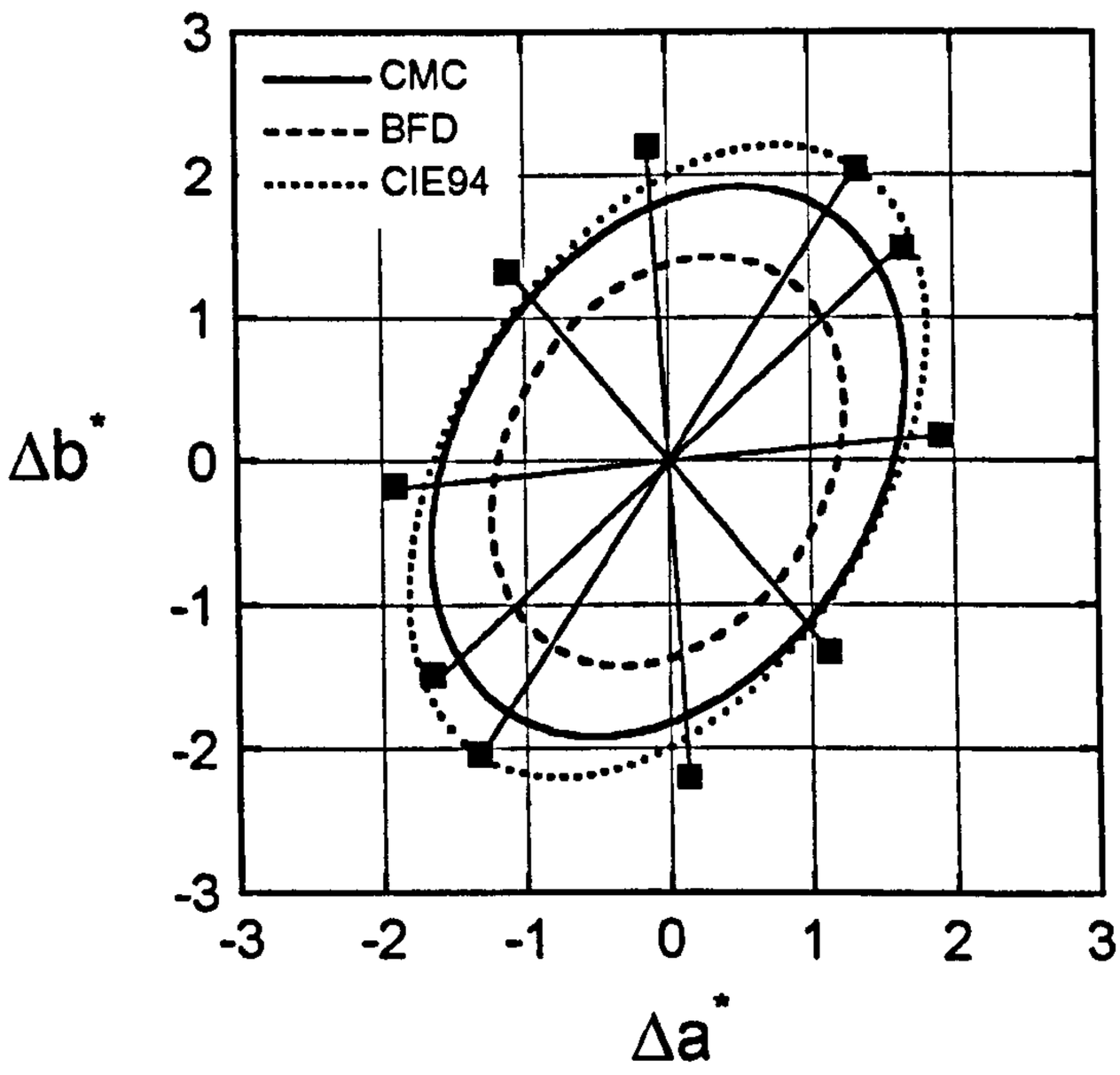

Figure 3-3. Sampling of colour-differences around the greenish blue (GB) centre.

3.2.4 Standard pairs

Three standard colour-difference pairs were prepared and used. All of them are near-neutral grey sample pairs and exhibit both lightness and chromatic differences. Standard pair no.1 ($\Delta E^* = 1.1$) was used to investigate the effect of background lightness (Part 1 and lightness tolerances in Part 2). For testing of the gap effect in Part 1, standard pair no.2 ($\Delta E^* = 0.5$) and standard pair no.3 ($\Delta E^* = 2.0$ with 5mm gap between samples) were additionally used.

3.2.5 Grey scale

When the samples in a pair are separated (gap), it is not easy to scale colour differences using the paired-comparison method. As the gap largely decreases observers' sensitivity, most of test colour differences are then perceived to be smaller than the standard colour difference. Since, as appropriately pointed out by Bartleson [2], the paired-comparison method works best only when the stimuli are similar enough to be confused often, another scaling method (grey-scale method) was used together with (Part 2), or instead of, the paired-comparison method (Part 3).

Colour differences of the grey scale specified in the British Standard (Fastness testing for assessing change of colour) [3] seem to be too large to scale small to medium colour differences typically encountered in colour-difference assessment. Thus, a new grey-scale (a series of 7 neutral grey panels) of the same size and material as the test panel was prepared. From left to right, pairing adjacent panels produces 6 colour-difference pairs that serve as the reference scale. Grey-scale grades and the colour differences are shown in Table 3-3.

Table 3-3. Grey-scale grades and colour differences.

GS-Grade	Colour-Difference ΔE^*			
	Aim	Part 2		Part 3
		SPIN	(SPEX)	SPEX
9	0.25	0.19	(0.22)	0.12
8	0.50	0.38	(0.39)	0.43
7	0.75	0.60	(0.58)	0.67
6	1.00	0.98	(1.03)	0.95
4	1.50	1.64	(1.67)	1.42
2	2.00	2.00	(1.93)	1.93

The equation that relates the GS grade to ΔE^* value was found by use of the standard curve-fitting software (Fig.3-4). The ΔV values (the differences seen) obtained from the observers selected are hence the same as ΔE^* values for Parts 2 and 3.

Part 2: $$\Delta V = 2.59 - 0.27\ GS \quad (3\text{-}1)$$

Part 3: $$\Delta V = 2.45 - 0.255\ GS \quad (3\text{-}2)$$

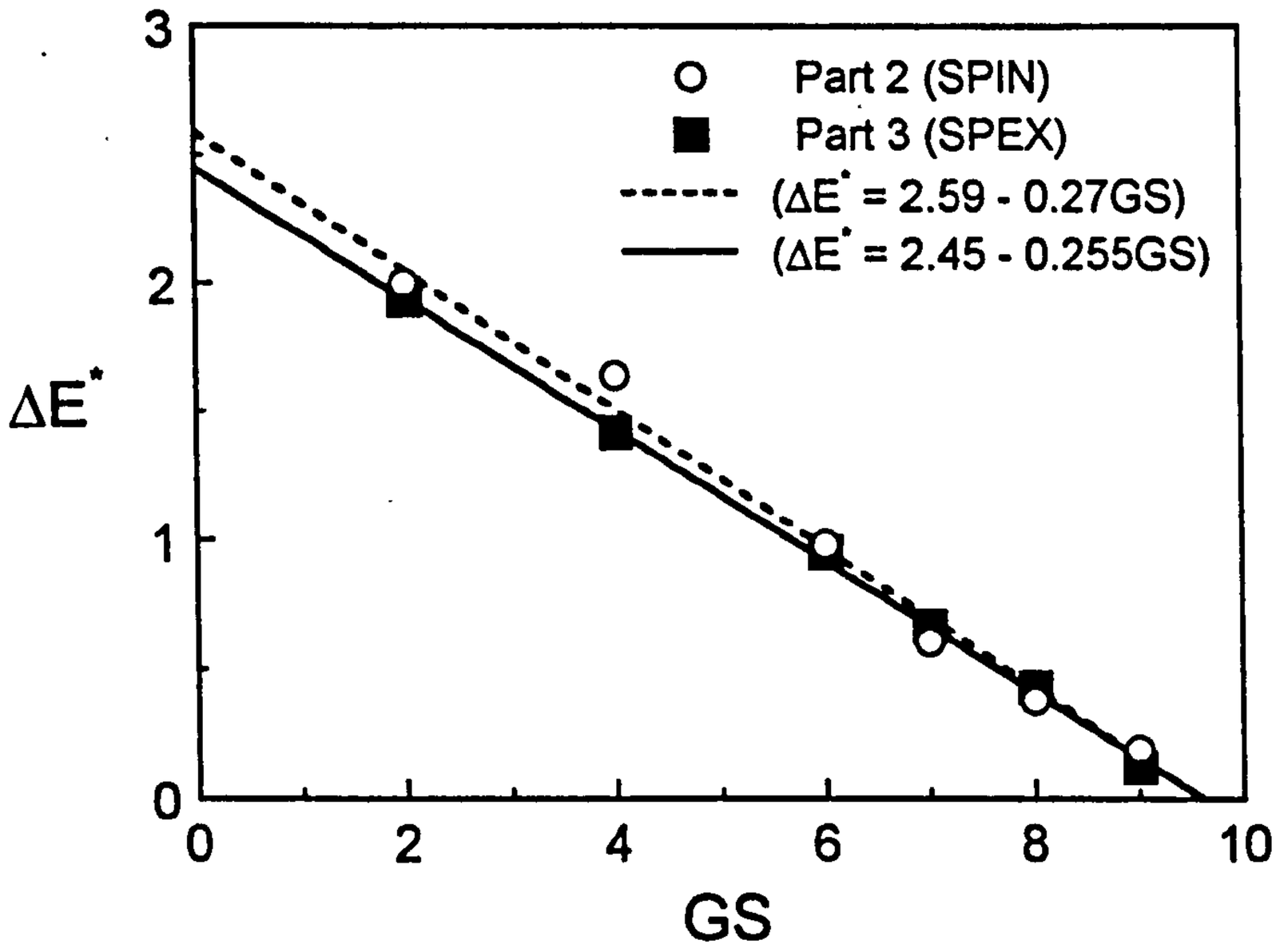

Figure 3-4. ΔE^* vs. GS.

3.3 Sample Preparation

Painted samples were produced using the Artilene Pigment Pastes supplied by Clariant[4]. (Table 3-4) These are a range of binder-free concentrated aqueous pigment pastes that stir readily into: emulsion paints - decorative and industrial, aqueous wood stains, and water based printing inks.

The colour formulation was achieved by the Colorgen match prediction software [5]. First, the colour matching recipe of a target colour (entered to the program with CIELAB co-ordinates) was produced. Following the recipe, pigment pastes were mixed and these were applied to paper boards using the K Hand Coater [6], which consists of

wire wound K Bars and the Impression Bed. Taking the K-Bar no.8 (or no.5) and drawing down one or more times produced about 40μ dry coat thickness. The dried samples were cut into 5.0 × 6.5 cm^2 rectangles, and the cut samples were attached to stiff card board side-to-side in close contact to each other. The sample size led to 10° viewing field at a normal viewing distance of about 50cm.

Table 3-4. Characteristics of pigments used in sample preparation.

Product Name	Specific Gravity	% Pigment Content	Light Fastness	Chemical Fastness
Artilene White RC	2.20	58	7	5
Black PBN	1.10	40	7	5
Red FBLC	1.15	40	7	5
Red PBL	1.19	42	7	3
Orange 2GCN	1.15	50	7	5
Oxide Yellow TGL	1.95	60	7	3
Yellow GCN	1.20	50	6 - 7	3
Green 4GLC	1.45	50	7	5
Blue BCN	1.30	48	7	5
Violet BL	1.10	26	8	5
Bordeaux 2RC	1.10	40	6	5
Vinyl Silk Extender Base(*)	1.114	60	-	-

(*) Used as a diulent.

3.4 Colour Measurements

Colour panels were measured by use of a Colorgen CS-1100 Spectrophotometer [7]. The CS-1100 is an abridged dual-beam reflectance spectrophotometer containing an integrating sphere, whose optical characteristics are:

Wavelength: 380-720 nm (Bandwidth: 10 nm)

Light source: Tungsten halogen lamp

Sample illumination size: 12.5 mm standard (6.25 mm optional)

Geometry: 6°/d, SPIN or SPEX (controlled via software)

Accuracy and Precision: < 0.12 ΔE^* and < 0.07 ΔE^*, respectively.

Two spots on each sample were measured. Averaged CIELAB co-ordinates of samples in each pair and colour-difference of each pair were calculated for the Standard

Illuminant D65 and the 10° Observer. Colour measurements were repeated 3-5 times throughout (i.e., before, during and after) the observer tests, and the standard deviation of each colour-difference value was calculated.

The samples were measured in specular component included (Parts 1 and 2) and excluded (Part 3) modes. There was essentially no difference between colour difference values calculated from SPIN or SPEX modes, as the samples have matte surfaces and are not extremely dark. However, the increase of gloss on the samples of dark neutral grey pairs (i.e., colour centre L30 of Part 2) was apparent. Thus, these 5 pairs (10 samples) were measured in both gloss included and excluded modes to test the gloss effects on colour-difference measurements. As the metric colour differences vary along only one direction (ΔL^*), it is natural that if the colour-difference is larger then the grey-scale grade (GS) should be smaller or the observer response probability (P_i) should be greater.

In Table 3-5, colour-difference values from the SPEX mode evidently relate to observer judgements better than those from the SPIN mode. The result is consistent with that of Atkin [8], that is, the colour-difference measurement of glossy sample pairs should be made excluding the specular component.

Table 3-5. Gloss effect on colour-difference measurement (Grey BG).

Pair No.	ΔE^*(SPIN)	ΔE^*(SPEX)	GS	P_i
N31	**1.74**	**1.34**	**6.71**	**0.13**
N32	**1.45**	**1.48**	**4.33**	**0.63**
N33	1.74	1.90	3.67	0.69
N34	2.37	2.38	2.94	0.94
N35	2.67	2.47	2.46	1.00

[The colour measurement uncertainties of the present study are given in Section 5.2.]

3.5 Visual Assessments

3.5.1 Viewing conditions

Observations were carried out in a dark room with an ICS-TEXICON viewing cabinet. Three backgrounds (grey, black, and white) were made by painted wood boards with a lightness L^* of 49, 30, and 95, respectively. For the black background the bottom of the

viewing booth was covered with a matt paper of $L^* = 25$ as the wood board has high glossy surface. The gap between a pair of samples was achieved by the rectangular window of grey cardboard having 5mm vertical stripe in the centre. It corresponds to the angular subtense of 0.5° separation at about 50cm viewing distance. The arrangement of colour-difference pairs in gap viewing condition is shown in Fig.3-5.

Colour-difference stimuli were illuminated by the THORN EMI tubes simulating Illuminant D65. The 0/45 illumination/viewing geometry was used. Within viewing geometry the observers were allowed to freely change the position of standard pair and sample pair in each presentation, and also the order of presentations was completely randomised by the experimenter to avoid non-random judgements.

3.5.2 Observer judgements

Twelve to 15 observers, mainly postgraduate students of the Colour Chemistry Department of the Leeds University, took part in the visual tests. The number of judgements for each parametric viewing conditions in each part of tests are summarised in Table 3-6.

Table 3-6. Summary of observer judgements.

Part	Scale method	Number							
		Colour	Pair	Observer		Judgement			
						Grey	Black	White	Gap
1	PC[a]	1	45	15		60	30	30	30
2	PC[a]	13	105	12		14	14	14	-
	GS[b]	13	105	12		12	12	12	12
3	GS[b]	21	98	10	OG[c]	10	10	10	10
				1	DK[d]	10	10	10	10
				1	CY[e]	10	10	10	10

(a) Paired-comparison method, (b) Grey-scale method
(c) Observer group, (d) Observer DK, (e) Observer CY

Before the main test each observer examined the Ishihara test [9]. There were no colour defectives. Observers also read the judgement instruction before the test. Those for the paired-comparison and the grey-scale methods are given below.

Standard Pair (No.2)

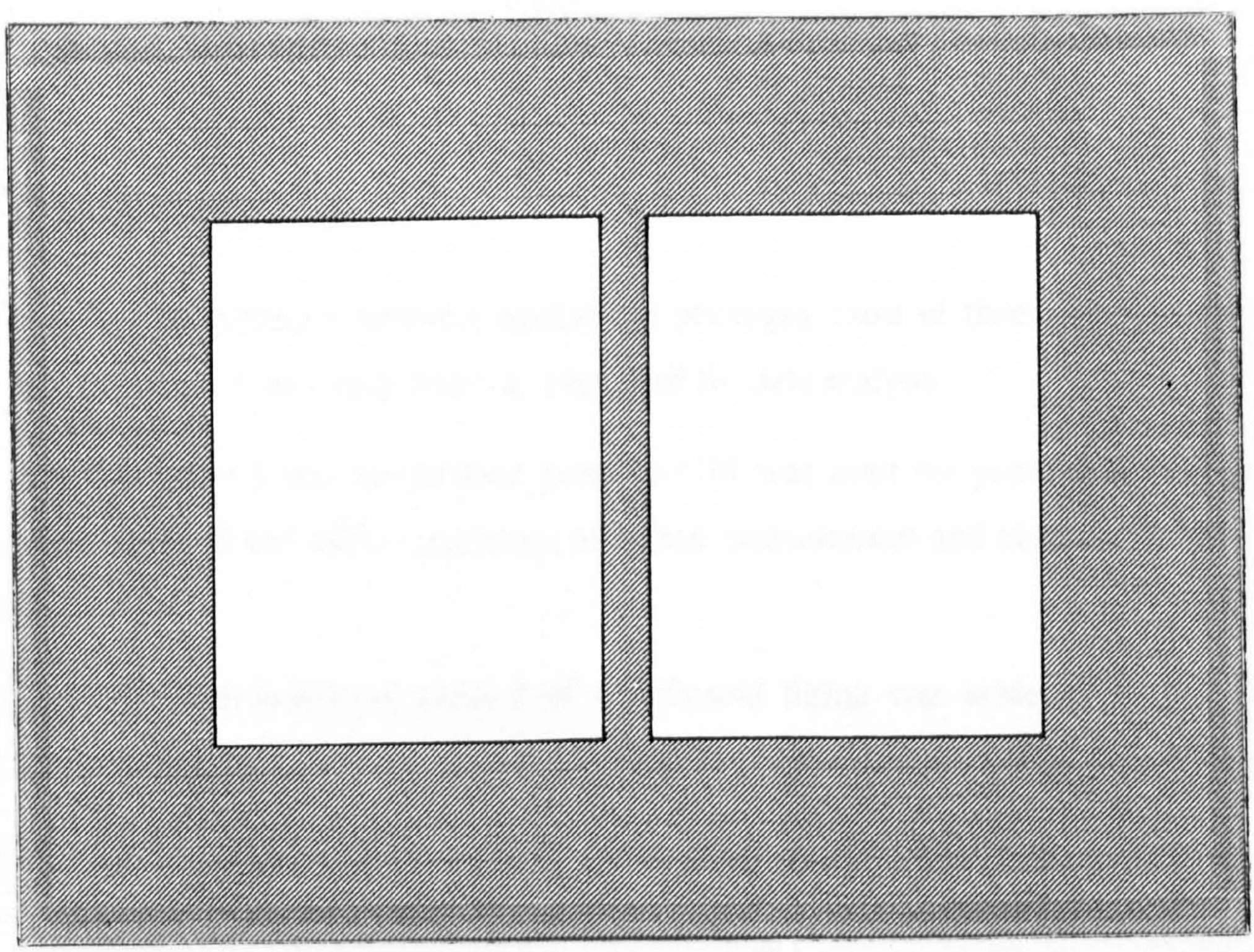

Test Pair (with Gap)

Figure 3-5. Arrangement of colour-difference pairs (actual sizes) in a paired-comparison method.

3.5.2.1 Paired-comparison method

This test is intended to investigate the appearance of small colour differences. Your task is, first, to take the test colour-difference pairs one by one and then to compare the colour-difference of a test pair to that of the standard pair. If it is thought to be smaller, then say '0'(zero) or 'no'. If it were larger, say '1'(one) or 'yes'.

3.5.2.2 Grey-scale method

This observer test is intended to study the appearance of small colour differences. Your task is to take the test colour-difference pairs one by one, and to compare the colour-difference of a test pair to those of grey scales (GS). Then, estimate the closest GS-grade. Answers are to be given up to 1 decimal place (e.g., grade 7.2, grade 4.6).

[The observer uncertainties of the present study are given in Section 5.3.]

3.6 Software Packages

The following computer software application packages, most of them provided by the Leeds University Computing Service, were used for data analysis.

The Microsoft Excel spreadsheet program [10] was used for processing raw data: storage, retrieval and basic calculation of colour measurement and observer judgement data.

The maximum-likelihood method of an ellipsoid fitting was achieved by use of a simplex routine (written in QuickBASIC) in the Numerical Recipes example book [11].

For the least-square ellipsoid fitting, the fit program of the Microcal Origin graphics software [12] was used. The Origin was also used to draw most of the graphs of the thesis.

The statistical package SPSS [13] was used for both the probit and the principal component analyses (PCA). The PCA was done using the EIGEN procedure of the SPSS built-in matrix language, which returns eigenvectors and eigenvalues of a symmetric matrix. Ellipsoid principal axes were also calculated by this procedure.

3.7 References

1. A.R.Robertson, CIE Guidelines for Coordinated Research on Colour-Difference Evaluation, Col. Res. Appl., **3**, 149-151 (1978).

2. C.J.Bartleson and F.Grum (Eds.), Optical Radiation Measurements, Vol.5: Visual Measurements, Academic, London, 1984.

3. BS1006: Colour Fastness of Textiles and Leather, A02: Grey Scale for Assessing Change in Colour, BSI, 1990.

4. Clariant (UK) Ltd., Pigments & Additives, Calverley Lane, Horsforth, LEEDS LS18 4RP.

5. PaintMatch (Version 6.74) User's Manual, Colourgen Ltd. (Available from J.H.Nobbs, Department of Colour Chemistry and Dyeing, University of Leeds, LEEDS LS2 9JT)

6. RK Print-Coat Instruments Ltd., South View Laboratories, Litlington, Royston, HERTS SG8 0QZ.

7. Colorgen Ltd. (X-Rite Ltd.), Lower Walshford Mill, Millstreet, Buglawton, Congleton, Cheshire CW12 2AD.

8. D.S.J.Atkin, E.Coates and B.Rigg, Effects of Gloss on Colour-Difference Measurements, JSDC, **97**, 333-334 (1981).

9. S.Ishihara, Tests for Colour-Blindness, 2nd ed., Kanehara Shuppan, Tokyo, 1959.

10. Microsoft Excel (Version 5.0) User's Guide, Microsoft Corporation, 1993-1994.

11. J.C.Sprott, Numerical Recipes: Routines and Examples in Basic, Cambridge Univ. Press, New York, 1991.

12. Origin (Version 3.78) User's Manual, Microcal Software Inc., One Roundhouse Plaza, Northampton, MA 01060, USA.

13. M.J.Norusis, SPSS for Windows: Advanced Statistics (Release 6.0), SPSS Inc., USA, 1993.

4. RESULTS AND DISCUSSION
PART I - 5 CIE COLOUR CENTRES

The results of colour discrimination around the 5 CIE colour centres [1], confined to the reference condition (grey background), are covered in this chapter. The full set of results is given in Tables A-2 to A-4 in Appendix 1. The detailed description and discussion about the results of parametric effects (background and gap), observer variability, and colour measurement error are covered in Chapter 5.

4.1 Red Centre

As was intended, the red colour centre was used to test the data analysis methods: logistic and probit models. The following Tables 4-1 and 4-2 show the detailed description of the logistic and the probit analyses that produced Figs. 4-1 and 4-2.

Table 4-1. Logistic model.

(a) Ellipsoid coefficients and principal axes

Param. Estimate Model: $P_i = \dfrac{1}{1+e^{\alpha-\beta\Delta E_i}}$

$$\Delta E^2 = b_{11}(\Delta a^*)^2 + b_{22}(\Delta b^*)^2 + b_{33}(\Delta L^*)^2 + 2b_{12}\Delta a^*\Delta b^* + 2b_{13}\Delta a^*\Delta L^* + 2b_{23}\Delta b^*\Delta L^*$$

Ellipsoid Coeff.

b_{11}	b_{22}	b_{33}	b_{12}	b_{13}	b_{23}	α	$\beta(=\alpha/\Delta E_{std})$	ΔE_{std}
4.80	**6.32**	**23.51**	**-3.44**	**-3.93**	**5.86**	**4.34**	**3.94**	**1.10**
0.31	0.41	1.51	-0.22	-0.25	0.38	($\leftarrow b_{ik}$ divided by β^2)		

Mean (μ) and Standard Deviation (σ)

$\mu = \alpha / \beta = \Delta E_{std} = 1.10$

$\sigma = 1.7 / \beta = 0.43$

Coeff. Matrix

$B =$

0.31	-0.22	-0.25
-0.22	0.41	0.38
-0.25	0.38	1.51

Axis	λ	u	v
C	**1.70**	-0.23	0.33
B	**0.40**	1.66	-1.83
A	**0.13**	-17.96	-15.70

Axis	ΔL^*	Δa^*	Δb^*	**length**	ϕ	θ
A	0.12	-2.09	-1.83	**2.78**	-138.8	87.6
B	0.59	0.98	-1.09	**1.58**	-47.9	68.0
C	0.71	-0.17	0.24	**0.77**	125.3	22.1

Table 4-1. (Continued)

(b) Ellipsoid tilting (→ displacement of the highest point)

$$\Delta L^*_m = \left[\frac{B_{33}}{|B|}\right]^{1/2} = 0.93$$

$$\Delta a^*_m = \left(\frac{b_{12}b_{23} - b_{22}b_{13}}{b_{11}b_{22} - b_{12}^2}\right)\Delta L^*_m = 0.24$$

$$\Delta b^*_m = \left(\frac{b_{12}b_{13} - b_{11}b_{23}}{b_{11}b_{22} - b_{12}^2}\right)\Delta L^*_m = 0.74$$

(c) Ellipse parameters for each plane

In the a*b* plane, $\theta = 0.5\tan^{-1}\left(\frac{2b_{12}}{b_{11} - b_{22}}\right) = 38.8$

$$A = \frac{1}{\sqrt{b_{22} + b_{12}\cot\theta}} = 2.76$$

$$B = \frac{1}{\sqrt{b_{11} - b_{12}\cot\theta}} = 1.31$$

Plane	θ	A	B
a*L*	11.4	1.97	0.80
b*L*	162.9	1.86	0.78

Table 4-1. (continued)

(d) Colour-difference values and observer responses (total number of judgements: 60). The calculated values are for the ellipsoid model in Table 4-1-a.

Pair No.	Colour Difference ΔL^*	Δa^*	Δb^*	Freq. (Obs.) Unfiltered	Filtered	Prob. (P_i) Obs/Unfil	Cal.
RA1	0.54	0.04	0.11	**2**	2	**0.03**	0.17
RA2	0.80	0.18	-0.05	**12**	10	**0.20**	0.35
RA3	1.33	-0.06	-0.17	**38**	38	**0.63**	0.88
RA4	1.57	0.02	-0.06	**50**	50	**0.83**	0.96
RA5	1.68	0.09	-0.24	**49**	58	**0.82**	0.97
RB1	0.18	1.00	-0.07	**6**	3	**0.10**	0.10
RB2	0.24	1.41	-0.04	**12**	8	**0.20**	0.19
RB3	0.06	1.98	0.09	**22**	24	**0.37**	0.44
RB4	-0.11	2.32	0.56	**41**	38	**0.68**	0.55
RB5	-0.07	2.47	0.49	**39**	53	**0.65**	0.63
RC1	-0.06	0.02	0.89	**0**	0	**0.00**	0.10
RC2	-0.15	-0.08	1.09	**2**	1	**0.03**	0.15
RC3	0.00	-0.17	1.30	**10**	10	**0.17**	0.30
RC4	0.03	0.03	1.60	**46**	36	**0.77**	0.43
RC5	-0.03	0.04	2.01	**39**	52	**0.65**	0.64
RD1	0.01	1.02	1.10	**2**	0	**0.03**	0.11
RD2	0.00	1.47	1.23	**7**	1	**0.12**	0.17
RD3	0.03	1.43	1.57	**6**	5	**0.10**	0.24
RD4	0.00	1.64	1.70	**17**	17	**0.28**	0.29
RD5	-0.02	2.50	2.37	**41**	45	**0.68**	0.65
RE1	0.00	-0.87	0.77	**11**	6	**0.18**	0.29
RE2	-0.04	-1.02	1.04	**14**	15	**0.23**	0.49
RE3	-0.11	-1.20	1.03	**26**	24	**0.43**	0.53
RE4	-0.01	-1.29	1.20	**45**	45	**0.75**	0.71
RE5	-0.08	-1.31	1.59	**52**	55	**0.87**	0.84
RJ1	0.60	0.63	0.06	**2**	1	**0.03**	0.17
RJ2	0.70	0.95	0.09	**15**	9	**0.25**	0.26
RJ3	0.95	1.16	-0.08	**39**	33	**0.65**	0.50
RJ4	0.94	1.47	0.09	**37**	50	**0.62**	0.54
RJ5	1.63	1.65	0.13	**60**	60	**1.00**	0.96
RK1	-0.35	0.51	0.10	**1**	1	**0.02**	0.11
RK2	-0.55	0.77	-0.09	**49**	38	**0.82**	0.37
RK3	-1.02	1.18	0.06	**46**	56	**0.77**	0.87
RK4	-1.45	1.38	0.00	**59**	59	**0.98**	0.99
RK5	-1.57	1.95	-0.03	**60**	60	**1.00**	1.00
RL1	0.26	-0.06	0.26	**2**	0	**0.03**	0.07
RL2	0.41	-0.02	0.41	**32**	24	**0.53**	0.16
RL3	0.52	-0.04	0.68	**34**	41	**0.57**	0.35
RL4	0.81	0.02	0.91	**53**	54	**0.88**	0.74
RL5	1.59	-0.03	1.13	**59**	59	**0.98**	0.99
RM1	-0.45	-0.03	0.31	**2**	0	**0.03**	0.08
RM2	-0.67	0.00	0.71	**6**	6	**0.10**	0.19
RM3	-1.00	0.12	0.96	**39**	33	**0.65**	0.48
RM4	-1.08	0.04	1.13	**45**	53	**0.75**	0.57
RM5	-1.58	-0.03	1.45	**60**	60	**1.00**	0.91

Table 4-2. Probit model (for vector direction A).

(a) Principal component analysis (PCA)

Sample	L^*	a^*	b^*
RA1-L	45.27	37.07	22.80
RA2-L	45.14	37.00	22.88
RA3-L	44.88	37.12	22.94
RA4-L	44.76	37.08	22.88
RA5-L	44.70	37.05	22.97
RA1-R	45.81	37.11	22.91
RA2-R	45.94	37.18	22.83
RA3-R	46.21	37.06	22.77
RA4-R	46.33	37.10	22.82
RA5-R	46.38	37.14	22.73

① Simple Statistics

	L^*	a^*	b^*
Mean	45.54	37.09	22.85
StD	0.63	0.05	0.07

② Covariance Matrix

	L^*	a^*	b^*
L^*	0.3994	0.0134	-0.0352
a^*	0.0134	0.0023	-0.0009
b^*	-0.0352	-0.0009	0.0052

③ Eigenvalues of the Covariance Matrix

	Eigenvalue	Proportion	Cumulative
PC1	0.4030	0.9902	0.9902
PC2	0.0023	0.0057	0.9960
PC3	0.0016	0.0040	1.0000

④ Eigenvectors

	PC1	PC2	PC3
L^*	-0.996	-0.054	0.077
a^*	-0.034	-0.561	-0.827
b^*	0.088	-0.826	0.556

(b) Probit analysis

Param. Estimate Model: $z(P_i) = c_0 + c_1 \cdot \Delta E^*$

c_0 or c_1	Reg. Coeff.	Std. Err.	Coeff./S.E.
c_0	-3.3859	0.3267	-10.3643
c_1	2.8518	0.2506	11.3811

Pearson Goodness-of-Fit $\chi^2 = 2.28$, DF = 3, P:$\chi^2 = 0.52$

Mean (μ) and Standard Deviation (σ)

$\mu = -c_0 / c_1 = 1.1873$

$\sigma = 1 / c_1 = 0.3507$

95% Confidence Limits for μ

Prob.	$\Delta E^*(\mu)$	Lower CL	Upper CL
0.50	1.1873	1.1189	1.2519

Observed and Expected Frequencies

ΔE^*	Tot. No.	Freq.		Resid.	Prob.
	Obs.	Obs.	Exp.		Exp.
0.55	60	2	2.08	-0.08	0.0346
0.82	60	10	8.85	1.15	0.1475
1.34	60	38	40.11	-2.11	0.6684
1.57	60	50	51.75	-1.75	0.8625
1.70	60	58	55.69	2.31	0.9282

For the comparison of the two analysis methods, the fit of observer responses (from two methods) to the assumed normal distribution was examined first. In Fig.4-1, observer probability for positive (larger than) responses are plotted against the calculated colour differences. Fig.4-1-a shows the unfiltered probability vs. colour-difference calculated from the fitted ellipsoid equation, and Fig.4-1-b shows the filtered probability vs. CIELAB colour-difference normalised by the mean tolerance for each vector direction obtained by the probit method. These correspond to the logistic model and the probit model, respectively. The parameters α and β of the logistic curve in fig.(a) are 4.34 and 3.94, respectively. As reviewed earlier (Fig.2-1), we can estimate the standard deviation of the observer judgements by use of the logistic curve. Regarding the colour-difference magnitude of the standard pair ($\Delta E^* = 1.1$) as the mean, then the standard deviation is approximated as $\sigma = 1.7/\beta = 0.43$. Thus, the coefficient of variation (CV) of the logistic model is 39%. The average CV for the 9 vector directions of the probit analysis is 24%. The two figures in Fig.4-1 show these facts. In the logistic model the data points are more scattered about the cumulative normal (logistic) curve, while in the probit model they are rather better fitted to a steeper logistic curve (bold line). The increase of the slope of the fitted logistic curve means a decrease in the population standard deviation (Fig.2-1). It could be confirmed by the following simple calculation. That is, the α and β parameters of the logistic curve in fig.(b) estimated are 7.01 and 6.42, respectively. It produces $\mu = 1.09$ and $\sigma = 0.26$, and thus a CV of 24% (which is interestingly exactly the same value as that obtained from the probit model). The reduction of the experimental variability in the results of the probit model is more or less expected, because the ΔE values in fig.(a) were obtained from only 1 ellipsoid equation while those in fig.(b) were from 9 regression equations.

Fig.4-2 displays the chromaticity ellipses from logistic function and the tolerance vectors from probit analysis. As shown in the figures, the main differences between the ellipse and the vectors occurred along the lightness and hue directions (roughly equivalent to the vector directions A and E, respectively). Robertson [1] claimed that the deviations from ellipsoidal contours of equal perceived colour-difference might occur in the direction of the dichromatic confusion points in CIExyY space. As long as we represent the colour-discrimination boundary as the ellipse (or the ellipsoid), it seems that the disagreement is inevitable. At present, there is no way to represent the contour into one single measure other than the ellipsoid.

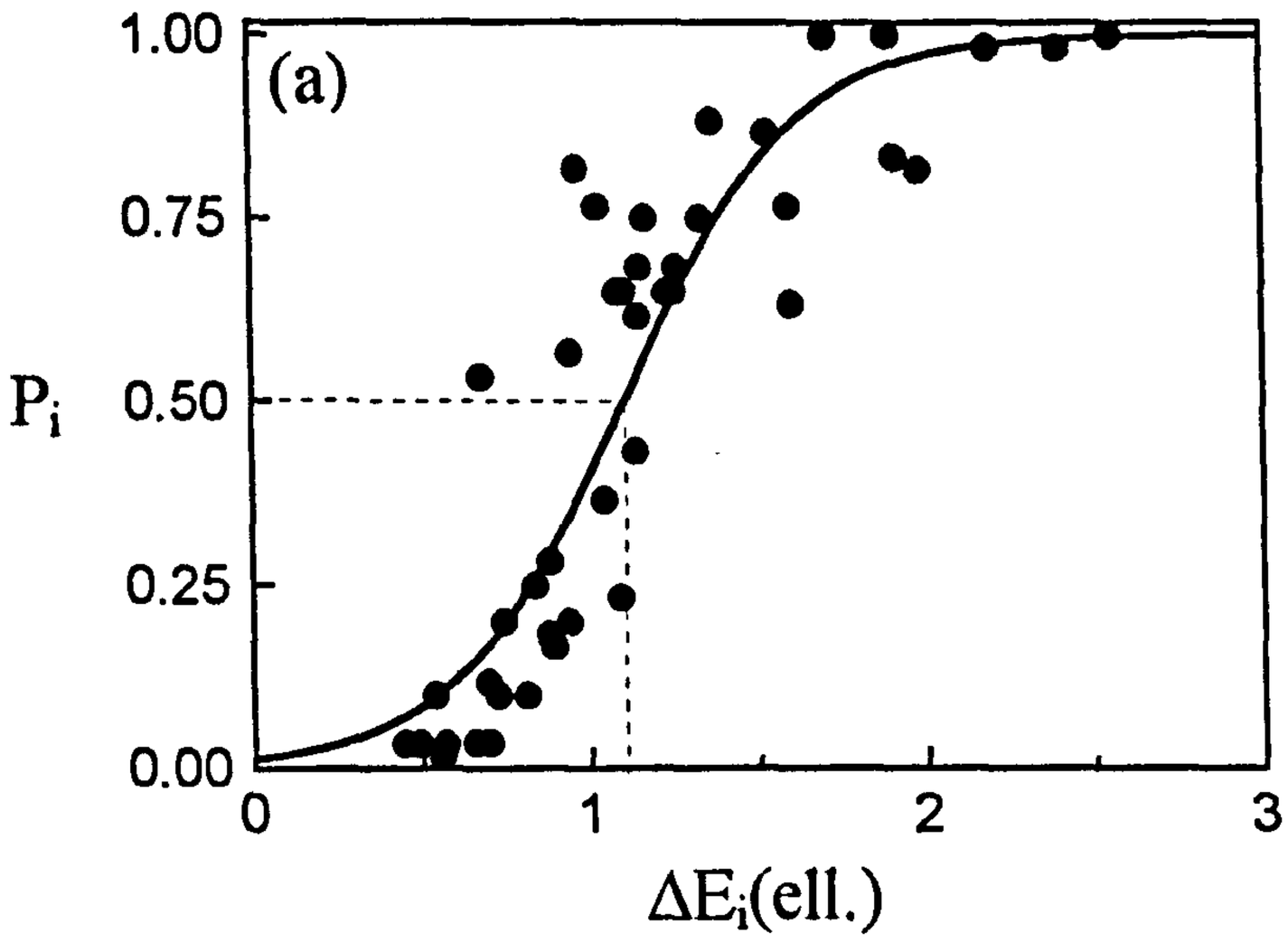

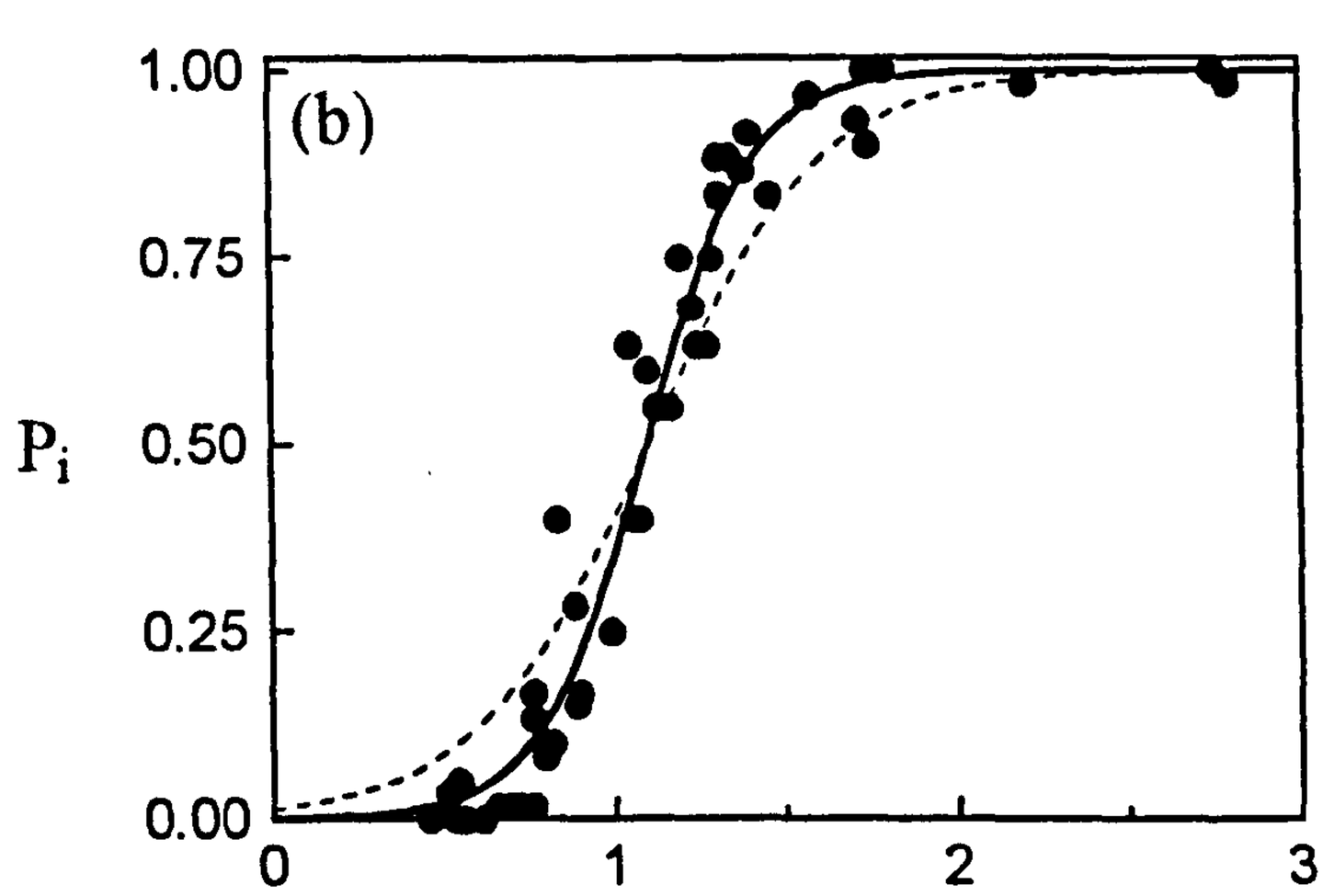

Figure 4-1. Probability of "greater" judgement vs. colour-difference calculated by: (a) logistic model, and (b) probit model.

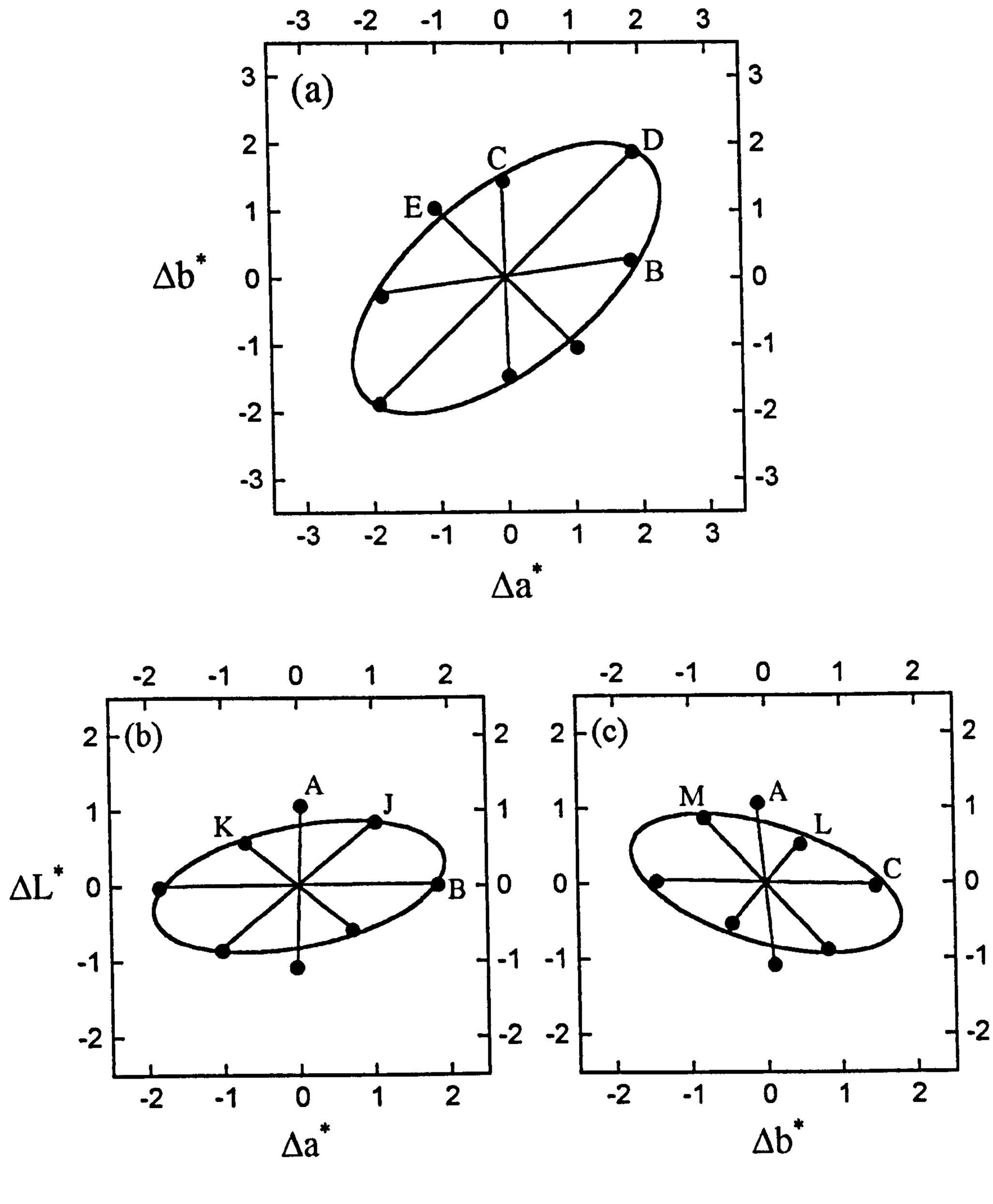

Figure 4-2. Chromaticity ellipses from maximum-likelihood method using logistic function and tolerance vectors from probit analysis: (a) a^*b^*, (b) a^*L^*, and (c) b^*L^* planes.

The ellipse parameters and the tolerance vectors of the red centre for other parametric conditions are given in Tables A-5 and A-6 in Appendix 2.

The problem of the probit analysis (more precisely, the paired-comparison method) is that it is desirable but not always possible to sample test colour-difference pairs which have a similar visual difference to that of the standard pair. (Section 3.2.5) In the study of the parametric effects, the observer sensitivity would vary greatly from one viewing condition to another in addition to the inherent variability of the experiment. The application of the probit analysis for all parametric conditions therefore seems to be undesirable.

Also, it is thought to be rather cumbersome to apply the probit model to the data analysis. That is, the tolerance vectors are obtained from 9 probit analyses and 9 principal component analyses (in this study), while the logistic colour-difference ellipsoid can be obtained from several repeated fittings (normally less than 10 times) of the data.

Table 4-3 shows the fit of major colour-difference formulae to the visual results. Smaller values (generally regarded as the better performance) in the case of the probit model do not mean the superiority of the probit analysis to the logistic model as it may be due to the uses of the filtering algorithm (Section 2.1.1.3) and the different type of measure. The CIE94 formula shows slightly better fit than CMC or BFD, but there is no significant difference between these 3 formulae for the red centre.

Table 4-3. Measures of fit for red centre.

Data analysis method	**Measure**	CIELAB	CMC (1:1)	BFD (1:1)	**CIE94** (1:1:1)
Logistic (unfiltered data)	**CV (%)**	45	29	31	**28**
Probit (filtered data)	**TSD (%)**	40	20	21	**19**

In summary, both the logistic and the probit models produced virtually identical results but the probit analysis yielded more uniform results because it is experimentally and computationally a more intensive method than the logistic analysis.

4.2 Grey Centre

The colour co-ordinates and the observer responses for the tests around the grey centre are given in Table A-3 (Appendix 1). The results of the fitting process are summarised in Table A-7 (Appendix 2).

The difficulty of evaluating colour-difference of the grey (achromatic) samples arises from the fact that the partition of total colour-difference to its components usually does not correspond to true visual results. Hence, in the BS 6923 [2], it was recommended that "for the colours of $C^* \leq 4$ the partition of total colour-difference is only valid for lightness difference and not for that of chroma or hue."

As shown in Table 4-5, the use of hue-angle dependence terms in both CMC and BFD does not seem to improve the fit of these formulae to visual results compared to CIELAB (CIE94). The average colour co-ordinates of the grey centre produced were $L^* = 50.0$, $a^* = -0.4$, $b^* = 0.6$. The lengths of semi-axes of the unit ellipse for the neutral grey colour ($a^* = b^* = 0$) calculated by CMC, BFD, and CIE94 formulae are shown in Table 4-4.

Table 4-4. Semi-axes lengths of CMC, BFD, and CIE94 unit ellipses.

Formula	S_C	S_H
CMC	0.638	0.638
BFD	0.521	0.521
CIE94	1.000	1.000

All three formulae assume the circular boundary of chromaticity discrimination and their lengths are to be equal regardless of the lightness of the samples. The results from this study showed that this is not the case. The colour-difference ellipse is slightly oriented towards the b^* axis and the ratio of minor axis to major axis lengths is about 0.6.

Therefore, the ellipse shape of neutral samples were checked by analysing earlier data sets; that of Luo [3] (translated to CIELAB by Melgosa [4]), and Berns [5]. Interestingly, Table 4-6 and Fig.4-3 showed that in most cases the ellipses obtained were all toward to b^* axis ($\theta \cong 95°$) and the minor to major axes ratio was average 0.6.

The first attempt to correct the anomalies with near neutral samples was, thus, simply change the weightings of Δa^* and Δb^* in the CIELAB formula.

$$\Delta E = \left[\left(\Delta L^*\right)^2 + \left(\frac{\Delta a^*}{0.6}\right)^2 + \left(\Delta b^*\right)^2 \right]^{1/2} \qquad (4\text{-}1)$$

The fit of Eq.(4-1) to grey samples was checked by use of data from this study, from Berns (three greys, $L^* \cong 14$, 59 and 83, respectively), and Cheung [6] (one grey $L^* = 62$, textile samples). The results were very satisfactory. The empirical Eq.(4-1) out-performed the other 4 formulae. (Table 4-5)

From Table 4-6, it seems that the ellipse sizes of the neutral samples are dependent upon the lightness of samples rather than chroma or hue. If we fix the minor to major axes ratio, then we could propose a simple relationship of the length of the major semi-axis to the L^* of the sample.

The three ellipses from Berns data were systematically bigger than other ellipses from Luo data. Thus, all 3 major semi-axes lengths were divided by that of $L^* \cong 59$. The relation between L^* and major semi-axes lengths (approximately tolerance along b^* axis) are plotted in Fig.4-4.

The new ΔL^* weighting function S_L (obtained independently from this study; see Chapter 5) would probably be used for the weighting of both ΔL^* and Δb^* as well as $\Delta a^*/0.6$ without causing any further complication. That is,

$$\Delta E = \frac{1}{S_L}\left[\left(\Delta L^*\right)^2 + \left(\frac{\Delta a^*}{0.6}\right)^2 + \left(\Delta b^*\right)^2 \right]^{1/2} \qquad (4\text{-}2)$$

where $S_L = 0.95 - 0.009\,L^* + (0.014\,L^*)^2$. The form of S_L is shown by the curve in Fig.4-4.

Eq.(4-2) was also tested using the same data sets. The results were nearly identical to those from Eq.(4-1). It is certain that we could make the empirical colour-difference formula for neutral samples ($C^* \leq 4$) by simple modification of the CIELAB formula. However, it is not easy to incorporate it to the existing weighted CIELAB formulae as it could cause the discontinuity of colour-difference calculation and makes the formula quite complicated.

It is interesting that the relation between L^* and major axes of grey samples is very similar to a new lightness weighting function.

Table 4-5. Measures of fit for grey centre.

Data	Measure	CIELAB (CIE94)	CMC (1:1)	BFD (1:1)	ΔE_{GC1}[a]	ΔE_{GC2}[b]	ΔE_6[c]
This Study[d] (29 pairs)	PF/4	26	**22**	23	18	-	13
Berns (24 tol.)	TSD (%)	**21**	28	26	19	20	-
Cheung[e] (68 pairs)	PF/4	**25**	30	36	24	23	14

(a) $$\Delta E_{GC1} = \left[\left(\Delta L^*\right)^2 + \left(\frac{\Delta a^*}{0.6}\right)^2 + \left(\Delta b^*\right)^2 \right]^{1/2}$$

(b) $$\Delta E_{GC2} = \frac{1}{\ell S_L} \left[\left(\Delta L^*\right)^2 + \left(\frac{\Delta a^*}{0.6}\right)^2 + \left(\Delta b^*\right)^2 \right]^{1/2}$$

where $S_L = 0.95 - 0.009 L^* + (0.014 L^*)^2$ (→ See Chapter 5)

(c) Optimised ellipsoid equation

(d) Results from the grey-scale method

(e) All formulae tested with setting $\ell = 1.5$

Table 4-6. Ellipse parameters of neutral samples.

Data Set		Centre Co-ordinates			Ellipse Parameter			
		L^*	C^*	h°	θ	A	B/A	Area
Luo	MCD 14	37.6	0.6	65	62.3	0.71	0.67	1.08
	MMB DG	38.3	0.4	29	82.9	0.74	0.67	1.15
	BFD CA43	45.2	3.8	222	136.3	0.88	0.85	2.07
	CISCC GY	53.0	0.3	142	104.1	1.04	0.64	2.17
	MCD 33	54.2	1.0	86	77.3	0.95	0.79	2.24
	CIE GY	61.3	0.6	34	86.8	0.98	0.57	1.72
	MMB SG	66.6	3.9	116	112.0	1.21	0.55	2.50
	VVVR W	87.0	4.1	240	87.9	1.37	0.57	3.37
	BFD AAK37	90.8	2.6	145	92.5	1.71	0.43	3.96
Berns	Black	14.1	0.6	137	95.0	1.47	0.54	3.64
	Medium gray	59.4	1.3	126	101.0	1.49	0.54	3.79
	Light gray	83.5	0.4	35	103.7	2.55	0.38	7.88
This Study[a]		50.0	0.7	119	87.2	0.96	0.52	1.52
Overall					**94.7**		**0.60**	

(a) Average results of both a paired-comparison and a grey-scale methods

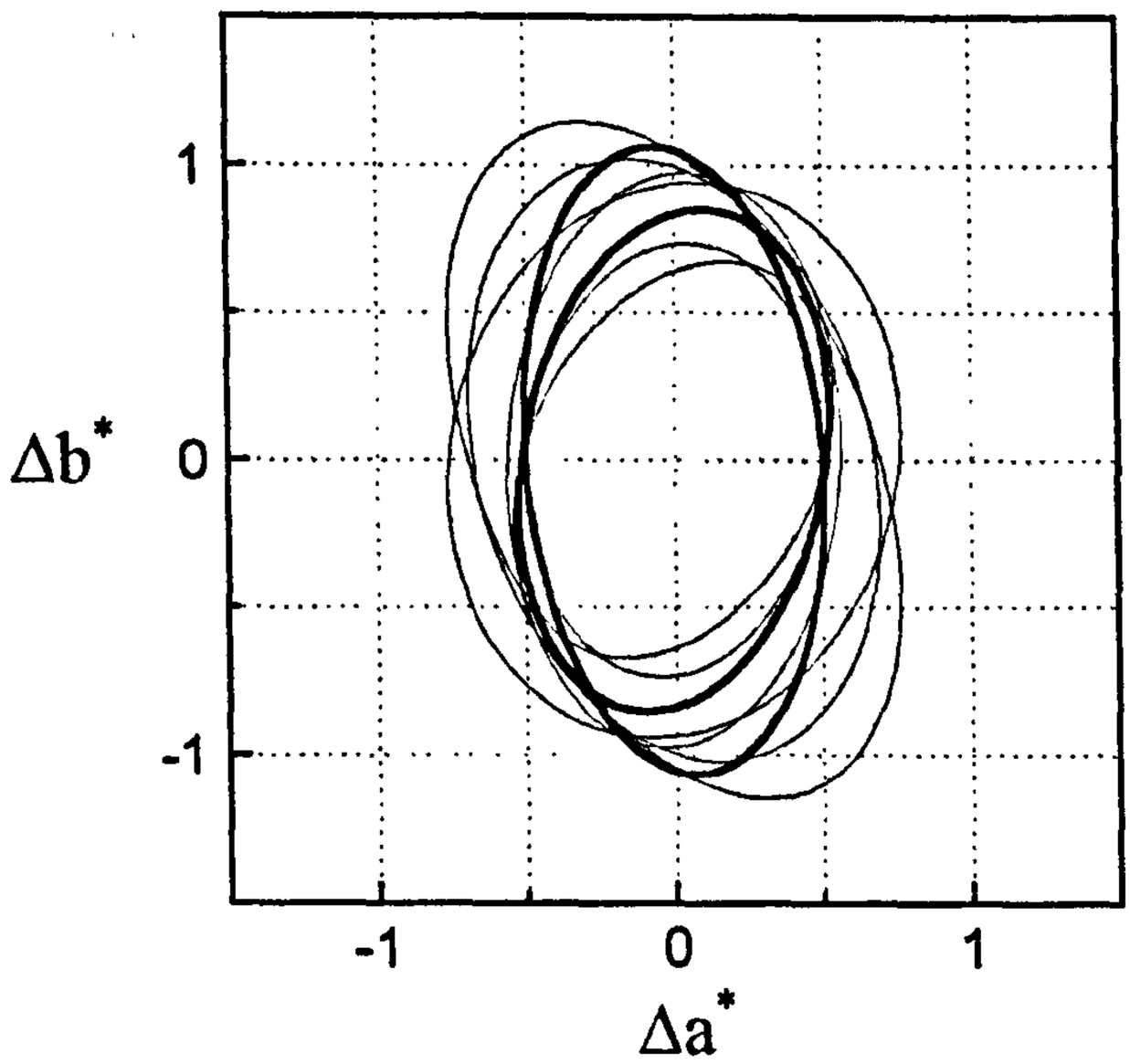

Figure 4-3. Chromaticity ellipses for neutral colours (bold lines: this study)

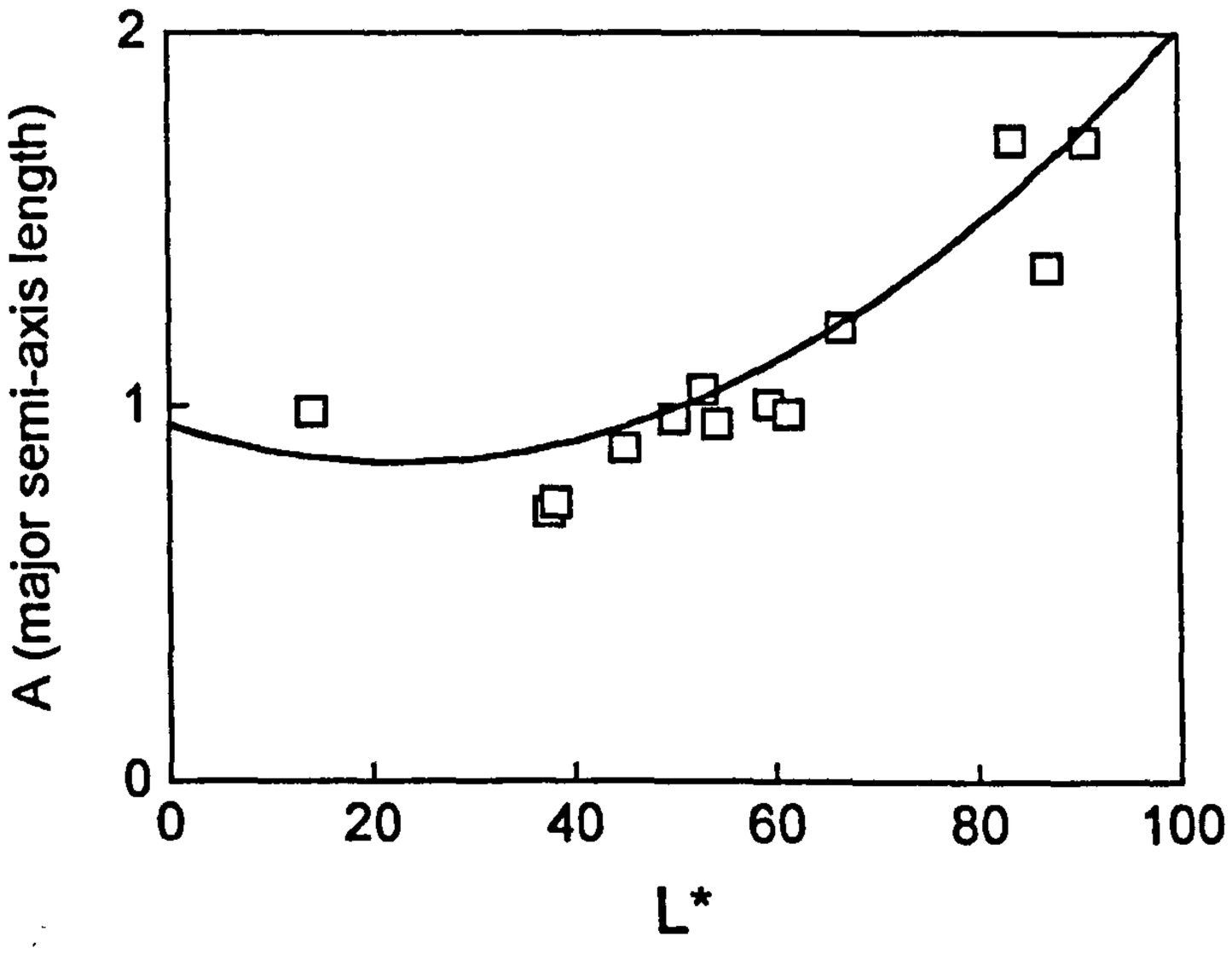

Figure 4-4. Dependency of the length of major semi-axis to L^* in grey samples.

4.3 Blue Centre

The colour co-ordinates and the observer responses for the tests around the blue centre are given in Table A-3 (Appendix 1). The results of the fitting process are summarised in Table A-8 (Appendix 2).

As claimed by Luo [7] and implied by the BFD formula, the chromaticity-discrimination ellipses are not always toward to the origin in a^*b^* plane. The degree of ellipse rotation is also known to be prominent in the blue region ($h^\circ \cong 270$). Like most of earlier worker's data [3,5], it is again confirmed by the data from this study (Table 4-7). Thus, in effect, either a $\Delta a^*\Delta b^*$ or a $\Delta C^*\Delta H^*$ term is needed for the more exact calculation of a colour-difference.

The ellipse in the a^*b^* chromaticity plane and corresponding ellipse parameters can be easily converted to $\Delta C^*\Delta H^*$ microplane. The a^*b^* ellipse is defined as Eq.(2-29).
The ellipse parameters θ, A, and B calculated from ellipse coefficients b_{ik} are given by Eqs.(2-37) and (2-38).
Conversely, b_{ik} values in terms of θ, A, and B are given by Eq.(2-39).

In the C^*H^* ellipse, A and B are retained but θ is replaced by $\Delta\theta$ -orientation from the hue angle h° (Fig.2-4). The ellipse equation, parameters and coefficients of a C^*H^* ellipse are given by Eqs.(2-40), (2-41), and (2-42), respectively.

The conversion to and from between b_{ik} and s_{ik} is also given by Eqs.(2-44) and (2-43) respectively.

The BFD unit ellipse is given by

$$\Delta E^2 = \left(\frac{\Delta C^*}{D_C}\right)^2 + \left(\frac{\Delta H^*}{D_H}\right)^2 + R_H R_C \frac{(\Delta C^*)(\Delta H^*)}{D_C D_H} \qquad (4\text{-}3)$$

The coefficients of the rotation term ($R_H R_C / D_C D_H$) seem to be redundantly over-complicated as both R's and D's are dependent on chroma and hue-angle.

Let us set the general form of the colour-difference formula as below:

$$\Delta E = \left[\left(\frac{\Delta L^*}{S_L}\right)^2 + \left(\frac{\Delta C^*}{S_C}\right)^2 + \left(\frac{\Delta H^*}{S_H}\right)^2 + S_R(\Delta C^*)(\Delta H^*)\right]^{1/2} \qquad (4\text{-}4)$$

Ignoring the first term in the right side (lightness tolerance) and comparing Eq.(2-40) with Eq.(4-4) and the first equation of Eq.(2-41) leads to the following:

$$s_{11} = \frac{1}{S_C^{\,2}} \qquad s_{22} = \frac{1}{S_H^{\,2}}$$

$$S_R = 2s_{12} = \tan(2\Delta\theta)(s_{11} - s_{22})$$

$$\therefore \quad S_R = \tan(2\Delta\theta)\left(\frac{1}{S_C^{\,2}} - \frac{1}{S_H^{\,2}}\right) \tag{4-5}$$

S_R also could be expressed by the following form (by the third equation of Eq.2-42):

$$S_R = \sin(2\Delta\theta)\left(\frac{1}{A^2} - \frac{1}{B^2}\right) \tag{4-6}$$

The coefficient S_R accounts for the ellipse rotation similar to the BFD formula. Strictly speaking, S_C and S_H, and A and B are quite different when the extent of ellipse rotation is big enough, but to make the derivation of S_R as simple as possible, let us assume A = S_C and B = S_H. Also, it is assumed that $\Delta\theta$ varies only with h° and both S_C and S_H are only functions of metric chroma C^*. Then, Eq.(4-6) leads to

$$S_R = S_{RH} S_{RC} \tag{4-7}$$

where, $S_{RH} = \sin(2\Delta\theta) = f_1(h^\circ)$, and $S_{RC} = \left(\frac{1}{S_C^{\,2}} - \frac{1}{S_H^{\,2}}\right) = f_2(C^*)$.

The CIE94 formula assumes the same form of metric chroma dependence for both S_C and S_H, if we put this into $f_2(C^*)$, then the form of S_{RC} becomes:

$$S_{RC} = \frac{k_1 C^*}{(1 + k_2 C^*)^3} \tag{4-8}$$

By fitting the S_{RC} function to data obtained by using the CIE94 formula for S_C and S_H, we could obtain coefficients of Eq.(4-8). (Fig.4-5)

$$S_{RC} = \frac{-0.05463 C^*}{(1 + 0.02545 C^*)^3} \tag{4-9}$$

The variation of $\Delta\theta$ according to the change of h° follows the pattern shown in Fig.4-6 that is from Luo data [3,4] (also referring to Cui [8]). Eqs.(4-4) and (4-7) provide more comprehensive and direct information about ellipse rotation compared to the BFD formula. Furthermore, it is perfectly compatible with CIE94, but much simpler than BFD.

For example, if we assume the ellipse rotation occurs only in the blue region near

$235 < h° < 305$ and the maximum rotation angle is 35° at $h° = 270$, then $\Delta\theta$ could be the following form.

$$\Delta\theta = 0 \qquad \text{if } h° \le 235 \text{ or } h° \ge 305, \qquad \text{otherwise}$$

$$\Delta\theta = -\left[0.169(h° - 270)\right]^2 + 35 \qquad (4\text{-}10)$$

Above setting was checked for the blue samples by use of data from this study (average $h° = 262$), Berns (two blues, $h° = 267$ and 282, respectively), and Cheung (one blue, $h° = 280$). The results are quite satisfactory. (Table 4-7)

In conclusion, both CMC and CIE94 formulae are significantly improved by the inclusion of one more term which could reflects the ellipse rotation, and the method shown above is one kind of simple approach in a practical sense. The rotation term in the BFD formula is, in fact, over-complicated and is not soundly based on the ellipse geometry.

Table 4-7. Measures of fit for blue centre.

Data	Measure	CIELAB	CMC (1:1)	BFD (1:1)	CIE94 (1:1:1)	ΔE_{BC}[a]	ΔE_6[b]
This Study[c] (31 pairs)	PF/4	38	27	**19**	27	20	17
Berns (18 tol.)	TSD (%)	44	30	**17**	30	17	-
Cheung[d] (67 pairs)	PF'/3	46	32	**28**	32	29	20

(a) $$\Delta E_{BC} = \left[\left(\frac{\Delta L^*}{\ell S_L}\right)^2 + \left(\frac{\Delta C^*}{S_C}\right)^2 + \left(\frac{\Delta H^*}{S_H}\right)^2 + S_R(\Delta C^*)(\Delta H^*)\right]^{1/2}$$

where $S_R = S_{RH}\, S_{RC}$

$$S_{RC} = \frac{-0.05463C^*}{(1 + 0.02545C^*)^3}$$

$S_{RH} = \sin(2\Delta\theta)$

$\Delta\theta = 0$ if $h° \le 235$ or $h° \ge 305$, otherwise

$\Delta\theta = -[0.169(h° - 270)]^2 + 35$

and S_L, S_C and S_H are the same as those of CIE94.

(b) Optimised ellipsoid equation

(c) Results from the grey-scale method

(d) All formulae tested with setting $\ell = 1.5$

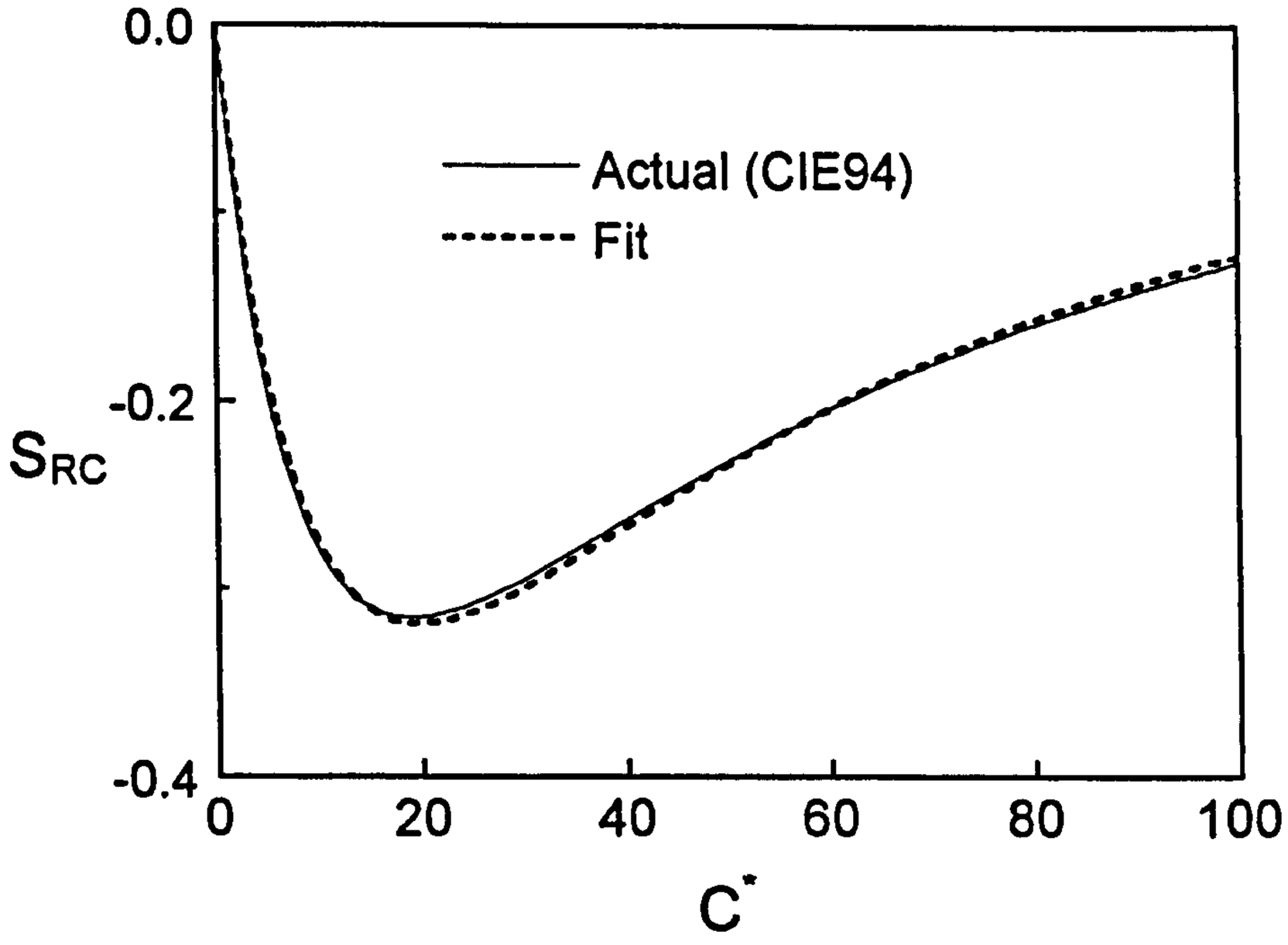

Figure 4-5. Variation of the ellipse-rotation coefficient(S_{RC}) with C^*.

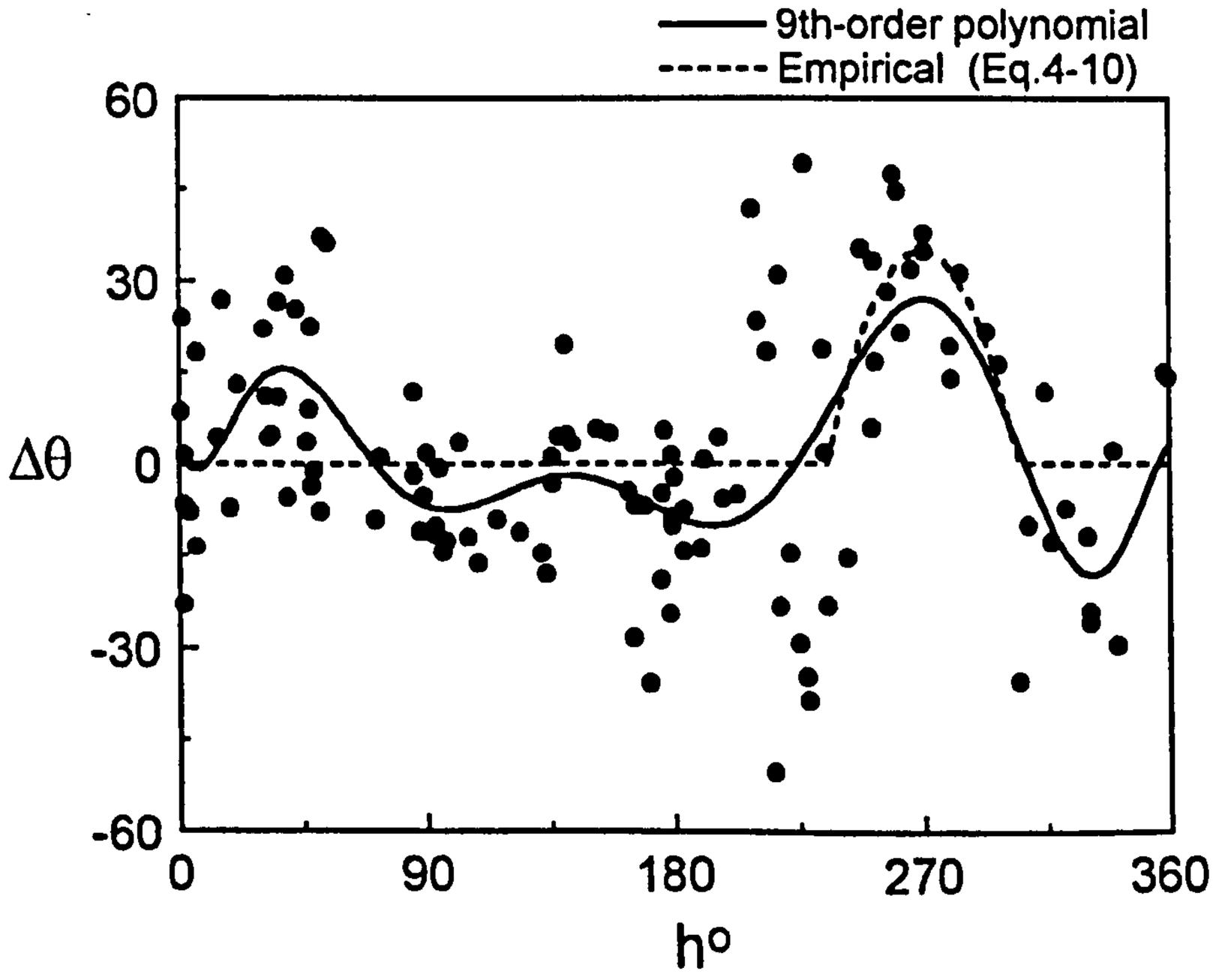

Figure 4-6. Relation between $\Delta\theta$ and h° from Luo data [3,4].

4.4 Yellow and Green Centres

For the yellow and the green centres, colour-difference pairs were not specifically prepared to obtain colour-difference ellipsoids. Using a small number of colour-difference pairs, the lightness tolerances and the chromaticity discrimination (around each of yellow and green centres) were investigated separately in Parts 2 and 3 of the experiments. Therefore, the experimental results and the discussions are not given independently in this section, but are dealt in the next section together with other CIE colour centres. The colour co-ordinates and observer responses of yellow and green pairs can be found in Tables A-3 and A-4 (Appendix 1). The coefficients and the parameters of the fitted ellipses for these centres are shown in Table A-10 (Appendix 3).

4.5 Comparison with Previous Studies

Two earlier studies – Cheung [6] and Berns (RIT) [5] – which include the colour difference ellipsoids for the 5 CIE colour centres were chosen for the comparison to those from this study. The Cheung data was obtained by use of textile samples and the ratio method while the Berns data was made by use of painted samples and the paired-comparison method / probit analysis. Only the results from the grey-scale method (under the grey background condition) of this study were used for the comparison. However, in the red colour centre of this study, the visual data is in a different form: i.e., observer response probability obtained by a paired comparison method. Hence, those from the logistic analysis were converted to the visual difference (ΔV) values and the ellipsoid was re-fitted by use of a least-square method. The parameters of the 5 fitted ellipsoids for each of three data sets are shown in Table 4-11.

Table 4-8. Number of sample pairs of three data-sets used in the comparison.

Colour Centre (abbr.)	Data Sets		
	Cheung	Berns[(a)]	This Study
GREY (N)	68	10	36
RED (R)	59	10	53
YELLOW (Y)	62	9	13
GREEN (G)	61	14	12
BLUE (B)	67	11	38
Total	317	54	152

(a) number of colour-difference tolerances

4.5.1 Overall fit of colour-difference formulae

CIELAB, CMC, BFD and CIE94 formulae were used to test the fit to the visual results. It seems to be meaningless to compare the performances of these formulae without adjusting the relative tolerances of the component colour differences, as all 3 data sets were made by use of different substrates and different scaling methods. Thus, setting the ℓ values (or K_L in CIE94) either 0.5, 0.67, 1, 1.5 or 2, the fit of each formula was tested. Tables 4-9 and 4-10 shows the performance testing results.

With optimised ℓ value, the BFD formula always fits best to all 3 data sets (Table 4-9), CMC and CIE94 follows the next showing similar performances while CIELAB shows the worst fit. The balance of the weighting between the lightness and chromaticness (both chroma and hue) differences in BFD seems to be rather wrongly adjusted. In many cases the BFD(0.67:1) formula showed the best fit to the perceptibility data, especially for painted samples [9-12]. This seems to be related to the fact that BFD was developed by use of the textile samples. That is, the optimum ℓ value of BFD for the Cheung data (textile samples) is close to 1 in Table 4-9. The BFD(0.67:1) formula is, in effect, equivalent to the BFD(1:1.5) formula. In other words, both the chroma and hue differences in BFD are fundamentally under-weighted compared to the lightness difference. Thus, as it is not always possible to adjust the relative tolerances in every case, it is better to increase the ΔC^* weighting function D_C in BFD by 1.5 times. Were it increased, the modified BFD(1:1), BFD(1.5:1) formulae would show best fits to the painted sample and textile sample data sets, respectively.

The different optimised ℓ values of the CMC, BFD and CIE94 formulae to the 3 data sets revealed the fact that these 3 formulae have different structures for weighting the component colour differences and calculating total colour difference. (This is further studied in Chapter 5 with a wider range of standard colour positions in the CIELAB space.)

For the blue centre, with identical ℓ value, the fit of BFD to the visual data is significantly better than CMC or CIE94. (Table 4-10) This, as was discussed in Section 4.3, strongly supports the fact that an additional term is actually needed in CMC or CIE94 to account for the rotation of an ellipse from the hue axis near the blue region.

Table 4-9. Overall fit of colour-difference formulae to 3 visual data sets. (The best fit value is printed bold.)

Data	Msr.	ℓ	CIELAB	CMC	BFD	CIE94
Cheung	PF'/3	0.67	48	46	37	61
		1	**45**	34	**28.6**	45
		1.5	49	**31**	29.4	34
		2	54	34	34	**31**
Berns	TSD (%)	0.5	**27**	25	17	33
		0.67	29	**21**	**16**	24
		1	35	24	23	**19**
		1.5	41	30	30	23
This Study	PF'/3	0.5	55.1	43	37	56
		0.67	**54.9**	36	**33**	46
		1	60	**35**	36	**38**
		1.5	69	42	46	39

Table 4-10. Fit of colour-difference formulae to each of 5 CIE colour centres. (Values referred to in the text are shown bold.)

Data	Msr.	Cnt.		CIELAB	CMC	BFD	CIE94
Cheung	PF'/3	N	ℓ	2	1	1	2
				21	21	21	21
		R	ℓ	1	1.5	(1.5)	2
				38	27	26	28
		Y	ℓ	1.5	2	(1.5)	2
				35	31	30	**38**
		G	ℓ	0.67	1.5	1	1.5
				28	25	23	23
		B	ℓ	0.67	1.5	(1.5)	1.5
				42	32	**28**	32
Berns	TSD (%)	N	ℓ	1	0.5	(0.5)	1
				16	15	15	15
		R	ℓ	0.5	1	(0.67)	1
				19	12	14	12
		Y	ℓ	0.67	1	(0.5)	1.5
				16	9	8	8
		G	ℓ	0.5	0.67	(0.5)	1
				18	13	9	9
		B	ℓ	0.5	0.67	(0.67)	0.67
				39	32	**17**	32
This Study	PF'/3	N	ℓ	1.5	1	(0.67)	1.5
				22	21	21	21
	CV	R	ℓ	0.5	0.67	(0.67)	1
				30	28	27	27
	PF'/3	Y	ℓ	0.5	1	(0.5)	1.5
				31	23	17	19
	PF'/3	G	ℓ	0.5	0.67	(0.5)	1
				22	21	19	19
	PF'/3	B	ℓ	0.5	1	1	1
				31	26	**20**	26

4.5.2 Principal axes, tilting and ellipse parameters

The ellipsoid (ellipse) parameters in Table 4-11 are calculated by use of the same procedure described in Table 4-1. Among three principal axes of an ellipsoid, the axis close to the L^* axis is designated as L, and two axes close to the a^*b^* plane designated as C (long axis) and H (short axis). In most cases, these are roughly equivalent to the tolerance sizes along the lightness, chroma, and hue directions in the CIELAB space. When it is difficult to assign the proper axis directions due to the significant tilting of an ellipsoid, the highest point of an ellipsoid (ΔL^*_m) is denoted as L, and the major and minor axes of an ellipse (cross section of an ellipsoid projected onto the a^*b^* plane) are denoted as C and H, respectively. The L, and C and H values for yellow and green centres of this study were obtained from the results of independent experiments of the lightness tolerance and the chromaticity discrimination, respectively.

It is difficult to find any general trend about the tilting of the colour-difference ellipsoid. That is, yellow and green ellipsoids of the Cheung data and a grey ellipsoid of the Berns data are significantly tilted (about 50°) from the L^* axis. While, 3 ellipsoids (grey, red, and blue ellipsoids) of this study are tilted to a lesser extent.

It seems that in all 3 data sets there are little differences between the lightness tolerances of samples of L^* between 35 to 60. But, for the light colour (yellow centre in this case), the lightness tolerance seems to be significantly increased compared to that of other colour centres. The worst performance of CIE94 to the Cheung yellow centre, even after increasing the ℓ value to 2, illustrates this fact. (Table 4-10)

The orientation (θ) and the shape (H/C ratio) of the chromaticity ellipses for the grey centre are in good agreement between 3 data sets as was studied in Section 4.2: that is, $\theta \cong 90°$ and $B/A \cong 0.6$. In the green region, the H/C ratios of the ellipses from 3 studies are also very similar (about 0.5).

For each of the red, yellow and blue centres, the shapes of ellipses are rather in poor agreement between the three studies. In addition to the rotation from the hue axis, the blue ellipse seems to be more elongated compared to those for the other colour centres.

The variation in Table 4-10 illustrates the importance of testing data sets drawn from as many different experiments as possible. Work based on a single set may lead to false conclusions.

Table 4-11. Ellipsoid (ellipse) parameters for 5 CIE colour centres.

Data	Cnt.	L^*	C^*	h°	L	(tilt.)	C	H	θ	Δθ	H/C	Area
Cheung	N	62	0	30	1.69	11	1.14	0.65	86	.	0.57	2.34
	R	45	45	31	1.72	12	3.08	1.28	41	10	0.41	12.33
	Y	86	47	97	2.89	**51**	2.40	1.30	80	-17	0.54	9.79
	G	56	32	180	1.62	**47**	2.57	1.29	177	-3	0.50	10.43
	B	36	31	280	1.70	22	4.80	0.96	118	18	0.20	14.46
Berns	N	59	1	126	0.90	**46**	1.45	0.86	103	.	0.59	3.92
	R	42	42	31	0.93	20	2.40	1.43	32	1	0.60	10.80
	Y	78	36	87	1.11	16	2.11	1.27	80	-7	0.60	8.41
	G	56	28	175	0.94	17	2.57	1.34	168	-7	0.52	10.87
	B	36	28	267	0.86	13	3.30	1.10	117	**30**	0.33	11.41
This	N	50	1	118	1.33	36	0.86	0.51	80	.	0.59	1.37
Study	R	45	43	31	1.06	27	2.93	1.30	41	10	0.45	11.99
	Y	86	47	98	1.62	.	4.17	1.54	93	-5	0.37	20.17
	G	55	32	179	1.08	.	2.95	1.51	165	-14	0.51	13.96
	B	36	28	261	1.22	37	2.68	1.27	111	**30**	0.47	10.67

4.6 References

1. A.R.Robertson, CIE Guidelines for Coordinated Research on Colour-Difference Evaluation, Col. Res. Appl., **3**, 149-151 (1978).

2. BS 6923: Calculation of Small Colour Differences, BSI, 1988..

3. M.R.Luo and B.Rigg, Chromaticity-Discrimination Ellipses for Surface Colours, Col. Res. Appl., **11**, 25-42 (1986).

4. M.Melgosa, E.Hita, J.Romero and L.Jimenez del Barco, Color-Discrimination Thresholds Translated from the CIE (x,y,Y) Space to the CIE 1976 (L^*,a^*,b^*), Col. Res. Appl., **19**, 10-18 (1994).

5. R.S.Berns, D.H.Alman, L.Reniff, G.D.Snyder and M.R.Balonon-Rosen, Visual Determination of Suprathreshold Color-Difference Tolerances Using Probit Analysis, Col. Res. Appl., **16**, 297-316 (1991).

6. M.Cheung, Three-Dimensional Aspects of Color Discrimination, Ph.D. Thesis, University of Bradford, 1984.

7. M.R.Luo and B.Rigg, BFD(ℓ:c) Colour-Difference Formula: Part 1 – Development of the Formula, JSDC, **103**, 86-94 (1987).

8. C.Cui and J.K.Hovis, A General Form of Color Difference Formula Based on Color Discrimination Ellipsoid Parameters, Col. Res. Appl., **20**, 173-178 (1995).

9. M.R.Luo and B.Rigg, BFD(ℓ:c) Colour-Difference Formula: Part 2 – Performance of the Formula, JSDC, **103**, 126-132 (1987).

10. M.R.Luo, M.C.Lo and W.G.Kuo, The LLAB(ℓ:c) Colour Model, Col. Res. Appl., **21**, 412-429 (1996).

11. S.S.Guan, Private Communication.

12. Chapter 6 of this thesis.

5. RESULTS AND DISCUSSION PART II – PARAMETRIC EFFECTS

In this chapter, the results and discussion of experiments on parametric effects (background and gap) are given. The measures for the observer variability and the colour measurement error for each part of the experiments are also given here. The raw data (experimental results) is shown in Tables A-2 to A-4 of Appendix 1.

5.1 Physical Parameters - Background and Gap

5.1.1 Effects on lightness difference

5.1.1.1 Lightness differences under standard condition

As appropriately pointed out by Rigg [1], the lightness difference (ΔL^*) weighting functions (S_L) of the major colour-difference formulae evaluate the lightness difference quite differently from one to another (Fig.5-3). Unlike the chromaticness (both chroma and hue) differences, almost all colour-difference data sets include only a very small portion of colour-difference pairs which exhibit purely lightness differences (normally, less than 20%). Thus, the comparison by previous workers of the reliability of the ΔL^* weighting functions seems to be not properly carried out. The result is greatly dependent upon the particular data set which is used.

As a first step, earlier data sets - Fong [2], Badu [3] and Berns [4] - which include entirely or mostly lightness difference pairs were gathered and compared to that from this study. A brief description of each data set is as follows:

(a) Fong : small colour differences (1-2 ΔE^*)
43 pairs including chromatic samples (also very dark neutral samples)
ratio method (standard pair $L^* = 63.5$, $\Delta E^* = 1.6$)
background $L^* = 46$
(The results for $\Delta L^*/\Delta V$ for the 25 pairs with a significant lightness difference are shown in Fig.5-1-a.)

(b) Badu : medium (relatively large) colour differences about 5 ΔE^* unit
14 pairs all achromatic samples
grey-scale and ratio method (standard pair $L^* = 51.7$, $\Delta E^* = 5.0$)

background $L^* \cong 42$

(The results for $\Delta L^*/\Delta V$ for both assessment methods are shown in Fig.5-1-b)

(c) Berns : small colour differences of 1-2 ΔE^*

19 tolerance vectors (each from 5-7 pairs) including 3 neutral colours

paired-comparison / probit analysis (standard pair $L^* = 49.2$, $\Delta E^* = 1.0$)

background $L^* \cong 38$

(The results for the unit visual difference ($\Delta L^*/\Delta V$) are shown in Fig.5-1-c.)

(d) This study

sample pair colour-difference: 0.5 - 3.0 ΔE^*

78 pairs in 11 colour centres (7 achromatic and 4 chromatic colours)

grey-scale, and paired-comparison / probit analysis (std pair $L^* = 49.2$, $\Delta E^* = 1.1$)

background $L^* = 49$ (black BG $L^* = 25$, and white BG $L^* = 95$)

(The lightness difference test results under the reference grey background condition for both scaling methods are represented in Fig.5-1-d. The probit analyses results are also given in Table A-9 of Appendix 2.)

It can be seen in Fig.5-1 that for any data set the second order polynomial (parabolic) function of L^* would be most likely to satisfy the variation of lightness tolerances ($\Delta L^*/\Delta V$) according to L^*. However, it is difficult to find a single curve which could describe the general trend of lightness differences for all data sets. For this reason, the three data sets were combined with the average data at each lightness value from this study (Fig.5-2) and the best fit to this combined data was sought. As each data has slightly different scaled values for lightness tolerances, in each data set the $\Delta L^*/\Delta V$ values were normalised by dividing the value with that for the neutral grey pair nearest to $L^* \cong 50$. The results are shown in Table 5-1.

In Fig.5-2, some common facts could be found. First, the data points of L^* over 40 show a fairly good agreement. That is, the lightness tolerances increase with increasing metric lightness and the rate of increase is more rapid as the lightness increases. The ΔL^* weighting functions of CMC, BFD, and CIE94 (identical to CIELAB) were compared in Fig.5-3. The CMC S_L function and that of BFD show quite similar shapes, as both are based on the Fong data. However, for very dark colours, the S_L analogue of the BFD formula is very different from that of CMC, and it is thought to be the major source of

difference in their performance in this comparison. (BFD shows a better fit to all data sets tested than CMC; Fig.5-4) That is, the CMC S_L function weights for ΔL^* are too small for dark colours and thus evaluates too large a colour difference. It also evaluates the colour difference of the light samples ($L^* \geq 70$) bigger than the BFD formula. As implied by Fig.5-2, it would be better to change the hyperbolic CMC S_L function to a parabolic function, at least, for the lightness range of L^* over 50.

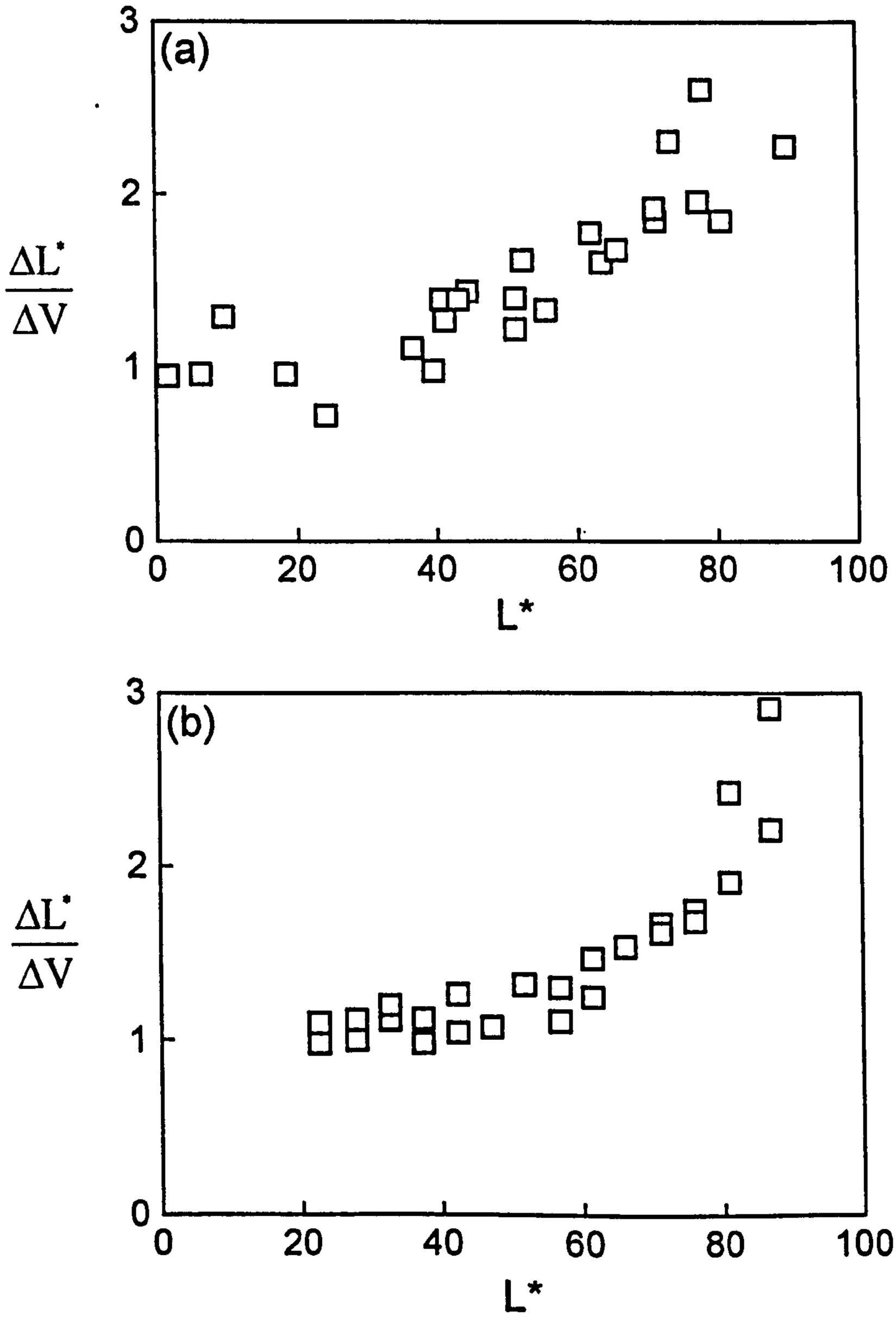

Figure 5-1. $\Delta L^*/\Delta V$ for (a) Fong, and (b) Badu data sets.

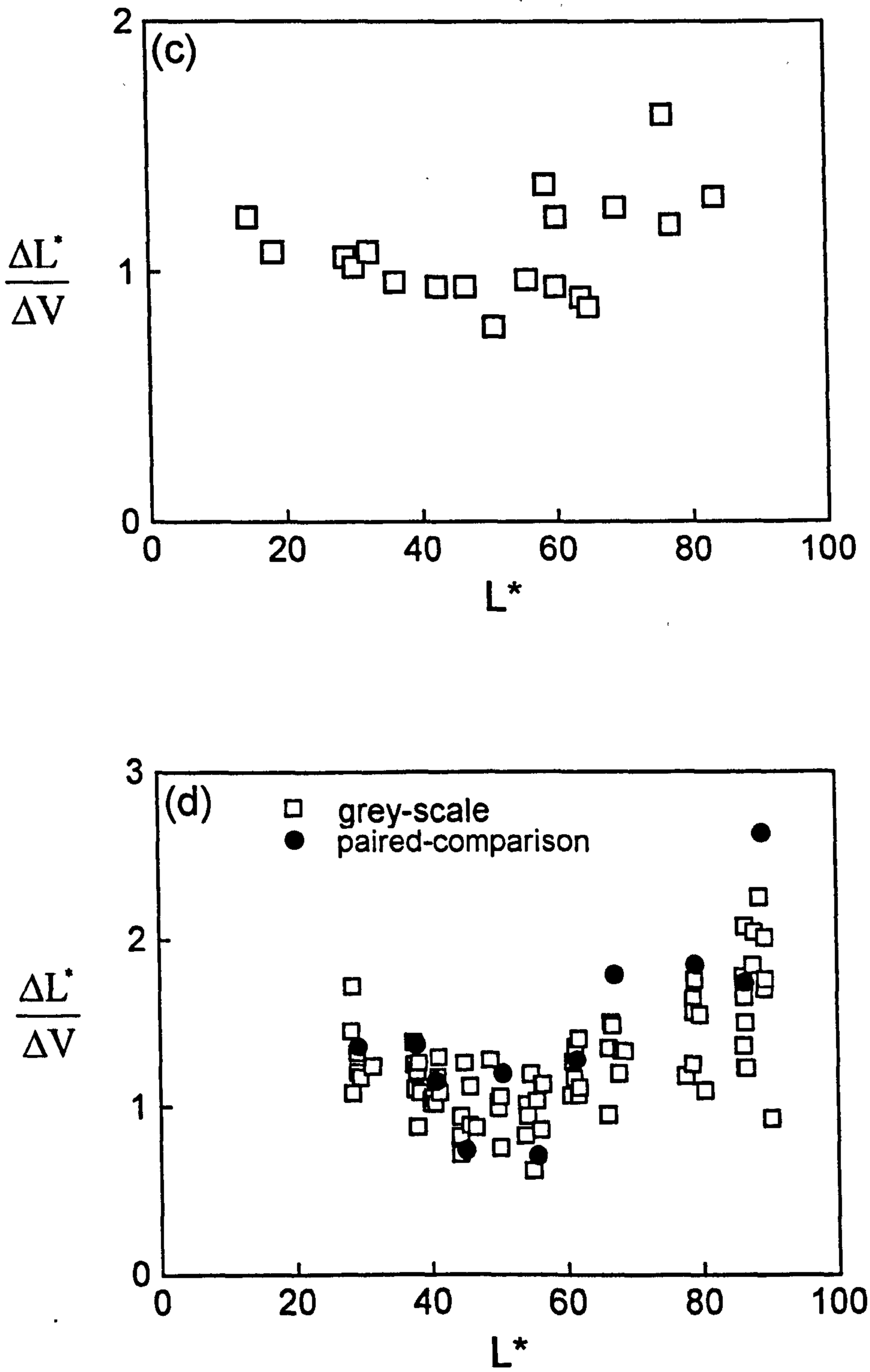

Figure 5-1. Continued; $\Delta L^*/\Delta V$ for (c) Berns data, and (d) this study.

Table 5-1. $\Delta L^*/\Delta V$ values shown in Fig.5-2. (Bold figures in parentheses indicate the original $\Delta L^*/\Delta V$ values of the grey pairs used for rescaling other $\Delta L^*/\Delta V$ values.)

Neutral samples

Data Set	Pair No. (Col.Cnt.)	L^*	$\Delta L^*/\Delta V$	
Fong	NM	1.63	0.65	
	NL	6.32	0.67	
	NK	9.58	0.92	
	NJ	18.42	0.68	
	NI	24.11	0.52	
	NH	39.39	0.69	
	NG	44.37	1.03	
	NF	**51.12**	**1.00**	**(1.40)**
	NE	63.51	1.15	
	ND	71.21	1.32	
	NC	77.36	1.39	
	NB	80.56	1.31	
	NA	89.78	1.60	
Badu①	L20/25	22.45	0.79	
	L25/30	27.70	0.80	
	L30/35	32.50	0.88	
	L35/40	37.25	0.79	
	L40/45	42.25	0.87	
	L45/50	47.05	0.82	
	L50/55	**51.70**	**1.00**	**(1.32)**
	L55/60	56.80	0.91	
	L60/65	61.45	1.02	
	L65/70	66.10	1.16	
	L70/75	71.20	1.25	
	L75/80	76.05	1.30	
	L80/85	81.05	1.61	
	L85/90	86.90	1.91	
Berns②	Blk	14.55	1.30	
	Mdm-Gry	**59.78**	**1.00**	**(0.94)**
	L-Gry	83.38	1.36	
This Study	L30	29.15	1.26	
	L40	40.56	1.06	
	L50	**50.94**	**1.00**	**(0.98)**
	L60(Grey)	61.35	1.22	
	L70	67.08	1.36	
	L80	78.98	1.43	
	L90	88.88	1.89	

Chromatic samples

Data Set	Pair No. (Col.Cnt.)	L^*	$\Delta L^*/\Delta V$
Fong	RF	36.52	0.72
	RE	40.69	0.98
	BE	41.10	0.86
	YF	42.98	0.95
	BC	51.16	0.83
	RD	52.27	1.08
	RC	55.54	0.93
	RB	62.00	1.25
	BB	65.63	1.12
	YC	71.06	1.31
	SYC	73.20	1.64
	YB	77.82	1.86
Berns②	VDR	18.24	1.13
	Mdr-R-Brn	28.89	1.12
	D-Blu	30.13	1.08
	D-Blu-Grn	32.26	1.09
	Mdr-Blu	36.11	1.01
	DRO	42.33	1.00
	Gry-Prp	46.48	1.00
	Mdr-Grn-Blu	50.65	0.83
	Mdr-Blu-Grn	55.58	1.03
	Mdr-Prp-Pnk	58.42	1.39
	Brl-Grn-Blu	59.95	1.29
	L-Brn	63.54	0.95
	Gry-Y-Grn	64.60	0.91
	L-Blu-Grn	68.77	1.34
	SOY	75.90	1.68
	Mdr-Y	76.86	1.27
This Study	Blue	37.79	1.16
	Red	45.07	0.92
	Green	55.43	1.07
	Yellow	86.32	1.56

① Averaged data from two scaling methods (grey-scale and ratio) were used.

② Colour centre names were abridged. (Blk = black, Mdm = medium, Gry = Gray or Grayish, L = light, V = very, D = dark, R = red or reddish, Mdr = moderate, Brn = brown, Blu = blue or bluish, Grn = Green or Greenish, O = orange, Prp = purple or purplish, Pnk = pink, Brl = brilliant, Y = yellow, and S = strong)

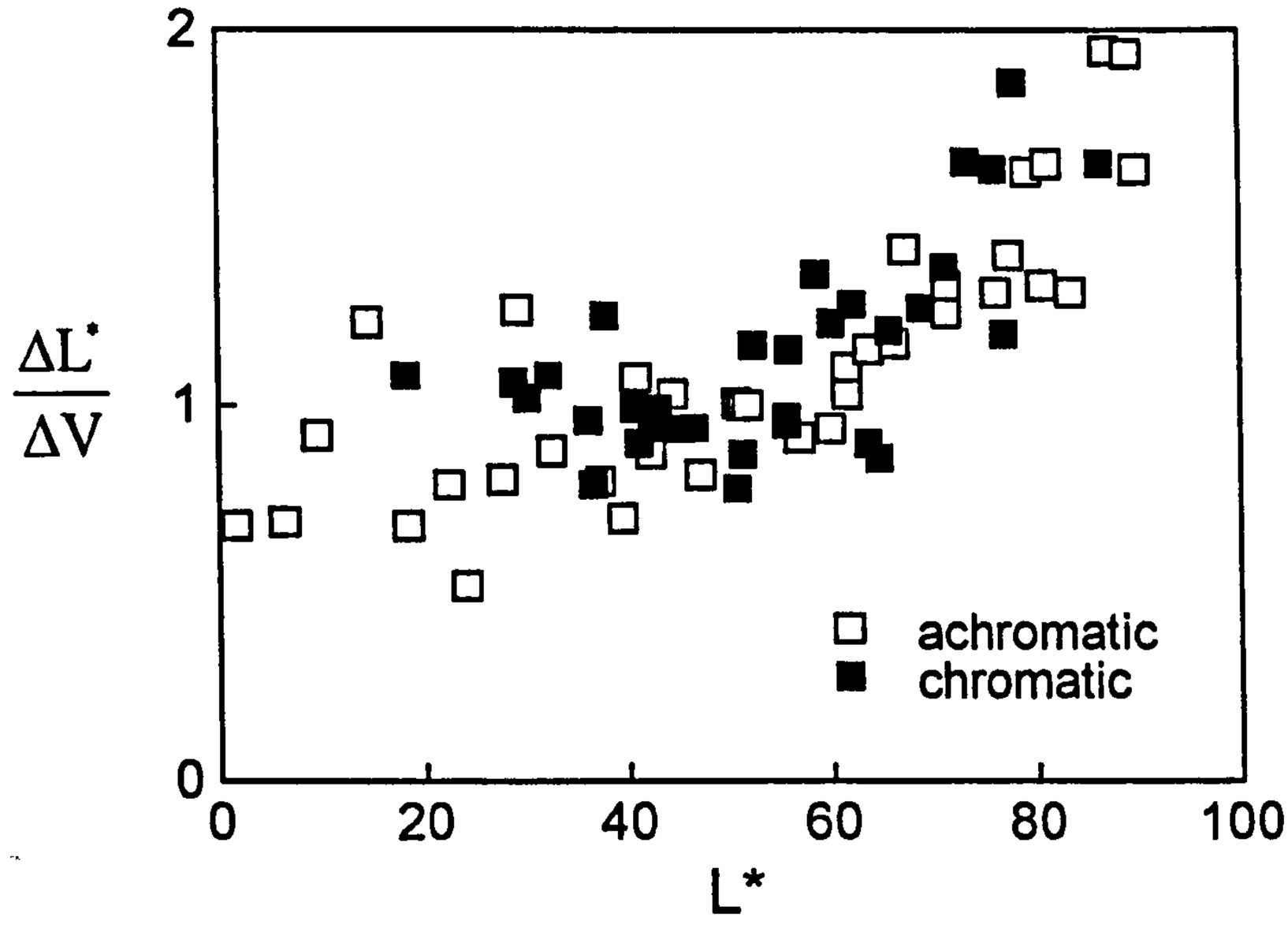

Figure 5-2. Combined data: equal visual lightness differences for achromatic(□) and chromatic(■) colours.

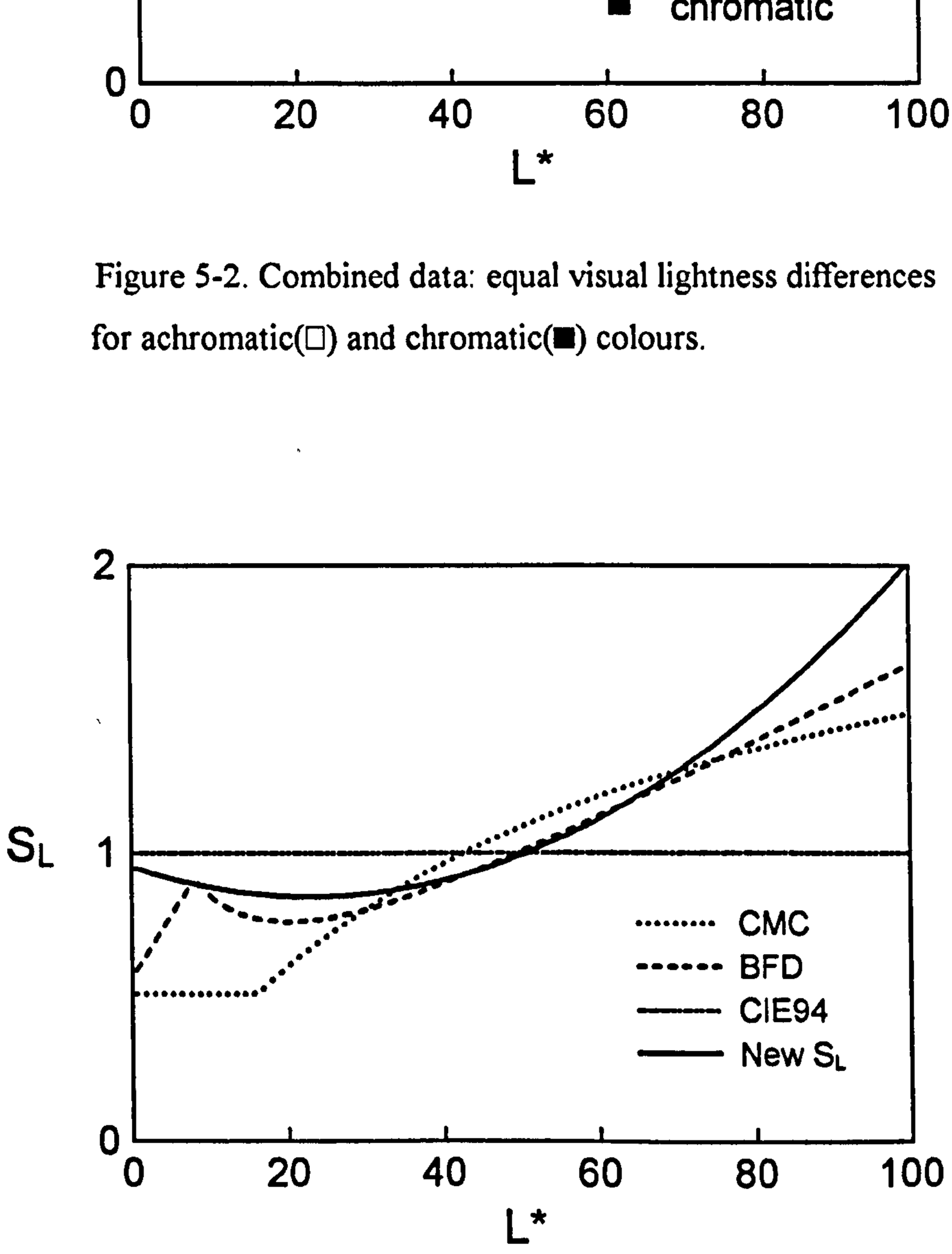

Figure 5-3. ΔL^* weighting functions. (The new S_L function is explained in the text.)

For the samples of L^* below 40, there are serious differences in lightness tolerances from the different data sets and thus it is much more difficult to find the general tendency. It is in part due to the very small number of dark sample pairs in each data set. Unfortunately, additional data for dark colours is not available, a new ΔL^* weighting function was fitted keeping all the data points. (Figs.5-2 and 5-3) It is given by

$$S_L = 0.95 - 0.009\,L^* + (0.014L^*)^2 \qquad (5\text{-}1)$$

The 95% confidence limits for the regression coefficients are ±0.10, ±0.004, ±0.001, respectively.

The performance of new S_L function is examined using the above 4 data sets and an additional 30 pairs ($|\Delta L^*/\Delta E^*| > 0.85$) of the Luo data [5]. For the visual results from this study, those obtained from the grey-scale method was used as it is more readily comparable to other data sets than that from the paired-comparison method. As Fong and Luo data include many pairs not entirely showing just lightness differences, each colour-difference formula was tested by only changing the ΔL^* weighting function. (i.e., Δa^* and Δb^* or ΔC^* and ΔH^* values are identical to the CIELAB formula.) Also, to avoid any variation in colour-difference calculation due to change of the position of standard and test colours, all possible combination in each pair was used as well. For Berns data, as all colour differences were calculated for unit visual differences (i.e., tolerance vector), correlation coefficient between ΔV and ΔE was not obtainable. As explained in Chapter 2, the TSD (tolerance standard deviation) is used instead.

Fig.5-4-a clearly shows the superior performance of each S_L function to its basis data. That is, both CMC and BFD S_L functions to the Fong data and CIE94 S_L function to the Berns (RIT-Dupont) data. However, the new S_L function gives not only a similar quality of fit as the other S_L functions for their basis data but quite even performances for all data.

The new S_L function is still thought to be not wholly satisfactory in evaluating lightness difference of very dark samples. But the effectiveness of the four data points at low L^* level shown in Figure 5-1-a (Fong data) is questionable, because the $\Delta L^*/\Delta V$ values at similar L^* level scattered up to a factor of 2 as shown in Figure 5-1-d (this study). For the time being, the new S_L function could be used for most practical application as lower L^* value is very rare and thus not so important.

In most of the range of L^* (= 20 – 80), the new S_L function evaluates ΔL^* similar to the

BFD formula. However, it is more convenient and easy to use compared to BFD as it only changes ΔL^* weighting other than the lightness scale itself.

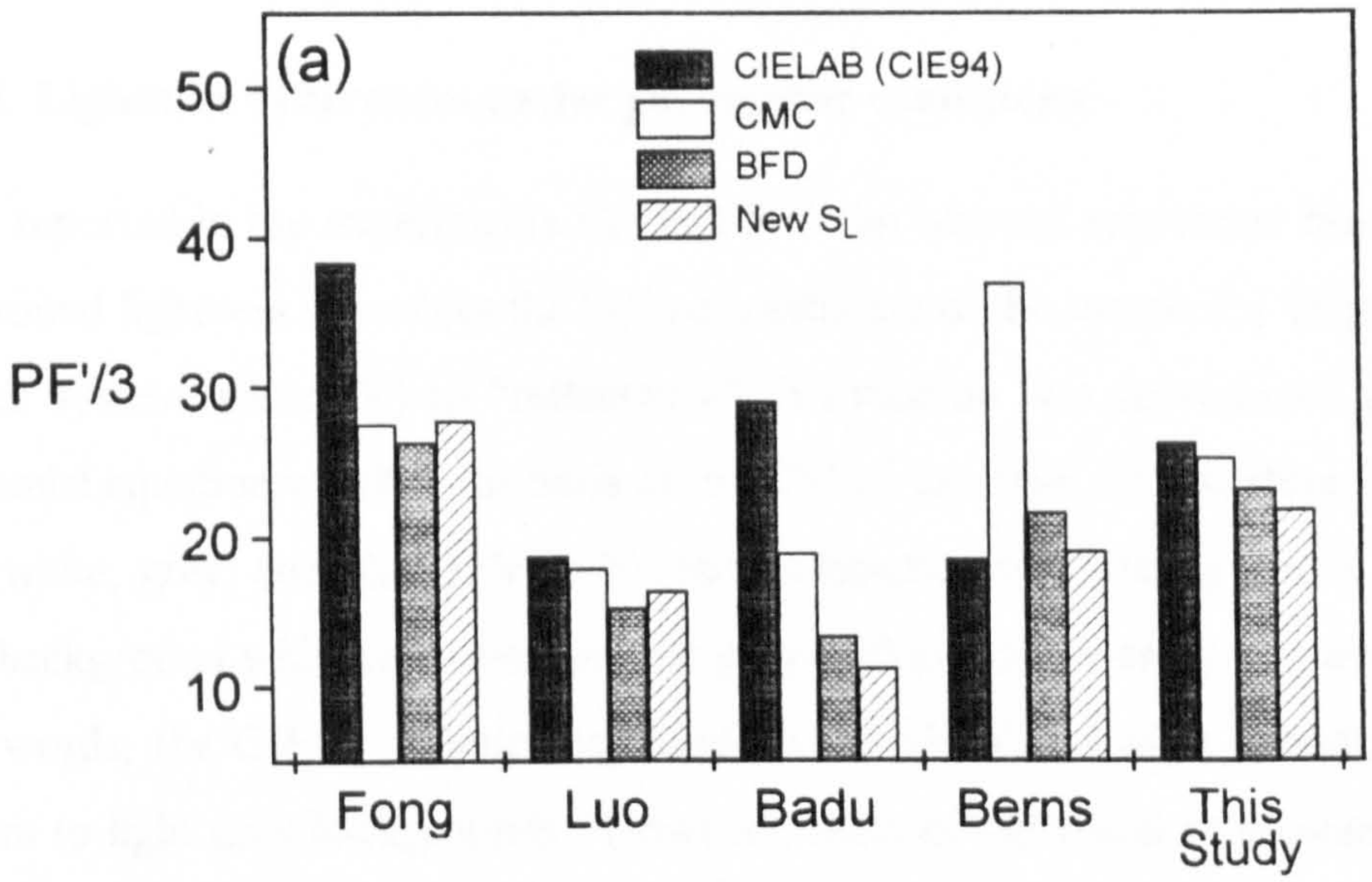

Figure 5-4. Comparison of the fit between CIELAB, CMC, BFD and new S_L function: (a) for data sets, and (b) for parametric conditions.

The $\Delta L^*/\Delta V$ values range from 0.85 ($L^* = 23$) to 2.01 for ΔL^* values calculated from the new S_L function. The CMC S_L function gives $\Delta L^*/\Delta V$ values ranging from 0.51 to 1.48. That is, the maximum to minimum ratio of $\Delta L^*/\Delta V$ values is less than a factor of 2.4 for the new S_L, while in CMC it is about a factor of 2.9. Hence, the new S_L weights the lightness difference (for colours of $L^* = 0 - 100$) more uniformly compared to CMC.

5.1.1.2 Lightness differences under parametric conditions

It was reported in the experiments which led to the Munsell renotation system that the background lightness influences the lightness estimate of the sample [6]. (Fig.5-5) In the Munsell system, value (V) to "reflectance" (Y) relation was represented by a quintic polynomial equation which is the basis of the CIE L^* function. Of the three backgrounds used (white, grey, and black), V to Y relation function was greatly out of line for the black background while the white and the grey backgrounds were in fair agreement. In other words, the CIE L^* function is based on the visual estimates obtained under the medium to light grey backgrounds. However, most of the visual assessments of colour difference have been practically carried out under the medium to dark (mainly, dark) background ($L^* \cong 40$). It might cause the inconsistency between Munsell based ΔL^* and ΔV from the colour-difference data sets.

Badu [3] performed colour-difference experiments concentrating on the background (and also the gap) effect and did not find any effect. It is possible that this may be due to the use of relatively large differences ($\Delta E^* \cong 5$) so that when the colour-difference is clearly visible, even if the experimental condition is changed, the sensation hardly changes.

The pattern of the change of lightness tolerances (according to the sample lightness) under three parametric conditions (Fig.5-6) were similar to that obtained under the grey background (Fig.5-1-d). The shapes of the graphs for the black and white backgrounds, and gap resemble each other, that is, it is concave near the average lightness of the grey scale (or standard pair) used. The degree of concavity is greater in the black background results than in the white. This suggests that the black background generally enhances contrast while the white background decreases it. (Compare Fig.5-6-a, b with Fig.5-1-d.)

The performance of the colour difference formulae (CIELAB, CMC, BFD and new

S_L) was tested on each of the parametric data sets by the same procedure as described in Section 5.1.1.1. The results are shown in Fig.5-4-b where it is seen that for the grey, black and gap conditions the sequence is new S_L (best) > BFD > CMC > CIELAB (worst). It is interesting to note that the CIELAB (CIE94) formula gives the best fit to the visual data obtained under the white background (Fig.5-4-b), the condition under which the L^* function was derived from Munsell V.

The parametric effect that has been neglected in all studies is the influence of the average lightness of the standard pair (i.e., paired-comparison or grey-scale methods) on the assessment of the perception of lightness differences. Thus, though it is unlikely in the practical situation, the question still remains whether the analogous trend of Figs.5-1-d and 5-6 could also occur if we use a white or a black standard pair instead of a grey one.

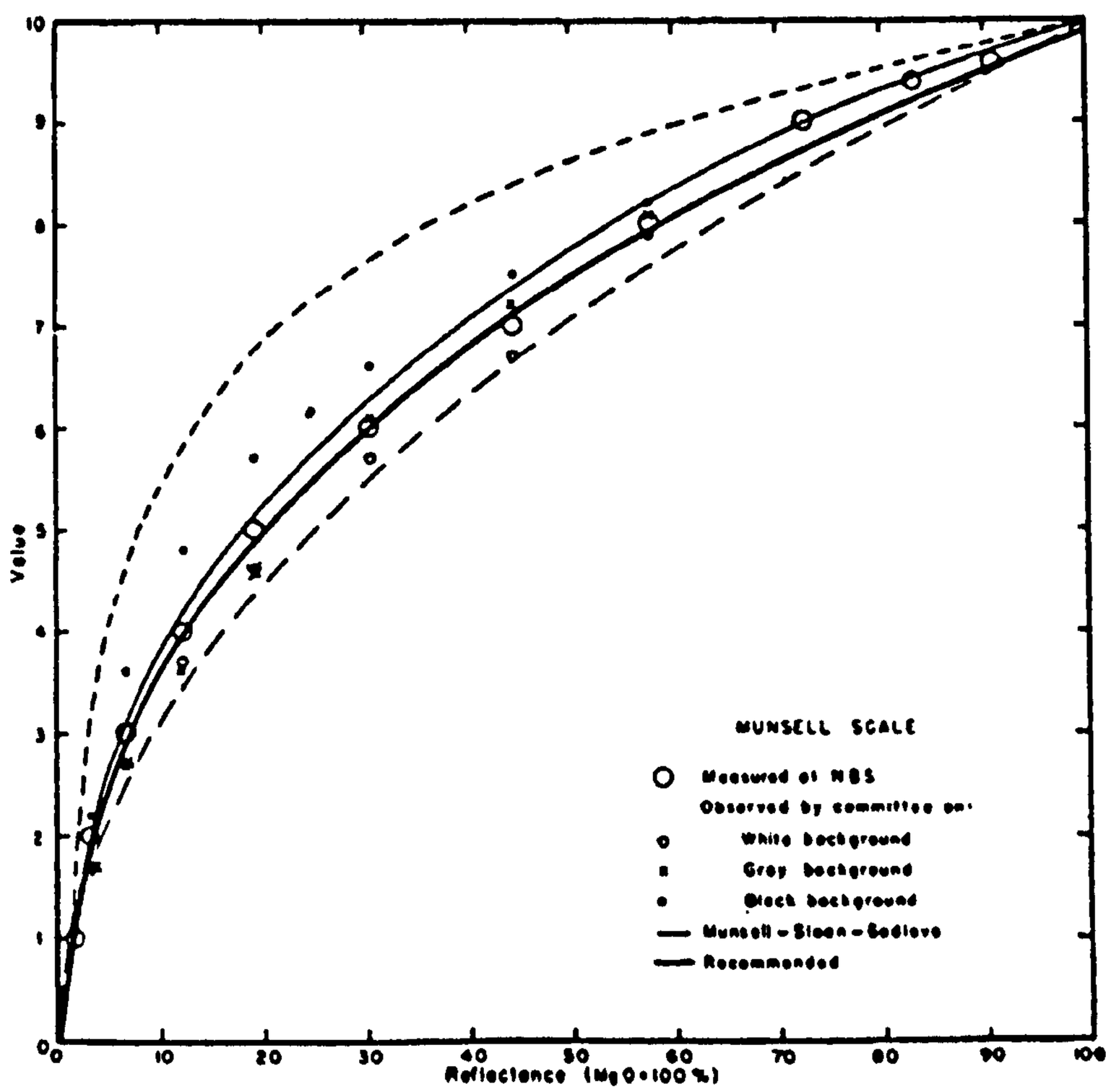

Figure 5-5. Munsell value (V) as a function of reflectance (Y) [6]. (Upper and lower dashed curves: $Y = k$ anti-log V and $Y = V^2$, respectively)

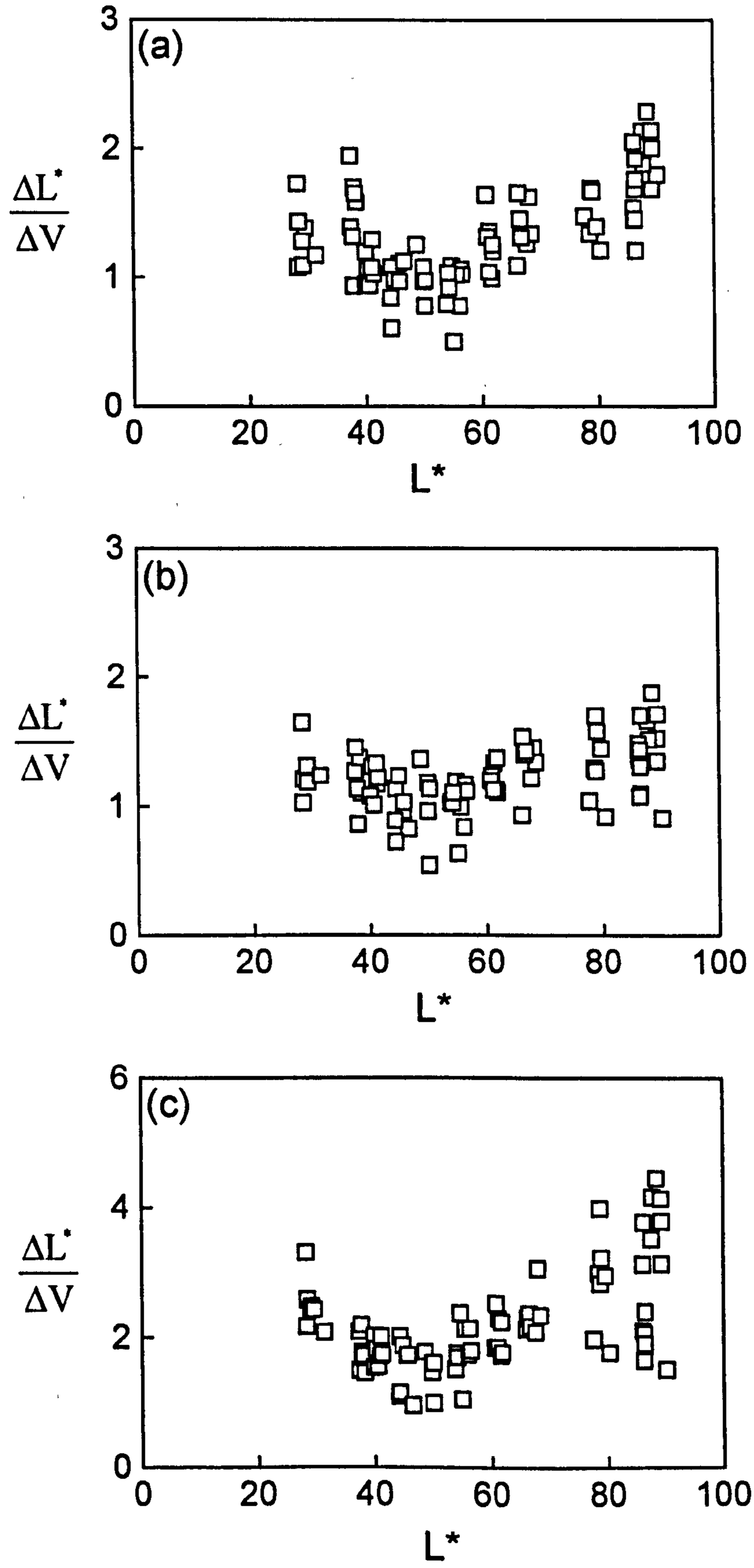

Figure 5-6. $\Delta L^*/\Delta V$ for parametric conditions:
(a) black, (b) white backgrounds, and (c) gap

5.1.1.3 Parametric correction factors for lightness difference

The role of the parametric correction factor (here, K_L) is described in Section 2.6.

(a) Background factor

Table 5-2 gives the correction factors for the lightness-difference on change of background lightness. Both sets of the results from the two scaling methods commonly revealed the fact that, overall, the visual judgement of colour difference was not significantly influenced by the lightness of the neutral background. The value of K_L was between 0.9 and 1.1 for all but two colour centres (from a grey-scale method). The average value was 1.0 for each background.

However, the change from a grey to a black background had increased the lightness tolerance of the dark blue (K_L = 1.3) while the change from a grey to a white background had decreased that of the light grey $L^* \cong 90$ (K_L = 0.8). In terms of the crispening effect [7] (when the sample lightness is close to background lightness, the visual differences are much larger than that for the same sample pair on a different background), a very weak effect did occur in case of the light grey. The opposite effect of the dark blue can be explained as the result of the local adaptation to the lightest element of the visual field [8].

(b) Gap factor

Like the background, the gap between samples in a pair is a parameter of great interest in the coloration industry. McDonald [9] has attributed the reason for the increase of ΔL^* weighting by a factor of 2 in the acceptability test to the colourist's nature of judgement. That is, in acceptability matching, the dyer is more biased against hue differences but more lenient to lightness differences, and most samples used in acceptability experiments are textile samples. It was also explained as due to the unclear dividing line between the samples [10].

The gap factors for lightness differences obtained in this study are given in Table 5-2-a together with those from Witt experiments ([11], Table 2-3). The average gap factor for the 5 CIE colour centres and 6 additional grey samples is 1.7, while that obtained by Witt from 5 CIE threshold ellipsoids is 1.9. In the Witt study, the K_L value for the blue

centre is very large (2.9), which could be due to the use of very small colour differences. As a result, a small error in the threshold ellipsoid would produce a large error in the parametric factor. For both the dark and light grey samples, the gap factors were larger than that for medium grey sample ($L^* = 50$). In addition, except for the green centre, the gap factors for chromatic samples were smaller than those for the neutral samples.

Table 5-2. ΔL^* correction factors (K_L) for 3 parametric conditions. (Bold figures are explained in the text)

(a) Grey-scale method (① results from Witt study [11])

Colour Centre	Co-ordinates			K_L			
	L^*	a^*	b^*	Black BG	WhiteBG	Gap	Gap①
L30	29.2	-0.1	0.6	1.0	1.0	**1.9**	
Blue	37.8	-6.3	-26.8	**1.3**	1.0	1.5	**2.9**
L40	40.6	-0.2	0.3	1.0	1.1	1.6	
Red	45.1	37.0	22.2	1.0	1.0	1.6	1.7
L50	50.9	-0.3	0.0	1.0	1.1	1.5	
Green	55.4	-32.0	0.1	0.9	1.0	1.8	1.5
L60 (Grey)	61.3	-0.3	0.0	1.0	1.0	1.7	2.0
L70	67.1	-0.2	0.0	1.1	1.0	1.8	
L80	79.0	-0.3	-0.5	1.1	0.9	1.9	
Yellow	86.3	-6.4	45.8	1.0	0.9	1.5	1.4
L90	88.9	-0.5	-0.3	1.1	**0.8**	**2.0**	
Overall				1.0	1.0	1.7	1.9

(b) Paired-comparison / probit analysis

Colour Centre	Co-ordinates			K_L	
	L^*	a^*	b^*	Black BG	White BG
L30	29.3	-0.2	0.5	0.9	1.0
Blue	37.8	-6.2	-26.7	1.2	1.1
L40	40.8	-0.2	0.3	1.0	1.2
Red	45.1	36.9	22.2	1.3	1.1
L50	50.6	-0.3	0.0	1.0	1.0
Green	55.7	-31.9	0.1	1.3	1.3
L60 (Grey)	61.4	-0.3	-0.1	1.0	1.1
L70	67.1	-0.2	0.0	0.9	0.9
L80	79.1	-0.4	-0.5	0.9	0.8
Yellow	86.3	-6.5	46.0	1.0	0.9
L90	89.1	-0.5	-0.4	0.8	0.6
Overall				1.0	1.0

As can be seen in Table 5-3, when the relative tolerance is increased by a factor of 2.0, the fit of each colour difference formula is improved. The results could be a partial explanation of the use of factor 2 in acceptability experiments (mainly textile samples). Considering from the results of this study it seems to be reasonable to set the gap factor (k_L or ℓ) to about 2.

Table 5-3. Measure of fit (PF/4) for gap viewing condition.

ℓ (or K_L)	CIELAB	CMC	BFD	New S_L
1.0	34.8	31.5	28.0	25.4
1.5	33.7	30.2	26.6	23.8
1.7	33.3	29.8	26.2	23.4
2.0	**32.8**	**29.4**	**25.8**	**22.9**
2.5	32.4	29.4	25.7	22.9
3.0	32.5	30.0	26.3	23.8

5.1.2 Effects on chromaticity discrimination

5.1.2.1 Chromaticity discrimination under standard condition

Similar to the lightness-difference study, first, previous data sets - Luo [12,13] and Berns[4] - were collected and compared to that from the present study. Each data set is summarised as follows.

(a) Luo ellipse data

The original Luo ellipse data [12] includes 132 xy chromaticity discrimination ellipses, which is translated to the CIELAB space by Melgosa [13]. Each a^*b^* ellipse which is represented by its colour centre co-ordinates and its parameters (i.e., orientation angle θ, and major and minor semi-axes, A and B) is further transformed to C^*H^* in this study by the following procedures:

From θ, A, and B values, the a^*b^* ellipse coefficients b_{11}, b_{12} and b_{22} were obtained by using Eq.(2-39). The b_{ik} values for each ellipse were then transformed to s_{ik} values of an C^*H^* ellipse by using Eq.(2-43). The differences along the chroma and hue directions for

the unit visual difference, ΔC^* and ΔH^*, are given by (Section 4.3, Eqs.4-4 and 4-5)

$$\Delta C^* = \frac{1}{\sqrt{s_{11}}}, \quad \text{and} \quad \Delta H^* = \frac{1}{\sqrt{s_{22}}} \tag{5-2}$$

Among the 132 C^*H^* ellipses, eight ellipses for grey centres ($C^* \leq 4$) were excluded as the chromaticity discrimination of the grey samples are unlikely to show either the metric chroma or hue angle dependence. An ellipse with a much higher chromatic colour (C^* = 101, Set VVVR Y in Table III of Refs.[12,13]) than any other in the data set was also excluded in the comparison of this study.

The 123 C^*H^* ellipses give the total number of 246 tolerances (123 tolerances along the directions to ΔC^* and ΔH^*, respectively). These 246 tolerances were used to study the dependence of the chroma or hue differences (ΔC^* or ΔH^*) on the metric chroma or hue angle (C^* or h°), and to test the fit of major colour-difference formulae.

(b) Berns tolerance data

A part of the Berns tolerance data was already used in the lightness difference study. For 19 colour centres, the colour-difference ellipsoids were fitted by use of the tolerance data. Among the 3 ellipsoid principal axes of each ellipsoid, two axes close to the a^*b^* chromaticity plane were selected, and from these ΔC^* and ΔH^* values were obtained by the same procedure as above.

For the testing of the colour-difference formulae, the 67 tolerances which vary only in the a^*b^* plane were selected.

(c) Present study

The chromaticity discrimination (or chromaticness differences, i.e., both chroma and hue differences) around the 15 colour centres was examined by use of the 75 colour-difference pairs (Chapter 3). In each colour centre, 12 chromaticity ellipses (4 parametric conditions × 3 observer groups) were fitted. The coefficients and parameters of all 180 ellipses obtained are given in Tables A-10 and A-11 (Appendix 3). The fit of the colour-difference formulae were tested by use of the 70 colour-difference pairs (excluding 5 grey pairs).

5.1.2.1.1 Chroma dependence of chroma and hue differences

Table 5-4 shows the measures of fit of the 4 colour-difference formulae - CIELAB, CMC, BFD, and CIE94 for the chromaticness differences. The BFD formula always gave the best fit, CIE94 and CMC followed next, and CIELAB was worst. The best performance of BFD to the 3 data sets can be due to the use of both the hue-angle dependence in the hue weighting D_H (S_H) and the addition of the ellipse rotation term to the formula. But it is more likely to be due to the latter, as CMC which also assumes a hue angle dependence of the hue difference showed no better performance than CIE94 which does not.

It is interesting that CIE94 shows similar performance to BFD to the Luo data. It is believed that the CIE94 chroma and hue weighting functions S_C and S_H were, in effect, developed on the basis of the Luo data. As shown in Fig.5-8, the Berns data does not include a wide chroma range, and thus it is impossible to obtain the reliable relations between C^* and ΔC^*, and between C^* and ΔH^* without using the Luo data.

For the Berns data, the fits of both CMC and BFD improved greatly if the tolerances for grey samples were excluded to give 58 pairs. It means that, as studied in Section 4.2, for the neutral grey colours the semi-axes lengths show hardly any dependence upon the metric chroma (C^*) but only on the metric lightness (L^*). It was also shown in Section 4.2 that the grey ellipse generally oriented along the b^* axis regardless of its hue angle (h°).

Table 5-4. Fit of colour-difference formulae to chromaticness differences.
(Each formula tested by setting the lightness weighting function S_L =1)

Data Set	Measure	No. of Pairs	Parametric Condition	CIELAB	CMC	BFD	CIE94
Luo	TSD (%)	246 tol.	.	50	26	**22**	23
		123 ΔC^*	.	44	26	**24.2**	24.4
		123 ΔH^*	.	31	26	**19**	21
Berns	TSD (%)	67 tol.	.	37	26	**22**	23
		58 tol.	.	35	22.2	**18**	21.8
Present Study	PF'/3	70	Grey BG	35	23	**20**	22
		70	Black BG	33	22	**19**	21
		70	White BG	31	19.9	**18**	20.0
		70	Gap(K_{CH}=1.5)	32	22	**19**	20

Figs.5-7 and 5-8 show the metric chroma dependence of chroma and hue differences of the three data sets. The present data set also lacks the chroma or hue differences for the high chroma samples like the Berns data. Therefore, the chroma dependence was studied by only using the Luo data and not using the combined data.

In many studies [14,15,16], it was shown that the chroma difference has a strong dependence to the metric chroma (C^*) of the standard colour. In fact, so long as the chroma difference is concerned, there is little dispute about the C^* dependence, though the three modified CIELAB formulae (CMC, BFD and CIE94) have different forms (either hyperbolic or linear) of the chroma weighting functions. It can be seen in Fig.5-9-a, both chroma weighting functions of BFD and CIE94 similarly vary with C^*. Hence, the hyperbolic BFD D_C function may be simplified to a linear function of C^*. The CMC S_C function is substantially different from the other two chroma weighting functions. It is not easy to determine which S_C (D_C) function is better between that of CMC and that of BFD or CIE94. However, in terms of the Luo data, possibly the linear CIE94 S_C function describes better the variation of the chroma difference with the chroma of the standard colour than the hyperbolic CMC S_C function. Therefore, it is difficult to justify the additional complexity of a nonlinear weighting function.

It is uncertain whether the hue difference varies only with the metric chroma, as does the CIE94 hue weighting function S_H. The hue difference may have the dependence on both the metric chroma (C^*) and the hue angle (h°), as in the CMC or BFD. But, as mentioned above and claimed by Berns [16], the use of the hue-angle dependence term in the hue weighting function could have little advantage in practice.

Because the direct comparison of the variations of the hue weighting functions with C^* is not possible, the relation between the metric chroma and the prediction of the hue difference by the CMC, BFD and CIE94 S_H functions using the Luo data was studied (Fig.5-9-b). As expected, the CIE94 S_H function varies linearly with C^* while both the CMC S_H and BFD D_H functions are scattered around the linear CIE94 S_H. A more random nature of the variation of the CMC S_H with C^* compared to that of the BFD D_H indicates that the CMC S_H has a more strong dependence on h° but the BFD D_H is rather weakly influenced by h°. It is interesting that the BFD D_H varies more uniformly (less scattered data points) with C^* than the CMC S_H. Assuming that the hue weighting function is dependent only on C^*, then it would be best represented by a linear function of C^* as the CIE94 S_H.

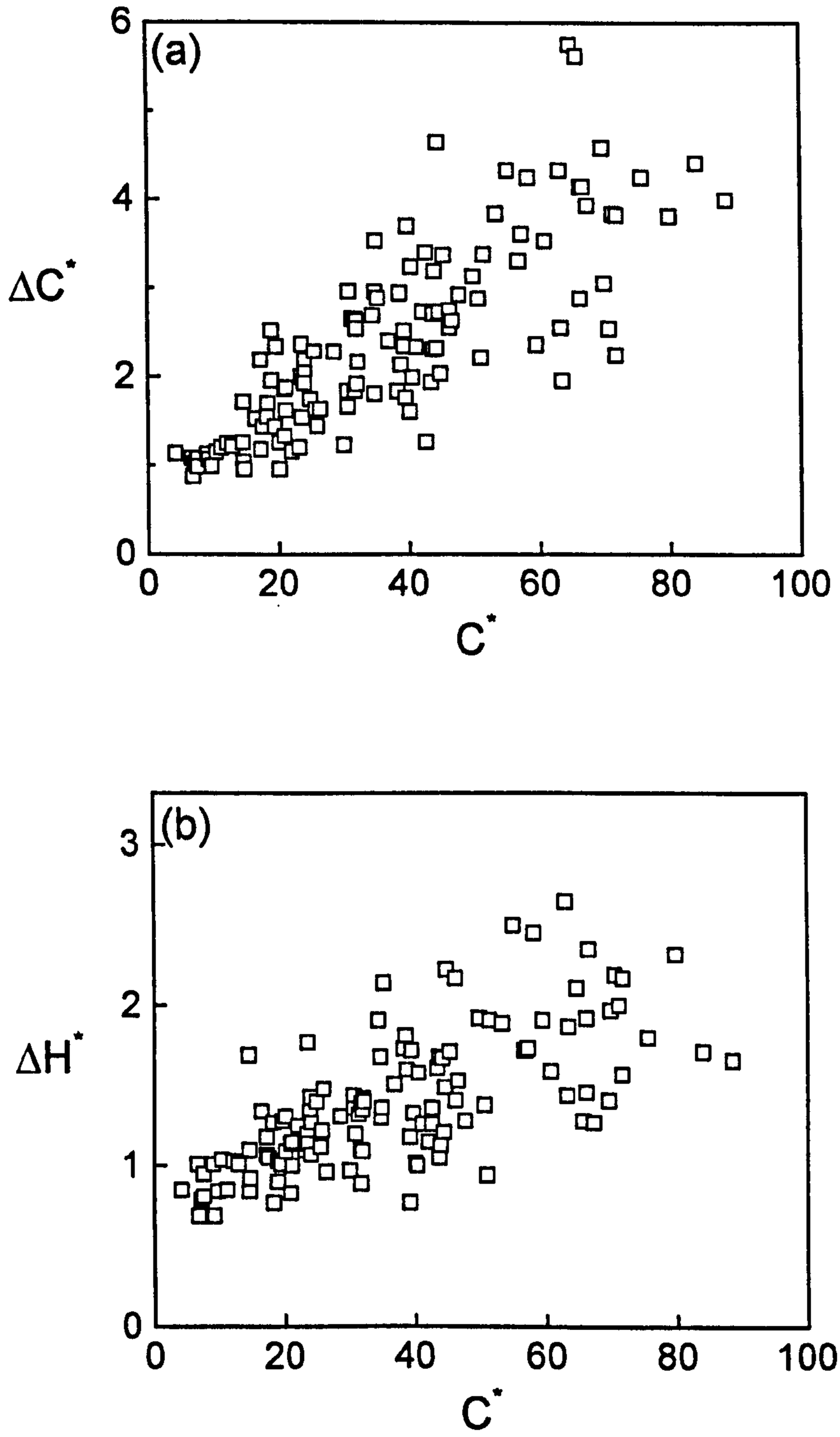

Figure 5-7. Chroma dependence of chroma and hue differences of the Luo data: (a) C^* vs. ΔC^*, and (b) C^* vs. ΔH^*.

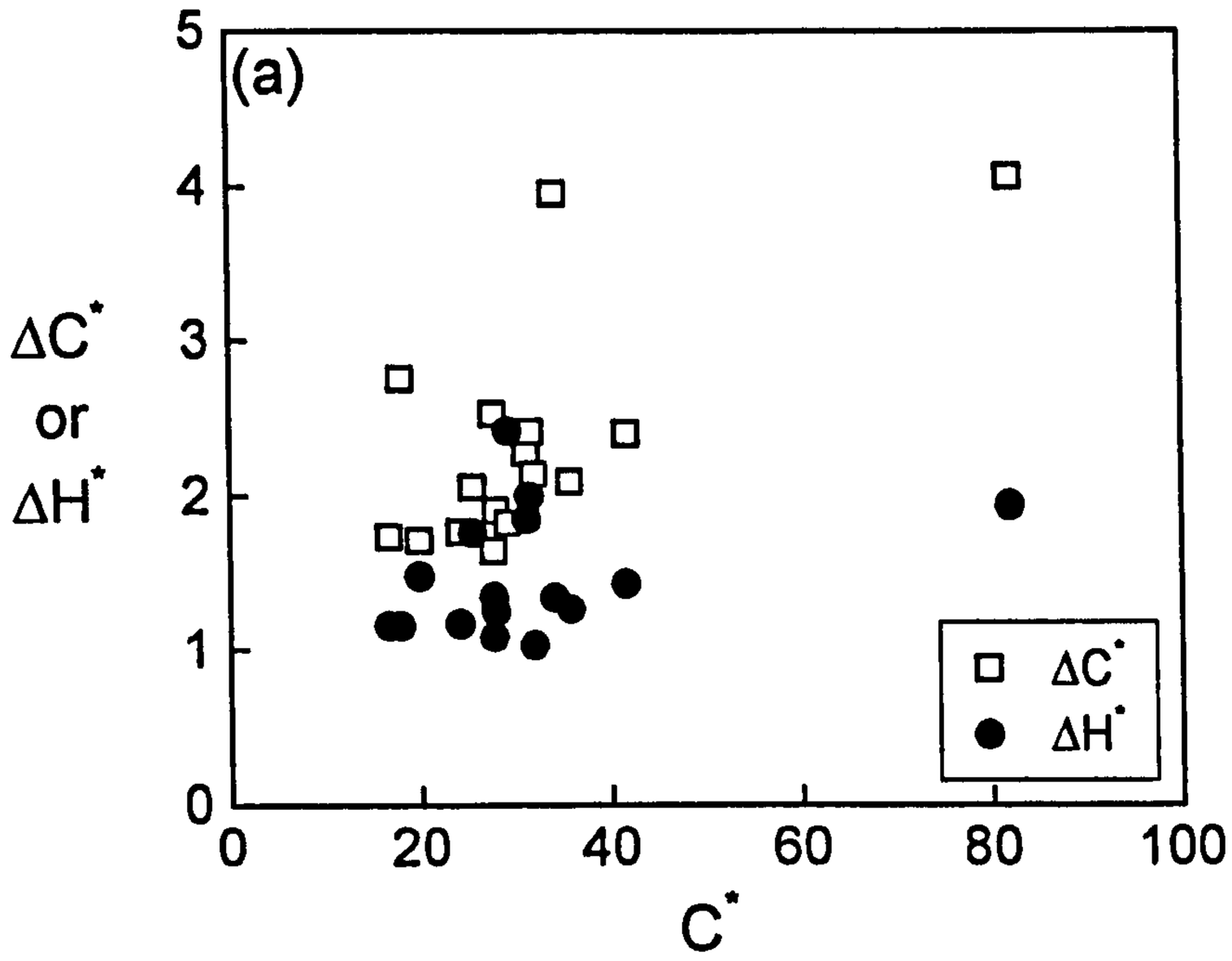

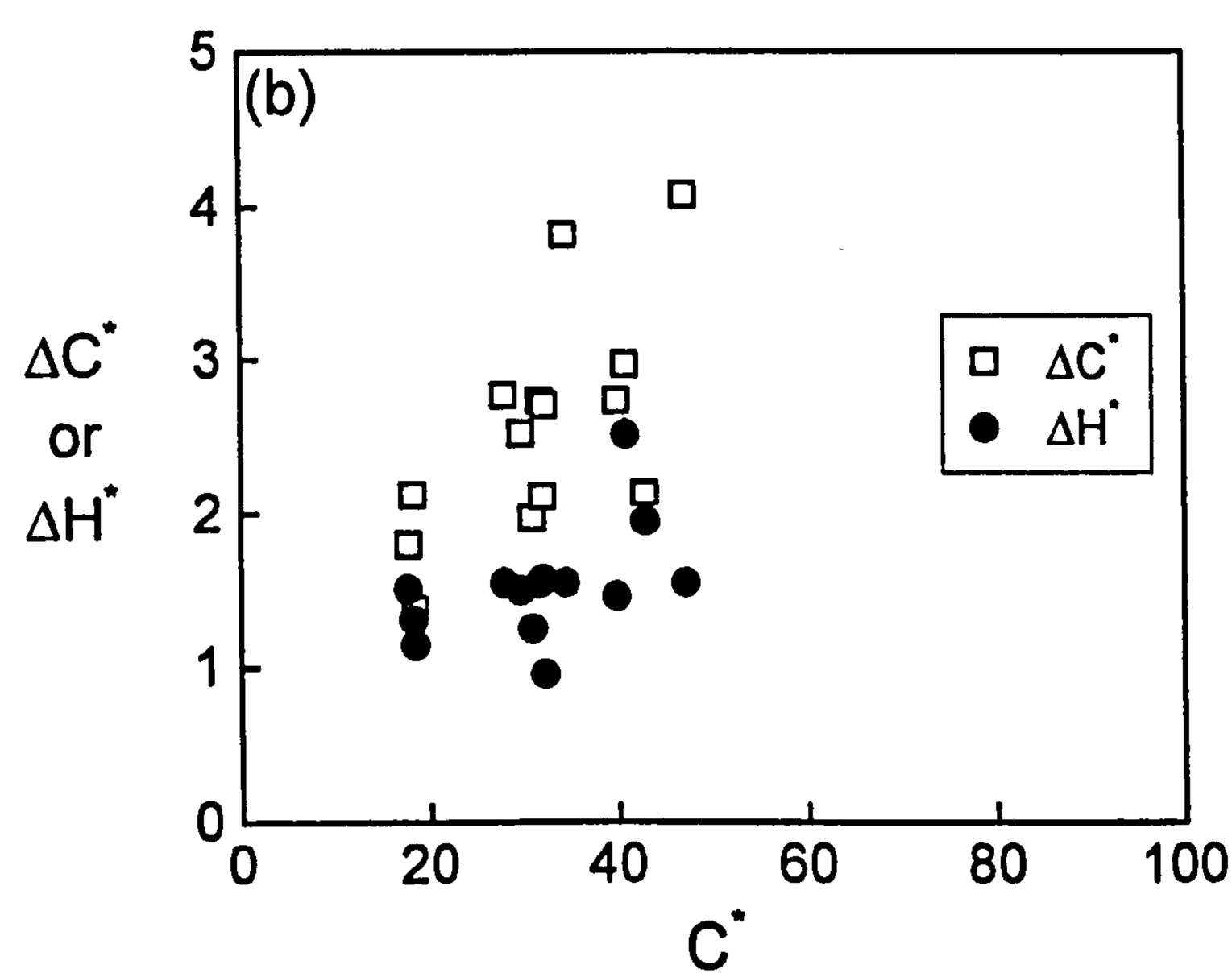

Figure 5-8. Chroma dependence of chroma or hue differences: (a) Berns data, and (b) present study.

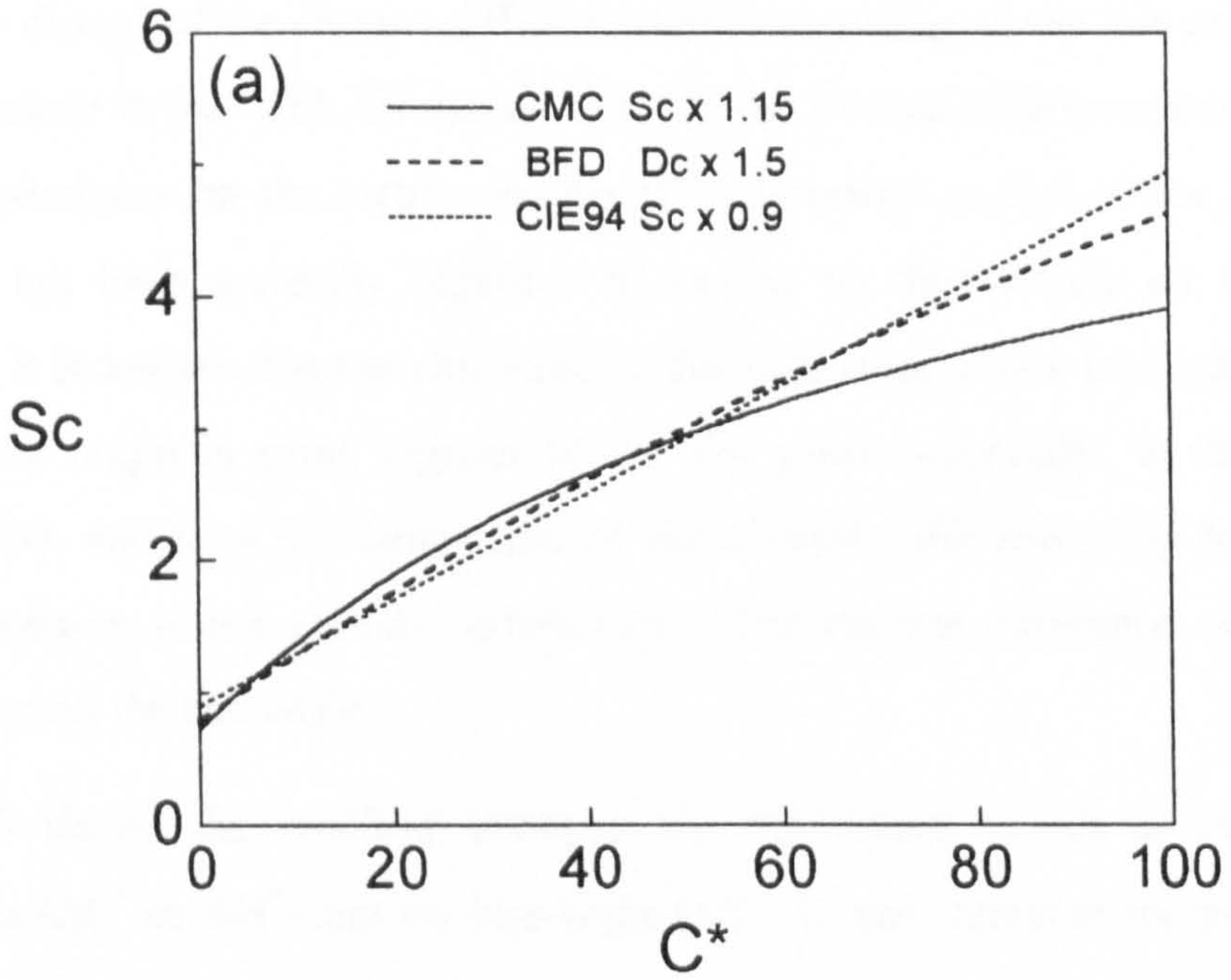

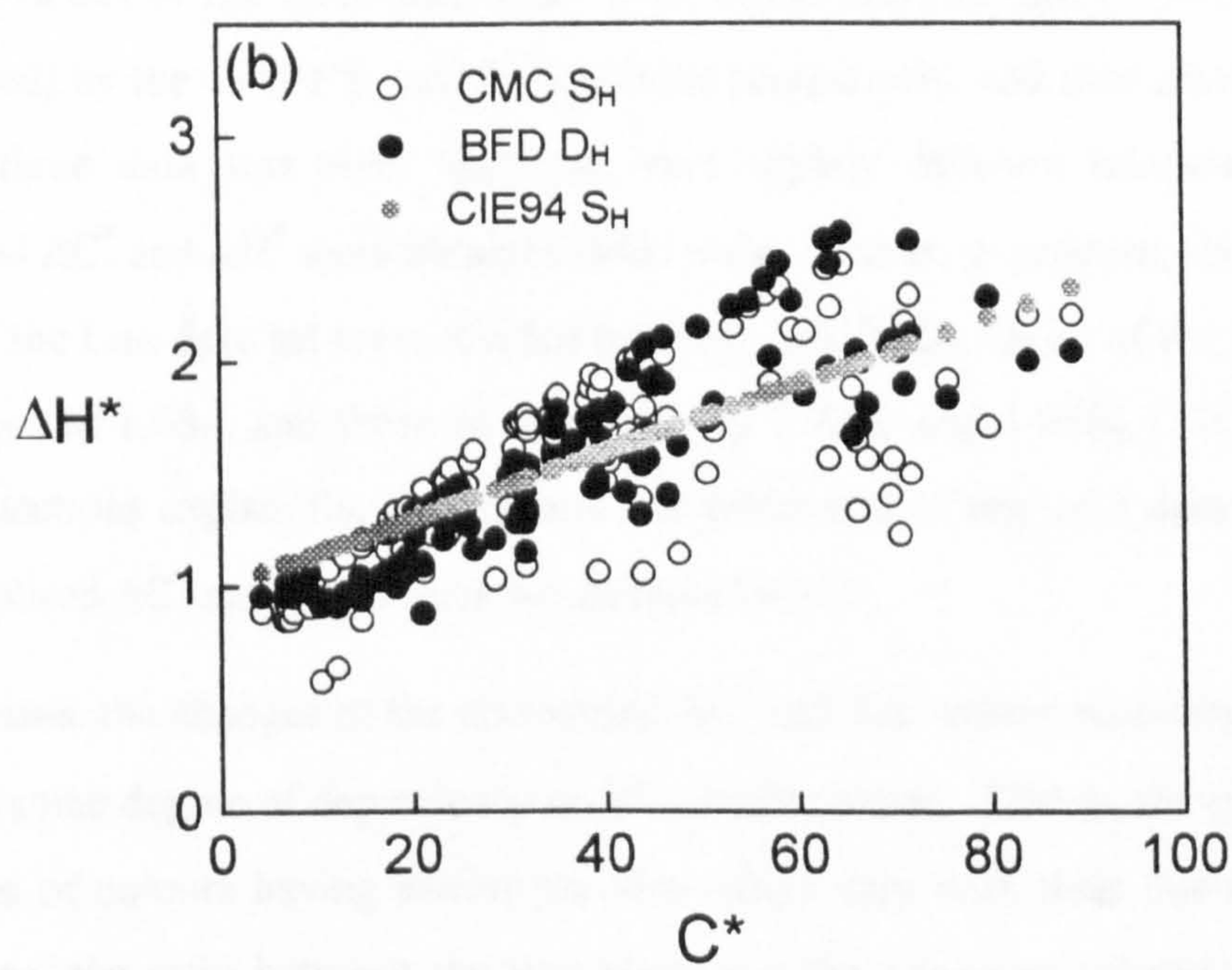

Figure 5-9. Chroma and hue weighting functions: (a) S_C (or D_C) function, and (b) prediction of ΔH^* by S_H (or D_H) function.

5.1.2.1.2 Hue dependence of chroma and hue differences

All three modified CIELAB colour-difference formulae (CMC, BFD and CIE94) assume there is no change of the chroma difference (ΔC^*) according to the hue-angle (h°) of the standard colour in the CIELAB space. Because the chroma difference shows a relatively strong dependence on the metric chroma (C^*) compared to that of the hue difference (ΔH^*), it has been generally regarded as having no dependency on the hue-angle. However, it is known that the chromaticity discrimination ellipse is not always directed towards the origin in some regions of the a^*b^* plane (especially, in the blue region, Section 4.3), and thus the description of the chroma difference only by the standard chroma position is not entirely satisfactory. The chroma difference may have some dependence on the hue angle.

Fig.5-10 shows the relations between the normalised values of chroma or hue differences (ΔC^* or ΔH^*) and the hue-angle (h°). It was shown in the previous section that the CIE94 S_C and S_H functions reasonably well describe the variation of ΔC^* and ΔH^* according to the metric chroma (C^*). Hence, in figures (a) and (b), ΔC^* and ΔH^* tolerance values of the three data sets - Luo, Berns and this study - were first divided (normalised) by the CIE94 S_C and S_H functions respectively, and then plotted against h°. [As the three data sets were found to have slightly different tolerance values, the normalised ΔC^* and ΔH^* were obtained differently. That is, in practice, the ΔC^* and ΔH^* values of the Luo data set were divided by $0.9S_C$ and $0.9S_H$, those of the Berns data set by $0.95S_C$ and $1.0S_H$, and those of this study by $1.05S_C$ and $1.05S_H$.] If the CIE94 S_C and S_H functions explain the chroma and hue tolerances of any of 3 data sets perfectly, the normalised ΔC^* and ΔH^* values would have been 1.

In both cases, the changes of the normalised ΔC^* and ΔH^* values according to h° are not great but some degree of dependency on h° certainly exists. That is, the chroma and hue tolerances of colours having similar chroma values vary with their hue-angles. In the worst case, the ratio between the maximum and the minimum tolerance values, even after adjusted with their chroma position, can be more than a factor of two. The fit lines in figures (a) and (b), which were obtained by optimising the combined data set, may be used to correct the unsatisfactory CIE94 formula by proposing that both the chroma and hue weighting functions S_C and S_H are hue-angle dependent and can be rewritten as follows:

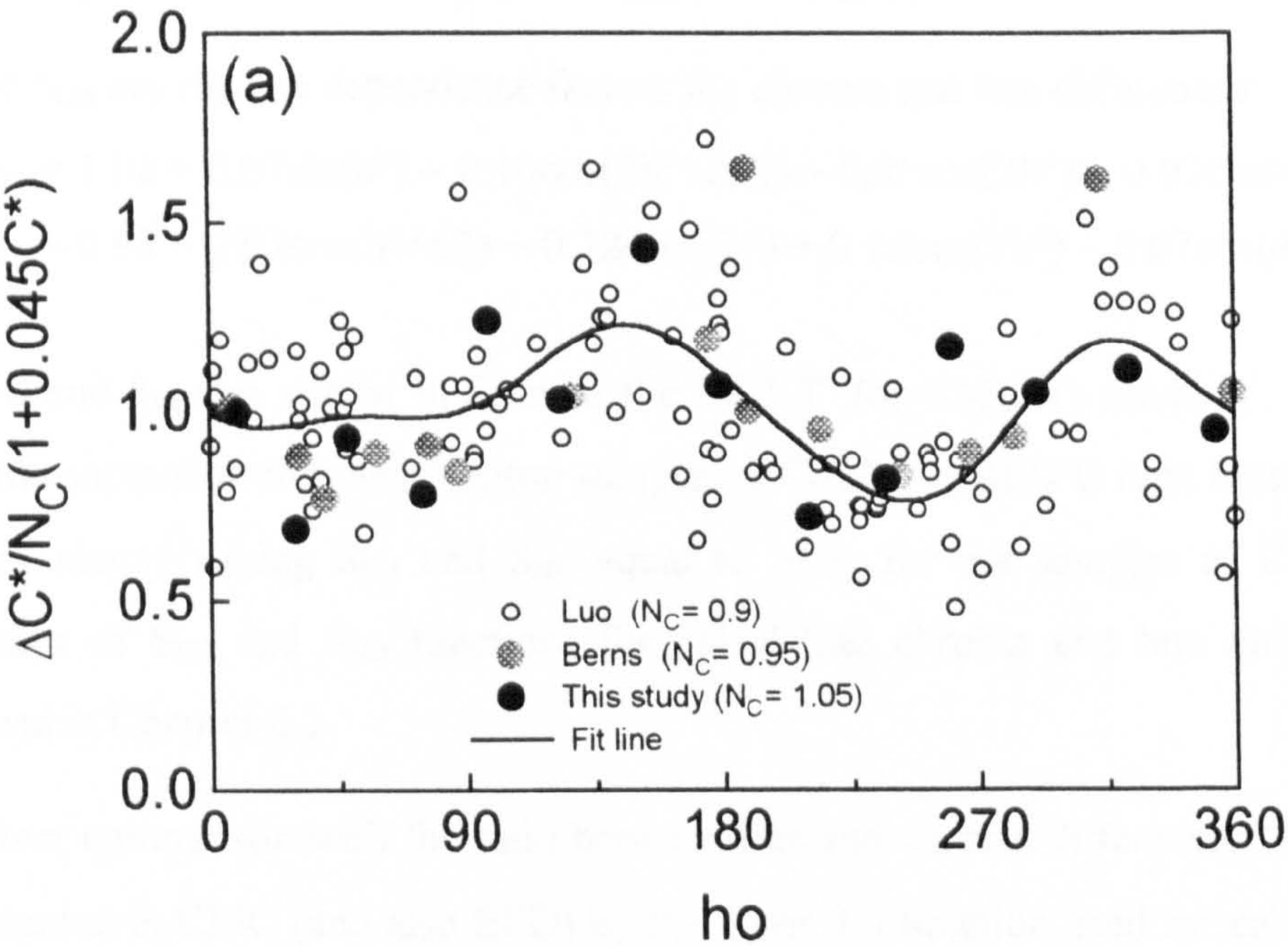

Figure 5-10. Hue dependence of chroma and hue differences of 3 data sets: (a) h° vs. $\Delta C^*/N_C(1+0.045C^*)$, and (b) h° vs. $\Delta H^*/N_H(1+0.015C^*)$.

$$S_C = S_{CC} \cdot S_{CH} \qquad \text{and} \qquad S_H = S_{HC} \cdot S_{HH} \tag{5-3}$$

where S_{CC} and S_{HC} are identical to the CIE94 S_C and S_H functions, that is,

$$S_{CC} = 1 + 0.045C^* \qquad \text{and} \qquad S_{HC} = 1 + 0.015C^*. \tag{5-4}$$

S_{CH} and S_{HH} are the hue dependence factors for chroma and hue differences:

$$S_{CH} = 1.02 + 0.07\sin(h°) - 0.16\cos(2h°+250) - 0.05\cos(3h°) - 0.03\cos(4h°)$$
$$S_{HH} = 0.98 - 0.03\cos(h°+62) + 0.12\cos(2h°) + 0.12\cos(3h°) - 0.07\cos(4h°-46) \tag{5-5}$$

The S_{CH} and S_{HH} are similar in form to the BFD T′ (or CMC T) function. In order to avoid the anomalies with near neutral samples, a CMC f or BFD G type function may be used, or simply setting S_{CH} and S_{HH} equal to unity for the samples of $C^* \leq 4$. (The usefulness of S_{CH} and S_{HH} functions for calculating chroma and hue differences are examined in Chapter 6.)

A direct comparison with the ratio between hue and chroma differences ($\Delta H^*/\Delta C^*$) as implemented in CMC (and also BFD) by the T (or T′) function used for calculating hue differences can be made.

The $\Delta H^*/\Delta C^*$ ratios of the three data sets and the T functions are given in Fig.5-11. The fit line (T function) shown in both figures (a) and (b) is

$$T = 0.63 + 0.1\cos(h° + 105) + 0.11\cos(2h° + 300) + 0.1\cos(3h°) + 0.05\cos(4h° - 255) \tag{5-6}$$

As can be seen in Fig.5-11-a, the ratio $\Delta H^*/\Delta C^*$ can, in practice, be bigger than 1 due to the chromaticity ellipse rotation. The discounting of the hue-angle dependence of the chroma difference in both CMC and BFD does not allow values greater than 1. Therefore, the use of hue-angle dependence term only in the hue weighting function hardly seems to be an effective method of calculating chromaticness differences.

In figure (a), it can be seen that there is a sudden change of the ellipse shape ($\Delta H^*/\Delta C^*$ ratio) near the blue region ($h° \cong 270$). It is thought to be due to the significant ellipse rotation in this region. The new fit line (T function) of this study has a little similar trend with the hue-angle to that of BFD and a quite different form to that of CMC. The difference between the T functions of BFD and this study is somewhat bigger than expected. Because although the T function of this study is obtained by fitting the three data sets, but actually is biased towards the Luo data set as this has the largest number of data points.

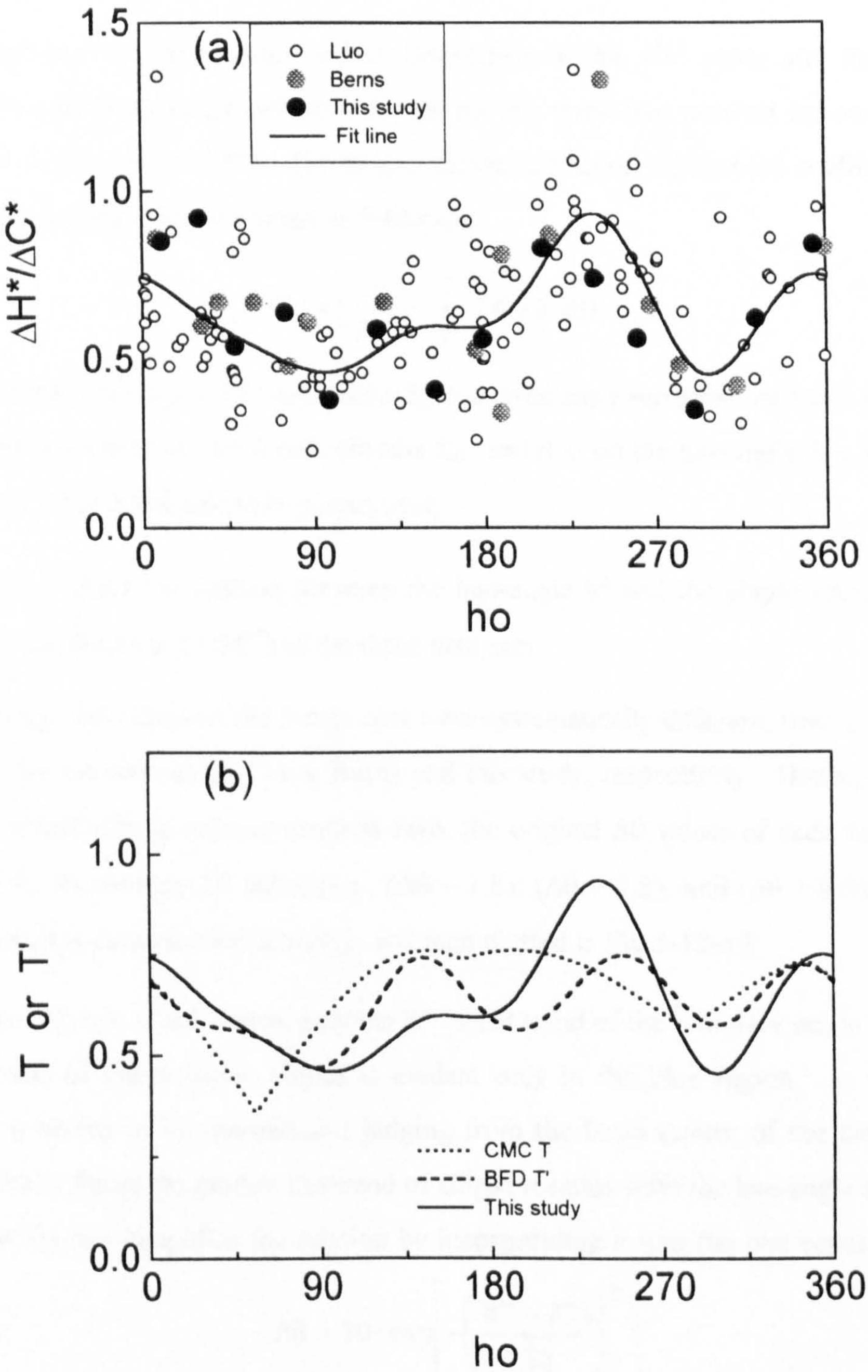

Figure 5-11. Hue-angle dependence of the ratio between hue and chroma differences: (a) h° vs. $\Delta H^*/\Delta C^*$, and (b) comparison of T (or T′) functions.

One possible explanation for this discrepancy is that the BFD T′ function may have been obtained without distinguishing the difference between the ellipse semi-axes (A and B) and chroma or hue tolerances (ΔC^* and ΔH^*).

The variation of chromaticity ellipse orientation in the a^*b^* plane and the general method of adding an additional term for taking this trend into account are reviewed in Section 4.3 (Eq.4-4 to 4-10). It was also shown in Section 4.3 that the coefficient (S_R) of the rotation term can be written as following:

$$S_R = \left(\frac{1}{A^2} - \frac{1}{B^2}\right) \sin(2\Delta\theta) \qquad (5\text{-}7)$$

As considered previously, the coefficient S_R is conveniently separated into two parts, i.e., a function dependent on the metric chroma S_{RC} and that on the hue-angle S_{RH}, which are set to $(1/A^2 - 1/B^2)$ and $\sin(2\Delta\theta)$, respectively.

Fig.5-12-a gives the relation between the hue-angle h° and the ellipse rotation angle $\Delta\theta$ (from the direction of ΔC^*) of the three data sets.

[The average $\Delta\theta$ values of the 3 data sets were systematically different, that is, 1.8, -3.8, and -8.8 for the data sets of Luo, Berns and this study, respectively. Hence, assuming that the overall ellipse rotation angle is zero, the original $\Delta\theta$ values of each data set are adjusted by its average $\Delta\theta$ value (i.e., $(\Delta\theta - 1.8)$, $(\Delta\theta + 3.8)$, and $(\Delta\theta + 8.8)$ for Luo, Berns, and this data set, respectively), and then plotted in Fig.5-12-a.]

Similar to Fig.4-6, which shows only the h° vs. $\Delta\theta$ trend of the Luo data set, in figure (a) the rotation of chromaticity ellipse is evident only in the blue region. In the other regions, it seems to be insignificant judging from the large scatter of the data points. The fit line in figure (a) models the trend of ellipse rotation with the hue-angle analogous to Eq.(4-10), but simplifies the relation by incorporating it into the one equation. It is given by:

$$\Delta\theta = 30 \cdot \exp\left[-\left(\frac{h^\circ - 275}{25}\right)^2\right] \qquad (5\text{-}8)$$

In Fig.5-12-b, the FFT filter smoothing was used for reducing the noise in the Luo data and thus making the comparison easier. It was applied to the original $\Delta\theta$ values by use of the routine in the Microcal Origin graphics software. Also, ten data points which surround one data point were considered at a time in the FFT filtering.

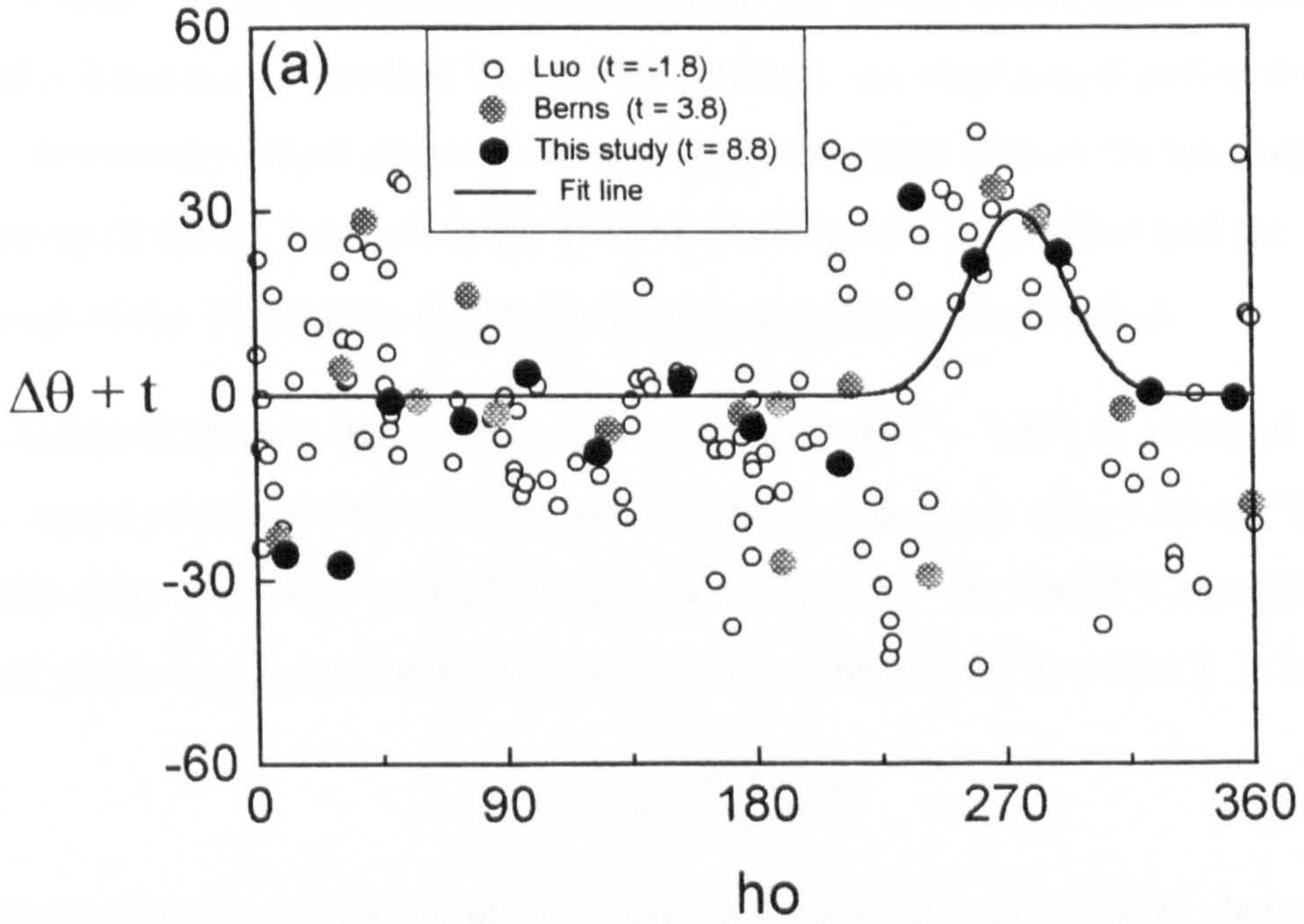

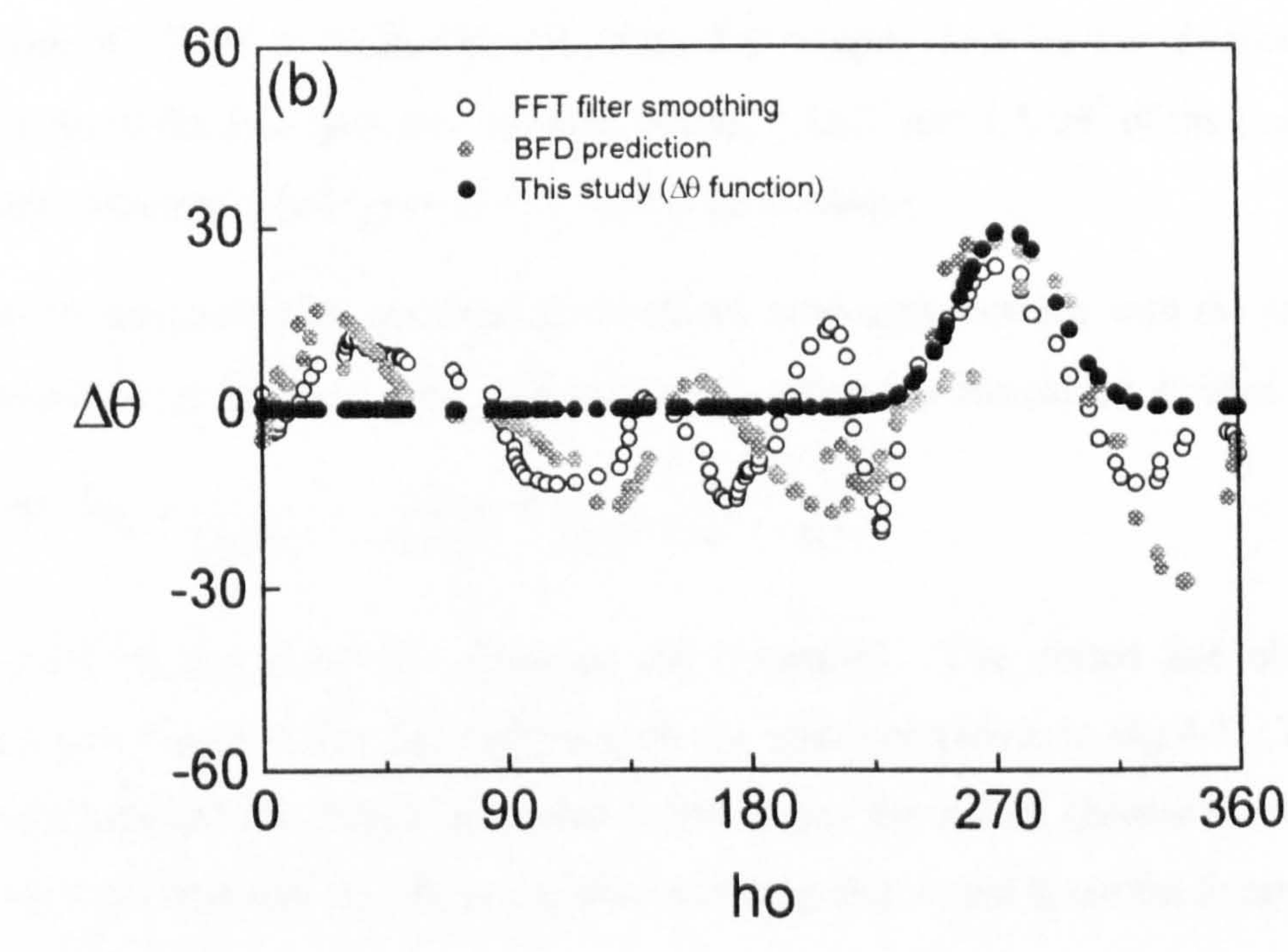

Figure 5-12. Ellipse rotation ($\Delta\theta$) as the function of metric hue -angle (h°): (a) three data sets and the fit line, and (b) comparison of $\Delta\theta$ between FFT filter smoothed Luo data and its predictions by BFD and this study.

The Fast Fourier Transform (FFT) filtered $\Delta\theta$ values of the Luo data are shown together with those predicted by the BFD formula and the $\Delta\theta$ function of this study in figure (b). It can be seen that the complicated BFD formula has a large discrepancy to the Luo data even after it has been smoothed by the FFT filtering. As emphasised earlier, the rotation of the chromaticity ellipse seems to be not significant other than in the blue region. The complexity of the R_T function in the BFD formula cannot be justified and the simplified form such as the $\Delta\theta$ function (Eq.5-8) of this study may be used instead.

The assumed chroma dependence function S_{RC} ($= 1/A^2 - 1/B^2$) is obtained using the actual values of ellipse semi-axes A and B of the Luo data set. (Fig.5-13-a) The fit line coincides reasonably well to the FFT filtered data points. (In the FFT smoothing, again ten data points which surround one data point were considered at a time.) It is given by

$$S_{RC} = \frac{-1.21C^*}{(2+0.07C^*)^3} \tag{5-9}$$

To incorporate it into the existing colour-difference formula (CIE94, here), the S_{RC} function must be rescaled. As explained in the first part of this section, both S_C and S_H functions of CIE94 multiplied by the factor 0.9 roughly describe the chroma and hue differences of the Luo data set. In other words, $1.1\Delta C^*$ and $1.1\Delta H^*$ of the Luo data set are approximately equal to the CIE94 S_C and S_H functions.

Therefore, assuming that the sizes of the ellipse semi-axes increase with the same order of magnitude as ΔC^* and ΔH^*, the original S_{RC} function should be divided by $(1.1)^2$ because $S_{RC} = \frac{1}{(1.1A)^2} - \frac{1}{(1.1B)^2} = \frac{1}{(1.1)^2}\left(\frac{1}{A^2} - \frac{1}{B^2}\right)$.

In Fig.5-13-b, the three S_{RC} functions are compared. The dotted line obtained by assuming $A = S_C$ and $B = S_H$ is identical to the solid line shown in Fig.4-5. The actual relations between the ellipse semi-axes A and B and the metric chroma C^* of the Luo data set were obtained by a fit to the data assuming that A and B are the linear functions of C^*. They are:

$$1.1A = 0.95759 + 0.05856\,C^*$$
$$1.1B = 0.86464 + 0.01644\,C^* \tag{5-10}$$

The dashed line is drawn by substituting above 1.1A and 1.1B values to the S_{RC} function. The solid line that is obtained by dividing Eq.(5-9) by 1.21 shows a very similar form to

the dashed line. (The performance improvement of the CIE94 formula obtained by adding the S_{RC} and S_{RH} function into it is tested in Chapter 6.)

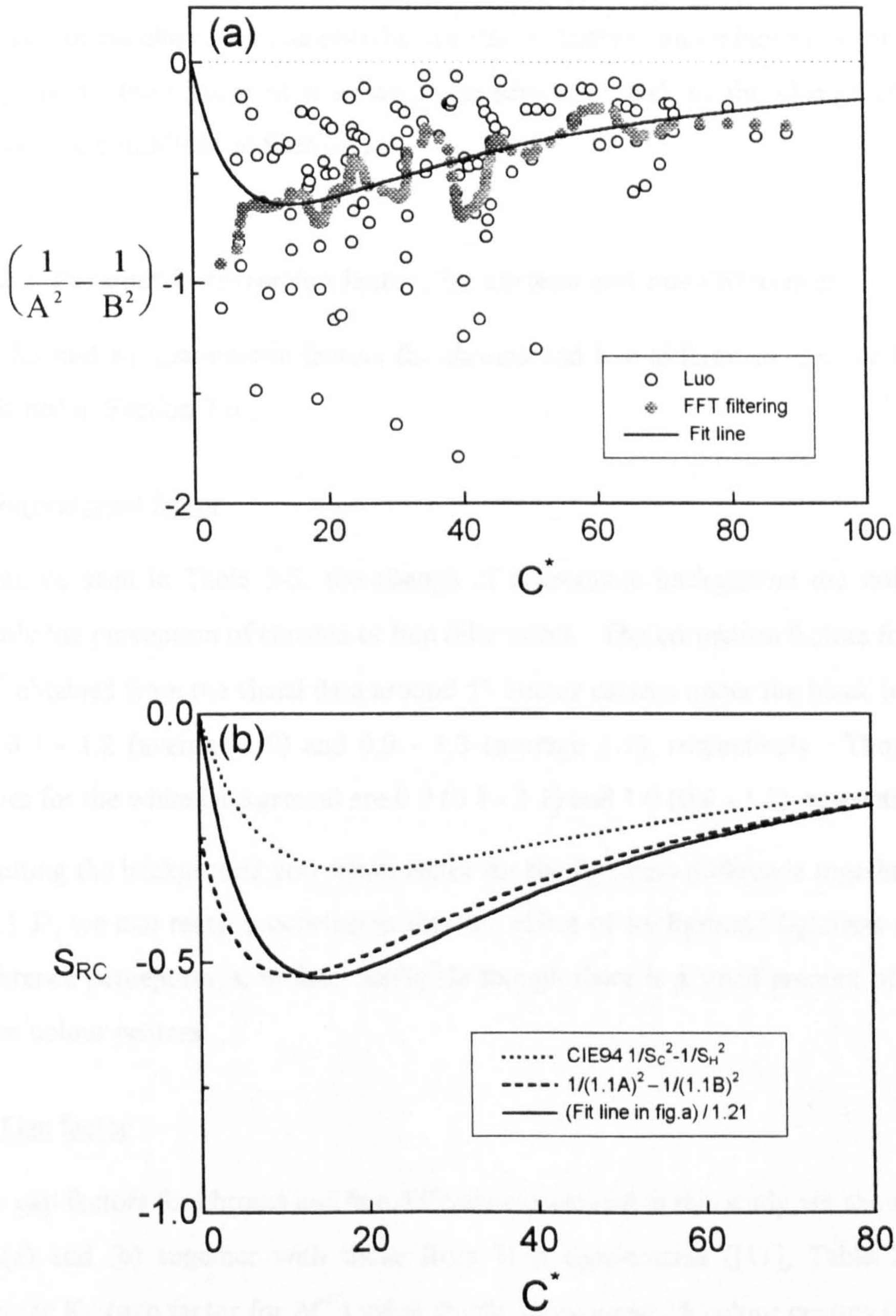

Figure 5-13. Chroma dependence function S_{RC} of the rotation term: (a) C^* vs. $(1/A^2 - 1/B^2)$, and (b) comparison of S_{RC} functions.

5.1.2.2 Chromaticity discrimination under parametric conditions

The results of the chromaticity discrimination under the 3 parametric conditions (black and white backgrounds, and gap) are not given explicitly. The parametric factors needed to correct the chroma and hue differences perception that is caused by the change of viewing condition from the reference grey background are given in the next section. The variation of the ellipse parameters (the orientation angle θ, and minor to major axes ratio B/A) due to the change of the viewing condition as well as the change of observer (group) are considered in Section 5.3.

5.1.2.3 Parametric correction factors for chroma and hue differences

The K_C and K_H (parametric factors for chroma and hue differences, ΔC^* and ΔH^*) are explained in Section 2.6.

(a) Background factor

It can be seen in Table 5-5, the change of achromatic background did not influence greatly the perception of chroma or hue differences. The correction factors for ΔC^* and ΔH^* obtained from the visual data around 15 colour centres under the black background are 0.8 - 1.2 (average 1.0) and 0.9 - 1.3 (average 1.1), respectively. Those average values for the white background are 0.9 (0.8 - 1.1) and 1.0 (0.8 - 1.2), respectively.

Putting the background correction factor for the lightness difference together (Section 5.1.1.3), we can reach a conclusion that the effect of background lightness on colour-difference perception is, in fact, negligible though there is a small amount of change in some colour centres.

(b) Gap factor

The gap factors for chroma and hue differences obtained in this study are shown in Table 5-5(a) and (b) together with those from Witt experiments ([11], Table 2-3). The average K_C (gap factor for ΔC^*) value of this study using 15 colour centres (including 5 CIE centres) is 1.5, while that of Witt using 5 CIE threshold ellipsoids is 2.0. The K_H (gap factor for ΔH^*) values shows fairly good agreement between the two studies, i.e., the averages values are 1.5 for this study and 1.6 for Witt study, respectively.

Table 5-5. Chroma and hue difference (ΔC^* and ΔH^*) correction factors for 3 parametric conditions. (① Results from Witt study[11], and bold figures are explained in the text)

(a) ΔC^* correction factor, K_C

Colour Centre	Co-ordinates			K_C			
	L^*	C^*	h°	Black BG	White BG	Gap	Gap①
1. N	49.4	0.9	108.4	1.1	1.1	1.4	1.3
2. PR	54.3	40.8	10.0	0.9	0.9	1.4	
3. R	43.7	42.9	30.0	1.2	0.9	1.7	2.4
4. YR	60.3	39.9	48.4	0.8	0.9	1.6	
5. RY	79.8	31.0	74.8	1.2	1.1	1.5	
6. Y	86.7	47.1	97.9	0.9	0.8	1.4	1.7
7. GY	66.4	29.7	123.0	1.0	0.9	1.5	
8. YG	60.8	34.4	153.4	0.9	0.9	1.0	
9. G	55.4	31.7	179.1	0.9	0.9	**1.2**	**2.7**
10. BG	52.8	18.5	210.3	1.0	1.0	1.6	
11. GB	61.1	32.0	237.3	1.0	0.9	1.7	
12. B	35.7	27.9	260.3	1.2	0.8	1.3	2.1
13. V	47.1	32.2	290.4	0.8	1.0	1.3	
14. P	45.8	18.2	322.9	1.0	0.9	1.3	
15. RP	53.2	17.7	353.6	1.0	1.0	1.6	
Overall				1.0	0.9	**1.5**	**2.0**

(b) ΔH^* correction factor, K_H

Colour Centre	K_H			
	Black BG	White BG	Gap	Gap①
1. N	1.0	1.1	1.5	1.3
2. PR	1.1	0.8	1.0	
3. R	0.9	1.1	**1.1**	**2.0**
4. YR	1.3	0.9	1.5	
5. RY	1.2	0.9	1.3	
6. Y	1.1	0.9	1.4	1.5
7. GY	1.1	1.0	1.3	
8. YG	1.1	1.0	1.3	
9. G	1.1	1.1	1.6	1.4
10. BG	1.1	0.9	1.8	
11. GB	1.2	1.2	2.2	
12. B	1.1	1.2	1.9	2.0
13. V	1.0	0.9	1.6	
14. P	1.0	0.9	1.4	
15. RP	1.0	0.8	1.0	
Overall	1.1	1.0	**1.5**	**1.6**

The largest discrepancy for K_C and K_H between the two studies is occurred in the green centre and the red centre, respectively. In the Witt study, the gap factors for some colour centres are extremely large. As explained earlier (Section 5.1.1.3, ΔL^* parametric factor K_L), this may be due to the fact that they were obtained from the threshold ellipsoids.

The K_C and K_H values obtained in this study produce, overall, a similar magnitude. This suggests that it is better to use the K_{CH}, the parametric factor for chromaticness difference, than to use the K_C and the K_H factors individually. Thus, in Section 2.6, a formula similar in form to Eq.(2-64) rather than Eq.(2-63) is preferred in practice. In the CMC formula (also in the BFD), the relative tolerances for lightness and chroma differences, ℓ and c, are defined but the equivalent term h for hue difference is omitted by assuming that the h is always unity. However, the c should be interpreted as the relative tolerances for both chroma and hue differences (chromaticness difference).

If we regard the K_L:K_{CH} ratio (or ℓ:c ratio) as the K_L (or ℓ) and also regard $K_{CH} = 1$ always, then we need to change only the K_L for the parametric changes, which is the convention normally used in the modified CIELAB formulae (CMC, BFD, and CIE94) nowadays.

5.1.3 Effects on colour discrimination around 3 CIE colour centres

The lightness, chroma and hue discriminations around each of the 5 CIE colour centres under the standard condition (grey background) and corresponding parametric effects caused by the change of viewing conditions (i.e., black and white backgrounds, and gap) were already given in Chapter 4 and in the previous sections of this chapter. The results shown in those chapters (or sections) are based on experiments conducted to study lightness tolerance and chromaticity discrimination independently. As mentioned in Chapter 4, colour-discrimination ellipsoids for the 3 CIE centres (red, grey and blue) under 4 viewing conditions were also obtained in this study. Although these do not offer any particular new information, the parametric effects on the colour difference ellipsoids of these three centres are briefly described here. The coefficients and parameters of these ellipsoids are shown in Appendix 2 (Tables A-5, A-7 and A-8).

Table 5-6 gives the tilting angle of an ellipsoid axis which is close to the lightness (L^*) axis, the minor to major axes ratio (B/A) and the rotation angle from the positive a^* axis of the cross section of an ellipsoid projected onto the a^*b^* plane, the parametric correction factor for total colour-difference K_E (i.e., the ratio between the geometric mean of three axes of an parametric ellipsoid and that of an ellipsoid obtained under the reference grey background condition), and the population standard deviation estimated from the parameter β of a logistic function.

The tilting, rotation and the shape (B/A ratio) of an ellipsoid seem to be, in general, insensitive to the parametric conditions. That is, the location and the orientation of a colour-difference ellipsoid are not greatly affected by the parametric changes.

It is disappointing that some ellipsoids were rather strongly tilted (about 40°). It means that existing weighted CIELAB colour-difference formulae, such as CMC, BFD and CIE94, which do not allow for the tilting of a tolerance ellipsoid cannot cope with this problem. Thus more sophisticated type formula, which include the interaction term between the lightness and chromaticness differences ($\Delta a^*\Delta L^*$ and $\Delta b^*\Delta L^*$, or $\Delta L^*\Delta C^*$ and $\Delta L^*\Delta H^*$), may be required for the precise description of a colour-difference.

The ellipsoids were more elongated when viewed under the gap condition, but it is not easy to verify whether this effect systematically occurs from the results obtained using only 3 colour centres.

The degree of rotation of the ellipsoids shows fairly good agreement (within 10°) except the blue ellipsoid which was obtained under the white background by use of a paired-comparison method.

The background showed no significant effect on colour-difference ellipsoid, a similar conclusion was drawn from the results which were reviewed in the previous sections. A blue ellipsoid under the black background judged by the paired-comparison method was extremely elongated along the lightness (L^*) axis, and thus produced a quite large parametric factor (K_E), unlike those of other ellipsoids obtained under the same viewing condition. Careful examination of the basic conditions for interpreting the ellipsoid fitted coefficients as an ellipsoid (Section 2.2.1) revealed the fact that the blue coefficients satisfy the conditions, i.e., the ellipsoid can be defined. The anomalous result is thought to be caused by poor sampling or by the lack of a sufficient number of colour-difference pairs, i.e., the test colours of colour-difference pairs of this centre do not satisfactorily

cover the various directions around the standard. Hence, errors may be involved in the ellipsoid fitting process.

The standard deviation which can be regarded as the observer variability was not much different from one background to another.

Table 5-6. Summary of variation of ellipsoids (ellipses) for 3 CIE centres due to the change of viewing conditions. (Values referred to in the text are shown bold.)

Colour Centre	Scale Method	Param. Cond.	tilt.	B/A	rot.	K_E ①	σ ②
Red	PC ③	GRY	22	0.50	39	1.0	0.33
		BLK	23	0.49	38	1.0	0.32
		WHT	**10**	0.67	38	1.0	0.31
		Gap1 ⑤	**45**	**0.33**	32	.	.
		Gap2 ⑥	**46**	**0.26**	37	.	.
Grey	GS ④	GRY	**36**	0.59	80	1.0	.
		BLK	22	0.64	78	0.9	.
		WHT	28	0.63	80	1.0	.
		GAP	26	**0.45**	82	1.2	.
	PC	GRY	25	0.47	95	1.0	0.24
		BLK	23	0.51	91	1.0	0.29
		WHT	21	0.52	94	1.0	0.24
Blue	GS	GRY	37	0.47	111	1.0	.
		BLK	42	0.50	116	1.1	.
		WHT	43	0.56	109	1.1	.
		GAP	42	**0.42**	103	1.4	.
	PC	GRY	39	0.58	102	1.0	0.35
		BLK	44	0.62	107	**1.6**	0.40
		WHT	39	0.63	**84**	1.0	0.33

① Parametric factor for total colour difference, i.e., the ratio between the cube-root of the volume of a parametric ellipsoid and that of a reference ellipsoid.
② Standard deviation estimated as $1.7/\beta$, where β is a parameter of the logistic function.
③,④ Paired-comparison and grey-scale methods, respectively.
⑤,⑥ Tests with standard pair no.2 and no.3, respectively.

5.2 Colour Measurement Error

The methods of the quantification of colour measurement errors were reviewed in Section 2.4, and the procedures of the instrumental measurement of the colour panels used in this experiment were also summarised in Section 3.4.

The German standard DIN55600 (Part 2) [17] and the ASTM standard E1345 [18]

provide more elaborate methods to quantify the colour-difference (or colour) measurement error than the simple method that only calculates the standard deviations of the measured colour-difference values. However, both the DIN and the ASTM methods are more or less cumbersome, i.e., they require many numbers of measurements (about ≥ 20) to calculate the error estimate. They are, in effect, aimed to test (a) the repeatability of the colour measuring instrument and (b) the reproducibility of a series of preparation, and (c) to reduce the variability of multiple colour measurements. Because both are thought to be impractical to quantify the overall measurement error of a large number of colour panels, it was decided in this study to use a simple method.

As mentioned in Section 2.4, the problem of using the simple method is that it does not coincide with the variation of the observed experimental results. That is, each of colour-difference scale values does not follow the underlying normal error distribution. Thus, the short-term repeatability of the spectrophotometer (Colourgen CS-1100) was tested first by use of both the DIN and the simple method. (Table 5-7)

Two panels of a colour-difference pair which has the similar colour co-ordinates and colour-difference value to the standard pair no.1 (Section 3.2.4) were measured one after another, each 20 times with nearly identical position, without re-calibrating the spectrophotometer. The standard deviations (1σ and 2σ) by the simple method are shown in the 3rd and 4th rows of Table 5-7, while the confidence limits (70% and 95%) by the DIN method are shown in the 5th and 6th rows of the same table. It can be seen that, as expected, in the DIN method the 95% confidence limits of colour-difference scale values are not twice those for the 70% confidence limits. Although the errors obtained by both methods are not identical, the simple method produces estimates not much different from the complicated DIN method. The simple method seems to produce reasonable estimates of the instrumental colour-difference measurement error and it has been used instead of a more sophisticated method.

Table 5-7. Short term repeatability of Colourgen CS-1100 spectrophotometer.

Mean & StD	ΔE^*	ΔL^*	Δa^*	Δb^*
μ	**1.00**	**0.67**	**-0.18**	**-0.72**
1σ	0.03	0.02	0.03	0.03
2σ	0.05	0.04	0.06	0.07
70% CI	0.04	0.04	0.04	0.04
95% CI	0.05	0.06	0.05	0.06

Table 5-8. Precision of instrumental colour-difference measurements.

Colour Centre	No. of Pairs	ΔE^*		
		Mean	StD	CV%
LD1①	55	1.49	0.07	4.4
LD2②	23	1.54	0.07	4.9
CHD③	75	1.87	0.07	3.6
Blue	26	2.16	0.07	3.3
Red	45	1.52	0.06	4.0
Grey	24	1.02	0.06	5.6
Total	248	**1.64**	**0.07**	**4.0**

Colour Centre	ΔL^*			Δa^*			Δb^*		
	$\lvert\Delta L^*\rvert$	StD	CV%	$\lvert\Delta a^*\rvert$	StD	CV%	$\lvert\Delta b^*\rvert$	StD	CV%
LD1	1.47	0.07	4.6	0.11	0.04	.	0.14	0.06	.
LD2	1.53	0.08	5.0	0.06	0.04	.	0.11	0.07	.
CHD	0.20	0.06	.	1.19	0.05	4.5	1.14	0.07	6.4
Blue	0.41	0.09	.	0.87	0.08	9.3	1.65	0.06	3.9
Red	0.56	0.08	14.6	0.79	0.04	5.4	0.69	0.07	9.9
Grey	0.41	0.07	15.7	0.46	0.04	8.2	0.61	0.06	9.4
Total	0.71	**0.07**	9.9	0.67	**0.05**	7.4	0.74	**0.07**	9.1

(①,② Lightness difference studies in experiment part 2 and 3, respectively.

③ Chromaticity discrimination study in experiment part 3.)

The results are based on 3 sets of measurement, i.e., before, during and after the visual assessments. Each set of measurements cotains 3 -5 readings of each sample.)

Table 5-8 shows the results of the colour measurement error of this study. The standard deviations of the total and the component colour differences were 0.07 except that for Δa^* (0.05). That is, the error in measured colour-difference value is well within the 0.1 ΔE^* unit.

The CV (coefficient of variation) for the total colour-difference (ΔE^*) was 4%. The CV, however, has not much meaning as an estimate of the colour-difference measurement error because it depends on the mean of the absolute values of individual differences. Luo [5,12] assumed a 5% error of each measured colour-difference values in xyY space for generating the colour measurement error ellipsoids. Considering the fact that the mean colour-difference of the Luo sample data [5] ($\Delta E^* = 4.4$) is about 3 times larger than that of this study ($\Delta E^* = 1.6$), the CV of this study is actually much smaller than that of Luo.

5.3 Observer Uncertainty

The errors of previous colour-difference evaluation studies and the estimation methods of the observer judgement error were described in Section 2.5. In that section, it was reviewed that the precision (standard error) of the Luo [5] and the Berns [4] data sets are ±8.9% and ±5.7%, respectively. The overall standard error of this study is ±7.0% for a standard grey background condition and observer groups (Table 5-9), which is between those of earlier studies. The observer tests of this study are, therefore, thought to be reasonably performed under well-controlled conditions, and the visual data-set can be regarded as self-consistent.

The errors involved in observer judgements under the different backgrounds (black and white backgrounds) are similar in magnitude to those under the reference grey background. Together with the parametric factors reviewed in previous sections, the change of a grey background seems to cause no significant variation in observer sensitivity.

However, the gap between a pair of samples caused more observer error (±10%) than other viewing conditions. It is thought to be that the observers are more uncertain in their assessments of colour-difference pairs having an unclear dividing line between samples (e.g., textile specimen) than those having sharp dividing line (e.g., paint specimen).

The single observer has made more precise judgements than the observer group (Table 5-9-b), except for the gap viewing condition. The error in the judgements of the observer CY under the gap condition is bigger than that for the observer group. Again, it is believed that the judgement of the colour-difference between separated samples is more difficult than those directly in contact with each other.

The variation of chromaticity discrimination ellipses according to the observers as well as parametric conditions is also studied (Table 5-10). Twelve ellipses (3 observer groups × 4 parametric conditions) were obtained for each of 15 colour centres. The orientation ($\Delta\theta$) and the shape (B/A ratio) of a chromaticity ellipse are, in general, not changed much by the observer or by the parameter (i.e., overall, the standard deviations of $\Delta\theta$ and B/A are 7.7 and 0.08, respectively). Near the red and blue region in the CIELAB space, however, the fitted ellipses show a rather greater variability.

Table 5-9. Precision (standard error) of visual data.

(a) Observer group

Colour Centre①	No. of Pairs	Grey BG	Black BG	White BG	Gap	Scale Method④
Red	45	5.0	5.9	**7.6**②	8.2	PA
LD1	55	7.4	7.9	6.0	**12.3**③	
Grey	29	6.2	4.3	7.0	8.9	GS
Blue	31	9.0	6.2	8.0	12.8	
CHD	75	7.5	9.5	8.4	10.1	
LD2	23	6.1	8.7	7.6	9.6	
Total	258	**7.0**	**7.5**	**7.5**	**10.4**	-

(b) Single observer

Colour Centre	Observer⑤	Grey BG	Black BG	White BG	Gap
CHD	DK	5.0	4.3	3.4	7.6
	CY	6.2	5.8	4.8	10.3
LD2	DK	4.8	4.6	4.8	9.0
	CY	5.5	4.4	3.9	13.2

(c) Example of an error estimation from the result of a grey-scale method.

GS & ΔV	Mean	StD	StD of MGS⑥	−1σ	+1σ	CV
GS	6.84	1.17	**0.34**	6.50	7.18	.
ΔV	0.74	0.09	.	0.65	0.83	**12.3**

① LD1, LD2, CHD: Lightness difference exps. in part 2 and 3, and chromaticity discrimination exp. in part 3, respectively.

② Obtained excluding the result of vector direction D.

③ From the simplified method assuming a normal distribution of the grey-scale values → Table 5-9-c.

④ Errors estimated from the results of probit analyses (PA) and grey-scale assessments (GS), respectively.

⑤ DK, CY: Observers DK and CY, respectively.

⑥ Standard deviation (StD) of the mean grey-scale, i.e., StD (1.17) divided by the square-root of the total number of judgement (here, 12) for each col. diff. pair.

Table 5-10. Variation of chromaticity ellipses according to observers and parametric conditions. (① Refer to Table 3-2)

Colour Centre①	h°	Δθ		B/A	
		Mean	StD	Mean	StD
PR	10	-32	**10**	0.65	**0.14**
R	30	-30	**13**	0.73	**0.14**
YR	48	1	**14**	0.53	**0.10**
RY	75	-1	6	0.54	0.06
Y	98	-5	4	0.40	0.03
GY	123	-10	5	0.57	0.04
YG	153	-2	6	0.48	0.06
G	179	-5	9	0.67	0.09
BG	210	-23	5	0.73	0.06
GB	237	25	**13**	0.80	**0.10**
B	260	1	**9**	0.65	**0.10**
V	290	13	2	0.32	0.05
P	323	-11	7	0.59	0.07
RP	354	-17	6	0.69	0.06
Overall		-6.8	**7.7**	0.60	**0.08**

Table 5-11. Change of parametric factors according to observers (① OG, DK, CY: observer group, observers DK and CY).

(a) Parametric factors K_L, K_C and K_H

Obs.①	Param.	K_L	K_C	K_H
OG	Black BG	1.1	1.0	1.1
	White BG	1.0	0.9	1.0
	Gap	**2.0**	**1.5**	**1.5**
DK	Black BG	1.1	1.0	1.0
	White BG	0.9	1.0	1.0
	Gap	**2.8**	**1.7**	**1.7**
CY	Black BG	1.0	1.0	1.0
	White BG	1.0	0.9	1.0
	Gap	**3.3**	**2.7**	**2.7**

(b) ℓ:c ratio for the gap parameter

Obs.	ℓ	c
OG	**1.4**	1.0
DK	**1.6**	1.0
CY	**1.2**	1.0

One possible explanation of this variability may be due to the rotation of an ellipse that is prominent in the blue region. It is not clear where the variation of red ellipses came from. More experiments are required to find the source of this kind of uncertainty.

The changes of parametric factors according to the observer (or observer group) are examined. Table 5-11 gives the results obtained by use of the 98 colour-difference pairs (23 pairs for lightness difference and 75 pairs for chromaticness difference) which were judged by one observer group (10 observers with single assessment each) and two single observers (10 repeated assessments each). The background factors were changed little not only from one background to another but observer to observer (or group to group). It also confirms the experimental results of previous sections that the background effect on colour-difference perception is negligible.

The gap factors were, on the other hand, considerably different between observers (groups). The ℓ and c values shown in Table 5-11-b were calculated by taking the ratios K_L/K_H and K_C/K_H, respectively. Considering the results shown in table (b), it deemed to be appropriate to set the ℓ value (or ℓ:c ratio) as about 1.5 for textile industry in using the weighted CIELAB formula.

5.4 References

1. B.Rigg, Colour-Difference Formulae - Recent Developments, JSDC, **111**, 267-271 (1995).

2. E.Coates, K.Y.Fong and B.Rigg, Uniform Lightness Scales, JSDC, **97**, 179-183 (1981).

3. S.Addae-Badu, Large Colour Differences between Surface Colours, Ph.D. Thesis, University of Bradford, 1986.

4. R.S.Berns, D.H.Alman, L.Reniff, G.D.Snyder and M.R.Balonon-Rosen, Visual Determination of Suprathreshold Color-Difference Tolerances Using Probit Analysis, Col. Res. Appl., **16**, 297-316 (1991).

5. M.R.Luo, New Colour-Difference Formulae for Surface Colours, Ph.D. Thesis, University of Bradford, 1986.

6. S.M.Newhall, D.Nickerson and D.B.Judd, Final Report of the O.S.A. Subcommittee on the Spacing of the Munsell Colors, J. Opt. Soc. Am., **33**, 385-418 (1943).

7. D.B.Judd and G.Wyszecki, Color in Business, Science and Industry, 3rd ed., John Wiley & Sons, New York, 1975.

8. CIE Publ. No.101, Parametric Effects in Colour-Difference Evaluation, CIE central Bureau, Vienna, 1993.

9. R.McDonald, The Effect of Colour Physics on the Textile Industry (Newton Lecture, City University, London, 1 Nov. 1995), The Colour Group [GB] Newsletter, Dec. 1995, 12-25.

10. R. G. Kuehni, Modification to the JPC79 Colour - Difference Formula (Correspondence), JSDC, **100**, 281 (1984).

11. K.Witt, Parametric Effects on Surface Color-Difference Evaluation at Threshold, Col. Res. Appl., **15**, 189-199 (1990).

12. M.R.Luo and B.Rigg, Chromaticity-Discrimination Ellipses for Surface Colours, Col. Res. Appl., **11**, 25-42 (1986).

13. M.Melgosa, E.Hita, J.Romero and L.Jimenez del Barco, Color-Discrimination Thresholds Translated from the CIE (x,y,Y) space to the CIE 1976 (L^*,a^*,b^*), Col. Res. Appl., **19**, 10-18 (1994).

14. R.McDonald, Industrial Pass/Fail Colour Matching - Part II. Methods of Fitting Tolerance Ellipsoids, JSDC, **96**, 418-433 (1980).

15. M.R.Luo and B.Rigg, BFD(ℓ:c) Colour-Difference Formula: Part 1 - Development of the formula, JSDC, **103**, 86-94 (1987).

16. R.S.Berns, The Mathematical Development of CIE TC 1-29 Proposed Color Difference Equation: CIELCH, Proc. 7th Cong. AIC COLOUR 93, Budapest, Vol.B, 1993, C19.1-19.4.

17. H.G.Völz, Industrial Color Testing: Fundamentals and Techniques, VCH, Weinheim, Germany, and New York, 1995.

18. ASTM E1345, Standard Practice for Reducing the Effect of Variability of Color Measurement by Use of Multiple Measurements, 1995 Annual Book of ASTM Standards, Vol.06.01.

6. NEW WEIGHTING FUNCTIONS FOR THE MODIFIED CIELAB COLOUR-DIFFERENCE FORMULA

In the previous two chapters, the new weighting functions (or the correction terms) for lightness, chroma and hue differences have been considered. The aim of Chapter 6 is to test these weighting functions with various data sets and thus to develop a reliable CIELAB-based ellipsoidal formula.

6.1 Specification of New Weighting Functions

Preliminary tests of colour-difference formulae based on component colour differences (Chapter 5) revealed the following:

The three modified CIELAB formulae (CMC, BFD and CIE94) show very similar performances to each other. They could be used for general application in their present forms. The CIE94 formula may be preferred, in practice, to the other two formulae as it has the simplest form but shows a reasonable performance. However, in some cases, CIE94 seriously mispredicts the colour tolerance volume from a standard colour.

First, the lightness tolerance shows some dependency on the lightness of a standard; in the case of light colours, it definitely increases with the lightness (Fig.5-2). The CIE94 formula proposes a constant lightness tolerance.

Second, the chromaticity ellipses in the blue region evidently rotate from the direction of chroma differences (Fig.5-12). Like the CMC formula, CIE94 has no means for reflecting this in the formula itself.

Third, the chroma or hue tolerances may differ by more than a factor of 2 for two colours having identical metric chromas (Hue-angle dependency, Fig 5-10). The CIE94 formula has no hue-angle dependency.

The simplicity itself may be one of great advantages of using CIE94. The flexibility allows the addition of new terms to the formula or the incorporation of new parametric factors. Therefore, it was decided to specify a new colour-difference formula similar in form to CIE94. The new formula would be compatible in most respects to CIE94 and nearly as simple as CIE94, but better in its performance than CIE94.

A general form of an ellipsoidal formula based on the CIELAB space can be written as

follows:

$$\Delta E = \left[\left(\frac{\Delta L^*}{\ell S_L} \right)^2 + \left(\frac{\Delta C^*}{S_C} \right)^2 + \left(\frac{\Delta H^*}{S_H} \right)^2 + S_R \Delta C^* \Delta H^* \right]^{1/2} \qquad (6\text{-}1)$$

The ℓ value should be read as the ratio between K_L and K_{CH} (Section 5.1.2.3). If the S_L, S_C, and S_H functions were the same as those of CIE94 and the S_R function that allows the chromaticity ellipse rotation was set to zero, then Eq.(6-1) is identical to CIE94.

Efforts were made in three aspects to improve the performance of Eq.(6-1) compared to CIE94: (1) lightness tolerance (S_L function), (2) hue-angle dependency of chroma and hue tolerances (S_C and S_H functions), and (3) chromaticity ellipse rotation (S_R function).

6.1.1 Lightness weighting function

The lightness weighting function is slightly modified from that originally obtained in Chapter 5 (Eq.5-1) for the following reasons.

The only data set including extremely dark samples is the Fong data set [1] which shows the lightness tolerances of medium to dark colours ($L^* < 50$) are generally smaller than those of the medium to light colours ($L^* \geq 50$). However, this is not the case in the other two data sets (Berns [2] and this study) which were carried out under very carefully controlled experimental conditions and thus are regarded as self-consistent. These suggest that the visual lightness tolerances of dark colours are bigger than those near medium lightness ($L^* \cong 50$), though the greatest tolerance magnitude is apparent for the light colours.

Each data point (tolerance value) of the Fong data was obtained using only one colour-difference pair, and thus the effectiveness of these data points (especially, those for very dark colours) is questionable.

To compromise for this situation, it may be better to set the lightness tolerances (S_L function) of medium to dark colours ($L^* = 0 \sim 50$) as unity and for the medium to light colours ($L^* = 50 \sim 100$), which show the clear trend of the increase of lightness tolerance with the lightness (L^*), as a second order polynomial of L^* (Fig.6-1-a). That is,

$$S_L = 1 - 0.01L^* + 0.0002(L^*)^2$$
$$\text{unless } L^* < 50 \quad \text{when } S_L = 1 \qquad (6\text{-}2)$$

This proposal satisfies the basic purpose of keeping the new weighting function as compatible as possible to CIE94, i.e., Eq.(6-2) is identical to that of the CIE94 S_L function for the colours of $L^* \leq 50$.

6.1.2 Chroma and Hue weighting functions

The original chroma and hue weighting functions S_C and S_H of CIE94 are thought to be insufficient to describe the chroma and hue tolerances for a wide range of colour positions (especially, with respect to the hue-angle of a standard). Thus, the S_{CH} and S_{HH} functions obtained in Section 5.1.2.1.2 were incorporated to the definition of S_C and S_H functions. The forms of S_C and S_H functions are as follows:

$$S_C = S_{CC} \cdot S_{CH}$$
$$S_H = S_{HC} \cdot S_{HH} \qquad (6\text{-}3)$$

where $S_{CC} = 1 + 0.045C^*$

$$S_{HC} = 1 + 0.015C^* \qquad (6\text{-}4)$$

$$S_{CH} = 1 + 0.07\sin(h^\circ) - 0.16\cos(2h^\circ+250) - 0.05\cos(3h^\circ) - 0.03\cos(4h^\circ)$$
$$S_{HH} = 1 - 0.03\cos(h^\circ+60) + 0.12\cos(2h^\circ) + 0.12\cos(3h^\circ) - 0.07\cos(4h^\circ-45)$$
$$\text{unless } C^*_{std} \leq 4 \quad \text{when } S_{CH} = S_{HH} = 1 \qquad (6\text{-}5)$$

(The S_{CH} and S_{HH} functions given in Eq.6-5 are a little changed from their original forms shown in Eq.5-5 to allow for the first term to be unity.)

6.1.3 Ellipse rotation function

The ellipse rotation function S_R is defined by Eq.(6-6) based on Eqs.(5-7), (5-8) and (5-9) of Section 5.1.2.1.2. As the $\Delta\theta$ function is essentially zero (and hence S_R also) except for the blue region (Fig.5-12-a), the form of Eq.(6-1) is identical to CIE94 except for the blue colours.

$$S_R = S_{RC} \cdot S_{RH}$$
$$S_{RC} = \frac{-C^*}{(2+0.07C^*)^3}$$
$$S_{RH} = \sin(2\Delta\theta) \quad \text{and} \quad \Delta\theta = 30 \cdot \exp\left[-\left(\frac{h^\circ - 275}{25}\right)^2\right] \qquad (6\text{-}6)$$

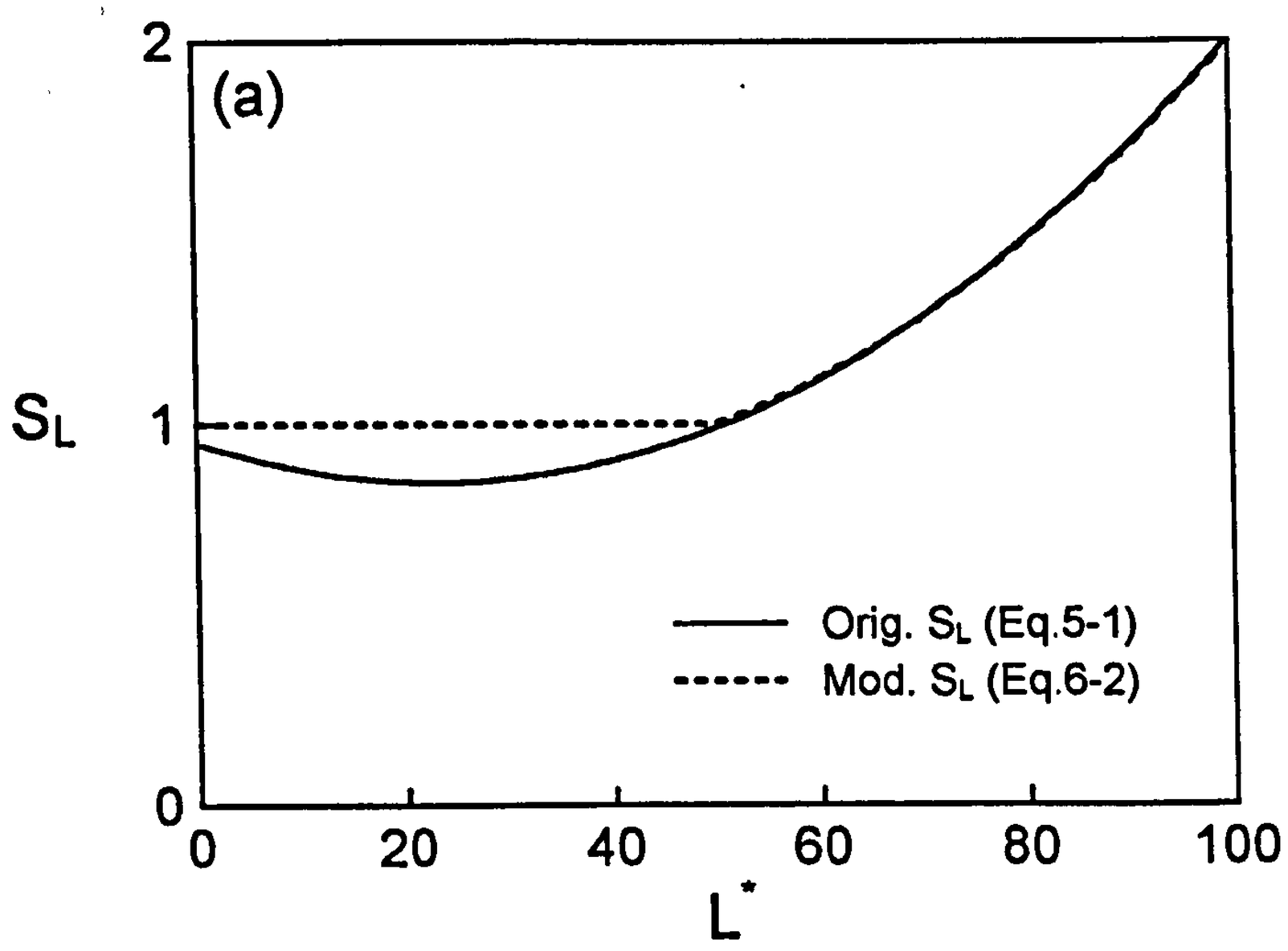

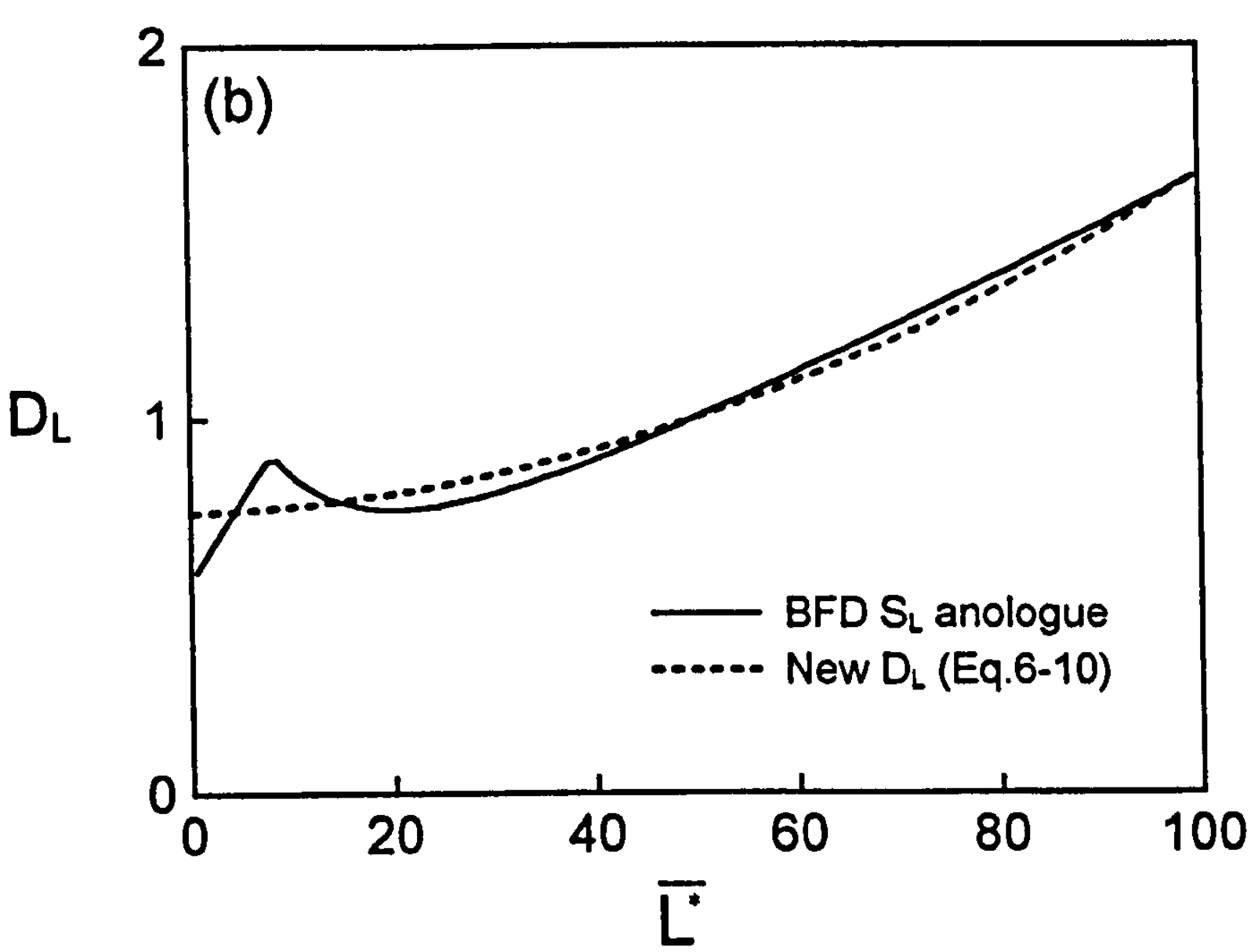

Figure 6-1. Lightness-difference (ΔL^*) weighting functions: (a) S_L functions of this study, and (b) D_L functions of the BFD formula.

6.1.4 Modification of the BFD weighting functions

The BFD formula usually shows the better performance than CMC or CIE94 formulae when the ℓ value is fully optimised for the individual data set tested. As it incorporates most features from a wide range of data sets available at the time of development (1987) and also has the most complex form among the three formulae, it may be a natural consequence. However, it sometimes shows the poorer performance even when it is tested with its original recommended ℓ value (1 for perceptibility and 1.5 for acceptability).

It is suspicious that the relative sizes of lightness and chroma (also hue) weighting functions of BFD were more or less unbalanced whereas in the other two formulae they are similar in size. The average size of the lightness weighting function of BFD is very similar to that of CMC or CIE94 (Fig.5-3). But, the chroma weighting function is much smaller than the other two formulae. Hence, an attempt was made to improve the reliability of the BFD formula by substituting the chroma weighting function D_C with a new one whose size is similar in magnitude to that of CMC or CIE94.

The general form of the BFD formula can be written:

$$\Delta E = \left[\left(\frac{\Delta L^*}{\ell D_L} \right)^2 + \left(\frac{\Delta C^*}{D_C} \right)^2 + \left(\frac{\Delta H^*}{D_H} \right)^2 + R_T \left(\frac{\Delta C^*}{D_C} \right) \left(\frac{\Delta H^*}{D_H} \right) \right]^{1/2} \qquad (6\text{-}7)$$

The original BFD D_C function is defined as follows:

$$D_C = \frac{0.035\,\overline{C^*}}{1 + 0.00365\,\overline{C^*}} + 0.521 \qquad (6\text{-}8)$$

Increasing the D_C function by 1.5 times (right-hand side) and simplifying the hyperbolic function yields the following (Fig.6-2):

$$D_C = \frac{\overline{C^*}}{19 + 0.07\,\overline{C^*}} + 0.78 \qquad (6\text{-}9)$$

The different lightness scale (the Fong L scale) of BFD may cause confusion with the CIELAB lightness scale (L^*) and is inconvenient in practical use. Hence, the analogue of the lightness weighting function of BFD is also replaced by the new one that is parallel in form to that of Eq.(6-2) by fitting the original BFD curve (Fig.6-1-b). It is given by

$$D_L = 0.75 + 0.001\overline{L^*} + (0.009\overline{L^*})^2 \qquad (6\text{-}10)$$

As can be seen in Fig.6-1-b, the new lightness weighting function D_L is very similar to the original one.

To make a distinction between the original BFD(ℓ:c) formula and the new one obtained by replacing the lightness and chroma weighting functions, the latter is denoted as the BFD-II(ℓ:c) formula. The D_H and R_T functions are identical between BFD and BFD-II formulae.

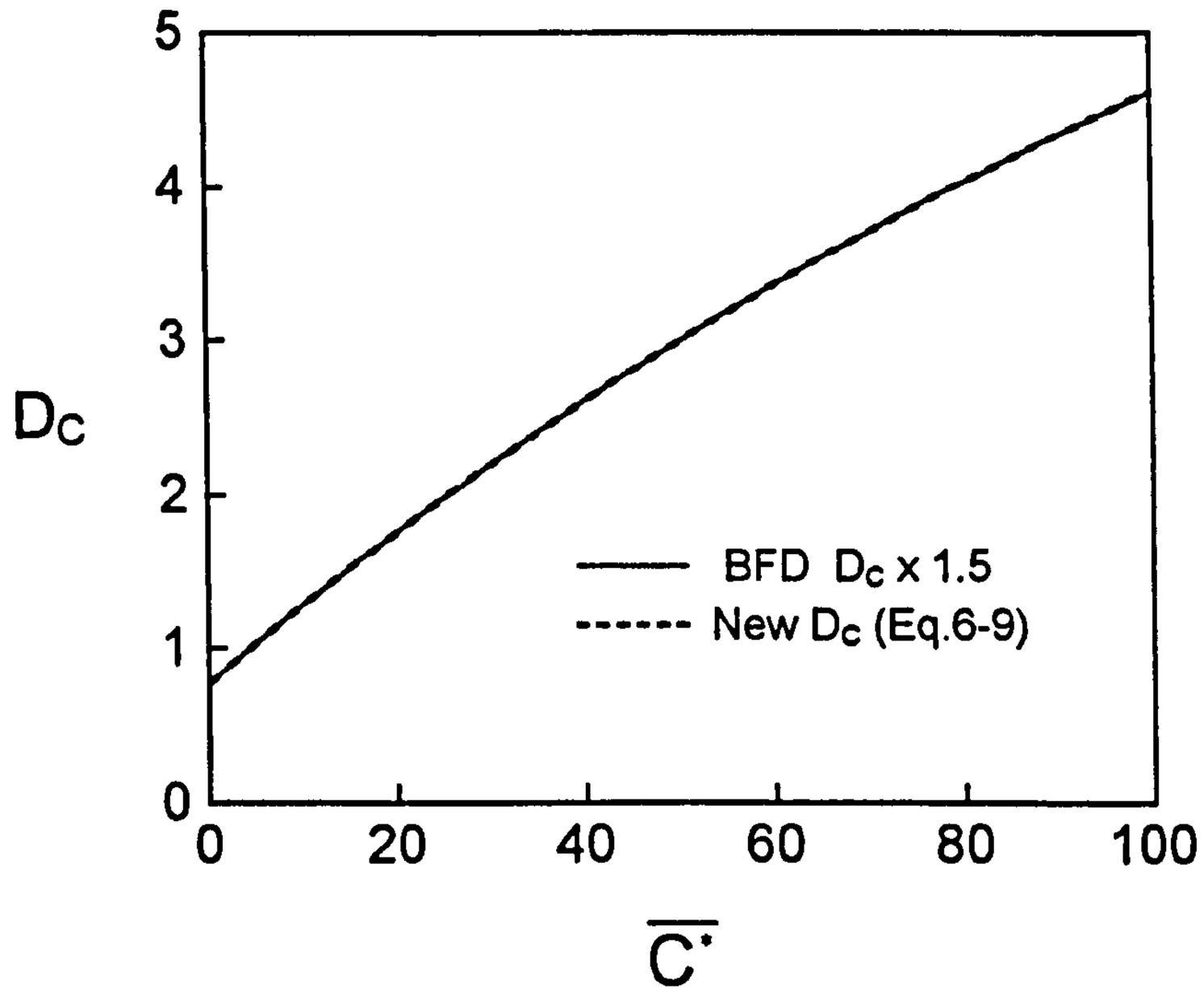

Figure 6-2. ΔC^* weighting functions (D_C) for the BFD formula.

6.2 Test of New Weighting Functions

The new weighting functions for the lightness, chroma and hue differences and the BFD-II formula described in the previous section together with 4 colour-difference formulae (CIELAB, CMC, BFD and CIE94) were tested by the 5 data sets summarised in Table 6-1.

Table 6-1. Five colour-difference data sets used in testing new weighting functions.

Data Set	Luo	Berns	This Study	Cheung	Gap	Total
Substrate	Textile	Paint	Paint	Textile	Paint	-
No.Col.Cnt.	≅ 70	19	21	5	21	-
No. Pairs	533	163[b]	244	317	203	1460
Measure	PF/4	TSD	PF'/3	PF'/3	PF'/3	-
ℓ (or K_L)[a]	1.5	1.0	1.0	1.5	1.5	-
Ref.	3	2	(c)	4	(d)	-

(a) Default value used in Table 6-2-a, i.e., $\ell = 1.5$ for textile, and $\ell = 1.0$ for paint samples

(b) Number of tolerance vectors

(c),(d) Data sets obtained in this study under the grey background and the gap conditions, respectively. The gap data is regarded as pseudo-textile data and thus ℓ is set to 1.5.

It can be seen in Table 6-2 that the performance of a particular formula depends greatly upon the basis data set it was developed. That is, the BFD and the CIE94 formulae show the best performance to the Luo and the Berns data sets, respectively. [The fit (PF/4 value) of BFD(1:1) or BFD-II(1.5:1) to the Luo dataset is 21(%).]

Three modified CIELAB formulae (CMC, BFD and CIE94) showed very similar performance when tested with ℓ (or K_L) values setting as 1.5 for textile samples and 1.0 for paint samples. Considering the fact that the optimisation of ℓ value is not always possible, it seems that there is no difference in performance among these three formulae. Thus, the CIE94 is actually preferred as it has the simplest form among three formulae.

The anomality of the BFD formula in the chroma weighting function D_C could also be found in both Tables 6-2(a) and (b). The BFD-II formula obtained by increasing the D_C function by 1.5 times (and by a minor change of its lightness weighting function) out-performed any other formulae tested. There was little change in the performance of BFD-II whether the ℓ value was optimised or not. In addition, the optimised ℓ values of BFD-II vary in a similar way to those for other weighted CIELAB formulae. The irregularity of the optimised ℓ values of the BFD formula for different data sets seems to be a serious defect in the practical application. Hence, it is believed that for the better performance, the BFD D_C function needs to be increased to have a size similar in magnitude to that of CMC or BFD.

The source of this anomaly may originate from the different method of combining the various data sets on the basis of the perceptibilty and acceptability criterion. The distinction between the perceptibilty and the acceptabilty judgements is rather ambiguous. According to Luo [5], the grey-scale assessment should come within the category of perceptibilty judgements irrespective of the substrates used. Then, the optimised ℓ values of modified CIELAB formulae for the Cheung and the gap (this study) data sets should be 1. However, this may not be the case at all, as pointed out by Berns [6], issues concerning perceptibilty and acceptability are not clear. It is, therefore, thought in this study to be better to use the textile and non-textile substrate criterion by setting $\ell = 1.5$ and 1, respectively.

The optimised ℓ value of a modified CIELAB formula also depends on the structure of a dataset. Almost all colour-difference pairs in the Luo sample data [3] are, in effect, chromaticness differences rather than lightness differences, as it was designed to study the chromaticity discrimination. This is thought to be the reason why the Luo data set requires a quite different ℓ value ($\cong$ 1) compared to the Cheung and the gap data sets.

Table 6-2 also revealed that the performance of CIE94 could be improved significantly if the weighting functions were replaced or the new function was added.

The dependency of lightness tolerance with metric lightness is probably not consistent in the case of dark colours but it shows the clear dependency in the case of medium to light colours. The lightness tolerance of a light colour ($L^* > 50$) is clearly bigger than that of a medium or a dark colour ($L^* \leq 50$) as shown and explained in Chapter 5 and Section 6-1. The CIE94 S_L function deliberately discounts this effect and thus seriously misleads in predicting the lightness tolerance of a light colour (e.g., yellow or white grey). For the two data sets of this study, which include relatively a large portion of lightness difference pairs, a considerable improvement in performance of CIE94 could be found when its S_L function is replaced by the new S_L function (Eq.6-2). The insensitivity of the performance in cases of the Luo data set is caused by its structure as explained earlier.

The dependence of hue tolerance (and also chroma tolerance) on hue-angle should be tested with the data set including a sufficient number of colour centres. In case of the Luo data set [3] which includes about 70 colour centres, the incorporation of the hue-angle dependence functions to the S_C and S_H functions of CIE94 and the addition of the

rotation function to CIE94 (i.e., CIE94 + S_{CH}, S_{HH} and S_R) clearly improved the performance of the formula. The reason no significant improvements are seen for other data sets could be explained by the lack of a sufficient number of colour centres. It cannot be justified to claim no hue-angle dependency by testing the formulae with a data set including only 19 colour centres [2,7].

It is worth noting that the C94LR (i.e., CIE94 + S_L and S_R) equation performs markedly better than the CIE94 formula except for the Luo data. Compared with the three existing weighted CIELAB formulae, it has the second simplest form. The most complex modified version C94LCHR (i.e., CIE94 + S_L, S_{CH}, S_{HH} and S_R) performs better than C94LR only for the Luo data. It means that the additional complexity of hue-angle dependence factors has not much benefit in practice.

Overall, the BFD-II formula suggested in this study performs best. [The BFD-II(1:1) and BFD-II(1.5:1) formulae correspond to the BFD(0.67:1) and BFD(1:1) formulae, respectively.] It may be partly because more than 1/3 of the test pairs are from the Luo data set. It is encouraging that the performance of C94LR is clearly better than CMC and CIE94, and nearly matches to that of BFD and BFD-II.

The performance testing results by Luo [8] in predicting various colour-difference data sets by the 5 colour-difference formulae are given in Table 6-3.

The discrepancy between the relative tolerances (ℓ) of colour-difference formulae for the Luo and Rigg datasets (Table 6-3-a) seems to be caused by the random effect of combining several datasets without distinguishing the substrate difference, as discussed above.

Similar optimised ℓ values (0.67 and 0.7) of the BFD formula for both the large colour-difference datasets (Table 6-3-b) and the Berns dataset (Table 6-2-b) means that the latter has the similar in structure to the colour order system. That is, it may be caused by the colour-difference pairs of the Berns dataset being sampled on the direction basis.

One of the advantages of using a colour appearance model in the colour-difference calculation may lie in the metamerism study (Table 6-3-c). However, if the simple colour-difference formula (e.g., CIE94) shows similar performance to the very complicated colour model (e.g., LLAB), there would be no reason to use the latter.

Table 6-2. Performance testing results of colour-difference formulae in predicting five different data sets.

(a) With default ℓ values (ℓ = 1.5 for textile, and ℓ = 1.0 for paint samples)

Formula	Data Set	Luo	Berns	This Study	Cheung	Gap	Overall
CIELAB		47	36	53	45	55	48
BFD (ℓ=1 textile, ℓ=0.67 paint)		21	21	30	29	32	26
BFD-II		**21**	**20**	**30**	**28**	**31**	**25**
CMC		29	28	32	31	34	31
CIE94		**26**	**21**	**36**	**34**	**38**	**30**
CIE94 + S_L		26	20	33	30	34	29
CIE94 + S_{CH}, S_{HH}		24	21	36	35	39	30
CIE94 + S_R		24	20	36	33	37	29
CIE94 + S_L, S_{CH}, S_{HH}		24	20	33	32	36	29
CIE94 + S_L, S_R ①		**25**	**18**	**32**	**29**	**33**	**27**
CIE94 + S_{CH}, S_{HH}, S_R		22	19	35	32	37	28
CIE94 + S_L, S_{CH}, S_{HH}, S_R ②		**22**	**18**	**32**	**29**	**34**	**26**

①,②: Denoted as C94LR and C94LCHR, respectively, in table (b) and in the text.

(b) With optimised ℓ values

Formula	Data Set										Overall
	Luo		Berns		This Study		Cheung		Gap		
	ℓ		ℓ		ℓ		ℓ		ℓ		
BFD	0.8	20	0.7	21	0.8	30	1.2	28	1.0	32	25
BFD-II	**1.2**	**20**	**1.0**	**20**	**1.1**	**29**	**1.7**	**27**	**1.4**	**31**	**25**
CMC	1.0	26	1.0	28	1.0	32	1.4	31	1.2	33	29
CIE94	1.4	26	1.1	21	1.3	34	2.0	31	1.7	37	29
C94LR	**1.2**	**24**	**1.0**	**18**	**1.1**	**30**	**1.8**	**28**	**1.4**	**33**	**26**
C94LCHR	1.3	21	1.0	18	1.1	31	1.6	29	1.3	34	26

Table 6-3. Summary of Luo's performance testing results (PF/4 values) [8] in predicting various colour-difference data sets by the 5 colour-difference formulae

(a) For the Luo and Rigg datasets

Formula	Data Set (No.Pairs)						Weighted Mean
	CP(2776)		CA(1613)		CILA(1053)		
	ℓ		ℓ		ℓ		
CIELAB	-	48	-	44	-	52	48
CMC	1.0	33	2.0	30	1.0	36	33
CIE94	2.0	33	2.0	30	2.0	35	33
BFD	1.0	28	1.5	28	1.0	35	29
LLAB	1.0	33	1.5	30	1.0	36	33

(b) For the large colour-difference datasets

Formula	ℓ	Data Set (No. Pairs)			Weighted Mean
		BFDB(408)	WW(214)	OSA(128)	
CIELAB	1	44	20	35	36
CMC	1	26	39	36	31
CIE94	1	23	29	28	26
BFD	1	27	28	35	29
LLAB	1	31	26	32	30
CIELAB	0.74	38	21	31	32
CMC	0.77	22	39	33	29
CIE94	1.00	23	29	28	26
BFD	0.67	20	28	30	24
LLAB	0.67	25	26	30	26

(c) For the Kuo and Luo's metamerism datasets

Formula	Light Source							Mean
	D65	A	TL84	TL83	W	WW	P27	
CIELAB	45	26	37	31	36	32	32	34
CMC(1:1)	40	25	25	21	28	25	20	26
CIE94	41	15	26	22	31	26	22	26
BFD(1:1)	37	22	25	20	24	21	21	24
LLAB	26	22	28	20	25	19	21	24

6.3 LCD - New Weighted CIELAB Formula

It was shown in the previous section that the performance of the CIE94 formula could be significantly improved when its weighting functions are replaced by more reliable ones.

Based on these results, the C94LR equation is proposed as a new modified CIELAB formula - the LCD (Leeds Colour Difference) formula - and is finally specified as follows:

$$\Delta E = \left[\frac{(\Delta L^*/S_L)^2}{K_L{}^2} + \frac{(\Delta C^*/S_C)^2 + (\Delta H^*/S_H)^2 + S_R \Delta C^* \Delta H^*}{K_{CH}{}^2} \right]^{1/2} \qquad (6\text{-}10)$$

where $S_L = 1 - 0.01L^* + 0.0002(L^*)^2$ unless $L^* < 50$ when $S_L = 1$

$S_C = (1 + 0.045C^*)\, S_{CH}$

$S_H = (1 + 0.015C^*)\, S_{HH}$

$S_R = [-C^*/(2 + 0.07C^*)^3] \sin(2\Delta\theta)$

and $S_{CH} = S_{HH} = 1$

$\Delta\theta = 30 \exp\{-[(h°-275)/25]^2\}$

$K_L = K_{CH} = 1$ for non-textile samples

$K_L = 1.5, K_{CH} = 1$ for textile samples

L^*, C^* and h° refer to the standard of a pair of samples. When neither of samples in a pair is easily assigned as standard, their mean L^*, C^* and h° values could be used instead.

The LCD formula is compatible with CIE94 in most respects and adopts its advantages (simplicity and flexibility), but improves the performance by smoothing the weighting functions according to the colour position in the CIELAB space, particularly for lightness tolerances for light colours and chromaticity discrimination in the near blue region.

As concluded earlier, the hue-angle dependency is more likely to exist. (To be exact, the chromaticity ellipse rotation should also be regarded as a kind of hue-angle dependency, because it depends on the hue-angle position and is used to correct the chroma and hue tolerances.) Thus, the hue-dependent factors (S_{CH} and S_{HH}) are incorporated in the LCD formula to leave room for further development. A Fourier type equation similar in form to the BFD T′ or R_H function may be used for S_{CH} and S_{HH}.

For the moment, however, S_{CH} and S_{HH} are set to unity from a practical point of view, since, as shown in Table 6-2, no substantial improvement in performance was observed between C94LR and C94LCHR compared with the extra complication of the latter (Eq.6-5).

The ellipse rotation is set to be effective only for the blue region. If more experimental data are accumulated and confirmed by earlier data, then the $\Delta\theta$ function could be further modified. The marginal improvement in performance of the more complex BFD formula approach (and the BFD-II formula proposed in this study) does not provide ground for this kind of refine over the LCD.

It was shown in Section 5.1.2.3 that the parametric factors K_C and K_H (or the relative tolerances ℓ and c) for chroma and hue differences have, overall, similar values. In the LCD formula, therefore, K_C and K_H are not separately used, but a common factor K_{CH} for both chroma and hue differences is used instead. Following a general convention of setting $K_C = K_H = 1$, K_{CH} may be omitted from the formula. For convenience of use, the formula would be named LCD(K_L): e.g., LCD(1) for non-textile samples and LCD(1.5) for textile samples. The optimum K_L value (especially, for textile samples) needs, of course, a further examination.

It is worth pointing out that the CIE94 optimisation was biased towards one colour difference dataset, the RIT-Dupont (Berns) dataset [2], but the LCD formula (C94LR in Table 6-2) is tested with five different datasets including a parametric dataset. In addition, LCD showed the best fit to the Berns data among the colour-difference formulae tested.

6.4 References

1. E.Coates, K.Y.Fong and B.Rigg, Uniform Lightness Scales, JSDC, **97**, 179-183 (1981).

2. R.S.Berns, D.H.Alman, L.Reniff, G.D.Snyder and M.R.Balonon-Rosen, Visual Determination of Suprathreshold Color-Difference Tolerances Using Probit Analysis, Col. Res. Appl., **16**, 297-316 (1991).

3. M.R.Luo, New Colour-Difference Formulae for Surface Colours, Ph.D. Thesis, University of Bradford, 1986.

4. M.Cheung, Three-Dimensional Aspects of Color Discrimination, Ph.D. Thesis, University of Bradford, 1984.

5. M.R.Luo and B.Rigg, Chromaticity-Discrimination Ellipses for Surface Colours, Col. Res. Appl., **11**, 25-42 (1986).

6. R.S.Berns, Deriving Instrumental Tolerances from Pass-Fail and Colorimetric Data, Col. Res. Appl, **21**, 459-472 (1996).

7. R.S.Berns, The Mathematical Development of CIE TC1-29 Proposed Color Difference Equation: CIELCH, Proc. 7th Cong. AIC COLOUR 93, Budapest, Vol.B, 1993, C19.1-19.4.

8. M.R.Luo, M.C.Lo and W.G.Kuo, The LLAB(ℓ:c) Colour Model, Col. Res. Appl, **21**, 412-429 (1996).

7. CONCLUSIONS

A practical and theoretical study of the influence of the parametric effects on the appearance of small colour differences was carried out and the following conclusions have been reached.

(1) It was found that the background lightness causes no significant change in perceived tolerance size, but the gap between samples in a pair does cause a significant decrease in perceived tolerance size. In the case of gap, the extent of decrease in perceived tolerance size was found to be greater for the lightness component than that for both the chroma and hue components.

(2) Compared with other earlier representative colour-difference studies, a similar level of error was found in this study in both colour measurements and observer judgements. Different scaling and data analysis methods were found to have little impact on the experimental results. Individual observers and groups were found to have substantially different tolerance sizes under the gap viewing condition and thus to produce different parametric factors.

(3) None of the lightness weighting functions of the three modified CIELAB formulae - CMC, BFD and CIE94 - was found to universally satisfy the various lightness difference data sets. A new lightness weighting function was obtained by fitting a combined lightness difference dataset and expressed by a second-order polynomial of the metric lightness. The new lightness weighting function was found to display a more even and generally better fit to the individual datasets than any of the other three weighted CIELAB formulae.

(4) The chroma and hue tolerances were found to have dependency upon both chroma and hue-angle of a standard colour rather than to have a single dependency upon chroma. This was confirmed by the performance improvement of the CIE94 formula to the dataset including a wide range of hue-angle positions when hue dependent factors were incorporated in both the chroma and hue weighting functions of the formula. The extent of the enhancement in performance was found to maximise if the hue-dependent factors were accompanied by a term allowing for chromaticity ellipse rotation.

Although no systematic study has ever been conducted, the background has long been regarded to have a great influence on colour-difference perception. However, it was found in this study that the background effect is unlikely to be as significant as previously considered. The parametric factors for lightness, chroma and hue differences (ΔL^*, ΔC^* and ΔH^*) due to the change of lightness of grey background were found to be between 0.8 and 1.2, except for that for lightness-difference of a blue colour under a black background (1.3). In view of the inherent uncertainty of the experiment, the small extent of change in perceived tolerance size is well within the experiment error.

The study of the gap effect upon colour-difference sensation has led to the finding of significant gap factors for all three colour-difference components ΔL^*, ΔC^* and ΔH^* (overall, 1.7, 1.5 and 1.5, respectively). As the parametric factors in CIE94 and the relative tolerances in CMC (also in BFD) are considered to both serve the same purpose, it follows that the assumption in CMC of a relative tolerance *h* to hue differences in the divisor of the term in ΔH^* as always being unity is not a good practice. The relative tolerance *h* should be explicitly given in the CMC formula as is the parametric factor K_H of CIE94.

Alternatively, since the parametric factors for chroma and hue differences are likely to have similar magnitude, as shown by the gap factors in this study, the relative tolerance *c* of CMC could be interpreted as applying to both chroma and hue differences. That is,

$$\Delta E_{CMC} = \left[\frac{\left(\Delta L^*/S_L\right)^2}{\ell^2} + \frac{\left(\Delta C^*/S_C\right)^2 + \left(\Delta H^*/S_H\right)^2}{c^2} \right]^{1/2} \qquad (7\text{-}1)$$

The implication of setting a relative tolerance *c* (or a parametric factor K_C in CIE94) usually as unity may be clarified as well. The value of a relative tolerance ℓ used has, in effect, always been the ratio between ℓ and *c*.

The errors in colour measurements were estimated by the simple method of calculating the standard deviations of colour-difference scale values. Though the DIN or the ASTM method is regarded as a more elaborate method, they have not been used in view of the more complex method of calculation and thus the lack of practicability.

The precision of instrumental colour-difference measurements was found to be good according to the result that the overall standard deviations of the total colour-difference

(ΔE^*) and the absolute values of component colour-difference scales (ΔL^*, Δa^* and Δb^*) were 0.07, 0.07, 0.05 and 0.07, respectively.

The standard error of this visual dataset, i.e., the precision of observer judgements, was found to be ±7.0% for a standard grey background condition and observer groups, this is comparable to that of the two earlier datasets: Luo (±8.9%) and Berns (±5.7%). The precision of repeated judgements by single observer was found to be better than that of the same number of judgements by an observer group (each making a single judgement) except when the dividing line between samples in a pair was not clear, i.e., gap. The gap factors for lightness difference (those for chroma and hue differences being set to be unity) were found to be different from one observer (group) to another: 1.4 for one observer group, and 1.6 and 1.2 for the two single observers, this is thought to be due to the inherent difference in tolerance size of individual observer.

The logistic and the probit data analysis methods for a paired-comparison scaling were compared by use of a set of red colour-difference pairs. It was found that both methods yielded virtually identical results but the probit analysis, that is experimentally and computationally intensive, produced more uniform results.

The paired-comparison method (with corresponding probit or logistic analyses) in contrast to the grey-scale method was found to be unsuitable for studying the parametric effects. The change of physical parameters would shift the observer sensitivity greatly and thus the observer may judge all test colour-difference pairs smaller or larger than the standard pair, and in this case the precision of the paired-comparison method is extremely poor.

Colour discrimination ellipsoids for the two CIE colour centres (grey and blue) were obtained separately from the lightness difference and chromaticity discrimination experiments. The cross-section of a grey ellipsoid in the a^*b^* plane was not found to be a circle as assumed in the existing four formulae: CIELAB, CMC, BFD and CIE94, but an ellipse of which the major axis is almost towards the b^* axis. A simple empirical formula developed for the grey centre was found to show a good fit to neutral grey (achromatic) centres. This formula, however, has not been considered further as it would cause a discontinuity of colour-difference calculation and make a general form of a formula quite complex.

The blue ellipse, i.e., the cross-section of a blue ellipsoid, was not found to be oriented toward the origin in the a^*b^* plane. A formula modified from CIE94, and reasonably based on the ellipse geometry, was developed and tested with colour-difference pairs of three datasets including this study. It gave remarkably improved performance compared to CIE94 as well as CMC. The result concurs with those confirmed by Luo and the implication of the BFD formula. This finding was further utilised in the development of the new modified CIELAB formula.

It was shown in the preliminary test of the four colour-difference formulae (CIELAB, CMC, BFD and CIE94) to the five datasets – two textile, two paint and one pseudo-textile dataset – that the three modified CIELAB formulae (CMC, BFD and CIE94) were evidently better in performance than CIELAB and there was little difference in performance among the three modified formulae. As the CIE94 formula has the simplest structure among the three formulae, it was thought to be more favoured in practice than the other two.

An attempt of improving the performance of CIE94 was thus made by systematically modifying the formula to produce seven colour-difference models (CDM). The models tried were:

CDM-1) CIE94 + S_L : replacement of the lightness weighting function by a new one

CDM-2) CIE94 + S_{CH} and S_{HH} : incorporation of hue-angle dependence factors into the chroma and hue weighting functions S_C and S_H

CDM-3) CIE94 + S_R : addition of a term for the ellipse rotation dominant in the blue region

CDM-4) CIE94 + S_L, S_{CH}, S_{HH}

CDM-5) CIE94 + S_L, S_R

CDM-6) CIE94 + S_{CH}, S_{HH}, S_R

CDM-7) CIE94 + S_L, S_{CH}, S_{HH}, S_R

Among the seven models, CDM-5 and CDM-7 were shown to give a better fit to the five datasets than the three modified formulae when the default setting ℓ values (ℓ = 1.5 for textiles and ℓ = 1 for paints) were used. With optimised ℓ values, the performances of the same two models were apparently better than CMC or CIE94, and were nearly a match for BFD.

The new formula, LCD, was finally proposed as the following form:

$$\Delta E = \left[\frac{(\Delta L^*/S_L)^2}{K_L^{\,2}} + \frac{(\Delta C^*/S_C)^2 + (\Delta H^*/S_H)^2 + S_R \Delta C^* \Delta H^*}{K_{CH}^{\,2}} \right]^{1/2} \qquad (7\text{-}2)$$

where $S_L = 1 - 0.01L^* + 0.0002(L^*)^2$ unless $L^* < 50$ when $S_L = 1$

$S_C = (1 + 0.045C^*)\, S_{CH}$

$S_H = (1 + 0.015C^*)\, S_{HH}$

$S_R = [-C^*/(2 + 0.07C^*)^3] \sin(2\Delta\theta)$

and $S_{CH} = S_{HH} = 1$

$\Delta\theta = 30 \exp\{-[(h° - 275)/25]^2\}$

$K_L = K_{CH} = 1$ for non-textile samples

$K_L = 1.5, K_{CH} = 1$ for textile samples

The LCD formula is comparable with CIE94 in the aspects of simplicity and flexibility but smoothes the weighting functions according to the colour position in the CIELAB space, especially for lightness tolerances for light colours and chromaticity discrimination near the blue region.

The reliability of the BFD formula in terms of performance and ease of use was found to be made better if the size of the chroma weighting function was increased by 1.5 times and the form of lightness weighting function was made parallel to those of the other modified CIELAB formulae. This formula was named as the BFD-II(ℓ:c) formula in this study, and it could be an alternative proposal for the new modified CIELAB formula instead of LCD. In the case of BFD-II, however, there is no room for further development because of its inherent complexity.

It was claimed in the recent paper[1] that the modified CIELAB formula allowing for the ellipse rotation in a^*b^* plane, e.g., LCD or BFD, is particularly useful for the instrumental method of fastness testing. It is known that in some cases the CMC formula indicates that the European blue wool standard grade 5 fades more than grade 4.

---

[1] T.Sato, N.Takada, M.Ueda, T.Nakamura and M.R.Luo, Comparison of Instrumental Methods for Assessing Colour Fastness. Part 1–Change in Colour, JSDC, 113, 17-24 (1997).

Now it is thought to be a proper time to consider the revision of the CMC formula. The original form of CMC has had a great influence on the later colour-difference formulae of this kind - BFD, CIE94 and LCD. However, it seems that the CMC lightness weighting function has not been considered seriously since the initial development and the formula itself does not give correct predictions for the chroma and hue tolerances of blue colours.

Followings may be suggested as the **future work**.

(1) It has been regarded that there are no fundamental differences in sizes between the chroma and hue tolerances of painted samples and those of textile samples, unlike the case of the lightness tolerance. However, the results obtained under the gap viewing condition implied that this may not be the case. Therefore, future work may be directed towards the visual experiments including the two sets (i.e., both types of substrates) of colour-difference pairs around as many colour centres as possible.

(2) Since, in many cases, colour-difference ellipsoids were found to be tilted from the lightness axis L^*, it may be also worth investigating the trend of ellipsoid tilting throughout the CIELAB colour space. This could lead to a more efficient way of describing a colour-difference by the inclusion of a further correction of a product type $\Delta a^*\Delta b^*$ or $\Delta C^*\Delta H^*$.

(3) It seems that the maximum achievable performance of a modified CIELAB formula in terms of the performance factor is about 15%. As further improvement in performance is not thought to be possible, other approaches such as the colour space model (e.g., DCI-95) may be considered instead. The type of response functions used for representing perceptual colour co-ordinates can be not only a cube-root or a logarithmic but also a hyperbolic function as in the case of colour appearance models.

(4) The amount of work - sample preparation, colour measurements and observer tests - necessary to obtain the experimental data and to evaluate the existing colour-difference formulae is enormous. Thus, the co-operation between academia and industry is strongly needed. Also, if the previous industrial data sets - e.g., those of Datacolor, and Marks and Spencer - were made available to the academic institutions, there would be a great improvement in this area of research.

Appendix 1. Experimental data

[Colour panels were mesured in SPIN (Tables A-2 and A-3, excluding the colour centre L30) or SPEX (Table A-4) mode, and all colour co-ordinates were calculated for the D_{65} Illuminant and the 10° Observer function.]

Table A-1. Colour co-ordinates of backgrounds, standard pairs and grey-scale.

(a) Background

Background	L^*	a^*	b^*
Grey	48.5	-0.8	-4.1
Black	29.7	0.2	-1.6
Black (bottom)	24.5	0.3	-1.1
White	95.3	-0.1	3.8

(b) Standard pairs

Exp.	Pair No.	Msr. Mode	L^*_1	a^*_1	b^*_1	L^*_2	a^*_2	b^*_2	ΔL^*	Δa^*	Δb^*	ΔE^*
Part 1	SP1	SPIN	48.53	0.42	-4.43	49.22	0.10	-5.19	0.69	-0.32	-0.76	1.08
	SP2		50.11	-0.42	-5.31	50.35	-0.54	-5.75	0.24	-0.12	-0.44	0.52
	SP3		48.93	0.00	-4.44	50.45	-0.52	-5.68	1.52	-0.52	-1.24	2.03
Part 2	SP1		49.20	0.04	-4.91	50.03	-0.05	-5.64	0.83	-0.09	-0.73	1.11
	SP1	SPEX	48.70	0.05	-5.06	49.52	-0.05	-5.77	0.82	-0.10	-0.71	1.09

(c) Grey-scale

Exp.	Grade	Msr. Mode	L^*	a^*	b^*	ΔL^*	Δa^*	Δb^*	ΔE^*
Part 2	STD	SPIN	47.21	-0.22	0.04				
	9		47.39	-0.25	-0.01	**0.18**	-0.03	-0.05	**0.19**
	8		47.77	-0.28	-0.02	**0.38**	-0.03	-0.01	**0.38**
	7		48.36	-0.20	0.08	**0.59**	0.08	0.10	**0.60**
	6		49.34	-0.18	0.14	**0.98**	0.02	0.06	**0.98**
	4		50.98	-0.20	0.18	**1.64**	-0.02	0.04	**1.64**
	2		52.97	-0.23	-0.02	**1.99**	-0.03	-0.20	**2.00**
	STD	SPEX	46.85	-0.24	0.09				
	9		47.03	-0.31	-0.01	**0.18**	-0.07	-0.10	**0.22**
	8		47.41	-0.33	-0.10	**0.38**	-0.02	-0.09	**0.39**
	7		47.97	-0.24	0.01	**0.56**	0.09	0.11	**0.58**
	6		48.99	-0.20	0.12	**1.02**	0.04	0.11	**1.03**
	4		50.66	-0.17	0.12	**1.67**	0.03	0.00	**1.67**
	2		52.58	-0.20	-0.06	**1.92**	-0.03	-0.18	**1.93**
Part 3	STD		46.59	-0.14	0.05				
	9		46.68	-0.19	-0.01	**0.09**	-0.05	-0.06	**0.12**
	8		47.11	-0.18	-0.04	**0.43**	0.01	-0.03	**0.43**
	7		47.77	-0.24	0.03	**0.66**	-0.06	0.07	**0.67**
	6		48.71	-0.16	0.16	**0.94**	0.08	0.13	**0.95**
	4		50.13	-0.12	0.17	**1.42**	0.04	0.01	**1.42**
	2		52.05	-0.18	-0.06	**1.92**	-0.06	-0.23	**1.93**

Table A-2. Experimental results from Part 1.

Colour Centre	Pair No.	L^*_1	a^*_1	b^*_1	L^*_2	a^*_2	b^*_2	ΔE^*
Red	RA1	45.27	37.07	22.80	45.81	37.11	22.91	0.55
	RA2	45.14	37.00	22.88	45.94	37.18	22.83	0.82
	RA3	44.88	37.12	22.94	46.21	37.06	22.77	1.34
	RA4	44.76	37.08	22.88	46.33	37.10	22.82	1.57
	RA5	44.70	37.05	22.97	46.38	37.14	22.73	1.70
	RB1	44.36	36.67	22.63	44.54	37.67	22.56	1.02
	RB2	44.33	36.47	22.61	44.57	37.88	22.57	1.43
	RB3	44.42	36.18	22.55	44.48	38.16	22.64	1.98
	RB4	44.51	36.01	22.31	44.40	38.33	22.87	2.39
	RB5	44.49	35.94	22.35	44.42	38.41	22.84	2.52
	RC1	44.48	37.06	21.68	44.42	37.08	22.57	0.89
	RC2	44.53	37.11	21.58	44.38	37.03	22.67	1.10
	RC3	44.45	37.16	21.47	44.45	36.99	22.77	1.31
	RC4	44.44	37.06	21.32	44.47	37.09	22.92	1.60
	RC5	44.47	37.05	21.12	44.44	37.09	23.13	2.01
	RD1	44.39	35.43	21.01	44.40	36.45	22.11	1.50
	RD2	44.39	35.21	20.95	44.39	36.68	22.18	1.92
	RD3	44.38	35.23	20.78	44.41	36.66	22.35	2.12
	RD4	44.39	35.12	20.71	44.39	36.76	22.41	2.36
	RD5	44.40	34.69	20.38	44.38	37.19	22.75	3.44
	RE1	44.44	37.50	21.39	44.44	36.63	22.16	1.16
	RE2	44.46	37.57	21.25	44.42	36.55	22.29	1.46
	RE3	44.50	37.66	21.26	44.39	36.46	22.29	1.59
	RE4	44.45	37.71	21.17	44.44	36.42	22.37	1.76
	RE5	44.48	37.72	20.98	44.40	36.41	22.57	2.06
	RJ1	43.62	35.98	22.65	44.22	36.61	22.71	0.87
	RJ2	43.57	35.82	22.64	44.27	36.77	22.73	1.18
	RJ3	43.45	35.71	22.72	44.40	36.87	22.64	1.50
	RJ4	43.45	35.56	22.64	44.39	37.03	22.73	1.75
	RJ5	43.11	35.47	22.62	44.74	37.12	22.75	2.32
	RK1	45.70	35.51	23.00	45.35	36.02	23.10	0.63
	RK2	44.33	37.20	23.16	43.78	37.97	23.07	0.95
	RK3	45.35	36.02	23.10	44.33	37.20	23.16	1.56
	RK4	45.23	36.59	23.07	43.78	37.97	23.07	2.00
	RK5	45.35	36.02	23.10	43.78	37.97	23.07	2.50
	RL1	44.03	37.04	22.70	44.29	36.98	22.96	0.37
	RL2	43.96	37.02	22.63	44.37	37.00	23.04	0.58
	RL3	43.90	37.03	22.49	44.42	36.99	23.17	0.86
	RL4	43.76	37.00	22.38	44.57	37.02	23.29	1.22
	RL5	43.37	37.03	22.27	44.96	37.00	23.40	1.95
	RM1	43.68	37.07	23.55	43.23	37.04	23.86	0.55
	RM2	45.93	37.10	21.39	45.26	37.10	22.10	0.98
	RM3	45.22	37.02	22.34	44.22	37.14	23.30	1.39
	RM4	45.26	37.10	22.10	44.18	37.14	23.23	1.56
	RM5	45.26	37.10	22.10	43.68	37.07	23.55	2.14

Table A-2. (Continued)[a]

Colour Centre	Pair No.	Black FT[d]	Black UF[e]	White FT	White UF	Gap1[b] FT	Gap1[b] UF	Gap2[c] FT	Gap2[c] UF
Red	RA1	**0**	2	**0**	2	**0**	0	**0**	0
	RA2	**7**	5	**3**	1	**2**	3	**1**	2
	RA3	**19**	22	**21**	23	**5**	5	**3**	4
	RA4	**27**	25	**26**	25	**6**	6	**3**	3
	RA5	**30**	29	**29**	22	**8**	4	**5**	3
	RB1	**0**	2	**1**	2	**0**	2	**0**	0
	RB2	**10**	11	**6**	6	**2**	1	**1**	3
	RB3	**13**	16	**13**	16	**4**	6	**2**	2
	RB4	**17**	13	**22**	19	**6**	7	**4**	8
	RB5	**22**	18	**24**	22	**10**	7	**10**	5
	RC1	**0**	0	**0**	0	**1**	2	**0**	0
	RC2	**0**	1	**0**	3	**3**	4	**0**	0
	RC3	**0**	0	**8**	5	**7**	5	**1**	1
	RC4	**12**	17	**22**	23	**12**	13	**8**	10
	RC5	**23**	18	**25**	23	**14**	12	**13**	11
	RD1	**0**	0	**0**	0	**0**	1	**0**	2
	RD2	**1**	11	**2**	6	**0**	0	**0**	1
	RD3	**11**	1	**5**	2	**1**	2	**0**	0
	RD4	**18**	19	**10**	10	**3**	2	**0**	0
	RD5	**27**	26	**24**	23	**7**	6	**1**	1
	RE1	**0**	2	**5**	10	**1**	3	**1**	1
	RE2	**3**	7	**10**	10	**4**	4	**4**	4
	RE3	**10**	8	**14**	14	**6**	6	**4**	5
	RE4	**21**	24	**26**	25	**9**	8	**7**	6
	RE5	**27**	24	**28**	27	**15**	14	**11**	11
	RJ1	**2**	5	**2**	3	**0**	1	**0**	0
	RJ2	**11**	13	**6**	8	**1**	2	**1**	1
	RJ3	**22**	19	**16**	16	**4**	6	**1**	2
	RJ4	**28**	27	**23**	20	**7**	4	**2**	1
	RJ5	**30**	30	**29**	29	**12**	12	**12**	12
	RK1	**3**	3	**0**	0	**1**	1	**0**	0
	RK2	**22**	23	**26**	29	**7**	11	**3**	6
	RK3	**27**	28	**29**	26	**13**	9	**6**	3
	RK4	**29**	27	**30**	29	**15**	15	**10**	10
	RK5	**29**	29	**30**	30	**15**	15	**15**	15
	RL1	**0**	0	**0**	0	**2**	2	**2**	2
	RL2	**3**	4	**11**	12	**8**	10	**6**	8
	RL3	**9**	10	**16**	15	**9**	11	**6**	8
	RL4	**21**	20	**29**	29	**12**	7	**8**	6
	RL5	**30**	30	**30**	30	**15**	15	**13**	12
	RM1	**0**	0	**0**	4	**0**	3	**0**	0
	RM2	**5**	6	**5**	2	**0**	0	**0**	0
	RM3	**21**	20	**20**	21	**4**	4	**1**	3
	RM4	**27**	27	**27**	26	**8**	7	**2**	3
	RM5	**30**	30	**30**	30	**15**	15	**10**	9

(a) Total number of judgements: black & white BGs → 30, gap1 & gap2 → 15
(b), (c): Tests with standard pairs 2 and 3, respectively.
(d), (e): Filtered and unfiltered frequencies, respectively.

Table A-3. Experimental results from Part 2.

Colour Centre	Pair No.	L^*_1	a^*_1	b^*_1	L^*_2	a^*_2	b^*_2	ΔL^*	Δa^*	Δb^*	ΔE^*
Grey (L60)	N61	60.26	-0.29	-0.09	61.00	-0.28	-0.03	**0.74**	0.00	0.06	**0.74**
	N62	61.38	-0.30	-0.10	62.45	-0.29	-0.07	**1.07**	0.02	0.03	**1.07**
	N63	61.00	-0.27	-0.07	62.37	-0.29	-0.06	**1.37**	-0.02	0.01	**1.37**
	N64	60.36	-0.31	-0.05	62.08	-0.31	-0.07	**1.72**	0.00	-0.02	**1.72**
	N65	60.46	-0.24	0.05	63.13	-0.27	-0.03	**2.67**	-0.03	-0.08	**2.67**
Red	R1	46.26	36.89	22.14	46.76	36.98	22.03	**0.50**	0.08	-0.11	**0.52**
	R2	43.82	37.20	21.68	44.56	37.15	21.58	**0.73**	-0.06	-0.10	**0.74**
	R3	43.86	36.96	22.41	44.78	36.94	22.20	**0.92**	-0.02	-0.22	**0.95**
	R4	43.99	37.08	23.21	45.61	36.70	22.47	**1.61**	-0.39	-0.74	**1.82**
	R5	44.86	36.54	21.91	46.67	36.93	22.14	**1.81**	0.39	0.23	**1.87**
Yellow	YA1	86.06	-6.51	46.07	86.66	-6.73	45.88	**0.60**	-0.22	-0.19	**0.67**
	YA2	85.94	-6.52	45.91	86.90	-6.82	46.07	**0.96**	-0.30	0.16	**1.02**
	YA3	85.48	-6.33	45.91	86.77	-6.73	46.04	**1.29**	-0.40	0.13	**1.36**
	YA4	85.61	-6.35	45.95	87.37	-6.87	46.28	**1.76**	-0.51	0.34	**1.86**
	YA5	85.35	-6.31	45.84	87.22	-6.07	45.77	**1.87**	0.24	-0.06	**1.88**
Green	GA1	54.71	-32.01	-0.02	55.17	-31.73	0.03	**0.46**	0.28	0.05	**0.54**
	GA2	55.47	-31.81	0.23	56.63	-31.96	0.24	**1.16**	-0.14	0.01	**1.17**
	GA3	53.74	-31.78	-0.04	55.63	-31.98	-0.14	**1.89**	-0.20	-0.11	**1.90**
	GA4	55.29	-31.81	0.12	57.29	-32.22	0.30	**1.99**	-0.42	0.18	**2.04**
	GA5	55.42	-31.67	0.23	57.58	-31.73	0.23	**2.16**	-0.07	0.01	**2.16**
Blue	BA1	36.86	-5.98	-26.46	37.84	-6.22	-26.68	**0.98**	-0.24	-0.22	**1.03**
	BA2	37.33	-6.13	-26.70	38.40	-6.31	-26.83	**1.07**	-0.18	-0.12	**1.09**
	BA3	37.79	-6.19	-26.81	38.86	-6.24	-27.00	**1.07**	-0.05	-0.19	**1.09**
	BA4	37.34	-6.22	-26.65	38.79	-6.45	-26.95	**1.44**	-0.23	-0.30	**1.49**
	BA5	36.60	-5.96	-26.41	38.23	-6.32	-26.83	**1.63**	-0.36	-0.42	**1.72**
L90	N91	90.01	-0.50	-0.27	90.36	-0.51	-0.07	**0.36**	-0.01	0.20	**0.41**
	N92	88.60	-0.49	-0.50	90.13	-0.49	-0.30	**1.53**	0.00	0.20	**1.54**
	N93	86.98	-0.47	-0.48	88.72	-0.53	-0.44	**1.74**	-0.05	0.04	**1.74**
	N94	88.44	-0.48	-0.52	90.22	-0.50	-0.17	**1.77**	-0.02	0.35	**1.81**
	N95	87.07	-0.47	-0.50	89.98	-0.50	-0.33	**2.91**	-0.03	0.17	**2.92**
L80	N81	77.29	-0.35	-0.44	77.96	-0.34	-0.51	**0.66**	0.01	-0.07	**0.67**
	N82	80.00	-0.36	-0.47	80.76	-0.38	-0.36	**0.76**	-0.03	0.11	**0.77**
	N83	78.03	-0.35	-0.53	79.54	-0.32	-0.58	**1.52**	0.03	-0.05	**1.52**
	N84	77.98	-0.34	-0.49	79.94	-0.33	-0.47	**1.96**	0.01	0.02	**1.96**
	N85	78.63	-0.37	-0.64	80.78	-0.36	-0.41	**2.15**	0.01	0.23	**2.17**
L70	N71	65.61	-0.20	0.01	66.75	-0.30	-0.10	**1.13**	-0.10	-0.11	**1.14**
	N72	66.99	-0.23	-0.04	68.19	-0.21	-0.06	**1.20**	0.02	-0.03	**1.20**
	N73	67.66	-0.24	-0.06	69.32	-0.23	0.00	**1.66**	0.01	0.06	**1.66**
	N74	65.49	-0.21	-0.03	67.54	-0.23	-0.10	**2.05**	-0.02	-0.07	**2.05**
	N75	65.55	-0.21	-0.01	67.98	-0.24	-0.07	**2.44**	-0.02	-0.06	**2.44**
L50	N51	49.93	-0.32	-0.18	50.27	-0.32	0.02	**0.34**	0.00	0.20	**0.40**
	N52	49.37	-0.31	-0.11	50.24	-0.28	0.00	**0.87**	0.03	0.10	**0.88**
	N54	53.50	-0.29	-0.10	54.87	-0.27	-0.04	**1.37**	0.02	0.07	**1.37**
	N53	49.33	-0.34	0.06	51.06	-0.35	-0.16	**1.73**	-0.01	-0.21	**1.74**
	N55	47.43	-0.30	0.12	49.91	-0.31	0.00	**2.49**	-0.02	-0.12	**2.49**
L40	N41	40.61	-0.25	0.34	41.54	-0.24	0.27	**0.93**	0.02	-0.07	**0.93**
	N42	39.46	-0.24	0.34	40.43	-0.22	0.38	**0.97**	0.02	0.04	**0.97**
	N43	39.92	-0.21	0.31	41.14	-0.22	0.28	**1.22**	-0.01	-0.03	**1.22**
	N44	40.37	-0.19	0.30	42.10	-0.27	0.04	**1.74**	-0.08	-0.26	**1.76**
	N45	39.91	-0.27	0.34	42.06	-0.33	0.22	**2.15**	-0.06	-0.12	**2.15**
L30	N31	27.74	-0.35	0.51	29.08	-0.31	0.38	**1.33**	0.03	-0.12	**1.34**
	N32	27.61	-0.11	0.36	29.09	-0.13	0.27	**1.48**	-0.02	-0.09	**1.48**
	N33	28.20	-0.08	0.68	30.09	-0.17	0.50	**1.89**	-0.10	-0.18	**1.90**
	N34	27.85	-0.32	0.36	30.23	-0.33	0.52	**2.37**	-0.02	0.16	**2.38**
	N35	30.11	-0.15	0.53	32.55	-0.02	0.82	**2.45**	0.13	0.29	**2.47**

Table A-3. (Continued)

Colour Centre	Pair No.	Visual Difference (ΔV) BLK	GRY	WHT	GAP	Rejection Probability BLK	GRY	WHT
Grey	N61	0.45	**0.70**	0.62	0.41	0.00	**0.00**	0.00
(L60)	N62	0.89	**0.96**	0.97	0.61	0.21	**0.00**	0.00
	N63	1.39	**1.29**	1.22	0.80	0.43	**0.50**	0.36
	N64	1.66	**1.48**	1.53	0.94	0.86	**0.93**	0.71
	N65	2.13	**1.90**	1.95	1.20	1.00	**1.00**	1.00
Red	R1	0.46	**0.60**	0.63	0.55	0.00	**0.00**	0.00
	R2	0.88	**0.90**	0.84	0.69	0.14	**0.29**	0.14
	R3	1.56	**1.32**	1.31	0.83	0.64	**0.86**	0.79
	R4	1.85	**1.44**	1.48	0.97	0.93	**1.00**	1.00
	R5	1.93	**1.67**	1.81	1.09	1.00	**1.00**	1.00
Yellow	YA1	0.40	**0.54**	0.62	0.41	0.00	**0.00**	0.00
	YA2	0.58	**0.68**	0.78	0.53	0.07	**0.00**	0.00
	YA3	0.66	**0.76**	0.91	0.65	0.21	**0.00**	0.21
	YA4	0.97	**0.90**	1.09	0.78	0.43	**0.29**	0.57
	YA5	1.30	**1.14**	1.31	0.91	0.50	**0.50**	0.79
Green	GA1	1.08	**0.88**	0.86	0.52	0.14	**0.36**	0.07
	GA2	1.50	**1.36**	1.40	0.68	0.64	**0.71**	0.71
	GA3	1.75	**1.60**	1.60	0.80	1.00	**1.00**	1.00
	GA4	1.93	**1.81**	1.76	0.96	1.00	**1.00**	1.00
	GA5	2.11	**1.92**	1.94	1.21	1.00	**1.00**	1.00
Blue	BA1	0.53	**0.75**	0.81	0.49	0.00	**0.07**	0.07
	BA2	0.64	**0.91**	0.94	0.62	0.00	**0.21**	0.14
	BA3	0.69	**1.01**	0.99	0.75	0.07	**0.29**	0.14
	BA4	0.90	**1.18**	1.08	0.87	0.21	**0.50**	0.21
	BA5	1.24	**1.38**	1.18	1.16	0.43	**0.64**	0.71
L90	N91	0.23	**0.44**	0.45	0.27	0.00	**0.00**	0.00
	N92	0.77	**0.77**	0.90	0.41	0.00	**0.00**	0.29
	N93	0.93	**0.85**	1.15	0.42	0.21	**0.00**	0.43
	N94	1.07	**1.03**	1.34	0.58	0.43	**0.14**	0.71
	N95	1.27	**1.30**	1.56	0.66	0.86	**0.50**	0.86
L80	N81	0.45	**0.57**	0.64	0.34	0.00	**0.00**	0.00
	N82	0.63	**0.70**	0.84	0.44	0.00	**0.00**	0.00
	N83	0.90	**0.97**	1.20	0.54	0.29	**0.21**	0.43
	N84	1.17	**1.12**	1.24	0.61	0.50	**0.36**	0.86
	N85	1.56	**1.40**	1.50	0.74	0.93	**0.64**	0.93
L70	N71	0.69	**0.85**	0.75	0.50	0.00	**0.00**	0.00
	N72	0.95	**1.01**	0.99	0.58	0.07	**0.00**	0.07
	N73	1.24	**1.25**	1.24	0.71	0.50	**0.14**	0.36
	N74	1.41	**1.36**	1.47	0.87	0.71	**0.64**	0.79
	N75	1.86	**1.65**	1.71	1.13	1.00	**0.93**	1.00
L50	N51	0.51	**0.53**	0.73	0.41	0.00	**0.00**	0.00
	N52	0.90	**0.86**	0.91	0.60	0.07	**0.00**	0.07
	N54	1.49	**1.45**	1.24	0.81	0.57	**0.64**	0.64
	N53	1.78	**1.65**	1.53	1.09	0.79	**1.00**	0.79
	N55	1.99	**1.95**	1.83	1.41	1.00	**1.00**	1.00
L40	N41	0.72	**0.72**	0.80	0.47	0.00	**0.00**	0.00
	N42	1.03	**0.95**	0.90	0.63	0.29	**0.14**	0.00
	N43	1.30	**1.20**	1.21	0.78	0.57	**0.36**	0.29
	N44	1.71	**1.62**	1.44	1.02	0.93	**1.00**	0.79
	N45	2.01	**1.84**	1.62	1.26	1.00	**1.00**	0.93
L30	N31	0.94	**0.78**	1.11	0.52	0.29	**0.14**	0.14
	N32	1.38	**1.38**	1.44	0.68	0.93	**0.71**	0.79
	N33	1.74	**1.58**	1.60	0.77	1.00	**0.86**	0.93
	N34	1.86	**1.80**	1.81	0.98	1.00	**0.93**	1.00
	N35	2.11	**1.99**	1.99	1.19	1.00	**1.00**	1.00

Table A-3. (Continued)

Colour Centre	Pair No.	L^*_1	a^*_1	b^*_1	L^*_2	a^*_2	b^*_2	ΔL^*	Δa^*	Δb^*	ΔE^*
Blue	BB1	36.72	-5.94	-26.23	36.97	-4.76	-25.85	0.24	1.18	0.38	1.26
	BB2	36.80	-6.02	-26.06	36.70	-4.75	-26.08	-0.09	1.27	-0.02	1.28
	BB3	36.68	-6.10	-26.36	36.82	-4.52	-26.25	0.13	1.58	0.11	1.59
	BB4	36.66	-6.05	-26.39	36.70	-4.27	-25.93	0.04	1.77	0.47	1.83
	BC1	36.73	-3.69	-29.90	36.65	-3.90	-27.75	-0.09	-0.21	2.15	2.17
	BC2	36.70	-3.81	-29.88	36.67	-4.04	-27.11	-0.03	-0.23	2.77	2.78
	BC3	36.84	-3.62	-30.56	36.60	-3.92	-27.15	-0.24	-0.31	3.41	3.43
	BD1	37.16	-5.45	-28.46	37.21	-4.72	-27.17	0.05	0.74	1.29	1.48
	BD2	37.27	-6.00	-29.78	37.10	-5.28	-28.40	-0.17	0.73	1.38	1.57
	BD3	37.11	-5.84	-29.29	37.18	-5.03	-27.51	0.07	0.82	1.79	1.97
	BD4	37.24	-5.68	-29.05	37.25	-4.78	-27.03	0.01	0.90	2.03	2.22
	BE1	34.29	-0.33	-28.63	34.32	-1.72	-26.02	0.03	-1.38	2.62	2.96
	BE2	34.29	-0.33	-28.62	34.37	-2.16	-25.45	0.08	-1.83	3.18	3.67
	BE3	34.21	-0.48	-28.02	34.71	-2.55	-24.60	0.50	-2.08	3.42	4.03
	BE4	34.36	-0.23	-28.71	34.67	-2.49	-24.58	0.31	-2.26	4.13	4.71
	BK1	35.21	-2.50	-27.78	35.01	-2.11	-27.81	-0.20	0.40	-0.02	0.44
	BK2	35.94	-3.93	-27.80	35.41	-2.71	-27.56	-0.53	1.23	0.23	1.36
	BK3	36.05	-3.59	-27.84	35.35	-2.19	-27.37	-0.70	1.40	0.47	1.64
	BK4	36.56	-3.86	-27.31	35.44	-2.55	-27.64	-1.12	1.31	-0.33	1.75
	BL1	37.73	-5.99	-28.65	38.47	-5.96	-27.08	0.74	0.04	1.57	1.74
	BL2	37.58	-5.93	-29.16	38.41	-6.05	-27.34	0.84	-0.12	1.82	2.01
	BL3	37.56	-5.83	-29.27	38.46	-5.96	-27.18	0.90	-0.14	2.09	2.28
	BL4	37.28	-6.14	-29.72	38.83	-6.04	-26.90	1.55	0.10	2.82	3.22
	BM1	34.30	-0.05	-27.59	33.78	-0.14	-26.61	-0.52	-0.08	0.98	1.11
	BM2	34.36	-0.15	-28.00	33.76	-0.31	-26.48	-0.60	-0.16	1.52	1.65
	BM3	34.58	0.00	-28.26	33.78	-0.25	-26.44	-0.80	-0.25	1.82	2.01
Grey	NR01	49.86	-0.50	1.29	50.06	-0.31	0.36	0.20	0.19	-0.93	0.97
	NR02	49.68	-0.90	0.51	50.16	-0.44	1.02	0.48	0.46	0.51	0.84
	NR03	50.07	0.05	1.79	50.16	0.08	0.70	0.08	0.03	-1.09	1.09
	NR04	49.63	-0.27	0.59	50.08	0.09	0.72	0.46	0.36	0.14	0.60
	NR05	49.71	-0.91	0.50	49.76	-0.53	1.33	0.05	0.38	0.83	0.91
	NR06	49.77	-0.01	0.35	50.16	-0.32	0.47	0.39	-0.31	0.12	0.51
	NR07	49.34	-0.15	0.39	49.79	-0.54	1.34	0.44	-0.39	0.95	1.12
	NR08	49.78	-0.55	1.29	50.11	0.05	1.92	0.33	0.60	0.63	0.92
	NR09	49.21	-0.06	0.42	49.52	-0.85	0.55	0.31	-0.79	0.13	0.86
	NR10	49.71	-0.07	0.49	49.73	-0.56	1.31	0.02	-0.49	0.82	0.96
	NR11	49.35	-0.12	0.43	49.99	0.03	0.69	0.65	0.15	0.25	0.71
	NR12	49.78	-0.56	1.26	50.24	0.07	0.51	0.46	0.63	-0.75	1.08
	NR13	49.60	-0.91	0.55	49.76	-0.04	0.34	0.17	0.87	-0.21	0.91
	NR14	49.60	-0.27	0.61	50.06	0.01	1.81	0.47	0.29	1.20	1.32
	NR15	49.63	-0.87	0.54	50.62	-1.51	0.34	0.98	-0.64	-0.20	1.19
	NR16	49.58	-0.26	0.53	50.27	-0.42	0.83	0.69	-0.16	0.31	0.78
	NR17	49.42	-0.10	0.48	50.01	0.02	1.81	0.59	0.12	1.33	1.46
	NR18	49.70	0.01	0.37	49.95	0.02	1.75	0.25	0.02	1.38	1.40
	NR19	49.96	-0.27	0.42	50.00	0.03	1.80	0.04	0.29	1.38	1.41
	NR20	49.71	-0.04	0.36	50.33	-0.46	0.90	0.62	-0.43	0.55	0.93
	NR21	49.34	-0.14	0.37	50.21	-0.32	0.51	0.87	-0.18	0.15	0.90
	NR22	50.59	-1.51	0.33	50.11	-0.32	0.46	-0.48	1.19	0.13	1.29
	NR23	50.68	-1.54	0.38	50.32	-0.47	0.92	-0.36	1.07	0.55	1.26
	NR24	49.70	-0.82	0.52	50.26	0.12	0.59	0.56	0.94	0.07	1.10

Table A-3. (Continued)

Colour Centre	Pair No.	Visual Difference (ΔV) BLK	GRY	WHT	GAP	Rejection Probability BLK	GRY	WHT
Blue	BB1	0.85	**0.86**	0.68	0.68	0.29	**0.21**	0.29
	BB2	1.11	**1.04**	0.90	0.87	0.43	**0.43**	0.29
	BB3	1.22	**1.17**	1.11	0.96	0.50	**0.64**	0.57
	BB4	1.53	**1.49**	1.50	1.22	0.86	**0.93**	0.79
	BC1	0.99	**0.91**	0.99	0.57	0.36	**0.21**	0.21
	BC2	1.29	**1.16**	1.21	0.76	0.57	**0.71**	0.79
	BC3	1.53	**1.38**	1.41	0.96	0.79	**0.93**	0.93
	BD1	0.80	**0.88**	0.77	0.51	0.21	**0.00**	0.00
	BD2	1.05	**1.00**	0.91	0.66	0.36	**0.07**	0.14
	BD3	1.31	**1.14**	1.05	0.71	0.57	**0.50**	0.43
	BD4	1.37	**1.25**	1.29	0.97	0.79	**0.57**	0.64
	BE1	1.31	**1.23**	1.38	0.81	0.71	**0.71**	0.93
	BE2	1.49	**1.47**	1.61	1.00	0.93	**0.79**	1.00
	BE3	1.72	**1.60**	1.78	1.25	1.00	**0.93**	1.00
	BE4	1.94	**1.66**	1.88	1.41	1.00	**1.00**	1.00
	BK1	0.66	**0.83**	0.76	0.60	0.00	**0.00**	0.07
	BK2	1.24	**1.31**	1.17	0.84	0.57	**0.50**	0.43
	BK3	1.45	**1.43**	1.47	0.95	1.00	**0.93**	0.86
	BK4	1.60	**1.57**	1.58	1.20	1.00	**1.00**	0.93
	BL1	0.97	**0.97**	0.95	0.64	0.43	**0.14**	0.21
	BL2	1.13	**1.09**	1.11	0.70	0.86	**0.50**	0.43
	BL3	1.50	**1.27**	1.23	0.81	0.93	**0.64**	0.71
	BL4	1.85	**1.62**	1.45	0.97	1.00	**1.00**	0.93
	BM1	0.79	**0.99**	0.81	0.49	0.14	**0.21**	0.21
	BM2	0.91	**1.09**	1.05	0.61	0.29	**0.50**	0.36
	BM3	1.15	**1.26**	1.22	0.90	0.57	**0.79**	0.57
Grey	NR01	1.61	**1.20**	1.47	1.11	0.29	**0.29**	0.29
	NR02	1.58	**1.48**	1.47	1.10	0.50	**0.64**	0.64
	NR03	1.65	**1.42**	1.53	1.07	0.43	**0.43**	0.36
	NR04	1.04	**1.09**	1.24	1.00	0.07	**0.07**	0.00
	NR05	1.44	**1.31**	1.40	1.02	0.71	**0.57**	0.64
	NR06	1.13	**1.08**	1.11	0.84	0.14	**0.00**	0.07
	NR07	1.81	**1.76**	1.67	1.29	1.00	**0.64**	0.64
	NR08	1.62	**1.62**	1.60	1.30	0.93	**0.86**	0.79
	NR09	1.93	**1.85**	1.75	1.54	0.86	**1.00**	1.00
	NR10	1.75	**1.42**	1.52	1.36	0.64	**0.57**	0.71
	NR11	1.08	**1.01**	1.05	0.70	0.07	**0.14**	0.00
	NR12	1.81	**1.65**	1.67	1.49	0.93	**0.79**	0.86
	NR13	1.86	**1.74**	1.76	1.54	1.00	**1.00**	1.00
	NR14	1.72	**1.62**	1.63	1.14	0.79	**0.79**	1.00
	NR15	1.77	**1.80**	1.81	1.53	0.93	**1.00**	0.93
	NR16	1.20	**1.20**	1.08	0.86	0.29	**0.21**	0.07
	NR17	1.89	**1.60**	1.68	1.09	0.86	**0.93**	0.93
	NR18	1.92	**1.76**	1.80	1.06	1.00	**0.86**	0.86
	NR19	1.98	**1.69**	1.80	1.17	0.93	**0.93**	1.00
	NR20	1.49	**1.54**	1.54	1.24	0.57	**0.79**	0.50
	NR21	1.11	**1.21**	1.11	0.88	0.21	**0.07**	0.07
	NR22	2.14	**1.87**	2.04	1.88	1.00	**1.00**	1.00
	NR23	2.14	**1.89**	1.89	1.89	1.00	**1.00**	0.93
	NR24	2.04	**1.83**	1.86	1.67	1.00	**1.00**	1.00

Table A-4. Experimental results from Part 3.

Colour Centre	Pair No.	L^*_1	a^*_1	b^*_1	L^*_2	a^*_2	b^*_2	ΔL^*	Δa^*	Δb^*	ΔE^*
1. N	NH1	49.14	-0.81	0.43	49.31	-0.44	1.43	0.16	0.37	1.00	**1.07**
	NH2	49.70	0.13	0.78	49.78	0.10	1.83	0.08	-0.03	1.05	**1.05**
	NH3	49.66	-0.25	0.36	49.38	-0.46	1.31	-0.28	-0.22	0.95	**1.02**
	NH4	49.33	0.04	0.49	49.35	-0.48	1.31	0.02	-0.52	0.82	**0.97**
	NH5	49.43	0.10	0.36	49.30	-0.85	0.50	-0.14	-0.95	0.14	**0.97**
2. PR	PR1	54.80	37.72	7.11	54.40	40.99	7.49	-0.40	3.27	0.38	**3.32**
	PR2	54.83	37.80	7.13	54.50	39.52	7.75	-0.33	1.71	0.62	**1.85**
	PR3	54.02	38.92	6.28	54.29	40.99	7.39	0.26	2.08	1.11	**2.37**
	PR4	54.04	38.97	6.33	54.36	39.62	7.73	0.32	0.65	1.40	**1.57**
	PR5	53.74	44.41	6.28	53.99	42.96	7.61	0.26	-1.45	1.33	**1.98**
3. R	RH1	43.30	34.66	20.02	43.59	36.87	21.06	0.29	2.21	1.04	**2.46**
	RH2	43.87	35.63	21.29	44.07	37.13	22.70	0.20	1.50	1.42	**2.08**
	RH3	43.45	38.10	20.99	43.63	37.98	23.03	0.18	-0.13	2.04	**2.05**
	RH4	43.45	37.83	21.08	43.45	36.52	22.28	0.01	-1.32	1.20	**1.78**
	RH5	43.99	39.07	20.99	43.75	37.40	21.29	-0.25	-1.67	0.30	**1.71**
4. YR	YR1	58.95	23.46	27.41	59.18	25.62	28.29	0.23	2.16	0.88	**2.34**
	YR2	61.62	23.60	29.09	61.46	26.05	30.66	-0.16	2.45	1.57	**2.91**
	YR3	60.82	30.47	31.40	61.20	32.09	32.99	0.38	1.62	1.60	**2.30**
	YR4	59.27	25.56	28.18	59.94	25.76	30.02	0.67	0.20	1.84	**1.97**
	YR5	60.03	26.81	29.78	60.14	25.35	30.13	0.11	-1.46	0.35	**1.51**
5. RY	RY1	80.17	7.68	29.28	79.98	8.92	29.98	-0.19	1.24	0.70	**1.43**
	RY2	79.73	7.98	29.10	79.43	9.03	30.89	-0.31	1.05	1.79	**2.09**
	RY3	79.34	7.88	29.98	79.14	8.53	31.46	-0.20	0.65	1.48	**1.63**
	RY4	79.58	7.99	29.17	79.13	8.53	31.50	-0.45	0.55	2.34	**2.44**
	RY5	80.85	7.71	28.58	81.02	6.78	28.98	0.17	-0.93	0.40	**1.02**
6. Y	YH1	85.63	-6.88	44.01	85.41	-5.04	44.91	-0.21	1.84	0.91	**2.06**
	YH2	86.47	-7.01	45.37	86.88	-6.13	47.56	0.41	0.88	2.20	**2.40**
	YH3	86.75	-6.71	46.24	87.28	-6.29	49.87	0.53	0.43	3.63	**3.69**
	YH4	86.98	-6.07	47.36	87.28	-6.28	49.83	0.30	-0.21	2.47	**2.50**
	YH5	87.09	-6.38	45.62	87.21	-7.99	46.13	0.13	-1.61	0.52	**1.69**
7. GY	GY1	67.11	-20.18	24.97	66.72	-18.40	25.16	-0.39	1.77	0.20	**1.83**
	GY2	66.68	-15.31	24.53	66.49	-13.89	25.01	-0.19	1.42	0.48	**1.51**
	GY3	66.79	-15.39	24.53	66.91	-15.38	26.46	0.12	0.01	1.93	**1.93**
	GY4	66.56	-14.27	24.13	66.81	-15.40	26.38	0.25	-1.13	2.26	**2.53**
	GY5	65.08	-16.04	23.43	65.21	-17.74	24.73	0.12	-1.70	1.30	**2.15**
8. YG	YG1	60.82	-33.04	16.03	61.01	-30.89	16.12	0.19	2.15	0.09	**2.16**
	YG2	60.78	-30.08	14.46	60.75	-28.77	15.64	-0.03	1.31	1.18	**1.77**
	YG3	60.72	-30.02	14.49	60.93	-30.06	15.84	0.21	-0.05	1.35	**1.36**
	YG4	60.77	-30.01	14.43	60.95	-30.81	16.14	0.18	-0.80	1.71	**1.90**
	YG5	60.72	-30.82	14.78	60.73	-32.98	16.04	0.01	-2.16	1.26	**2.50**
9. G	GH1	55.47	-32.09	-0.06	55.61	-29.98	0.43	0.14	2.11	0.48	**2.17**
	GH2	55.31	-32.09	-0.10	55.32	-30.31	1.43	0.01	1.78	1.53	**2.34**
	GH3	55.33	-32.00	-0.08	55.21	-32.26	1.40	-0.12	-0.26	1.48	**1.51**
	GH4	55.37	-31.99	-0.07	55.32	-32.93	1.61	-0.05	-0.94	1.69	**1.93**
	GH5	55.47	-30.45	0.21	55.53	-32.92	0.24	0.07	-2.48	0.03	**2.48**
10. BG	BG1	53.50	-18.74	-8.33	53.27	-17.31	-8.32	-0.23	1.43	0.01	**1.45**
	BG2	52.64	-16.33	-9.67	52.76	-14.68	-9.04	0.13	1.65	0.63	**1.77**
	BG3	52.63	-16.35	-9.68	52.87	-15.01	-8.42	0.24	1.34	1.26	**1.85**
	BG4	52.42	-14.94	-10.45	52.65	-14.68	-9.03	0.23	0.26	1.42	**1.46**
	BG5	52.53	-15.00	-10.52	52.61	-16.34	-9.65	0.08	-1.34	0.88	**1.60**

Table A-4. (Continued)

Colour Centre	Pair No.	L^*_1	a^*_1	b^*_1	L^*_2	a^*_2	b^*_2	ΔL^*	Δa^*	Δb^*	ΔE^*
11. GB	GB1	60.97	-18.41	-26.64	60.87	-16.50	-26.47	-0.10	1.91	0.17	**1.92**
	GB2	61.97	-16.53	-26.40	61.87	-14.87	-24.91	-0.09	1.66	1.49	**2.23**
	GB3	60.75	-17.81	-28.52	60.75	-16.48	-26.48	0.00	1.34	2.04	**2.44**
	GB4	61.20	-18.27	-28.85	60.90	-18.40	-26.65	-0.29	-0.13	2.20	**2.22**
	GB5	60.95	-17.33	-28.07	60.97	-18.44	-26.75	0.02	-1.12	1.32	**1.73**
12. B	BH1	36.10	-6.78	-26.53	36.13	-5.11	-26.39	0.02	1.67	0.14	**1.68**
	BH2	36.48	-6.41	-29.55	36.73	-5.23	-27.71	0.25	1.18	1.84	**2.20**
	BH3	36.32	-4.08	-30.09	36.05	-4.23	-27.91	-0.27	-0.15	2.18	**2.20**
	BH4	33.48	-1.55	-28.26	33.67	-2.15	-26.22	0.18	-0.59	2.04	**2.13**
	BH5	36.18	-4.98	-26.41	36.30	-6.56	-26.32	0.12	-1.59	0.10	**1.59**
13. V	VH1	47.08	11.32	-30.78	47.16	12.38	-30.43	0.09	1.06	0.35	**1.12**
	VH2	46.89	10.07	-30.88	47.20	10.84	-29.60	0.31	0.77	1.28	**1.53**
	VH3	46.78	11.15	-31.06	47.08	11.54	-29.81	0.30	0.38	1.25	**1.34**
	VH4	47.14	11.27	-30.82	47.41	10.47	-28.99	0.27	-0.80	1.82	**2.01**
	VH5	47.14	12.34	-30.33	47.20	10.86	-29.44	0.06	-1.49	0.89	**1.73**
14. P	PH1	45.94	13.01	-10.90	46.06	14.67	-10.61	0.12	1.66	0.29	**1.69**
	PH2	46.00	14.61	-10.53	46.02	15.74	-9.90	0.02	1.14	0.64	**1.30**
	PH3	46.18	16.48	-11.47	45.87	15.77	-9.87	-0.31	-0.71	1.61	**1.78**
	PH4	46.20	16.50	-11.46	45.93	14.73	-10.53	-0.27	-1.77	0.93	**2.02**
	PH5	44.64	12.70	-12.68	44.84	11.35	-12.12	0.19	-1.35	0.56	**1.47**
15. RP	RP1	52.73	16.71	-3.17	53.05	18.06	-2.91	0.32	1.36	0.26	**1.42**
	RP2	52.81	16.67	-3.22	52.80	17.24	-2.29	-0.01	0.56	0.93	**1.09**
	RP3	53.33	17.68	-2.15	53.34	17.58	-1.06	0.01	-0.10	1.09	**1.10**
	RP4	53.87	18.21	-1.66	54.16	17.04	-0.87	0.29	-1.17	0.80	**1.45**
	RP5	53.06	19.59	-1.45	53.35	17.56	-1.09	0.29	-2.03	0.36	**2.08**
3. R	LR1	45.10	36.75	22.47	46.18	36.92	22.24	1.08	0.17	-0.23	**1.12**
	LR2	43.60	37.30	22.57	44.97	37.16	22.40	1.37	-0.14	-0.17	**1.39**
6. Y	LY1	85.98	-6.43	45.73	87.03	-6.36	45.56	1.05	0.07	-0.16	**1.07**
	LY2	85.31	-6.22	45.67	87.17	-6.01	45.51	1.86	0.22	-0.15	**1.88**
	LY3	85.03	-5.81	45.77	87.25	-6.02	45.56	2.22	-0.21	-0.20	**2.24**
9. G	LG1	54.93	-32.43	0.27	56.02	-32.47	0.37	1.09	-0.04	0.10	**1.09**
	LG2	53.34	-31.98	-0.02	54.84	-32.08	0.06	1.50	-0.09	0.08	**1.50**
12. B	LB1	37.38	-6.63	-26.86	38.33	-6.82	-27.06	0.95	-0.19	-0.20	**0.99**
	LB2	36.86	-6.64	-26.84	38.49	-6.56	-27.05	1.63	0.08	-0.21	**1.64**
16. N9	L91	86.58	-0.49	-0.26	88.61	-0.53	-0.25	2.03	-0.05	0.02	**2.03**
	L92	88.44	-0.49	-0.40	90.12	-0.50	-0.05	1.68	-0.01	0.35	**1.72**
17. N8	L81	77.85	-0.32	-0.39	79.35	-0.31	-0.43	1.50	0.01	-0.04	**1.50**
	L82	77.71	-0.33	-0.36	79.83	-0.33	-0.41	2.12	0.01	-0.06	**2.12**
18. N7	L71	65.32	-0.19	0.05	66.63	-0.20	0.02	1.31	-0.02	-0.03	**1.31**
	L72	67.12	-0.22	-0.06	68.93	-0.18	0.02	1.80	0.04	0.08	**1.80**
19. N6	L61	60.53	-0.27	0.05	62.00	-0.25	0.00	1.48	0.03	-0.05	**1.48**
	L62	60.05	-0.28	0.00	61.79	-0.28	-0.07	1.75	-0.01	-0.07	**1.75**
1. N	L51	53.14	-0.23	-0.08	54.46	-0.21	-0.01	1.32	0.02	0.07	**1.32**
	L52	49.02	-0.26	-0.09	50.67	-0.25	-0.13	1.65	0.01	-0.04	**1.65**
20. N4	L41	39.31	-0.12	0.40	40.56	-0.12	0.33	1.25	0.00	-0.07	**1.25**
	L42	39.35	-0.12	0.37	41.07	-0.09	0.35	1.72	0.03	-0.02	**1.72**
21. N3	L31	29.09	-0.02	1.01	30.09	0.00	0.99	1.00	0.02	-0.02	**1.00**
	L32	27.35	0.11	0.96	29.09	0.08	0.96	1.75	-0.03	-0.01	**1.75**

Table A-4. (Continued)

Colour Centre	Pair No.	ΔV_{GRY}			ΔV_{BLK}			ΔV_{WHT}			ΔV_{GAP}		
		OG	DK	CY	**OG**	DK	CY	**OG**	DK	CY	**OG**	DK	CY
1. N	NH1	**1.26**	1.30	1.61	**1.29**	1.12	1.61	**1.22**	1.21	1.76	**0.83**	0.81	0.88
	NH2	**1.35**	1.20	1.48	**1.28**	1.03	1.63	**1.31**	1.16	1.63	**0.82**	0.88	0.93
	NH3	**1.25**	1.01	1.35	**1.07**	0.95	1.46	**0.96**	0.98	1.48	**0.79**	0.91	0.79
	NH4	**1.28**	1.34	1.48	**1.32**	1.11	1.43	**1.16**	1.20	1.53	**1.02**	1.03	0.96
	NH5	**1.62**	1.69	1.76	**1.54**	1.43	1.79	**1.33**	1.46	1.76	**1.08**	1.47	1.38
2. PR	PR1	**1.10**	0.93	1.07	**1.23**	0.92	1.25	**1.21**	0.92	1.10	**0.69**	0.55	0.44
	PR2	**0.81**	0.75	0.74	**0.80**	0.79	0.89	**0.90**	0.82	0.95	**0.71**	0.45	0.36
	PR3	**0.74**	0.72	0.92	**0.77**	0.73	0.87	**1.01**	0.89	1.23	**0.56**	0.46	0.32
	PR4	**0.76**	0.58	0.54	**0.67**	0.55	0.82	**0.84**	0.72	0.97	**0.62**	0.42	0.31
	PR5	**0.56**	0.55	0.59	**0.65**	0.61	0.79	**0.76**	0.63	0.87	**0.63**	0.42	0.33
3. R	RH1	**0.95**	0.78	0.77	**0.78**	0.84	0.51	**1.13**	0.92	0.95	**0.59**	0.59	0.27
	RH2	**1.22**	1.21	1.10	**1.11**	1.16	0.82	**1.15**	1.05	1.02	**0.73**	0.70	0.35
	RH3	**1.08**	0.89	1.05	**1.11**	0.91	0.89	**1.12**	0.92	0.92	**0.95**	0.68	0.28
	RH4	**0.83**	0.79	0.79	**0.90**	0.84	0.69	**0.74**	0.83	0.74	**0.71**	0.65	0.32
	RH5	**0.79**	0.69	0.64	**0.69**	0.69	0.54	**0.80**	0.84	0.79	**0.64**	0.56	0.24
4. YR	YR1	**0.93**	0.96	1.15	**1.06**	1.03	1.10	**1.30**	1.07	1.25	**0.67**	0.55	0.36
	YR2	**1.07**	1.00	1.23	**1.04**	0.96	1.07	**1.24**	1.02	1.35	**0.69**	0.54	0.50
	YR3	**0.75**	0.81	0.84	**0.77**	0.82	0.77	**0.97**	0.86	1.02	**0.45**	0.33	0.24
	YR4	**1.05**	1.00	0.89	**0.74**	0.88	0.92	**1.07**	1.01	1.30	**0.66**	0.40	0.26
	YR5	**0.84**	0.91	1.02	**0.87**	0.88	0.95	**1.07**	0.91	1.12	**0.54**	0.44	0.24
5. RY	RY1	**0.88**	0.82	1.05	**0.80**	0.74	1.12	**1.05**	0.92	1.05	**0.68**	0.40	0.46
	RY2	**0.97**	0.88	1.00	**1.00**	0.88	1.12	**0.99**	0.92	1.07	**0.67**	0.46	0.40
	RY3	**0.79**	0.73	0.82	**0.72**	0.83	0.84	**0.80**	0.89	0.92	**0.67**	0.40	0.45
	RY4	**1.26**	0.86	1.07	**0.95**	0.92	1.23	**1.12**	1.05	1.10	**0.77**	0.56	0.50
	RY5	**0.79**	0.81	1.00	**0.73**	0.69	0.87	**0.93**	0.91	1.00	**0.61**	0.37	0.37
6. Y	YH1	**1.25**	1.15	1.43	**1.11**	1.06	1.40	**1.38**	1.25	1.40	**0.84**	0.60	0.78
	YH2	**0.77**	0.83	0.95	**0.72**	0.89	0.97	**1.06**	0.93	1.07	**0.70**	0.45	0.45
	YH3	**0.99**	1.02	1.05	**0.87**	1.05	0.97	**1.14**	1.02	1.00	**0.54**	0.51	0.45
	YH4	**0.57**	0.56	0.79	**0.69**	0.60	0.74	**0.74**	0.79	0.87	**0.52**	0.44	0.32
	YH5	**1.03**	0.87	1.10	**0.98**	0.97	1.18	**1.26**	0.93	1.23	**0.69**	0.44	0.59
7. GY	GY1	**1.17**	0.98	1.40	**1.12**	0.89	1.38	**1.20**	0.98	1.40	**0.83**	0.55	0.73
	GY2	**1.04**	0.93	1.35	**0.95**	0.96	1.43	**1.12**	0.93	1.35	**0.82**	0.58	0.69
	GY3	**0.79**	0.83	1.02	**0.77**	0.77	1.10	**0.80**	0.82	1.05	**0.63**	0.54	0.68
	GY4	**0.87**	0.95	1.15	**0.94**	0.91	1.15	**1.15**	0.88	1.35	**0.62**	0.46	0.45
	GY5	**1.16**	0.87	1.25	**1.03**	0.86	1.30	**0.94**	0.87	1.30	**0.75**	0.47	0.61
8. YG	YG1	**0.84**	0.63	1.20	**0.79**	0.60	1.05	**0.87**	0.68	1.12	**0.77**	0.45	0.41
	YG2	**1.22**	0.82	1.35	**0.97**	0.83	1.30	**1.19**	0.83	1.18	**0.76**	0.46	0.56
	YG3	**0.68**	0.64	0.87	**0.70**	0.63	0.89	**0.79**	0.60	0.87	**0.60**	0.38	0.44
	YG4	**0.75**	0.64	1.00	**0.82**	0.65	0.72	**0.72**	0.73	1.07	**0.74**	0.38	0.44
	YG5	**0.68**	0.61	0.82	**0.76**	0.67	0.95	**0.78**	0.64	1.00	**0.59**	0.44	0.30
9. G	GH1	**0.89**	0.79	1.05	**0.85**	0.86	1.05	**0.76**	0.81	1.07	**0.83**	0.51	0.46
	GH2	**1.38**	1.03	1.43	**1.10**	0.97	1.30	**1.27**	0.93	1.25	**0.80**	0.63	0.44
	GH3	**0.92**	0.81	0.92	**1.00**	0.84	0.92	**0.95**	0.81	0.87	**0.66**	0.47	0.38
	GH4	**1.03**	0.92	1.10	**0.97**	0.79	1.00	**1.00**	0.87	1.18	**0.71**	0.51	0.46
	GH5	**0.93**	0.83	1.10	**1.09**	0.83	1.20	**1.08**	0.77	1.23	**0.64**	0.44	0.28
10. BG	BG1	**0.94**	0.82	1.02	**0.94**	0.79	1.07	**1.03**	0.89	1.23	**0.66**	0.36	0.23
	BG2	**1.32**	1.06	1.23	**1.23**	1.01	1.38	**1.20**	0.98	1.35	**0.72**	0.58	0.35
	BG3	**1.38**	1.06	1.38	**1.25**	1.20	1.40	**1.32**	1.09	1.46	**0.83**	0.61	0.55
	BG4	**1.26**	1.21	1.35	**1.31**	1.23	1.46	**1.44**	1.16	1.38	**0.82**	0.65	0.46
	BG5	**1.30**	0.98	1.30	**1.05**	0.98	1.28	**1.27**	1.02	1.25	**0.62**	0.56	0.44

Table A-4. (Continued)

Colour Centre	Pair No.	ΔV_{GRY}			ΔV_{BLK}			ΔV_{WHT}			ΔV_{GAP}		
		OG	DK	CY	**OG**	DK	CY	**OG**	DK	CY	**OG**	DK	CY
11. GB	GB1	**1.06**	0.93	1.25	**1.11**	0.83	1.35	**1.03**	0.91	1.25	**0.57**	0.32	0.27
	GB2	**1.37**	0.92	1.30	**1.26**	0.96	1.38	**1.22**	0.89	1.38	**0.60**	0.40	0.32
	GB3	**1.13**	1.00	1.33	**1.16**	0.96	1.38	**1.17**	0.91	1.38	**0.70**	0.41	0.35
	GB4	**0.86**	0.98	1.28	**0.88**	0.87	1.20	**1.14**	0.89	1.33	**0.55**	0.40	0.27
	GB5	**1.19**	0.75	1.12	**0.81**	0.68	0.95	**0.88**	0.78	1.00	**0.50**	0.32	0.28
12. B	BH1	**1.11**	0.92	1.05	**0.92**	0.88	1.05	**0.98**	0.73	1.18	**0.71**	0.47	0.24
	BH2	**1.04**	0.82	1.18	**0.79**	0.82	0.97	**0.99**	0.79	1.23	**0.65**	0.42	0.28
	BH3	**0.73**	0.79	0.84	**0.79**	0.77	1.02	**1.02**	0.78	1.28	**0.66**	0.37	0.27
	BH4	**0.77**	0.69	1.07	**0.71**	0.77	1.02	**0.97**	0.91	1.33	**0.54**	0.44	0.32
	BH5	**1.03**	0.82	1.02	**1.08**	0.88	1.00	**0.84**	0.82	1.10	**0.47**	0.42	0.22
13. V	VH1	**1.22**	0.88	1.43	**1.19**	0.89	1.46	**1.27**	0.89	1.43	**0.79**	0.68	0.61
	VH2	**1.41**	0.89	1.48	**1.43**	0.91	1.43	**1.50**	0.95	1.51	**0.80**	0.56	0.72
	VH3	**1.15**	0.79	1.30	**1.16**	0.79	1.33	**1.22**	0.87	1.51	**0.75**	0.50	0.52
	VH4	**0.67**	0.59	0.77	**0.81**	0.60	0.92	**0.69**	0.51	1.00	**0.56**	0.50	0.31
	VH5	**0.85**	0.54	1.10	**0.86**	0.65	1.10	**1.01**	0.65	1.28	**0.69**	0.54	0.41
14. P	PH1	**1.25**	0.95	1.35	**1.25**	0.95	1.40	**1.29**	0.97	1.35	**0.75**	0.64	0.51
	PH2	**0.89**	0.87	1.20	**0.94**	0.92	1.28	**1.06**	0.92	1.33	**0.75**	0.59	0.45
	PH3	**0.91**	0.84	0.89	**0.83**	0.86	0.84	**0.96**	0.92	0.95	**0.66**	0.56	0.37
	PH4	**1.03**	0.74	1.12	**0.96**	0.87	1.15	**1.02**	0.91	1.30	**0.68**	0.56	0.42
	PH5	**0.67**	0.83	0.95	**0.89**	0.86	0.92	**0.88**	0.89	1.18	**0.66**	0.56	0.44
15. RP	RP1	**0.92**	0.79	1.05	**0.95**	0.81	1.12	**1.16**	0.89	1.10	**0.61**	0.52	0.38
	RP2	**0.68**	0.68	0.89	**0.78**	0.70	0.92	**0.83**	0.77	0.97	**0.67**	0.44	0.41
	RP3	**0.70**	0.70	0.78	**0.64**	0.68	0.77	**0.86**	0.79	0.92	**0.68**	0.52	0.44
	RP4	**0.89**	0.72	0.95	**0.85**	0.74	0.89	**0.89**	0.86	0.92	**0.73**	0.51	0.42
	RP5	**1.02**	0.92	1.07	**0.94**	0.87	1.07	**0.99**	0.92	1.23	**0.65**	0.59	0.46
3. R	LR1	**1.26**	1.09	1.10	**1.01**	1.03	0.92	**1.16**	1.18	1.05	**0.65**	0.55	0.26
	LR2	**1.48**	1.51	1.20	**1.29**	1.32	1.15	**1.22**	1.44	1.02	**0.69**	0.70	0.37
6. Y	LY1	**0.87**	0.96	0.89	**0.88**	0.77	1.23	**0.98**	0.98	1.00	**0.45**	0.31	0.37
	LY2	**1.10**	1.42	1.25	**1.30**	1.47	1.33	**1.38**	1.93	1.20	**0.50**	0.45	0.37
	LY3	**1.64**	1.63	1.46	**1.45**	1.84	1.48	**1.61**	1.91	1.43	**0.72**	0.52	0.55
9. G	LG1	**1.06**	0.96	1.02	**1.07**	0.92	1.12	**1.10**	0.95	1.15	**0.51**	0.42	0.35
	LG2	**1.48**	1.48	1.40	**1.45**	1.37	1.33	**1.46**	1.67	1.28	**0.86**	0.69	0.50
12. B	LB1	**1.13**	1.14	1.30	**1.06**	1.01	1.25	**1.15**	1.05	1.35	**0.59**	0.52	0.33
	LB2	**1.49**	1.15	1.38	**1.25**	0.97	1.20	**1.45**	1.23	1.33	**0.75**	0.52	0.41
16. N9	L91	**1.10**	1.06	1.10	**0.95**	0.89	1.23	**1.22**	1.24	1.33	**0.58**	0.23	0.22
	L92	**1.01**	1.01	1.20	**0.80**	0.89	1.15	**1.12**	1.18	1.18	**0.42**	0.16	0.21
17. N8	L81	**1.20**	1.11	1.20	**1.12**	1.09	1.20	**1.16**	1.39	1.28	**0.50**	0.32	0.26
	L82	**1.29**	1.26	1.35	**1.26**	1.11	1.40	**1.25**	1.34	1.51	**0.53**	0.35	0.31
18. N7	L71	**1.38**	1.12	1.46	**1.19**	1.05	1.48	**1.41**	1.34	1.53	**0.62**	0.36	0.44
	L72	**1.35**	1.06	1.35	**1.11**	1.15	1.46	**1.24**	1.29	1.48	**0.59**	0.40	0.44
19. N6	L61	**1.09**	1.18	1.43	**1.09**	1.06	1.46	**1.11**	1.30	1.56	**0.65**	0.46	0.56
	L62	**1.38**	1.32	1.56	**1.33**	1.39	1.58	**1.42**	1.47	1.51	**0.70**	0.49	0.64
1. N	L51	**1.61**	1.40	1.58	**1.67**	1.29	1.69	**1.28**	1.39	1.53	**0.88**	0.69	0.65
	L52	**1.67**	1.23	1.40	**1.53**	1.11	1.48	**1.40**	1.24	1.43	**1.03**	0.89	0.78
20. N4	L41	**1.21**	1.11	1.23	**1.05**	1.09	1.25	**1.04**	1.12	1.20	**0.62**	0.58	0.45
	L42	**1.63**	1.37	1.48	**1.62**	1.33	1.38	**1.32**	1.14	1.48	**0.95**	0.77	0.60
21. N3	L31	**0.85**	0.91	1.00	**0.72**	0.87	1.18	**0.81**	0.86	1.15	**0.41**	0.38	0.33
	L32	**1.20**	1.19	1.33	**1.01**	1.19	1.30	**1.06**	1.02	1.33	**0.53**	0.47	0.38

Appendix 2. Ellipsoid (ellipse) coefficients and parameters for 3 CIE centres and tolerance vectors for the red and for lightness difference of 11 centres.

Table A-5. Red centre - ellipsoids.

(a) Ellipsoid coefficients

Param.①	b_{11}	b_{22}	b_{33}	b_{12}	b_{13}	b_{23}	α	ΔE^*_{STD}	β	σ②
GRY	8.57	11.17	42.36	-5.84	-6.97	10.63	5.71	1.10	5.19	0.33
	0.32	0.42	1.57	-0.22	-0.26	0.40	(← b_{ik} divided by β^2)			
BLK	9.57	12.79	47.52	-6.65	-9.79	11.67	5.79	1.10	5.27	0.32
	0.35	0.46	1.71	-0.24	-0.35	0.42	(← b_{ik} divided by β^2)			
WHT	8.94	10.67	43.44	-3.69	-2.12	5.37	5.98	1.10	5.44	0.31
	0.30	0.36	1.47	-0.12	-0.07	0.18	(← b_{ik} divided by β^2)			
Gap1	4.07	8.33	13.34	-4.53	-3.66	5.03	4.33	.	.	.
Gap2	4.09	6.57	9.88	-4.49	-2.04	4.35	4.89	.	.	.

(b) Ellipsoid axes

Param.①	Axis	ΔL^*	Δa^*	Δb^*	length	ϕ	θ (tilt)	V③
GRY	A	0.13	-1.98	-1.76	2.65	-138.4	87.2	13.19
	B	0.58	0.99	-1.08	1.58	-47.3	68.3	
	C	0.70	-0.16	0.23	0.75	124.8	21.9	
BLK	A	0.05	2.02	1.52	2.53	37.0	89.0	11.76
	B	0.60	0.85	-1.14	1.55	-53.4	67.1	
	C	0.66	-0.18	0.22	0.72	129.5	23.0	
WHT	A	0.11	-1.70	-1.45	2.23	-139.5	87.1	11.68
	B	0.27	0.99	-1.14	1.53	-49.0	80.0	
	C	0.80	-0.06	0.13	0.82	114.7	10.4	
Gap1	A	0.04	0.79	0.47	0.92	30.7	87.3	0.37
	B	0.26	0.15	-0.28	0.41	-61.6	50.0	
	C	0.18	-0.08	0.12	0.23	124.0	40.1	
Gap2	A	0.20	-1.03	-0.91	1.39	-138.6	81.8	0.66
	B	0.30	0.24	-0.20	0.43	-40.6	46.0	
	C	0.18	-0.10	0.16	0.26	123.2	45.2	

(c) Highest point of an ellipsoid and ellipse parameters in a^*b^* plane

Param.①	L^*_m	A	B	B/A	θ (rot.)	V③
GRY	0.92	2.63	1.30	0.50	38.7	13.19
BLK	0.89	2.53	1.24	0.49	38.2	11.76
WHT	0.85	2.22	1.48	0.67	38.4	11.68
Gap1	0.32	0.92	0.30	0.33	32.4	0.37
Gap2	0.40	1.22	0.32	0.26	37.3	0.66

① Parametric condition: **GRY** = grey background (bg), **BLK** = black bg, **WHT** = white bg, **Gap1** = test with standard (std) pair no.2, and **Gap2** = test with std pair no.3

② Standard deviation estimated as 1.7/β

③ Volume of an ellipsoid

Table A-6. Red centre - tolerances.

(a) Probit analysis:

Mean tolerance with LCL, UCL (lower and upper confidence limits), SD (standard deviation), and P:χ^2 (probability of χ^2 test)

Param.①	Vector	Mean	LCL	UCL	SD	P:χ^2
GRY	A	1.19	1.12	1.25	0.35	0.52
	B	2.06	1.82	2.33	0.57	0.10
	C	1.60	1.47	1.78	0.29	0.11
	D	2.94	2.62	3.52	0.63	0.06
	E	1.62	1.57	1.67	0.31	0.24
	J	1.47	1.41	1.53	0.28	0.99
	K	1.00	.	.	0.34	0.00
	L	0.77	.	.	0.35	0.00
	M	1.32	1.26	1.37	0.24	0.52
BLK	A	1.21	1.12	1.29	0.28	0.84
	B	2.03	1.88	2.17	0.60	0.89
	C	1.56	1.22	2.14	0.31	0.01
	D	2.80	2.62	3.04	0.66	0.51
	E	1.54	1.46	1.62	0.33	0.21
	J	1.49	1.38	1.59	0.41	0.92
	K	0.87	.	.	0.20	0.00
	L	0.78	0.56	1.07	0.26	0.09
	M	1.25	1.16	1.33	0.26	0.92
WHT	A	1.15	1.05	1.24	0.31	0.15
	B	2.10	1.49	3.42	0.78	0.06
	C	1.76	1.68	1.86	0.27	0.19
	D	2.47	1.85	8.70	0.56	0.01
	E	1.70	1.64	1.77	0.22	0.38
	J	1.30	1.21	1.38	0.30	0.99
	K	0.93	.	.	0.57	0.00
	L	1.04	0.94	1.15	0.31	0.81
	M	1.24	1.15	1.32	0.26	0.97
Gap1	A	1.66	1.45	2.13	0.61	0.76
	B	2.38	2.15	2.80	0.68	0.57
	C	1.37	1.24	1.51	0.35	0.82
	D	3.43	3.03	4.40	0.86	0.52
	E	1.63	1.54	1.74	0.27	0.62
	J	1.85	1.68	2.08	0.47	0.86
	K	1.07	0.90	1.25	0.37	0.72
	L	0.73	0.53	0.90	0.48	0.46
	M	1.53	1.43	1.74	0.20	0.99
Gap2	A	2.04	1.70	4.36	0.72	0.83
	B	2.51	2.29	2.98	0.57	0.27
	C	1.66	1.54	1.79	0.26	0.64
	D	4.36	.	.	0.62	1.00
	E	1.80	1.66	2.03	0.44	0.94
	J	2.05	1.88	2.32	0.41	0.33
	K	1.63	1.42	1.85	0.54	0.31
	L	1.06	0.79	1.39	0.84	0.66
	M	1.98	1.81	2.26	0.37	0.99

(① Refer to Table A-5)

Table A-6. (Continued)

(b) Principal component analysis (PCA): Centre position of each vector

Vector	Centre Co-ordinates			Eigenvector			Eigenvalue
	L^*	a^*	b^*	ΔL^*	Δa^*	Δb^*	
A	45.54	37.09	22.85	-0.996	-0.034	0.088	0.9902
B	44.45	37.17	22.59	-0.010	-0.990	-0.139	0.9834
C	44.45	37.07	22.12	-0.022	-0.016	1.000	0.9943
D	44.39	35.94	21.56	0.000	-0.713	-0.701	0.9982
E	44.44	37.06	21.77	-0.031	-0.705	0.709	0.9947
J	43.92	36.29	22.68	-0.641	-0.767	-0.039	0.9908
K	44.70	36.85	23.09	0.634	-0.773	-0.009	0.9929
L	44.16	37.01	22.83	0.755	-0.016	0.655	0.9850
M	44.59	37.09	22.75	-0.733	0.005	0.680	0.9941

Table A-7. Grey centre

(Coefficients, principal axes, highest point and volume of an ellipsoid).

(a) Grey-scale method

Param.	b_{11}	b_{22}	b_{33}	b_{12}	b_{13}	b_{23}
GRY	3.78	1.44	0.92	-0.43	-0.06	0.71
BLK	4.44	2.00	0.94	-0.55	0.07	0.47
WHT	3.94	1.66	0.80	-0.43	-0.01	0.59
GAP	3.41	0.75	0.41	-0.39	-0.04	0.19

Param.	Axis	ΔL^*	Δa^*	Δb^*	length	ϕ	θ (tilt)	V
GRY	A	1.26	-0.09	-0.91	1.56	-95.9	36.0	2.44
	B	0.43	0.15	0.58	0.73	75.9	54.3	
	C	0.03	-0.50	0.10	0.51	168.7	86.1	
BLK	A	1.07	-0.09	-0.43	1.16	-101.1	22.5	1.57
	B	0.27	0.14	0.63	0.69	77.7	67.5	
	C	0.00	-0.46	0.10	0.47	167.9	89.6	
WHT	A	1.26	-0.08	-0.67	1.43	-96.9	28.0	2.18
	B	0.34	0.13	0.63	0.73	78.1	62.1	
	C	0.02	-0.49	0.09	0.50	169.2	87.9	
GAP	A	1.58	-0.07	-0.76	1.76	-95.5	25.8	4.48
	B	0.49	0.16	1.01	1.13	81.1	64.2	
	C	0.01	-0.53	0.08	0.54	171.7	88.7	

Param.	L^*_m	A	B	B/A	θ (rot.)	V
GRY	1.33	0.86	0.51	0.59	79.8	2.44
BLK	1.10	0.73	0.47	0.64	77.9	1.57
WHT	1.31	0.80	0.50	0.63	79.7	2.18
GAP	1.66	1.20	0.54	0.45	81.8	4.48

Table A-7. (Continued)

(b) Paired-comparison method ($\Delta E^*_{STD} = 1.1$)

Param.	b_{11}	b_{22}	b_{33}	b_{12}	b_{13}	b_{23}	α	β	σ
GRY	196.92	44.52	38.39	12.53	-16.06	2.61	7.73	7.03	0.24
BLK	132.45	34.84	21.83	1.82	-7.57	6.93	6.36	5.78	0.29
WHT	177.28	49.19	32.12	8.10	1.08	7.59	7.80	7.10	0.24

b_{ik} divided by β^2

Param.	b_{11}	b_{22}	b_{33}	b_{12}	b_{13}	b_{23}
GRY	3.98	0.90	0.78	0.25	-0.32	0.05
BLK	3.96	1.04	0.65	0.05	-0.23	0.21
WHT	3.52	0.98	0.64	0.16	0.02	0.15

Param.	Axis	ΔL^*	Δa^*	Δb^*	length	ϕ	θ (tilt)	V
GRY	A	1.07	0.14	-0.49	1.19	-73.5	25.3	2.59
	B	0.43	-0.03	0.95	1.04	92.0	65.4	
	C	0.05	-0.49	-0.04	0.50	-175.5	84.4	
BLK	A	1.24	0.09	-0.53	1.35	-80.3	23.4	2.67
	B	0.37	0.01	0.86	0.94	89.1	66.9	
	C	0.03	-0.50	-0.01	0.50	-179.2	86.2	
WHT	A	1.22	0.02	-0.47	1.31	-88.0	21.1	2.89
	B	0.36	-0.06	0.92	0.99	93.9	68.9	
	C	0.01	0.53	0.03	0.53	3.6	89.4	

Param.	L^*_m	A	B	B/A	θ (rot.)	V
GRY	1.16	1.07	0.50	0.47	95	2.59
BLK	1.29	0.98	0.50	0.51	91	2.67
WHT	1.28	1.02	0.53	0.52	94	2.89

Table A-8. Blue centre (Ellipsoid's coefficients, axes, highest point and volume)

(a) Grey-scale method

Param.	b_{11}	b_{22}	b_{33}	b_{12}	b_{13}	b_{23}
GRY	0.56	0.20	0.73	0.17	-0.17	-0.08
BLK	0.57	0.26	0.41	0.20	-0.24	0.01
WHT	0.50	0.21	0.58	0.11	-0.26	-0.08
GAP	0.35	0.08	0.38	0.06	-0.07	-0.04

Param.	Axis	ΔL^*	Δa^*	Δb^*	length	ϕ	θ(tilt)	V
GRY	A	0.06	-0.96	2.51	2.68	111.0	88.8	17.34
	B	0.86	1.08	0.39	1.44	20.1	53.0	
	C	0.86	-0.60	-0.25	1.07	-157.3	37.0	
BLK	A	1.35	1.62	-2.20	3.05	-53.6	63.7	24.38
	B	1.25	0.41	1.07	1.69	69.2	42.4	
	C	0.57	-0.91	-0.32	1.13	-160.5	59.5	
WHT	A	0.17	0.92	-2.25	2.43	-67.7	86.0	20.85
	B	1.25	1.24	0.60	1.86	26.0	47.6	
	C	0.81	-0.71	-0.23	1.10	-162.1	42.6	
GAP	A	0.36	-0.79	3.93	4.02	101.4	84.9	46.58
	B	1.24	1.37	0.16	1.86	6.8	48.1	
	C	1.10	-0.96	-0.29	1.49	-163.0	42.4	

Param.	L^*_m	A	B	B/A	θ (rot.)	V
GRY	1.22	2.68	1.27	0.47	111.5	17.34
BLK	1.93	2.46	1.23	0.50	115.7	24.38
WHT	1.50	2.43	1.37	0.56	109.4	20.85
GAP	1.70	3.95	1.66	0.42	102.8	46.58

Table A-8. (Continued)

(b) Paired-comparison method ($\Delta E^*_{STD} = 1.1$)

Param.	b_{11}	b_{22}	b_{33}	b_{12}	b_{13}	b_{23}	α	β	σ
GRY	12.65	4.75	14.41	1.81	-2.92	-1.39	5.28	4.80	0.35
BLK	10.67	4.91	5.54	1.91	-6.06	1.69	4.72	4.29	0.40
WHT	15.27	6.13	11.30	-0.95	-4.59	-0.76	5.63	5.12	0.33

b_{ik} divided by β^2

Param.	b_{11}	b_{22}	b_{33}	b_{12}	b_{13}	b_{23}
GRY	0.55	0.21	0.63	0.08	-0.13	-0.06
BLK	0.58	0.27	0.30	0.10	-0.33	0.09
WHT	0.58	0.23	0.43	-0.04	-0.18	-0.03

Param.	Axis	ΔL^*	Δa^*	Δb^*	length	ϕ	θ (tilt)	V
GRY	A	0.19	-0.43	2.27	2.31	100.6	85.3	16.68
	B	0.92	1.15	0.14	1.48	7.0	51.6	
	C	0.91	-0.70	-0.21	1.16	-163.5	38.7	
BLK	A	6.63	4.63	-4.28	9.15	-42.7	43.5	74.03
	B	0.74	0.35	1.52	1.73	77.1	64.7	
	C	0.60	-0.94	-0.08	1.12	-175.2	57.3	
WHT	A	0.69	0.52	1.98	2.16	75.2	71.5	18.70
	B	1.34	0.85	-0.69	1.73	-39.0	39.2	
	C	0.65	-1.00	0.04	1.20	177.8	56.9	

Param.	L^*_m	A	B	B/A	θ (rot.)	V
GRY	1.30	2.30	1.33	0.58	102.3	16.68
BLK	6.70	2.06	1.28	0.62	106.8	74.03
WHT	1.64	2.08	1.31	0.63	84.1	18.70

Table A-9. Lightness tolerances of 11 colour centres.

(a) Position of each centre ← PCA

Colour Centre	Centre Co-ordinates			Eigenvector			Eigenvalue
	L^*	a^*	b^*	ΔL^*	Δa^*	Δb^*	
Grey(L60)	61.45	-0.29	-0.05	1.000	-0.002	-0.006	0.9978
Red	45.12	39.94	22.18	-0.996	0.057	0.062	0.8434
Yellow	86.34	-6.52	45.97	-0.980	0.177	-0.088	0.8904
Green	55.69	-31.87	0.12	0.995	-0.047	0.087	0.9734
Blue	37.80	-6.20	-26.73	0.959	-0.166	-0.230	0.9892
L90	89.05	-0.49	-0.36	0.995	-0.009	0.100	0.9954
L80	79.09	-0.35	-0.49	1.000	-0.004	0.027	0.9965
L70	67.11	-0.23	-0.05	1.000	-0.005	-0.008	0.9987
L50	50.59	-0.31	-0.04	1.000	0.005	-0.018	0.9982
L40	40.75	-0.24	0.28	0.997	-0.023	-0.080	0.9943
L30	29.26	-0.20	0.49	-0.997	-0.031	-0.065	0.9880

(b) Mean tolerance, LCL, UCL, SD and P:χ^2 ← Probit analysis

Param.	Col. Cnt.	Mean	LCL	UCL	SD	P:χ^2
Grey BG	Grey	1.41	1.30	1.52	0.18	0.77
	Red	0.82	0.74	0.89	0.12	0.99
	Yellow	1.92	.	.	0.17	0.84
	Green	0.78	0.43	1.01	0.49	0.85
	Blue	1.51	1.35	1.87	0.50	0.65
	L90	2.90	2.55	3.69	0.69	0.40
	L80	2.03	1.83	2.40	0.51	0.80
	L70	1.97	1.83	2.12	0.29	0.97
	L50	1.32	.	.	0.13	1.00
	L40	1.27	1.17	1.47	0.20	0.54
	L30	1.50	.	.	0.44	0.05
Black BG	Grey	1.39	1.26	1.56	0.31	0.85
	Red	1.04	.	.	0.37	0.05
	Yellow	1.90	1.69	2.40	0.58	0.91
	Green	0.99	0.76	1.20	0.38	0.95
	Blue	1.78	1.61	2.26	0.35	0.63
	L90	2.20	1.98	2.55	0.58	0.20
	L80	1.80	1.61	1.97	0.37	0.40
	L70	1.75	1.61	1.90	0.34	0.50
	L50	1.38	1.20	1.56	0.37	0.86
	L40	1.24	1.12	1.40	0.30	0.22
	L30	1.36	0.58	1.47	0.20	0.21
White BG	Grey	1.54	1.41	1.70	0.26	0.71
	Red	0.86	0.79	0.94	0.11	1.00
	Yellow	1.70	1.56	1.86	0.34	0.59
	Green	0.99	0.79	1.20	0.30	1.00
	Blue	1.61	1.45	1.95	0.42	0.41
	L90	1.83	1.54	2.14	0.78	0.22
	L80	1.61	1.40	1.76	0.34	0.95
	L70	1.77	1.63	1.92	0.31	0.75
	L50	1.35	1.17	1.53	0.37	0.66
	L40	1.54	1.39	1.70	0.33	0.36
	L30	1.45	.	.	0.24	0.11

Appendix 3. Coefficients and parameters of 180 chromaticity ellipses.

Table A-10. Coefficients of chromaticity ellipses (① Observer Group, ② observer DK and ③ observer CY).

Col. Cnt.	Elps. Coeff.	Grey BG			Black BG			White BG			GAP		
		OG①	DK②	CY③	**OG**	DK	CY	**OG**	DK	CY	**OG**	DK	CY
1. N	b_{11}	**2.70**	3.20	3.47	**2.63**	2.26	3.42	**1.94**	2.36	3.48	**1.28**	2.17	1.98
	b_{12}	**-0.12**	0.06	0.17	**-0.01**	0.04	0.20	**0.11**	0.05	0.31	**-0.19**	-0.26	-0.04
	b_{22}	**1.48**	1.22	2.00	**1.35**	0.94	2.21	**1.27**	1.14	2.43	**0.62**	0.62	0.64
2. PR	b_{11}	**0.10**	0.08	0.11	**0.13**	0.09	0.14	**0.13**	0.08	0.10	**0.05**	0.03	0.02
	b_{12}	**0.05**	0.03	0.03	**0.02**	0.02	0.02	**0.05**	0.05	0.09	**0.01**	0.01	0.00
	b_{22}	**0.18**	0.13	0.12	**0.14**	0.14	0.25	**0.29**	0.23	0.47	**0.18**	0.08	0.04
3. R	b_{11}	**0.17**	0.14	0.11	**0.12**	0.15	0.06	**0.19**	0.20	0.18	**0.09**	0.09	0.02
	b_{12}	**0.02**	0.01	0.00	**-0.02**	0.01	-0.03	**0.04**	-0.01	0.01	**-0.04**	-0.02	0.00
	b_{22}	**0.31**	0.25	0.30	**0.34**	0.25	0.21	**0.30**	0.22	0.21	**0.21**	0.12	0.02
4. YR	b_{11}	**0.26**	0.28	0.39	**0.29**	0.28	0.34	**0.44**	0.30	0.46	**0.12**	0.08	0.03
	b_{12}	**-0.17**	-0.19	-0.19	**-0.01**	-0.16	-0.20	**-0.23**	-0.19	-0.29	**-0.08**	-0.04	0.00
	b_{22}	**0.34**	0.33	0.27	**0.18**	0.26	0.28	**0.38**	0.33	0.54	**0.13**	0.05	0.02
5. RY	b_{11}	**0.57**	0.56	0.89	**0.48**	0.41	0.80	**0.81**	0.70	0.88	**0.34**	0.12	0.14
	b_{12}	**-0.17**	-0.10	-0.21	**-0.05**	-0.06	-0.10	**-0.19**	-0.18	-0.17	**-0.07**	-0.03	-0.03
	b_{22}	**0.33**	0.17	0.27	**0.18**	0.18	0.27	**0.27**	0.27	0.27	**0.13**	0.07	0.05
6. Y	b_{11}	**0.42**	0.32	0.53	**0.37**	0.33	0.56	**0.58**	0.39	0.59	**0.20**	0.09	0.16
	b_{12}	**0.02**	0.05	0.01	**-0.02**	0.03	0.01	**0.03**	0.03	0.00	**0.01**	0.00	0.00
	b_{22}	**0.06**	0.06	0.08	**0.06**	0.07	0.07	**0.09**	0.08	0.09	**0.03**	0.02	0.01
7. GY	b_{11}	**0.45**	0.30	0.65	**0.38**	0.28	0.68	**0.43**	0.31	0.65	**0.23**	0.10	0.17
	b_{12}	**0.09**	0.10	0.19	**0.07**	0.09	0.21	**0.11**	0.10	0.15	**0.08**	0.05	0.09
	b_{22}	**0.15**	0.19	0.28	**0.16**	0.17	0.32	**0.22**	0.18	0.32	**0.10**	0.07	0.10
8. YG	b_{11}	**0.17**	0.09	0.27	**0.13**	0.08	0.27	**0.18**	0.09	0.24	**0.10**	0.04	0.03
	b_{12}	**0.16**	0.07	0.24	**0.09**	0.06	0.19	**0.15**	0.07	0.14	**0.07**	0.02	0.04
	b_{22}	**0.32**	0.21	0.47	**0.29**	0.21	0.36	**0.33**	0.22	0.44	**0.21**	0.07	0.10
9. G	b_{11}	**0.14**	0.11	0.20	**0.17**	0.12	0.22	**0.15**	0.11	0.25	**0.09**	0.04	0.02
	b_{12}	**0.08**	0.01	0.07	**-0.01**	0.02	0.04	**0.02**	0.01	-0.02	**0.02**	0.02	0.00
	b_{22}	**0.42**	0.28	0.43	**0.34**	0.25	0.35	**0.38**	0.25	0.36	**0.17**	0.10	0.07
10. BG	b_{11}	**0.50**	0.30	0.49	**0.39**	0.28	0.53	**0.46**	0.32	0.60	**0.16**	0.08	0.03
	b_{12}	**-0.05**	-0.04	-0.09	**0.01**	-0.01	-0.04	**-0.10**	-0.06	-0.03	**0.01**	-0.01	0.00
	b_{22}	**0.78**	0.62	0.89	**0.72**	0.68	0.93	**0.93**	0.60	0.83	**0.28**	0.20	0.13
11. GB	b_{11}	**0.44**	0.22	0.44	**0.35**	0.19	0.46	**0.29**	0.22	0.41	**0.09**	0.03	0.02
	b_{12}	**-0.04**	-0.02	-0.06	**0.03**	0.01	0.01	**0.00**	-0.03	-0.01	**0.00**	0.00	0.00
	b_{22}	**0.19**	0.18	0.32	**0.16**	0.15	0.27	**0.25**	0.15	0.33	**0.07**	0.03	0.02
12. B	b_{11}	**0.43**	0.28	0.42	**0.36**	0.29	0.39	**0.31**	0.23	0.49	**0.13**	0.08	0.02
	b_{12}	**0.02**	-0.01	0.01	**-0.04**	-0.02	-0.06	**-0.02**	-0.04	-0.07	**0.01**	-0.01	0.00
	b_{22}	**0.11**	0.11	0.19	**0.10**	0.11	0.20	**0.20**	0.14	0.33	**0.08**	0.03	0.02
13. V	b_{11}	**0.80**	0.33	1.11	**0.76**	0.39	1.07	**0.97**	0.42	1.22	**0.35**	0.22	0.20
	b_{12}	**0.51**	0.22	0.59	**0.49**	0.21	0.55	**0.56**	0.25	0.60	**0.16**	0.07	0.12
	b_{22}	**0.42**	0.22	0.48	**0.47**	0.21	0.52	**0.45**	0.21	0.60	**0.17**	0.09	0.10
14. P	b_{11}	**0.41**	0.29	0.59	**0.45**	0.33	0.64	**0.49**	0.34	0.72	**0.21**	0.14	0.09
	b_{12}	**0.19**	0.14	0.28	**0.19**	0.13	0.33	**0.24**	0.12	0.24	**0.09**	0.06	0.03
	b_{22}	**0.40**	0.34	0.45	**0.34**	0.34	0.45	**0.47**	0.37	0.44	**0.21**	0.14	0.07
15. RP	b_{11}	**0.32**	0.24	0.39	**0.31**	0.23	0.42	**0.38**	0.27	0.46	**0.13**	0.10	0.06
	b_{12}	**0.04**	0.07	0.13	**0.11**	0.08	0.19	**0.18**	0.08	0.19	**0.03**	0.02	0.01
	b_{22}	**0.43**	0.42	0.62	**0.44**	0.42	0.61	**0.65**	0.56	0.76	**0.45**	0.21	0.17

Table A-11. Parameters of chromaticity ellipses (①, ② and ③: Refer to Table A-10).

Col. Cnt.	Elps. Param.	Grey BG			Black BG			White BG			GAP		
		OG①	DK②	CY③	**OG**	DK	CY	**OG**	DK	CY	**OG**	DK	CY
1. N	θ	**84.4**	91.7	96.6	**89.4**	91.9	99.1	**98.9**	92.4	105.2	**74.7**	80.6	88.4
	A	**0.83**	0.91	0.71	**0.86**	1.03	0.68	**0.89**	0.94	0.65	**1.33**	1.32	1.25
	B	**0.61**	0.56	0.54	**0.62**	0.66	0.54	**0.72**	0.65	0.53	**0.87**	0.67	0.71
2. PR	θ	**155.5**	156.0	139.4	**144.7**	162.1	169.4	**163.0**	163.1	167.0	**176.3**	172.5	177.6
	A	**3.66**	3.81	3.48	**2.94**	3.53	2.73	**3.01**	4.12	3.54	**4.61**	6.08	7.36
	B	**2.26**	2.66	2.59	**2.52**	2.65	1.97	**1.81**	2.01	1.43	**2.37**	3.50	4.85
3. R	θ	**173.8**	172.6	0.4	**6.2**	176.3	9.8	**161.2**	25.8	170.3	**17.6**	25.2	29.0
	A	**2.41**	2.71	3.05	**2.87**	2.57	4.24	**2.39**	2.30	2.39	**3.70**	3.58	7.61
	B	**1.79**	2.01	1.83	**1.72**	2.01	2.15	**1.79**	2.11	2.18	**2.12**	2.74	6.11
4. YR	θ	**38.6**	41.3	53.5	**83.2**	46.8	49.6	**48.7**	42.9	40.9	**43.2**	55.1	73.0
	A	**2.84**	2.92	2.79	**2.34**	2.99	2.99	**2.41**	2.76	2.19	**4.49**	6.73	7.88
	B	**1.45**	1.42	1.37	**1.84**	1.52	1.40	**1.25**	1.41	1.12	**2.23**	3.03	5.69
5. RY	θ	**62.0**	76.4	72.7	**81.0**	76.8	79.6	**72.8**	70.2	75.4	**73.8**	63.6	74.5
	A	**2.05**	2.65	2.21	**2.44**	2.43	2.00	**2.17**	2.21	2.09	**3.02**	4.38	4.71
	B	**1.23**	1.31	1.02	**1.44**	1.53	1.11	**1.07**	1.15	1.04	**1.67**	2.72	2.63
6. Y	θ	**92.8**	100.5	91.9	**85.4**	96.4	91.1	**93.0**	94.9	89.7	**93.2**	92.4	91.8
	A	**4.17**	4.44	3.49	**4.04**	3.88	3.71	**3.37**	3.55	3.34	**5.97**	6.69	8.65
	B	**1.54**	1.74	1.38	**1.65**	1.72	1.34	**1.32**	1.60	1.30	**2.23**	3.38	2.54
7. GY	θ	**105.1**	120.4	112.8	**106.8**	118.0	114.8	**113.2**	119.2	110.8	**114.5**	126.4	122.9
	A	**2.84**	2.72	2.21	**2.73**	2.84	2.14	**2.45**	2.86	1.94	**3.91**	5.39	4.96
	B	**1.45**	1.66	1.17	**1.58**	1.74	1.14	**1.44**	1.66	1.19	**1.93**	2.68	2.08
8. YG	θ	**147.0**	155.6	146.2	**155.3**	157.7	142.0	**147.6**	156.2	152.8	**153.2**	151.7	154.5
	A	**3.95**	4.30	2.99	**3.38**	4.10	2.96	**3.45**	3.97	2.43	**3.93**	5.80	8.78
	B	**1.54**	2.06	1.26	**1.74**	2.07	1.40	**1.53**	2.01	1.40	**2.03**	3.58	2.90
9. G	θ	**165.1**	175.5	164.3	**4.7**	171.3	165.2	**173.9**	178.1	8.4	**169.2**	167.1	175.4
	A	**2.95**	2.97	2.37	**2.42**	2.95	2.16	**2.57**	3.09	2.02	**3.47**	5.61	6.97
	B	**1.51**	1.87	1.49	**1.72**	2.00	1.67	**1.62**	1.98	1.65	**2.38**	3.11	3.89
10. BG	θ	**10.4**	6.5	12.2	**178.6**	1.3	6.3	**11.8**	12.4	6.3	**173.7**	3.9	2.3
	A	**1.42**	1.84	1.46	**1.60**	1.90	1.38	**1.52**	1.80	1.30	**2.55**	3.62	5.60
	B	**1.12**	1.27	1.05	**1.18**	1.21	1.03	**1.02**	1.28	1.10	**1.90**	2.23	2.78
11. GB	θ	**80.9**	66.5	68.0	**98.1**	97.7	93.3	**86.4**	68.5	86.0	**88.1**	28.7	77.1
	A	**2.34**	2.43	1.82	**2.52**	2.60	1.92	**2.01**	2.67	1.74	**3.83**	5.89	7.52
	B	**1.49**	2.09	1.47	**1.68**	2.31	1.47	**1.85**	2.05	1.56	**3.34**	5.46	6.45
12. B	θ	**93.2**	87.7	91.6	**81.2**	82.6	74.8	**79.6**	68.5	68.7	**101.2**	80.2	57.9
	A	**2.96**	3.05	2.27	**3.32**	3.04	2.35	**2.26**	2.89	1.81	**3.66**	5.86	7.93
	B	**1.52**	1.90	1.55	**1.65**	1.85	1.57	**1.79**	2.01	1.39	**2.80**	3.57	6.65
13. V	θ	**124.9**	127.7	121.0	**126.8**	123.3	121.9	**122.6**	123.7	121.2	**119.7**	114.2	124.2
	A	**3.82**	4.35	2.84	**3.02**	3.73	2.36	**3.29**	4.52	2.04	**3.64**	4.26	8.64
	B	**0.93**	1.41	0.83	**0.94**	1.37	0.84	**0.87**	1.30	0.79	**1.50**	2.00	1.88
14. P	θ	**134.6**	139.8	127.7	**126.4**	136.3	126.9	**133.9**	138.8	120.1	**136.2**	135.8	126.1
	A	**2.16**	2.42	2.09	**2.26**	2.22	2.23	**2.05**	2.07	1.84	**2.88**	3.39	4.93
	B	**1.30**	1.47	1.11	**1.30**	1.48	1.06	**1.18**	1.45	1.08	**1.83**	2.25	2.96
15. RP	θ	**164.1**	160.3	155.6	**150.7**	160.7	148.1	**153.1**	165.9	154.0	**174.9**	171.0	172.8
	A	**1.81**	2.14	1.75	**1.99**	2.19	1.84	**1.87**	2.00	1.66	**2.84**	3.23	4.23
	B	**1.51**	1.51	1.21	**1.41**	1.49	1.17	**1.16**	1.31	1.09	**1.49**	2.15	2.44

Appendix 4. BFD(ℓ:c) colour-difference formula

The full specification of the BFD(ℓ:c) formula is given as follows.

$$\Delta E_{BFD} = \left[\left(\frac{\Delta L_{BFD}}{\ell} \right)^2 + \left(\frac{\Delta C^*}{c D_C} \right)^2 + \left(\frac{\Delta H^*}{D_H} \right)^2 + R_T \left(\frac{\Delta C^* \Delta H^*}{D_C D_H} \right) \right]^{1/2}$$

where

$$L_{BFD} = 54.6 \log(Y + 1.5) - 9.6$$

$$D_C = \frac{0.035 \overline{C^*}}{1 + 0.00365 \overline{C^*}} + 0.521$$

$$D_H = D_C (GT' + 1 - G)$$

$$G = \left[\frac{(\overline{C^*})^4}{(\overline{C^*})^4 + 14000} \right]^{1/2}$$

$$T' = 0.627 + 0.055 \cos(\bar{h} - 254°) - 0.04 \cos(2\bar{h} - 136°) + 0.07 \cos(3\bar{h} - 32°) + 0.049 \cos(4\bar{h} + 114°) - 0.015 \cos(5\bar{h} - 103°)$$

$$R_T = R_H R_C$$

$$R_H = -0.26 \cos(\bar{h} - 308°) - 0.379 \cos(2\bar{h} - 160°) - 0.636 \cos(3\bar{h} + 254°) + 0.226 \cos(4\bar{h} + 140°) - 0.194 \cos(5\bar{h} + 280°)$$

$$R_C = \left[\frac{(\overline{C^*})^6}{(\overline{C^*})^6 + 7 \times 10^7} \right]^{1/2}$$

(The terms $\overline{C^*}$ and $\bar{h}$ refer to the mean of the C^* and h° values for the standard and sample, these values and ΔC^* and ΔH^* being calculated from the CIELAB formula.)

$\ell = c = 1$ for perceptibility data

$\ell = 2, c = 1$ for acceptability data

$\ell = 0.67, c = 1$ for large colour differences